

**GREEN NANOTECHNOLOGY APPROACH FOR SYNTHESIS AND
ENCAPSULATION OF GOLD NANOPARTICLES FROM
AGRICULTURAL WASTE**

Kiruba Krishnaswamy

**A thesis submitted to McGill University
in partial fulfillment of the requirements of the degree of**

**Doctor of Philosophy
April, 2015**

**Department of Bioresource Engineering
McGill University, Canada**

Dedicated to

My Beloved Parents

ABSTRACT

Researchers in nanotechnology are turning towards “Nature” to provide inspiration to develop novel innovative methods for nanoparticle synthesis. Currently used chemical and physical methods of nanoparticles synthesis use toxic chemicals in their synthesis protocols. The toxic residues from these nanoparticles make them unsafe for food related applications. There is a need to develop nanoparticles using greener alternatives. Another challenging question that needs to be addressed is agricultural waste management. Merging these two problems led to the concept of creating wealth out of waste. Agricultural waste materials such as grape seeds, skin, stalk and organic waste generated during the Canadian fall season due to the fall of maple leaves and pine needles were used in this study to synthesize gold nanoparticles (AuNP).

The main goal of this study is to synthesize gold nanoparticles without using toxic chemicals in the synthesis protocol making them suitable for drug/functional food delivery systems. A green nanotechnology approach was followed by using water as the solvent throughout the study. This value addition to agricultural waste has led to the yield of high value and ecofriendly gold nanoparticles. From the transmission electron microscopy (TEM) micrographs of gold nanoparticles produced using grape seeds (GSE), skin (GSK), stalk (GST) and pine needle extract, nearly spherically- shaped AuNP about 20 - 25 nm in diameter were observed. Whereas the gold nanoparticles produced using maple leaf extract produced triangular prisms. This is the first study stating the use of maple leaf extracts to potentially synthesize gold nanoparticles.

As the plant matrix is a highly complex system, catechin, a polyphenolic compound present in grape seed, skin, and stalk, and in pine needles, was selected for further investigation. Gold nanoparticles were synthesized using different combinations of catechin (CAT), tannic acid (TAE), 1:1 CAT: TAE, 1:4 CAT: TAE. TEM images showed that gold nanoparticles synthesized using catechin were quasi-spherical in shape with 40 – 50 nm in size. All the gold nanoparticles produced by green synthesis method in this study were hydrophilic in nature.

In order to make hybrid organic-inorganic carriers for drug delivery systems, AuNP synthesized using catechin was encapsulated in maltodextrin and beta-cyclodextrin complexes. The method adopted for encapsulation of AuNP into maltodextrin followed a top-down approach. The complex formation of AuNP into beta-cyclodextrin followed a bottom-up approach. Three different encapsulation methods such as microwave assisted encapsulation, freeze drying encapsulation and simple inclusion encapsulation for maltodextrin and molecular inclusion encapsulation for beta-cyclodextrin were studied for encapsulation of AuNP. The scanning electron microscopy (SEM) images of the AuNP encapsulated powder showed interesting morphology when comparing microwave assisted encapsulation to freeze drying encapsulation in both maltodextrin and beta-cyclodextrin. It was found from this study that organic-inorganic hybrid carriers can be developed using water following a green nanotechnology approach.

RÉSUMÉ

Les chercheurs en nanotechnologie se concentrent sur “la nature” pour stimuler l’inspiration visant le développement de méthodes novatrices pour la synthèse de nanoparticules. Les méthodes chimiques et physiques courantes pour la synthèse de nanoparticules utilisent des produits chimiques toxiques dans leurs protocoles. La possibilité de résidus toxiques dans ces nanoparticules les rend non propre pour des applications alimentaires. Il existe donc un besoin de développer des nanoparticules par des méthodes plus vertes. Se jumèle à cette préoccupation la nécessité de mieux gérer les résidus agro-alimentaires. Ce jumelage nous amène le concept de créer de la richesse à partir de résidus. Des résidus organiques tels que les graines, la peau, les tiges du raisin, de même que les résidus domestiques typiques de l’automne canadien avec la chute des feuilles d’érable et des aiguilles de pins, ont été utilisés dans cette étude pour la synthèse de nanoparticules d’or (AuNP).

L’objectif principal de cette étude est la synthèse de nanoparticules d’or sans l’utilisation de produits chimiques toxiques dans le protocole de synthèse afin de les rendre utiles dans des systèmes de libération de médicaments/aliments fonctionnels. Une approche nano-technologique verte a été développée en utilisant de l’eau comme solvant. Cette valeur ajoutée aux résidus organiques a permis la production écologique de nanoparticules d’or de haute valeur. Grâce aux micrographies par microscopie électronique à transmission (TEM) des nanoparticules d’or produites en utilisant les graines, la peau, et les tiges de raisins et un extrait d’aiguilles de pin, des nanoparticules presque sphériques de 20 – 25 nm de diamètre ont été observées. Par contre les nanoparticules d’or produites avec les extraits de feuilles d’érable se sont avérées être des

prismes triangulaires. Ceci est la première étude à utiliser un extrait de feuille d'érable pour la synthèse de nanoparticules d'or.

Puisque la matrice organique est un système très complexe, la catéchine, un composé phénolique retrouvé dans la peau, les pépins et les tiges de raisins et dans les aiguilles de pin, a été choisie dans la poursuite de l'étude. Les nanoparticules d'or ont été synthétisées avec différentes combinaisons de catéchine (CAT) et d'acide tannique (TAE), 1:1 CAT: TAE, 1:4 CAT: TAE. Les images TEM ont montré que les nanoparticules d'or produites en utilisant la catéchine étaient quasi-sphériques et de 40-50 nm de dimensions. Toutes les nanoparticules d'or produites par cette méthode de synthèse verte étaient de nature hydrophile.

Dans le but de fabriquer un système de libération hybride organique/inorganique, les nanoparticules d'or synthétisées par catéchine ont été encapsulées dans des complexes de maltodextrine et de betacyclodextrine. La méthode d'encapsulation des AuNP avec la maltodextrine a suivi une approche descendante. La formation d'une matrice AuNP et betacyclodextrine a suivi une approche ascendante. Trois différentes méthodes d'encapsulation ont été étudiées, dont l'encapsulation par microonde, l'encapsulation par lyophilisation et l'encapsulation par inclusion simple pour la maltodextrine et l'encapsulation par inclusion moléculaire pour la betacyclodextrine. Les images par microscopie électronique à balayage (SEM) des poudres de nanoparticules d'or encapsulées ont montré une morphologie particulière en comparant l'encapsulation microonde à l'encapsulation par lyophilisation et ce pour la maltodextrine et pour la betacyclodextrine. Cette étude a démontré qu'un complexe organique-inorganique peut

être développé utilisant de l'eau comme solvant en suivant une approche nanotechnologique verte.

ACKNOWLEDGMENTS

I surrender myself before “The Almighty” whose blessings empowered me to complete this beautiful chapter of my life.

I would like to express my sincere thanks to my supervisor Dr. Valérie Orsat for her kindness, gracious guidance, encouragement and timely help during the course of my study. Language is inadequate to voice my deep sense of gratitude for believing in me and standing for me during times of trial. Thank you very much, I feel blessed to be your student.

Dr. G.S. Vijaya Raghavan, is the first person who introduced me to McGill University. Dr. Raghavan has inspired me since my undergraduate studies. I sincerely thank him for his visionary guidance and motivation. I would thank Prof. Raghavan and his wife Ms. Subhadra Raghavan for their support, kindness and care rendered during my stay in McGill and making me feel at home.

I humbly express my thanks to Mr. Yvan Gariépy for his technical guidance and support. His immense technical knowledge and his patience to explain the technicalities in detail have always amazed me. I would like to thank Dr. Darwin Lyew for being a good friend, his wise words has always boosted my confidence and made me optimistic. I would like to express my profound thanks to Dr. Alice Cherestes for her kindness, care and encouragement. Being a motivating mentor, she has guided me both personally and professionally. Thank you is a very small word to express my gratitude to her.

Dr. Salwa Karboune, for being kind and for providing me access to the particle size analyzer, Mr. John Gavita, Olympus Canada and Dr. Hojatollah Vali for providing access to transmission electron microscope. I would like to thank Ms. Gerry Chevalier, Residence Coordinator for her kindness and her willingness to help with a beautiful smile. I appreciate Ms. Susan Gregus, Ms. Abida Subhan and Ms. Patricia Singleton for their support and help in processing my administrative documents during my study.

I experienced a beautiful sisterly bond with my friends Simona, Yanti, Inneke and Sara for which I would always be grateful. I would like to thank my friends Ramesh Anna, Selva

Akka, Shrikalaa, Sriram, Prabha, Yashi, Nora, Navpreet, Paula, Amy and Winny for their encouragement and support during my study.

I would like to thank my comprehensive and defense committee members for spending their valuable time to read, evaluate my thesis and to provide valuable suggestions to improve the quality of this work. I am thankful to the Natural Science and Engineering Research Council of Canada (NSERC) for supporting this study.

Would like to thank all the amazing people I met in McGill University, those silent mornings in Mac Campus, where one could hear the mellifluous music of birds, the statue of Sir William Macdonald, who stands inert to time. The beautiful flowers in McEwen fields, cheered me to smile after a long day of lab work during spring and summer. The explosion of colors during fall by colorful trees, painting the clear blue sky with reddish - yellow hues on the banks of Lake Saint-Louis near Mac Campus. Graciously falling silver snowflakes knitting a white blanket of snow were the scenic view through my window. Living on campus made me feel close to Nature, the best teacher when carefully observed.

Amma (Ms. Shanthi Krishnaswamy), Appa (Mr. Krishnaswamy Subramaniam) and Thiruma, I feel blessed to be born in this beautiful family. Amma & Appa thank you very much, for teaching compassion is the true essence of life, trusting me and letting me follow my dreams. Thank you my dear Vinayagar and His family for being a good friend and guiding me through this journey called life.

I would like to thank all ‘My Gurus’.

Lessons learnt during my PhD would be cherished and treasured. The most valuable lesson learnt during my PhD is mentioned below.

“Known is a drop, unknown is an ocean” – Avvaiyar (Tamil Poet, 300 CE)

Thank you.

Sincerely,

Kiruba Krishnaswamy

CONTRIBUTIONS OF THE AUTHORS

In accordance with the McGill “Guidelines for a Manuscript Based Thesis”, the contributions made by the candidate and the co-authors to the completion of this dissertation are described below.

All the manuscripts presented in this dissertation are written by Ms. Kiruba Krishnaswamy and co-authored by Dr. Valérie Orsat, Department of Bioresource Engineering, McGill University. Ms. Kiruba Krishnaswamy was responsible for developing protocols, designing the experiments, conducting research, testing, and documentation. Dr. Valérie Orsat guided the candidate technically, financially and morally, proofread all manuscripts, and provided constructive criticisms and suggestions towards the research.

Dr. Hojatollah Vali, Facility for Electron Microscopy Research, McGill University helped with transmission electron microscopy (TEM) imaging for manuscript 1. Dr. Salwa Karboune, Department of Food Science and Agricultural Chemistry, McGill University helped with particle size analysis in manuscript 4.

The list of manuscript produced from this thesis:

1. Krishnaswamy, K., Vali, H., Orsat, V. [Value-adding to grape waste: Green synthesis of gold nanoparticles.](#) *Journal of Food Engineering*. 2014, 142, 210-220.
2. Krishnaswamy, K. and Orsat, V. [Insight into the nanodielectric properties of gold nanoparticles synthesized from maple leaf and pine needle extracts.](#) *Industrial Crops and Products*. 2015, 66, 131-136.

3. Krishnaswamy, K. and Orsat, V. [Gold nanofluids synthesised using antioxidant catechin, its characterization and studies on nucleation](#). *Journal of Experimental Nanoscience*. 2015, DOI: 10.1080/17458080.2015.1061217.
4. Krishnaswamy, K., Karboune, S., Orsat, V. Synthesis and characterization of maltodextrin encapsulated gold nanoparticles using freeze drying and microwave assisted encapsulation method. *Journal of Controlled Release*. (Submitted)
5. Krishnaswamy, K. and Orsat, V. Beta-cyclodextrin encapsulated gold nanoparticles by freeze drying encapsulation and microwave assisted encapsulation method ensuing green nanotechnology approach. *Journal of Nanoparticle Research*. (Submitted)

Selected results from the chapters were presented in annual conferences and meetings which are mentioned in the connecting text corresponding to each chapter.

TABLE OF CONTENTS

Abstract	I
Résumé	V
Acknowledgement	VIII
Contributions of Authors	X
List of Tables	XVIII
List of Figures	XX
List of Symbols and Abbreviations	XXV
CHAPTER I – INTRODUCTION	1
1.1 Problem statement	3
1.2 Objective	4
1.2.1 Specific objectives	4
1.3 Organization of the thesis	5
CHAPTER II – REVIEW OF LITERATURE	6
2.1 History and development of nanotechnology	6
2.1.1 Chronological highlights of events which led to the origin and development of nanotechnology	7
2.1.2 Terminology used in nanotechnology	14
2.2 Different forms of nanostructures	18
2.2.1 Quantum Dots	21
2.2.2 Buckminsterfullerene (or Fullerene)	21
2.2.3 Carbon nanotubes	22
2.2.4 Polymer nanoparticles	22

2.2.1 Metallic nanoparticles	25
2.3 Synthesis of gold nanoparticles (AuNP)	28
2.3.1 Bottom-up approach	28
2.3.2 Top-down approach	29
2.4 Transition towards green nanotechnology	31
2.4.1 Green Chemistry	32
2.4.2 Green Engineering	33
2.4.3 Green Nanotechnology	34
2.5 Green synthesis of gold nanoparticles from plant extracts	35
2.6 Characterization of nanoparticles	36
2.7 Summary	40
CONNECTING STATEMENT	41

CHAPTER III – VALUE-ADDING TO GRAPE WASTE: GREEN SYNTHESIS OF GOLD NANOPARTICLES	42
3.1 Abstract.....	42
3.2 Introduction.....	43
3.3 Materials and Methods	47
3.3.1 Sample preparation – synthesis of AuNP using grapes seed, skin and stalk ...	47
3.3.2 Synthesis of AuNP using catechin	47
3.3.3 Apparatus and measurements.....	47
3.3.4 Statistical design.....	50
3.4 Results and discussion.....	51
3.4.1 RSM for green synthesis of AuNP	65

3.4.2 Mechanism for green synthesis of gold nanoparticles by catechin	69
3.5 Conclusion	72
CONNECTING STATEMENT	74

CHAPTER 1V – GREEN SYNTHESIS OF GOLD NANOPARTICLES FROM MAPLE LEAF AND PINE NEEDLE EXTRACTS

4.1 Abstract.....	75
4.2 Introduction.....	76
4.3 Experimental details	78
4.4 Results and discussion.....	80
4.5 Conclusion	92
CONNECTING STATEMENT.....	93

CHAPTER V – GOLD NANOFLUIDS SYNTHESIZED USING CATECHIN AND ITS CHARACTERISATION

5.1 Abstract.....	94
5.2 Introduction.....	95
5.3 Materials and Methods	98
5.3.1 Sample preparation	98
5.3.2 UV-Vis Spectrophotometer.....	99
5.3.3 Differential Scanning Calorimeter	100
5.3.4 Dielectric Spectroscopy	100
5.3.5 Transmission electron microscopy	101

5.4 Results and discussion.....	101
5.4.1 Thermal properties of nanofluids	101
5.4.2 Dielectric properties of nanofluids	107
5.4.3 Interpretation of TEM micrographs.....	111
5.4.4 Spectral properties of nanofluids.....	115
5.4.5 Studies on nucleation of AuNP	119
5.5 Conclusion	123
CONNECTING STATEMENT	124

CHAPTER VI – SYNTHESIS AND CHARACTERISATION OF GOLD

NANOPARTICLES ENCAPSULATED IN MALTODEXTRIN MATRIX	125
6.1 Abstract.....	125
6.2 Introduction.....	126
6.3 Materials and Methods	130
6.3.1 Materials	130
6.3.2 Preparation of gold nanoparticles	130
6.3.3 Encapsulation methods	130
6.3.4 AuNP loading, encapsulation efficiency and yield	131
6.3.5 Particle size analysis	132
6.3.6 Differential Scanning Calorimeter	133
6.3.7 Scanning Electron Microscopy	133
6.3.8 Fourier Transform Infrared Spectroscopy	134
6.3.9 Statistical analysis	134
6.4 Results and discussion.....	134
6.4.1 Results from the statistical analysis.....	134

6.4.2 Interpretation of SEM images	141
6.4.3 Conformation of functional groups from FTIR spectra	147
6.4.4 Thermal analysis using differential scanning calorimeter (DSC)	150
6.5 Conclusion	158
CONNECTING STATEMENT	159

CHAPTER VII – BETA-CYCLODEXTRIN ENCAPSULATED GOLD NANOPARTICLES USING GREEN NANOTECHNOLOGY APPROACH 160

7.1 Abstract.....	160
7.2 Introduction.....	161
7.3 Materials and Methods	165
7.3.1 Materials	165
7.3.2 Preparation of gold nanoparticles	165
7.3.3 Encapsulation methods	165
7.3.4 AuNP loading, encapsulation efficiency and yield	166
7.3.5 Particle size analysis	167
7.3.6 Differential Scanning Calorimeter	167
7.3.7 Scanning Electron Microscopy	168
7.3.8 Fourier Transform Infrared Spectroscopy	168
7.3.9 Statistical analysis	169
7.4 Results and discussion.....	169
7.4.1 Interpretation of UV-Visible spectra for surface plasmon resonance (SPR).	169
7.4.2 Results from statistical analysis	172
7.4.3 Thermal analysis using differential scanning calorimetry (DSC)	174
7.4.4 Functional groups conformation using FTIR spectra	180

7.4.5 Interpretation of SEM micrographs	182
7.5 Conclusion	189
CONNECTING STATEMENT	191
 CHAPTER VIII – CURRENT STATUS, TRENDS AND APPLICATIONS OF NANOTECHNOLOGY	 192
8.1 Current status of nanotechnology	192
8.1.1 National Nanotechnology Initiatives (NNI) and budget allotted for R&D in nanotechnology	192
8.1.2 NNI investments by Program Component Areas for 2015	194
8.1.3 Position of Canada in R&D related to nanotechnology	197
8.2 Gold nanoparticles: current status and application	197
8.3 General applications of nanotechnology in agro-food systems	200
8.4 Potential applications of nanomaterials synthesized in this PhD study	203
8.5 Nanotechnology benefits, risk and challenges.....	204
8.5.1 Scientific gaps in knowledge	205
8.6 Sustainable gold nanoparticles.....	206
 CHAPTER IX – SUMMARY AND CONTRIBUTIONS TO KNOWLEDGE	 207
9.1 Summary	207
9.2 Contribution to knowledge	212
9.3 Recommendation for future research	214
 REFERENCES	 215

LIST OF TABLES

TABLE NO.	TITLE	PAGE NO.
2.1	Chronological highlights of event led to the development of nanotechnology	7
2.2	Terms and definitions related to nanotechnology (ISO/TS 80004-1: 2010)	15
2.3	Metallic nanoparticles and their synthesis conditions	26
2.4	Twelve Principles of Green Chemistry	31
2.5	Characterization methods used in nanoparticle analysis	38
3.1	Null and alternative hypothesis to study the effect of linear, quadratic and bilinear interactions of the variables	51
3.2	Code levels for independent variables in central composite design for the green synthesis of AuNP	51
3.3	Summary of TEM image analysis with particle size for the grape waste synthesized gold nanoparticles	58
3.4	Composition of phenolic compounds present in seed, stalk, skin in Merlot variety (Souquet et al., 2000).	63
3.5	Uncoded values and their corresponding response for face centered central composite design.	67
3.6	ANOVA table for green synthesis of gold nanoparticles from catechin.	68
5.1	Benefits of nanofluids containing nanoparticles versus microparticles	97
5.2	Composition of four different nanofluids synthesized using catechin (CAT) and tannic acid (TAE)	98
5.3	Particle size analysis of AuNP size in nanofluids	115
6.1	Full factorial design for the encapsulation of AuNP into a maltodextrin matrix	135
7.1	Properties of different cyclodextrins (Del Valle, 2004)	163

7.2	Encapsulation properties of AuNP encapsulated beta-cyclodextrin complex	172
8.1	Six key indicators of nanotechnology development in the world and the United States (Roco, 2011)	194
8.2	Application of nanotechnology in agro-food industry	201
8.3	Summary of current and projected applications of nanotechnology in the food production chain (Rossi et al., 2014)	202

LIST OF FIGURES

FIGURE NO.	TITLE	PAGE NO.
1.1	Comparing the size and shape of nanomaterials to more familiar materials	2
2.1	Nanomaterial Framework (ISO, 2010)	19
2.2	Different types of nanostructures and their dimensions	20
2.3	Top-down and Bottom-up approaches for synthesising polymeric nanoparticles	23
3.1	Flow chart showing the progressive transition towards green nanotechnology	43
3.2	Schematic flow diagram for the green synthesis of gold nanoparticles from grape waste, A) grape seed; B) grape skin; C) grape stalk	49
3.3	Changes in the absorbance of the grape seed, skin, stalk extracts and HAuCl ₄ solution over time	52
3.4	UV-Visible spectra recorded as a function of time of reaction between HAuCl ₄ and grape extracts. (a) grape seed extract synthesized gold nanoparticles (GSE+AuNP), (b) grape skin extract synthesized gold nanoparticles (GSK+AuNP), (c) grape stalk extract synthesized gold nanoparticles (GST+AuNP), (d) comparing the absorbance of grape extracts before the addition of HAuCl ₄ and after the formation of gold nanoparticles	55
3.5	a. TEM image of grape seed extract synthesized gold nanoparticles (GSE+AuNP) with size distribution graph (scale bars = 100 nm)	59
	b. TEM image of grape skin extract synthesized gold nanoparticles (GSK+AuNP) with size distribution graph (scale bars = 100 nm)	60
	c. TEM image of grape stalk extract synthesized gold nanoparticles (GST+AuNP) with size distribution graph (scale bars = 100 nm)	62
3.6	(a) HRTEM image of grape stalk extract synthesized AuNP showing atomic structures (scale bar = 2 nm), (b) corresponding EDX plot GST+AuNP showing elemental peak for gold, (c) image of GST + AuNP obtained from 3D laser microscope showing a thin film of grape matrix over gold nanoparticles	62

3.7	(a) UV-Vis spectra shows the reaction of catechin with HAuCl_4 solution over period of time, (b) TEM image of catechin synthesized gold nanoparticles	64
3.8	Response surface plot representing the effect of catechin and temperature on the green synthesis of gold nanoparticles using catechin	66
3.9	Schematic process flow for green synthesis of AuNP by catechin; reduction of catechin to quinone and generation of gold atoms by forming catechin+AuNP complex, (a) pictorial representation of gold nanoparticles surrounded by catechin molecule, (b) TEM image of catechin+AuNP showing a clear layer of catechin surrounding the gold nanoparticles (scale bars = 100 nm)	70
4.1	Schematic flow diagram for green synthesis of gold nanoparticles mediated through maple leaf and pine needle extracts	79
4.2	UV-Visible spectra recorded as a function of time of reaction between HAuCl_4 and plant extracts (a) maple leaf extract; (b) pine needle extract	81
4.3	TEM micrograph (scale bars = 20 nm) of gold nanoparticles synthesized using (a) maple leaf extract; (b) pine needle extract	82
4.4	DSC thermographs obtained for gold nanoparticles synthesized using maple leaf extract	85
4.5	DSC thermographs obtained for gold nanoparticles synthesized using pine needle extract	86
4.6	Graph showing (a) dielectric constant (ϵ'); (b) dielectric loss factor (ϵ''); (c) dissipation factor ($\tan \delta$) for gold nanofluids from plant extracts and Turkevich method over the frequency range from 200 MHz to 20 GHz	90
5.1	Green nanofluids containing gold nanoparticles	99
5.2	DSC thermogram for TAE +AuNP nanofluid (sample A)	102
5.3	DSC thermogram for 1:1 CAT: TAE + AuNP nanofluid (sample B)	103
5.4	DSC thermogram for 1:4 CAT: TAE + AuNP nanofluid (sample C)	104
5.5	DSC thermogram for CAT + AuNP nanofluid (sample D)	105
5.6	Overlay of DSC thermograms for the four different green synthesized AuNP nanofluids	106
5.7	Dielectric properties of green synthesized AuNP nanofluids, (a) Dielectric constant (ϵ'); (b) Dielectric loss factor (ϵ''); (c) Dissipation	109

	factor ($\tan \delta$)	
5.8	TEM micrograph of gold nanoparticles synthesized by TAE + AuNP	111
5.9	TEM micrograph of gold nanoparticles synthesized by 1:1 TAE: CAT + AuNP	112
5.10	TEM micrograph of gold nanoparticles synthesized by 1:4 CAT: TAE + AuNP	113
5.11	TEM micrograph of gold nanoparticles synthesized by CAT + AuNP, indicating clear encapsulation of gold nanoparticles by catechin layer (core and shell form)	114
5.12	UV- Vis spectra for gold nanofluids with SPR Peak, (a) TAE+AuNP; (b) 1:1 CAT:TAE+AuNP; (c) 1:4 CAT: TAE+AuNP; (d) CAT+AuNP	118
5.13	TEM image of Catechin on grid for CAT+AuNP Nanofluid	121
5.14	TEM image of reaction on grid for CAT+AuNP Nanofluid	122
6.1	Plot showing the effect of different encapsulation method on the % yield for encapsulation of AuNP into maltodextrin (MD)	136
6.2	Plot showing the effect of different encapsulation method on AuNP loading into maltodextrin (MD)	137
6.3	Graph showing the effect of AuNP loading for different encapsulation methods	138
6.4	Grid showing the mean of encapsulation efficiency for the three encapsulation methods for the three different concentrations	139
6.5	Graph representing the mean diameter of the encapsulated powder using the three encapsulation methods a) Freeze drying encapsulation (FE); b) Microwave assisted encapsulation (ME); c) Simple encapsulation (SE)	140
6.6	SEM micrograph of AuNP encapsulated powder at 100 x magnification. a) FE; b) ME; c) SE	142
6.7	SEM micrograph of AuNP encapsulated powder at 1000 x magnification. a) FE; b) ME; c) SE	145
6.8	Comparing the SEM micrographs for freeze drying and microwave assisted encapsulation methods	146
6.9	FTIR spectra for AuNP encapsulated powders for the three concentrations by a) Freeze drying encapsulation (FE); b) Microwave assisted encapsulation (ME); c) Simple encapsulation (SE)	149

6.10	DSC thermograph for AuNP encapsulated maltodextrin powder by freeze drying encapsulation method (1M)	151
6.11	DSC thermograph for AuNP encapsulated powder by microwave assisted encapsulation method (1M)	154
6.12	DSC thermograph for AuNP encapsulated powder by simple encapsulation method (1M)	156
7.1	Chemical structure and approximate geometric dimensions of α -cyclodextrins (α -CD), β -cyclodextrins (β -CD) and γ -cyclodextrins (γ -CD) (Astray et al., 2009)	162
7.2	Glycosidic oxygen bridge α (1,4) bond formation between two molecules of glucopyranose (Astray et al., 2009)	162
7.3	Surface plasmon resonance (SPR) plots for different concentrations of gold nanoparticles	170
7.4	Standard curve obtained for different concentration of gold nanoparticles	170
7.5	Surface plasmon resonance (SPR) plots for encapsulation of gold nanoparticles into beta-cyclodextrin complex	171
7.6	Prediction profiler plot showing the desirability functions for the three encapsulation methods	173
7.7	DSC thermograph for AuNP encapsulated beta-cyclodextrin powder produced by molecular inclusion method (MIB)	174
7.8	DSC thermograph for AuNP encapsulated beta-cyclodextrin powder produced by lyophilisation encapsulation method (FEB)	175
7.9	DSC thermograph for AuNP encapsulated beta-cyclodextrin powder produced by microwave assisted encapsulation method (MEB)	176
7.10	Overlay of DSC thermograph of (a) lyophilisation encapsulation method (FEB); (b) microwave assisted encapsulation method (MEB)	179
7.11	FTIR spectra for AuNP encapsulated beta-cyclodextrin powder by microwave assisted encapsulation (MEB); molecular inclusion method (MIB); lyophilisation encapsulation (FEB) overlay with FTIR spectra for pure beta-cyclodextrin	181
7.12	SEM micrograph of AuNP encapsulated powder obtained from beta-cyclodextrin at 100 x magnification. a) FEB; b) MEB; c) MIB	184
7.13	SEM micrograph of AuNP encapsulated powder obtained from beta-	186

	cyclodextrin at 1000 x magnification. a) FEB; b) MEB; c) MIB	
7.14	Comparing the SEM micrographs for microwave assisted encapsulation and lyophilisation encapsulation of AuNP within beta-cyclodextrin cavity	188
7.15	SEM micrograph of AuNP encapsulated in beta-cyclodextrin powder obtained from lyophilisation encapsulation method at 20,000 x magnification	189
8.1	Highlighted Program Component Areas (PCA) for NNI investment in 2015	195
8.2	Top 12 countries with high contribution of documents in research related to gold nanoparticles (Data retrieved from Scopus, April 2015 with search term ‘gold nanoparticles’)	199
8.3	Patent applications filled / obtained for gold nanoparticles in various disciplines (Data retrieved from Scopus, April 2015 with patent search term ‘gold nanoparticles’)	199
8.4	Number of nanotechnology publications per year in the Scopus database using the key terms as indicated (a) nanotechnology (b) nanotechnology and food (c) nanotechnology and agricultural related applications (d) nanotechnology and food related applications (Handford et al., 2014)	200
9.1	Summary of green synthesized gold nanoparticles (AuNP)	209
9.2	Summary of encapsulation of gold nanoparticles (AuNP)	211
9.3	Overall summary of this PhD thesis	213

LIST OF SYMBOLS AND ABBREVIATIONS

α - CD	-	Alpha cyclodextrin
β - CD	-	Beta cyclodextrin
γ - CD	-	Gamma cyclodextrin
μ	-	Micron
λ	-	Wavelength
\pm	-	Plus or minus
$<$	-	Less than
$>$	-	Greater than
ϵ'	-	Dielectric constant
ϵ''	-	Dielectric loss factor
%	-	Per cent
$^{\circ}\text{C}$	-	Degree Celsius
μg	-	Microgram
μm	-	Micrometer
\AA	-	Degree Angstrom
Abs	-	Absorbance
Conc.	-	Concentration
cm	-	Centimeter
Dia	-	Diameter
EHS	-	Environment, health and safety
ENMs	-	Engineered nanomaterials
etc.	-	<i>et cetera</i>
<i>et al.</i>	-	and others
FAO	-	Food and Agricultural Organisation
ISO	-	International Organization for Standardization
J	-	Joules
m	-	Meter
nm	-	Nanometer

Abbreviation's related to specific chapters

Chapter II

AES	- Auger electron spectroscopy
AFM	- Atomic force microscopy
CE	- Capillary electrophoresis
CFM	- Chemical force microscopy
CFUF	- Cross flow ultrafiltration
CPC	- Condensation particle counter
DSC	- Differential scanning calorimeter
FFF	- Field flow fractionation
FTIR	- Fourier transforms infrared spectroscopy
HDC	- Hydrodynamic chromatography
MS	- Mass spectrometry
NMR	- Nuclear magnetic resonance
SANS	- Small angle neutron scattering
SEC	- Size exclusion chromatography
SEC-ICP MS	- SEC- Inductively coupled plasma -mass spectrometry
SEM	- Scanning electron microscopy
SERS	- Surface enhanced Raman spectroscopy
SP-ICPMS	- Single particle- Inductively coupled plasma mass spectrometry
STEM	- Scanning transmission electron microscopy
STM	- Scanning tunneling microscopy
TEM	- Transmission electron microscopy
TEM -EDX	- TEM -Energy dispersive X-ray spectroscopy
UC	- Ultracentrifugation
XAS	- X-ray absorption spectroscopy
XPS	- X-ray photoelectron spectroscopy
XRD	- X-ray diffraction

Chapter III

AuNP	-	Gold nanoparticles
EC	-	(-) epicatechin
EGC	-	(-) epigallocatechin
GSE	-	Grape seed
GSE+AuNP	-	Gold nanoparticles synthesized from grape seed extract
GSK	-	Grape skin
GSK+AuNP	-	Gold nanoparticles synthesized from grape skin extract
GST	-	Grape stalk
GST+AuNP	-	Gold nanoparticles synthesized from grape stalk extract
HAuCl ₄	-	Hydrogen tetrachloroaurate (or) Chloroauric acid trihydrate

Chapter V

1:1 CAT: TAE+AuNP	-	Gold nanoparticles synthesized from 1:1 ratio of CAT:TAE
1:4 CAT: TAE+AuNP	-	Gold nanoparticles synthesized from 1:4 ratio of CAT:TAE
CAT	-	Catechin
CAT+AuNP	-	Gold nanoparticles synthesized from catechin

Chapter VI

DMAB	-	Didecyl dimethyl ammonium bromide
FE	-	Freeze drying encapsulation
ME	-	Microwave assisted encapsulation
SE	-	Simple encapsulation
TAE	-	Tannic acid
TAE+AuNP	-	Gold nanoparticles synthesized from tannic acid

Chapter VII

AuNP+BCD	-	AuNP encapsulated in beta-cyclodextrin
----------	---	--

BCD	-	Beta-cyclodextrin
CD	-	Cyclodextrin
FEB	-	Lyophilisation encapsulation
MEB	-	Microwave assisted encapsulation
MIB	-	Molecular inclusion encapsulation

CHAPTER 1

INTRODUCTION

The International Organization for Standardization (ISO) defines nanotechnology as the “application of scientific knowledge to manipulate and control matter at the nanoscale in order to make use of size- and structure- dependent properties and phenomena, as distinct from those associated with individual atoms or molecules or with bulk materials” (ISO, 2010). The International System of Units (Système International d'Unités, SI) definition for “nano” is, a prefix used to form decimal submultiples of the SI unit “meter”, designating a factor of 10^{-9} denoted by the symbol “n”.

Nanotechnology is the technology of working at extremely small scale of nanometer, where one nanometer is one billionth of a meter ($1 \text{ nm} = 0.000\ 000\ 001 \text{ m}$ or 10^{-9} m). Nanomaterials have unique properties that can be tailored to obtain new and modified functions (Figure 1.1). Due to the potential utilization of these nanomaterials in a variety of applications, research activities in the production of such materials are expanding. The major driving force that has led to the development of the field of nanoparticles synthesis is that they have distinct physical and chemical properties when compared to their bulk counterparts (Amato & Carroll, 1999; Hornyak et al., 2008; Poole Jr & Owens, 2003).

Over the past two decades, impressive progress has been made in the field of electronics especially in semiconductor quantum dots (Brust & Kiely, 2002; Khitrova & Gibbs, 2008). Nanotechnology has presented a possibility to be applied in various fields of study, where researchers, academicians, small and large scale industries are either developing or using engineered nanomaterials (ENMs) or products containing nanomaterials.

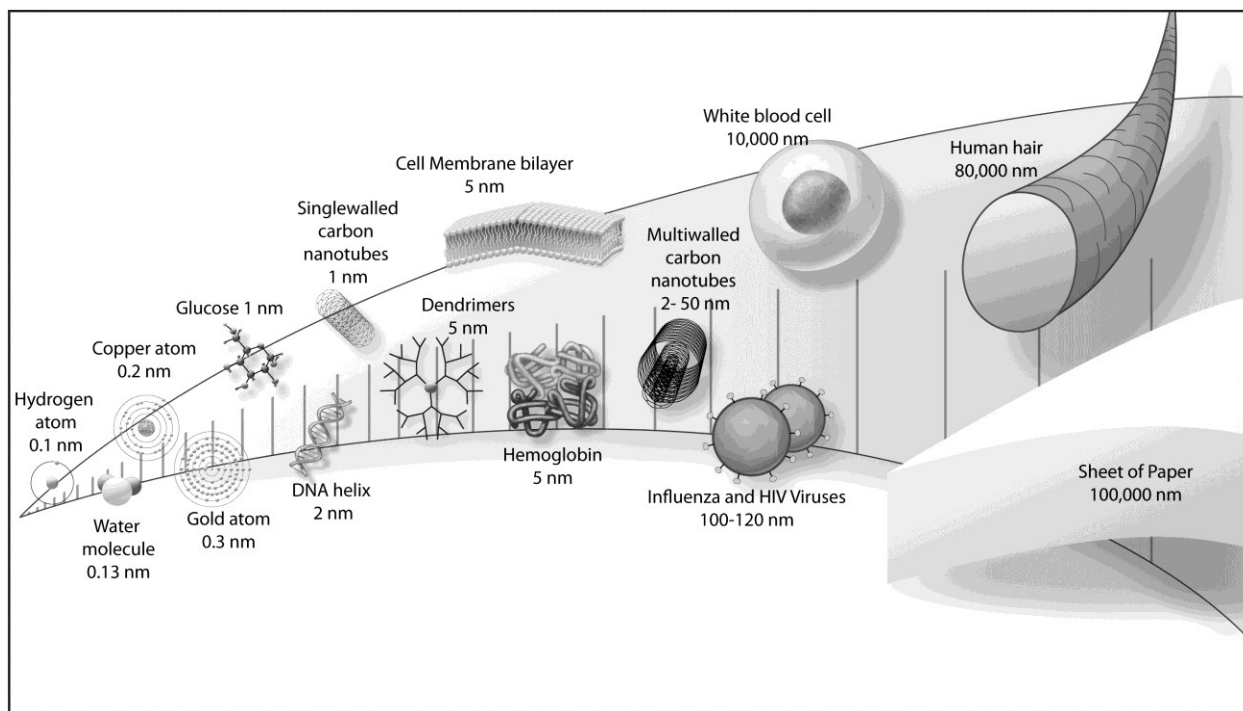


Figure 1.1 Comparing the size and shape of nanomaterials to more familiar materials (Yokel & MacPhail, 2011).

The production of nanoparticles of noble metals, such as gold nanoparticles (AuNP), is of great interest due to their novel characteristics that can be defined by manipulating their size and shape to produce unique properties which have potential applications in spectroscopy (Mulvaney, 1996), in biomedical applications such as drug delivery (Paciotti et al., 2004), tissue/tumor imaging (Jain et al., 2006), cancer therapy (Peng et al., 2009) and many other applications yet to be discovered.

Some of the commonly used reducing agents for chemical and physical methods for gold nanoparticle synthesis involves harsh chemicals such as hydrazine, sodium borohydride, dimethyl formamide, hydroxylamine hydrochloride, carbon monoxide, phosphorous in ether, hydrogen peroxide etc., which are hazardous in nature. The synthesis protocols to produce

polymeric nanoparticles use synthetic polymers like poly (D, L-lactide-co-glycolide), poly (ethylcyanoacrylate), poly (butylcyanoacrylate), poly (isobutylcyanoacrylate) and use organic solvents like dichloromethane and ethyl acetate, benzyl alcohol, cyclohexane, acetonitrile, acetone, etc., that are toxic. These methods produce nanoparticles efficiently, however downstream processing to separate them from the toxic substances is expensive and time consuming but necessary since the presence of even a small trace of hazardous compounds makes the AuNP unsuitable for biomedical/ food applications.

On the other hand, there is a huge challenge in the management of agricultural waste and post-harvest losses. For example, grape (*Vitis vinifera L.*) is one of the world's largest fruit crop with a global production of 68 million tonnes (2009) of which 38 million tonnes are processed. Annually around 2.5 million tonnes of grape waste are generated (FAOSTAT, 2012). In Canada, maple trees and pine trees shed their leaf / needles during the fall season which is considered as domestic yard waste, which often ends up in landfills.

Can such agricultural wastes be turned to high value products?

1.1 Problem statement

Problem statement 1: There is a need to develop a cleaner and greener method to produce nanoparticles that can be used in delivery systems in food/medical applications

Problem statement 2: There is a need to efficiently utilize agricultural waste

Solution: Integrating problem statement 2 to solve the issues of problem statement 1. This solution satisfies the criteria of “***Green Nanotechnology***”.

Green nanotechnology incorporates the principles of green chemistry into green engineering. It is about doing things right in the first place, about making nanomaterials and nanoparticles without toxic ingredients, using less energy and using renewable inputs wherever possible (Karn, 2008).

1.2 Objectives

The primary objective of this research is to assess the potential use of agricultural/organic wastes such as grape seed, skin, stalk, maple leaf and pine needles for synthesis of gold nanoparticles (AuNP) and in turn encapsulate them to form hybrid organic-inorganic carrier vehicles for delivery systems.

1.2.1 Specific objectives

- ☞ **Objective I:** To synthesize and characterize gold nanoparticles (AuNP) from grape seed, skin and stalk by green synthesis methods.
- ☞ **Objective II:** Green synthesis and characterisation of gold nanoparticles (AuNP) from maple leaf and pine needle extracts.
- ☞ **Objective III:** Determine the synthesis and characterisation of gold nanoparticles (AuNP) using catechin in aqueous solution.
- ☞ **Objective IV:** Developing methods for encapsulation of green synthesized gold nanoparticles into a maltodextrin matrix and their characterization.
- ☞ **Objective V:** Encapsulation of green synthesized gold nanoparticles into a beta-cyclodextrin cavity and their characterization.

1.2 Organisation of the thesis

Each specific objective of this PhD research has culminated into a manuscript for publication. This introduction is followed in Chapter II with a review of literature which provides information about the chronological development of nanotechnology and terminologies used in the field. Literature about different types of nanoparticles and the transition towards green nanotechnology has been also reviewed in Chapter II. The following Chapters III to Chapters VII are experimental research related to the specific objectives. Chapter VIII provides the current status of nanotechnology, statistics related to nanomaterials and applications in the food sector. Chapter XI being the last chapter encompasses the summary and contributions to knowledge from this PhD thesis along with recommendations for future research.

CHAPTER II

REVIEW OF LITERATURE

2.1 History and development of nanotechnology

The word “nano” in Greek means dwarf and one nanometer is defined as one billionth (1×10^{-9}) of a meter. Nanotechnology deals with extremely small sizes, where one nanometer (nm) is 1000 times smaller than a micron (Mansoori, 2005; Poole Jr & Owens, 2003). The adventure of nanotechnology starts with Nobel laureate Richard Feynman’s lecture “There’s Plenty of Room at the Bottom” at the American Physical Society meeting of the California Institute of Technology on Dec 29, 1959. This alerted the consciousness of the scientific community about the untapped potential of nanomaterials (Hornyak et al., 2008).

But the history of nanotechnology dates back to ancient civilizations of the world. The Lycurgus cup (400 AD), a stunning Roman treasure, contains glass with gold-silver alloyed nanoparticles. These nanoparticles are distributed in such a way that the glass looks green in reflected light, but glows brilliant red when light passes through the cup. Damascus steel swords (300 AD - 1700 AD), known for their exceptional sharp cutting edges and strength, contain nanoscale wire or tube like structures in their blades (Daniel & Astruc, 2004; Daw, 2012). Faraday’s prepared colloidal gold solutions, which he called ‘divided state of gold’, are still preserved in the Royal Institution, London (Edwards & Thomas, 2007).

The most ancient reported application of nanomedicine is in the traditional medicinal systems in India such as Ayurveda and Siddha in the form of bhasma (100 BC - 100 AD). In these Ayurvedic preparations, metals such as gold, silver, copper and other metals were processed into very fine powders leading to bhasmas which exhibited different colors which

were used to cure ailments (Kapoor, 2010; Paul & Chugh, 2011). The stained colored glass by the medieval artists of Europe (10-16th century) used metal nanoparticles in their colorful representations. All the artisans and craftsmen involved in creation of such beautiful artefacts were highly skilled but did not know that they were working at the nanoscale. The difference between the ancient nanotechnology examples and the present situation is the ability to understand or at least embark on the path towards understanding the fundamental underlying principles at the nanoscale which will assist us to systematically plan for the future of useful applications.

2.1.1 Chronological highlights of events which led to the origin and development of nanotechnology

In order to understand the growth of nanotechnology, it is important to review the events that led to the development of this field. The following Table 2.1 highlights some of those interesting events with their significance.

Table 2.1 Chronological highlights of event led to the development of nanotechnology

Year	Significance
About 400 B.C	Greek philosopher Leucippus (430 B.C) and his pupil Democritus (460-371 B.C) proposed that an atom is a discrete, indestructible, fundamental particle of which all matter is composed.
1803	English chemist John Dalton (1766-1844) revives the concept of an atom being hard, round, indestructible, fundamental particles of which all matter is composed. Dalton's atomic theory remained dominant for about another century.
1897	English physicist J.J. Thomson (1856-1940) discovered that atoms are made up of two charged parts, negatively charged electrons and a positive component as yet unidentified.

1926	Austrian physicist Erwin Schrödinger (1887-1961) formulated the wave equation, a series of partial differential equations that describes the property of electrons in an atom by assuming that they exist as waves. From this period onwards, scientists started thinking about the atom less in term of concrete, physical structures and more in terms of mathematical equations to explain its behavior.
1927	German physicist Werner Heisenberg (1901-1976) derives the Uncertainty Principle. The position (x) and momentum (p) of a particle cannot be simultaneously measured with arbitrarily high precision. This uncertainty arises from the wave properties inherent to the quantum mechanical description of nature. This principle has significant implications for small particles such as the electron that even with perfect measuring instruments, experimental methods and technique, the more precisely the position is determined the less precisely the momentum is known in that instant and vice versa.
1927	Solvay Physics Conference, Brussels, Belgium. By the end of the 1920's several eminent scientists, like Schrödinger, Heisenberg, Max Planck, Louis de Broglie, Albert Einstein, Max Born, Robert Oppenheimer and Paul Dirac, contributed to the theory of quantum mechanics. The most important implication of quantum theory is that matter has different properties at the microscopic or nanoscopic level than it does at the macroscopic level. The laws of physics and chemistry that apply to large masses of matter do not apply to small particles like electrons.
1931	German physicist Ernst Ruska (1906-1988) invented the first electron microscope.
1936	German physicist Erwin Wilhelm Müller (1911-1977) invents the field emission microscope (FEM). FEM consists of a thin metal needle inside a vacuum tube. Electrons are emitted from the tip when a strong current is applied to the needle. The image of the atomic structure of the metal that the needle is made up of is displayed on the conducting fluorescent screen. (Müller, 1955).
1953	Seventeen years later, Erwin Müller invents the field ion microscope (FIM) a

	modification of FEM, where charged atoms (ions) are accelerated instead of electrons. Müller and his co-workers were the first to experimentally observe atoms (Müller, 1957).
1959	American theoretical physicist Richard Phillips Feynman (1918-1988) delivers his classic talk "There's Plenty of Room at the Bottom"- An invitation to enter a new field of physics, on December 29 th , 1959, at the annual meeting of the American Physical Society at California Institute of Technology (Caltech), Pasadena, California. He suggested a new form of technology that involves manipulation of individual atoms and molecules to manufacture new materials and structures. Some interesting quotes from his talk, "I would like to describe a field, in which little has been done, but in which an enormous amount can be done in principle". He had a great vision that he was able to think ahead of his time, "In the year 2000, when they look back at this age, they will wonder why it was not until the year 1960 that anybody began seriously to move in this direction". During the conclusion of the talk, Feynman offered two \$1,000 prize, one to the first person who could "take the information on the page of a book and put it on an area 1/25,000 smaller in linear scale in such manner that it can be read by an electron microscope" and one to the first person who could make "a rotating electric motor which can be controlled from the outside and, not counting the lead-in wires, is only 1/64 inch cube" (Feynman, 1960).
1960	American electrical engineer William Howard McLellan (1924-2011) collects his \$1,000 cheque from Feynman the very next year, by building a working electric motor that meets the challenge conditions (Archives - California Institute of Technology).
1965	Gordon Moore (1929 -), co-founder of Intel Corporation, predicted that the number of circuits on a silicon chip would double every year. Later in 1975, he changed his projection to a doubling every 18-24 months. This prediction is popularly called "Moore's Law".

-
- 1974 Japanese professor of Tokyo University of Sciences, Norio Taniguchi (1912 – 1999) coined the term “Nanotechnology” (Taniguchi, 1974).
- 1981 German physicist Gerd Binnig (1947 -) and Swiss physicist Heinrich Rohrer (1933-2013) invented the scanning tunneling microscope (STM). Tunneling is caused by electrons ability to flow across small dimensions of nanometer scale. STM is based on this property of electrons, where measurements and observations are made at the nanoscale. It has the potential to pick and move individual atoms and molecules to construct nanoscale objects (Binnig & Rohrer, 1987).
- 1981 The first scientific paper on molecular nanotechnology is published by K. Eric Drexler, a graduate student at MIT (Massachusetts Institute of Technology) in the September 1981 issue of PNAS (Proceedings of the National Academy of Sciences) (Drexler, 1981).
- 1985 After 25 years, the prize for Feynman's second challenge was awarded to Tom Newman, graduate student at Stanford University. Newman reduced the original size of the first page of Charles Dickens's "A Tale of Two Cities" to 1/25,000 of its size using a focused beam of electrons to carve the lettering.
- 1985 Buckminsterfullerene or buckyball, a new allotrope of carbon was discovered by Richard Smalley, Robert Curl and Harold Kroto. It consists of 60 carbon atoms arranged in nearly spherical structure consisting of hexagons and pentagons. Soon after this discovery scientists were able to combine buckyballs together to form long tubes known as nanotubes (Kroto et al., 1985).
- 1986 Gerd Binnig, Calvin Quate and Christoph Gerber invented the atomic force microscope (AFM). AFM is a modification of the scanning tunneling microscope. In AFM, the microscope tip comes in contact with the surface under analysis, instead of being suspended above the surface in case of STM. AFM has significant applications
-

in the field of nanotechnology (Binnig et al., 1986).

- 1986 The Nobel Prize in Physics was divided, one half awarded to Ernst Ruska "*for his fundamental work in electron optics, and for the design of the first electron microscope*", the other half jointly to Gerd Binnig and Heinrich Rohrer "*for their design of the scanning tunneling microscope*" (Nobel Prizes 1986).
- 1986+ The discovery of the AFM heralded a new age of nanotechnology by providing scientists with the ability to move atoms and molecules into interesting shapes and structures. From this year onwards, numerous discoveries and inventions in nanotechnology arose from different parts of the world. Every contribution to the field of nanotechnology is important, but to provide a comprehensive presentation of all the advancement in the field of nanotechnology would far exceed the scope of this review. Hereafter this review will highlight certain important events and about progressive transitions towards green nanotechnology.
- 1988 The term "Quantum dot" is coined by Mark Reed (Reed et al., 1988).
- 1989 IBM Fellow Don Eigler becomes the first person in history to move and control individual atoms. Eigler and his team from IBM Almaden Research Centre spell out "IBM" by moving xenon atoms on the surface of nickel. The letter 'I' was made up of 9 xenon atoms, letter 'B' made of 13 atoms and letter 'M' of 13 atoms, with a total of 35 individual xenon atoms. This proved the feasibility and manipulation of individual atoms using STM with precision. This signaled a quantum leap forward in experimental nanoscience with an unprecedented ability to manipulate individual atoms (IBM, 2009).
- 1990 The world's first ever peer-reviewed journal in nanoscale science and engineering called "Nanotechnology" is launched by the Institute of Physics, UK
-

-
- 1991 American chemist Paul Anastas from Environmental Protection Agency (EPA), USA coined the word "Green Chemistry". He along with co-author John Warner postulated the 12 Principles of Green Chemistry (Anastas & Warner, 2000).
- 1991 Japanese electron microscopist Sumio Iijima discovers the presence of carbon nanotubes in soot produced by vaporization of carbon in an electric arc. This discovery sparks interest in carbon nanostructures and their applications (Iijima, 1991).
- 1994 Synthesis of thiol based gold nanoparticles by Burst and coworkers from University of Liverpool, UK. The interest in gold nanoparticle synthesis revived, finding its application in various sectors. Since then the literature in the field of gold nanoparticles has increased rapidly. To provide an overview of the growth in 1995, 11 articles were published related to gold nanoparticles, in 2000 it increased to 178 documents, while many more were published in 2005 (1430 documents), 2010 (3912 documents) and in 2014 (5590 documents). The total amount of literature available related to gold nanoparticles accounts to 40443 documents and 1485 patent results (Data retrieved from Scopus database, April 5, 2015).
- 1995 Stephen U.S. Choi and Jeffrey A. Eastman, from Argonne National Laboratory, USA proposed that nanoparticles could enhance the thermal conductivity of fluids. This has led to a new field of research into "nanofluids" (Choi & Eastman, 1995).
- 1996 Nobel Prize in Chemistry was awarded jointly to Robert F. Curl Jr., Sir Harold W. Kroto and Richard E. Smalley *"for their discovery of fullerenes"* (Nobel Prizes 1996).
- 1996 The world's smallest abacus is created out of 10 atoms by scientists at IBM, another major milestone in engineering at the nanoscale. Though this and the previously cited similar IBM achievements do not have a practical objective, it demonstrates the feasibility of manipulating individual atoms in a predetermined way.
-

2000	National Nanotechnology Initiative (NNI) is a U.S. Government research and development initiative formed in 2000.
2000+	A number of universities announce plans for, establishment of, or creation of research centers on nanoscience and/or nanotechnology. Number of international governmental organizations show interest in nanotechnology and announce establishment of new research centers in this field. Some examples include the National Center for Nanoscience and Technology, Beijing, China; MINATEC, research center for micro and nanotechnology at Grenoble, France; National Applied Research Labs, Hsinchu, Taiwan etc.,
2001	National Institute for Nanotechnology (NINT), Alberta, Canada was formed.
2003	Twelve principles of green engineering were postulated (Abraham & Nguyen, 2003; Anastas & Zimmerman, 2003).
2004	Concepts of green nanoscience start developing (McKenzie & Hutchison, 2004).
2008	‘The road to green nanotechnology’ is published by Barbara Karn of the U.S. Environmental Protection Agency (EPA) (Karn, 2008).
2009	Green Center Canada, funded by the governments of Ontario and Canada, was formed.
2014	Special Issue highlighting "Nanotechnology in Foods: Science behind and future perspectives" in Trends in Food Science & Technology (December 2014)

The collection of highlights presented in Table 2.1 has been adapted from Newton (2002) and IBM Research: Major Nanoscale Breakthroughs, and modified to suit this chapter accordingly.

2.1.2 Terminology used in nanotechnology

Before embarking on the journey to understand nanotechnology, it will be useful to become familiar with the terminology used in this field. The American Society for Testing and Materials developed the first nanotechnology standards (ASTM E 2456-06) in 2006 (ASTM, 2006). International Organization for Standardization (ISO) technical committee referred to the ASTM E 2456-06 to prepare ISO/TS 80004-1:2010, a list of terms and definitions related to core terms in the field of nanotechnologies (ISO, 2010).

For a Draft International Standard prepared by the ISO technical committees to be approved as International Standard, at least 75% of the member bodies should vote for approval. When there is an urgent market requirement, the technical committee publishes an ISO/Technical Specification (ISO/TS), to facilitate communication among members of business, research, legal, government and educational communities.

Due to advancement in the applications of nanotechnology in various fields, there is a need to provide a level playing field for industry and researchers with essential tools of terminology and definitions for common understanding. The part of ISO/TS 80004-1 containing the terms and definitions is provided in Table 2.2.

Table 2.2 Terms and definitions related to nanotechnology (ISO/TS 80004-1: 2010)

S.No.	Terms	Definitions
1.	<i>Nanoscale</i>	Size range from approximately 1 nm to 100 nm (Note: The lower limit in this definition (approximately 1 nm) is introduced to avoid single and small groups of atoms from being designated as nano-objects or elements of nanostructures, which might be implied by the absence of a lower limit.)
2.	<i>Nanoscience</i>	Study, discovery and understanding of matter in the nanoscale, where size- and structure-dependent properties and phenomena, as distinct from those associated with individual atoms or molecules or with bulk materials, can emerge
3.	<i>Nanotechnology</i>	Application of scientific knowledge to manipulate and control matter in the nanoscale in order to make use of size- and structure-dependent properties and phenomena, as distinct from those associated with individual atoms or molecules or with bulk materials (Note: Manipulation and control includes material synthesis.)
4.	<i>Nanomaterial</i>	Material with any external dimension in the nanoscale or having internal structure or surface structure in the nanoscale

		(Note: This generic term is inclusive of nano-object and nanostructured material.)
5.	<i>Nano-object</i>	Material with one, two or three external dimensions in the nanoscale (Note: Generic term for all discrete nanoscale objects.)
6.	<i>Nanostructure</i>	Composition of inter-related constituent parts, in which one or more of those parts is a nanoscale region (Note: A region is defined by a boundary representing a discontinuity in properties.)
7.	<i>Nanostructured material</i>	Material having internal nanostructure or surface nanostructure (Note: This definition does not exclude the possibility for a nano-object to have internal structure or surface structure. If external dimension(s) are in the nanoscale, the term nano-object is recommended.)
8.	<i>Engineered nanomaterial</i>	Nanomaterial designed for a specific purpose or function
9.	<i>Manufactured nanomaterial</i>	Nanomaterial intentionally produced for commercial purposes to have specific properties or specific composition
10.	<i>Incidental nanomaterial</i>	Nanomaterial generated as an unintentional by-product of a process (Note: The process includes manufacturing, bio-

	technological or other processes.)
11.	<i>Nanomanufacturing</i> Intentional synthesis, generation or control of nanomaterials, or fabrication steps in the nanoscale, for commercial purposes
12.	<i>Nanomanufacturing process</i> Ensemble of activities to intentionally synthesize, generate or control nanomaterials, or fabrication steps in the nanoscale, for commercial purposes
13.	<i>Nanoscale phenomenon</i> Effect attributable to nano-objects or nanoscale regions
14.	<i>Nanoscale property</i> Characteristic of a nano-object or nanoscale region

ISO/TS are accepted for publication if it is approved by 2/3rd members of the committee, casting vote. After 3 years of its initial publication ISO/TS is reviewed to decide whether it will be confirmed for a further period of three years, or revised to become an International Standard, or withdrawn (ISO, 2010).

Technical Committee ISO/TC 229, *Nanotechnologies*, and Technical Committee IEC/TC 113, *Nanotechnology standardization for electrical and electronic products and systems* were involved in the drafting of ISO/ Technical Specification (ISO/TS 80004-1). This draft was circulated for voting by the national bodies of International Organization for Standardization (ISO) and International Electrotechnical Commission (IEC).

Nanotechnology being an emerging and rapidly developing field, likewise there is an emerging vocabulary with expansion of knowledge. The development of terminology is

proceeding at an intensive phase (ISO, 2010). There is a challenging necessity to continually reevaluate or revise the terms and definitions. This evolution would create a robust terminology for nanotechnology which will not only capture and effectively convey the information about size and shape but also the performance aspects for nanomaterials in future (ASTM, 2006; Hornyak et al., 2008; ISO, 2010).

2.2 Different forms of nanostructures

In general there are two types of approaches in nanotechnology to produce nanoparticles or nanostructures (Nouailhat, 2008):

- a. ***Top-down approach:*** Reducing the size of bulk materials to nanosize. It refers to making nanostructures by templating, with size reduction by physical methods.
- b. ***Bottom-up approach:*** Applies to building organic and inorganic materials into defined nanostructures, atom-by-atom or molecule-by-molecule, often by self-assembly.

Figure 2.1 represents the hierarchical framework for terminologies in nanotechnology provided by ISO/TS 80004. The terminology related to the figure below defines the geometric boundaries and size to express the measurable and fundamental aspects of nanomaterials (ISO, 2010).

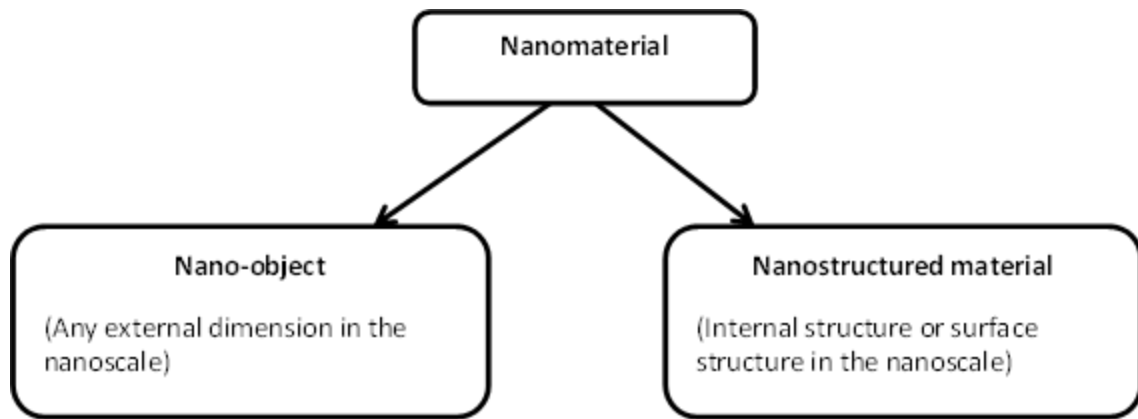


Figure 2.1 Nanomaterial Framework (ISO, 2010)

Nanomaterials can be classified more specifically as zero dimensional (0D) nanomaterials, wherein all the three dimensions are below 100 nm (eg. nanoparticles, quantum dots); one dimensional (1D) nanomaterials with two dimensions below 100 nm (eg. nanotubes, nanowires, nanorods); two dimensional (2D) nanomaterials containing one dimension below 100 nm (eg. nanofilms, nanoplates); three dimensional (3D) nanomaterials may not be of nanometer size but are constituted by the assembly of nanometer size elementary structures (eg. materials with nanocrystalline grains, cluster of engineered nanomaterials (ENMs), ENMs filling a host matrix or nanocomposites (Rossi et al., 2014). The different forms of nanomaterials along with their dimensional attributes are provided in Figure 2.2.

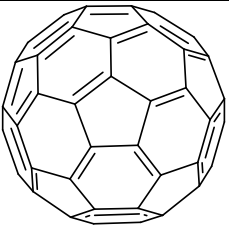
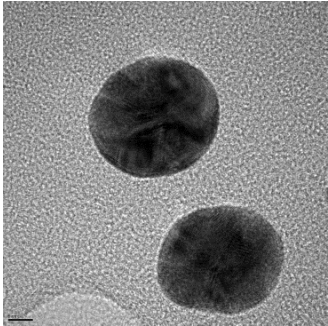
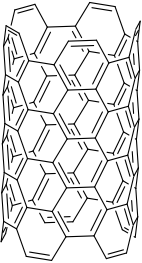
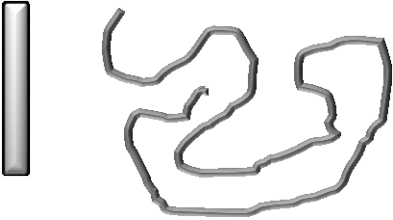
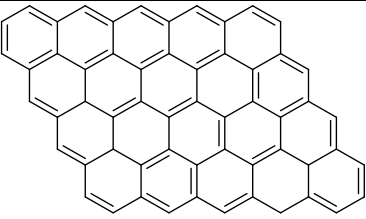
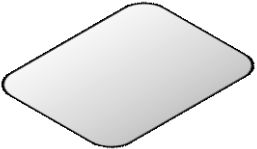
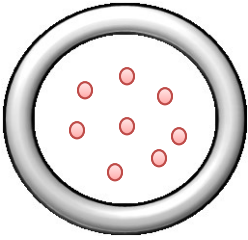
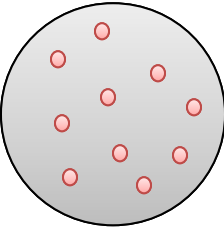
Dimension	Hollow	Solid
0D	 <p>Nanoclusters (C₆₀ Buckminsterfullerene)</p>	<p>Nanoparticles, Quantum dots</p> 
1D	 <p>Nanotube(Carbon nanotube)</p>	<p>Nanorods, Nanowires</p> 
2D	 <p>Graphene layer</p>	<p>Nanoplates,</p> 
3D	<p>Nanocapsules</p>  <p>● Bioactive compound</p>	<p>Nanospheres</p>  <p>● Polymer / lipid / carrier materials</p>

Figure 2.2 Different types of nanostructures and their dimensions

2.2.1 Quantum Dots

Quantum dots are one of the extensively researched nanoparticle systems. Their unique optical, photochemical, semiconductor, and catalytic properties are due to the quantum confinement. Quantum dots are nanoparticles having all three dimensions below 100 nm. ‘Quantum dots’ is a term used to refer to semiconductor nanoparticles, while ‘nanocrystal’ can be any inorganic entity that has a crystalline arrangement of atoms. Quantum size effects are manifested in a quantum dot when their electrons are confined to a point in space. They have no degrees of freedom in any dimension and the electrons are said to be localised at a point (Pradeep, 2007; Reed et al., 1988).

2.2.2 Buckminsterfullerene (or Fullerene)

Buckminsterfullerene (C_{60}) or buckyballs is an allotrope of carbon (distinctly different from graphite and diamond). Kroto and collaborators (1985), during an experiment aimed to understand the mechanism of carbon molecules formed in interstellar spaces, hit upon an unusual and extraordinary discovery in the history of chemistry for which they were awarded the Nobel Prize.

In their experiment, laser irradiation of graphite produced a remarkably stable cluster consisting of 60 carbon atoms. C_{60} molecule is a truncated icosahedron, a polygon with 60 vertices and 32 faces, 12 of which are pentagonal and 20 hexagonal. Initially clusters of C_n (with $n > 40$ atoms and even number) were found, later fullerenes with larger number of carbon atoms C_{70} , C_{76} , C_{80} , C_{240} , etc., were discovered (Kroto et al., 1985; Mansoori, 2005).

2.2.3 Carbon nanotubes

Carbon nanotubes were discovered by Sumio Iijima (1991), an electron microscopist while studying carbon graphite deposition in an electric arc evaporation reactor during the synthesis of fullerene. He reported the presence of helical microtubules of graphitic carbon rolled up to form a hollow tube, now familiarly called ‘nanotubes’.

A single sheet of graphite is called graphene, carbon nanotubes are formed by curling a graphene sheet. The nanotube diameter can range from one to several nanometers and can be single walled nanotube (SWNT) or multi walled nanotube (MWNT). Initially nanotubes were used in microelectronic circuitry and in microscopy, but now they are used in a wide range of applications (Iijima, 1991; Muralidharan & Subramania, 2008).

2.2.4 Polymer nanoparticles

Polymeric nanoparticles are researched widely as carriers in the pharmaceutical sector for controlled/sustained release in drug delivery systems. Polymeric nanoparticles can be either nanospheres or nanocapsules. Two main strategies used for preparation of polymeric nanoparticles are ‘top-down’ approach and ‘bottom-up’ approach. In the top-down approach a dispersion of preformed polymers produces polymeric nanoparticles while in the bottom-up approach polymerization of monomers leads to the formation of polymeric nanoparticles.

Different methods for producing polymeric nanoparticles are illustrated in Figure 2.3. This figure has been adapted from (Ezhilarasi et al., 2013; Rao & Geckeler, 2011; Sabliov & Astete, 2008) and modified accordingly.

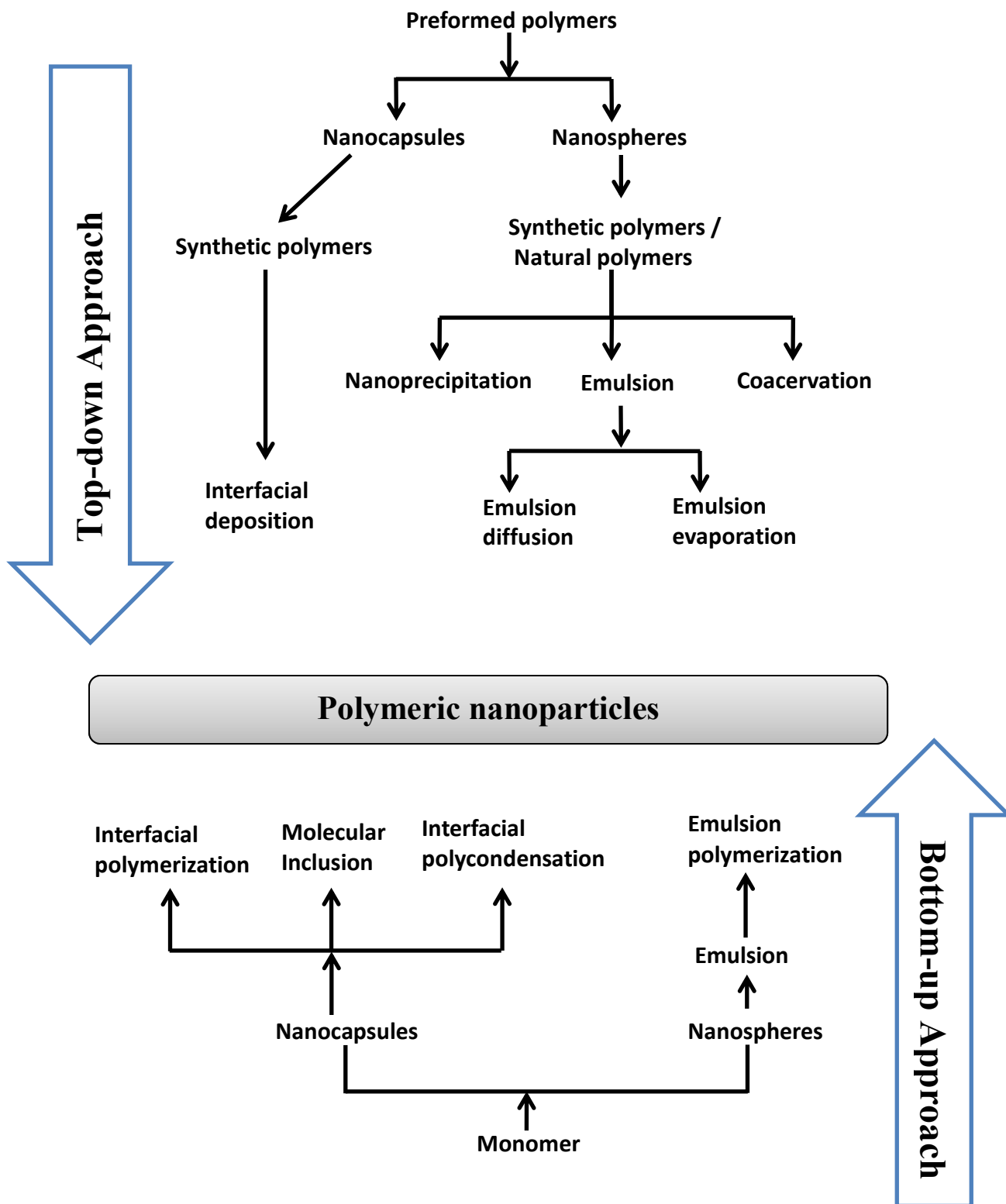


Figure 2.3 Top-down and Bottom-up approach for synthesising polymeric nanoparticles

The choice of selecting an appropriate method for producing polymeric nanoparticles depends on various factors such as, particle size, type of solvents and polymers used in the synthesis, area of application, etc. The ‘top-down’ method for producing polymeric nanoparticles includes solvent emulsification–evaporation (Emulsion evaporation method) (Bilati et al., 2005; Sabliov & Astete, 2008), solvent emulsification - diffusion (Emulsion diffusion method) (Cegnar et al., 2004; Csaba et al., 2005), coacervation (Jincheng et al., 2010; Wang et al., 2008) and nanoprecipitation (Solvent displacement method) (Galindo-Rodríguez et al., 2005).

Emulsion polymerization (Radwan & Aboul-Enein, 2002; Reis et al., 2006; Vauthier et al., 2003), interfacial polymerization (Watnasirichaikul et al., 2000), interfacial polycondensation and molecular inclusion use monomers as their starting point and come under the ‘bottom-up’ process to produce polymeric nanoparticles.

Both top-down and bottom-up methods use synthetic polymers / monomer like poly (D, L-lactide-co-glycolide), poly (ethylcyanoacrylate), poly (butylcyanoacrylate), poly (isobutylcyanoacrylate), poly (isohexylcyanoacrylate), stabilizers like poly (vinyl alcohol), didecyl dimethyl ammonium bromide and organic solvents like dichloromethane and ethyl acetate, benzyl alcohol, cyclohexane, acetonitrile, acetone, etc., that are toxic. Recently the scientific community is trying to find alternatives for synthetic polymers by using natural polymers and synthesis methods with less toxic solvents.

This review does not provide comprehensive information about all the synthesis protocols and methods used in preparing polymeric nanoparticles. However, some polymeric nanoparticles synthesis methods will be highlighted in Chapter VI. There are excellent reviews available in the literature that shed light on the different methods of polymeric nanoparticles

synthesis (Fathi et al., 2014; Liu et al., 2008; Mishra et al., 2010; Reis et al., 2006; Sabliov & Astete, 2008; Vrignaud et al., 2011).

2.2.5 Metallic nanoparticles

Nanoparticles of noble metals have received considerable attention from researchers due to their characteristic color and unique properties. Metal nanoparticles are made up of number of atoms or molecules bonded together and are intermediate in size between individual atoms and bulk materials. In the nanosize domain, physical, chemical, optical and electronic properties of the materials substantially differ from their constituent atoms and their bulk counterparts. These properties not only depend upon size but also their morphology described by their shape, structure and crystallinity. Just by varying their size or morphology new properties can be generated (Sau & Rogach, 2012).

Metal nanoparticles are formed when their metal salts are reduced to give zero-valent metal atoms. These metal atoms are formed in their embryonic stage of nucleation, they collide with other metal ions/atoms in the solution to form stable metal nuclei. The diameter of the metallic nanoparticle range from 1-100 nm, this depends on various factors like the redox potential between the metal salts and the reducing agent, strength of the metal-metal bonds, nature of solvent, type of stabilizing agent used, synthesis conditions, temperature etc. Some of the commonly synthesized metallic nanoparticles are of gold (Au), iron (Fe), silver (Ag), copper (Cu), cadmium (Cd), platinum (Pt), zinc (Zn) and palladium (Pd) (White et al., 2009). The Table 2.3 provides some information about the synthesis conditions of metallic nanoparticles of iron, silver and gold, adapted and modified from Das et al. (2008).

Table 2.3 Metallic nanoparticles and their conditions for synthesis

Metal NP	Starting Material	Reducing Agent	Medium	Stabilizers	Condition	Particle Diameter (nm)	Application	Reference
Fe	Fe(NO ₃) ₃ ·9H ₂ O	Hydrogen	Gas	No	160-300°C	300-500	Electronics, catalysis	(Bermejo et al., 1997)
	FeCl ₂	Sodium borohydride (NaBH ₄)	Triphase (xylene/water/pyridine)	TOPO (tri- <i>n</i> -octylphosphine oxide)	RT	3	Electro-catalysis	(Guo et al., 2001)
	Fe(CO) ₅	High temperature	Oleic acid	Oleic acid	300°C	11-20	Electronics, drug delivery	(Hyeon et al., 2001)
Ag	Silver bis(2-ethyl-hexyl) sulfo-succinate	Hydrazine	Water	Dodecane thiol	RT	3-4	Catalysis, optical and electronic devices	(Taleb et al., 1997)
	Ag (NO ₃)	Trisodium citrate	Water	Trisodium citrate	Boiling	40-60	Electronics	(Kamat et al., 1998)
	Ag (NO ₃)	NaBH ₄	Biphase (toluene/water)	1-Dodecane thiol	RT	5-8	Catalysis, optical and electronic devices	(Korgel et al., 1998)
	Ag (NO ₃)	Amine	Ethanol	Amine	60°C	1-2	Catalysis	(Frattini et al., 2005)
	Ag (NO ₃)	NaBH ₄ /ascorbic acid	Water	CTAB (cetyltrimethyl ammonium bromide)	RT	42 ± 3	Catalysis, optical and electronic devices	(Jana et al., 2001)

Au	HAuCl ₄	Sodium citrate	Water	Citrate ³⁻	RT	12-60	Sols	(Turkevich et al., 1951) (Frens, 1973) (De Mey & Moeremans, 1986)
	HAuCl ₄	Ethyl alcohol	Water	-	Ultrasound	10	Biology	(Baigent & Müller, 1980)
	HAuCl ₄	P (white) in ether	Water	-	Boiling	3-5	Biology	(Roth, 1982) (Faulk & Taylor, 1971)
	HAuCl ₄	Sodium citrate / tannic acid	Water	Citrate ³⁻ , tannic acid	Heating	3-17	Biology	(Mühlpfordt, 1982)
	HAuCl ₄	NaBH ₄	Water	Citrate ³⁻	4°C	4	Sols	(Birrell et al., 1987)
	HAuCl ₄	NaBH ₄	Biphase (toluene / water)	Thiol	RT	3	Powder, solutions	(Brust et al., 1994)
	HAuCl ₄	Sodium citrate / NaBH ₄	Water	Citrate ³⁻	0°C	4	Sensors	(Obare et al., 2002)

Where, RT – room temperature; NaBH₄ – Sodium borohydride;

TOPO – tri-*n*-octylphosphine oxide;

CTAB – cetyltrimethylammonium – bromide

2.3 Synthesis of gold nanoparticles (AuNP)

Most synthesis of gold nanoparticles is either by physical or chemical methods, which follow a top-down approach and bottom-up approach, respectively.

2.3.1 Bottom-up approach

Faraday was the first to report that metal particles displayed an unusual ruby-red color, as displayed by gold of very minute dimension. Faraday called the solution the ‘divided state of gold’. He used a two-phase preparation method by reducing aqueous solution of sodium tetrachloroaurate ($\text{Na}[\text{AuCl}_4]$) gold salts with a solution of phosphorus in carbon disulfide (Faraday, 1857). Faraday’s observations were the basis for the birth of colloidal science, where the term colloid was coined later. The size of colloidal gold particles fell below the resolution limit of the optical microscopes, hence they were impossible to be observed using optical microscopes. The importance of Faraday’s observations on metals colloids was realised nearly 150 years later. High resolution electron microscopic study of Faraday’s solution revealed the presence of gold at the nanoscale (Brust & Kiely, 2002; Edwards & Thomas, 2007).

With the development of the electron microscope, Turkevich was able to study the nucleation and growth of gold colloids in 1951. Electron microscopic investigation of various gold colloidal preparations was performed. They prepared a standard sodium citrate gold solution. Chlorauric acid solution (95 ml) was heated to 100°C and 5 ml of 1% sodium citrate solution was added to boiling solution with good mechanical stirring. Deep wine red colour gold colloidal solution was formed. The results from the electron microscopic study reported spherical particles and this method is considered as a standard method due to its high reproducibility (Turkevich et al., 1951).

Frens (1973) modified Turkevich's citrate reduction method to produce monodispersed gold suspensions with different sizes by varying the concentrations of sodium citrate. Gold particles ranging from 16 nm to 150 nm were synthesized.

Brust and colleagues (1994) reported a two-phase system containing water – toluene to reduce AuCl_4^- by sodium borohydride. Hydrogen tetrachloroaurate (AuCl_4^-) in aqueous solution was transferred to toluene using tetraoctylammonium bromide as phase-transfer agent and the solution was stirred vigorously. Dodecanethiol ($\text{C}_{12}\text{H}_{25}\text{SH}$) was added to the organic phase and aqueous solution of sodium borohydride was slowly added with vigorous stirring for 3 hours. The organic phase was separated and evaporated in a rotary evaporator. They reported the gold nanoparticles produced by their method to have applications in catalysis, sensors and molecular electronics (Brust et al., 1994).

The period after Brust et al. (1994) can be called the real renaissance of gold nanoparticles, as interest in both experimental and theoretical studies of optical properties of gold nanoparticles started growing. Functionalization of gold nanoparticles led to a wide range of applications in the field of sensors and molecular electronics. Another main reason for the tremendous growth in nanoparticle research is increase in the accessibility of electron microscopes.

2.3.2 Top-down approach

Laser induced size reduction is a powerful tool for size reduction and altering the structure of gold nanoparticles. Laser ablation/irradiation of solid metal targets in a liquid medium can be used to produce nanoparticles. After the nanoparticle synthesis using laser ablation methods, further post processing using laser irradiation can be applied to modify the size, shape and composition of the nanostructure (Zeng et al., 2012).

Gold nanoparticles can be prepared using laser ablation, with a metal plate of gold (>99.99%) placed in aqueous solution of sodium dodecyl sulfate (SDS). The gold nanoparticles obtained in SDS solution are subjected to laser fragmentation using a laser operating at 10 Hz (Mafuné et al., 2002).

Ultrasound is used in the production of novel nanomaterials. The acoustic cavitation leading to formation, growth and instantaneous collapse of bubbles is used in the modification of the shape of nanomaterials during ultrasonic irradiation. When a liquid is sonicated using high intensity ultrasound, high energy chemical reactions occur. A template of microsphere of silica present in a solution containing free metal atoms produced during ultrasonic irradiation, leads to deposition of atoms onto the template to form structured material (Baigent & Müller, 1980; Xu et al., 2013). Monodispersed gold nanoparticles can be produced using UV irradiation technique. HAuCl_4 and triton X-100, a nonionic surfactant having a hydrophilic polyethylene oxide chain was UV irradiated for 60 min to form gold nanoparticles of 15-20 nm (Mallick et al., 2001).

The physical methods require high temperature, pressure and instrumentation that are expensive and demands enormous consumption of energy. Developing methods for nanoparticle synthesis at room temperature with less expensive resources, involving non-toxic materials, with high yield of nanoparticles would be an ideal method that every researcher in nanoparticle synthesis is aiming to attain.

2.4 Transition towards green nanotechnology

Along with advancements in the field of nanotechnology in the 1990's there was another concept known as "Green chemistry" that was evolving. The Green Chemistry Institute was incorporated in 1997 and became a part of the American Chemical Society (ACS) in 2001. Green Chemistry involves the design of chemical products and processes that reduce or eliminate the use and generation of hazardous substances (Anastas & Warner, 2000). Green engineering is the development and commercialization of industrial processes that are economically feasible and reduce the risk to human health and the environment (ACS Green Chemistry Institute). The principles of Green Chemistry and Green Engineering are stated below.

2.4.1 Green Chemistry

The 12 Principles of Green Chemistry developed by Paul Anastas and John Warner, Environmental Protection Agency (EPA), USA, are provided in Table 2.4. This table provides a roadmap for chemists trying to implement green chemistry.

Table 2.4 Twelve Principles of Green Chemistry (Anastas & Warner, 2000)

S.No.	Principles of Green Chemistry
1.	Prevention It is better to prevent waste than to treat or clean up waste after it has been created.
2.	Atom Economy Synthetic methods should be designed to maximize the incorporation of all materials used in the process into the final product.
3.	Less Hazardous Chemical Syntheses Wherever practicable, synthetic methods should be designed to use and generate

substances that possess little or no toxicity to human health and the environment.

4. **Designing Safer Chemicals**

Chemical products should be designed to affect their desired function while minimizing their toxicity.

5. **Safer Solvents and Auxiliaries**

The use of auxiliary substances (e.g., solvents, separation agents, etc.) should be made unnecessary wherever possible and innocuous when used.

6. **Design for Energy Efficiency**

Energy requirements of chemical processes should be recognized for their environmental and economic impacts and should be minimized. If possible, synthetic methods should be conducted at ambient temperature and pressure.

7. **Use of Renewable Feedstocks**

A raw material or feedstock should be renewable rather than depleting whenever technically and economically practicable.

8. **Reduce Derivatives**

Unnecessary derivatization (use of blocking groups, protection/ deprotection, temporary modification of physical/chemical processes) should be minimized or avoided if possible, because such steps require additional reagents and can generate waste.

9. **Catalysis**

Catalytic reagents (as selective as possible) are superior to stoichiometric reagents.

10. **Design for Degradation**

Chemical products should be designed so that at the end of their function they

break down into innocuous degradation products and do not persist in the environment.

11. **Real-time analysis for Pollution Prevention**

Analytical methodologies need to be further developed to allow for real-time, in-process monitoring and control prior to the formation of hazardous substances.

12. **Inherently Safer Chemistry for Accident Prevention**

Substances and the form of a substance used in a chemical process should be chosen to minimize the potential for chemical accidents, including releases, explosions, and fires.

2.4.2 Green Engineering

The 9 Principles of Green Engineering, were developed during the Conference “Green Engineering: Defining the Principles” held at Sandestin, Florida during May, 2003. Scientists collectively agreed to compile a set of nine principles now known as “The Sandestin Declaration” which is stated below (Abraham & Nguyen, 2003):

1. Engineer processes and products holistically, use systems analysis, and integrate environmental impact assessment tools.
2. Conserve and improve natural ecosystems while protecting human health and well-being.
3. Use life-cycle thinking in all engineering activities.
4. Ensure that all material and energy inputs and outputs are as inherently safe and benign as possible.
5. Minimize depletion of natural resources.

6. Strive to prevent waste.
7. Develop and apply engineering solutions, while being cognizant of local geography, aspirations, and cultures.
8. Create engineering solutions beyond current or dominant technologies; improve, innovate, and invent (technologies) to achieve sustainability.
9. Actively engage communities and stakeholders in development of engineering solutions

2.4.3 Green Nanotechnology

The parallel development of nanotechnology with green chemistry and potential synergism between the two fields can lead to sustainable methods with reduced environmental impacts, and improved conservation and protection of resources and human health (McKenzie & Hutchison, 2004). With developments in nanotechnology, concerns of uncertainty and risk regarding environment, health and safety (EHS) must not be ignored. Thus the concept of “green nanotechnology” comes to the rescue. The two main goals of green nanotechnology are,

- Producing nanomaterials without affecting the environment or human health
- Producing nanomaterials that provide solutions to environmental problem

From a green engineering standpoint, the manufacture and design of nanoparticles involving the principles of green engineering will have a positive impact on the environment (Yates & Dionysiou, 2006). Therefore, efforts aimed at developing reasonable and meaningful protocols for generating nanomaterials is one of the main focus areas of green nanotechnology based research (Wong & Karn, 2012).

Green nanotechnology, by integrating the principles of green chemistry and green engineering, can produce eco-friendly, safe, metal nanoparticles that do not use toxic chemicals

in the synthesis protocol (Castro et al., 2011; Philip, 2009). This can be a viable substitute to the conventional physical and chemical methods of synthesizing nanoparticles (Karn, 2008; Schmidt, 2007; Schwarz, 2009).

2.5 Green synthesis of gold nanoparticles from plant extracts

With the initiation of green nanotechnology for nanoparticle synthesis, interest has grown to synthesize metallic nanoparticles from plant extracts (Betts, 2005). This section will highlight some of the plant materials used for the synthesis of gold nanoparticles. It has been reported that plant extracts / parts of plant such as rose (Ghoreishi et al., 2011), tea (Nune et al., 2009), honey (Philip, 2009), lemongrass leaf (Shankar et al., 2005), and tansy fruit (Dubey et al., 2010) have been used for the synthesis of gold nanoparticles. This area of gold nanoparticle synthesis using plant materials is under intense exploration (Nadagouda et al., 2009). Begum et al. (2009) reported that tea flavonoids were responsible for reduction of gold nanoparticles. They studied the biogenic synthesis of gold nanoparticles using three extracts namely black tea leaf broth, ethyl acetate extract and dichloromethane extract.

The first report using agricultural waste material for gold nanoparticle synthesis was reported in 2010. Banana peel extract precipitated in acetone and air-dried to form peel powder was used to reduce chloroauric acid. This study demonstrated the green route for synthesis of gold nanoparticles using banana peel (Bankar et al., 2010). Palm oil mill effluent was dried and was used for gold nanoparticle synthesis without adding an external surfactant, capping agent or template (Gan et al., 2012). Ahmad et al. (2012) reported the use of pomegranate peel extract for synthesis of gold nanoparticles. Recently, mango peel extract has been reported to reduce gold nanoparticles. This study also reported that the green synthesized gold nanoparticles using

mango peel extract showed no biological cytotoxicity on African green monkey kidney normal cells (CV-1) and normal human fetal lung fibroblast cells (WI-38) (Yang et al., 2014).

The plant materials used for green synthesis of AuNP are mostly in dried and pulverised form while very few have reported the use of fresh plant parts. The use of medicinal herbs and plant parts for green synthesis of gold nanoparticles are under intense investigation. But there are very few reports related to agricultural waste. To date, only four documents are available stating the use of agricultural waste materials for synthesis of gold nanoparticles (Ahmad et al. 2012; Bankar et al., 2010; Gan et al., 2012; Yang et al., 2014). Hence this proposed PhD study would open the possibility for exploring the use of agricultural waste materials in the production of high value nanomaterials.

2.6 Characterization of nanoparticles

In the vast array of analytical techniques provided in Table 2.5 (Tiede et al., 2008), three categories of detection and characterization are considered to be important for nanoparticle analysis. They are namely electron microscopy imaging, spectroscopic techniques and separation (Bouwmeester et al., 2014). Electron microscopy techniques are important in analysing size, shape and surface morphology of nanoparticles. When electron microscopes are coupled with X-ray spectroscopy (EDX), it can be used for elemental analysis. The commonly used electron microscopy techniques are transmission electron microscopy (TEM), scanning electron microscopy (SEM) and atomic force microscopy (AFM).

Single particle- Inductively coupled plasma mass spectroscopy (SP-ICPMS) has been developed for nanoparticle analysis in recent years. The individual nanoparticles are atomised and ionised in the ICP plasma and the resulting flume is detected by MS (Gray et al., 2012). The

advantage of SP-ICPMS is that it provides the size distribution in ng/L. UV- Vis spectroscopic methods are considered for determination of surface plasmon resonance of metallic nanoparticles (Salvati et al., 2005).

While there exists many techniques to characterise metallic nanoparticles, there is a limitation in techniques available for polymeric nanoparticles. In case of hybrids of organic-inorganic nanoparticles, new characterization methods have to be developed. Currently there is no single analytical method that can be used to detect all types of nanoparticles of various sizes, in different matrices (Bouwmeester et al., 2014). Hence new techniques and methods should be developed with specifics according to the sample.

Table 2.5 Characterisation methods used in nanoparticle analysis (Tiede et al., 2008).

Nanoparticle properties	Microscopy techniques	Chromatography techniques	Centrifugation/ filtration techniques	Spectroscopic techniques	Other techniques
Aggregation	STEM, TEM, SEM, AFM, STM			XRD, SANS	Zeta potential
Chemical composition	AEM, CFM			NMR, XPS, AES, MS	
Mass concentration	AEM, CFM				Gravimetry, thermal analysis
Particle number concentration					Particle counter, CPC
Shape	STEM, TEM, SEM, AFM, STM		UC		
Size	STEM, TEM, SEM, AFM, STM				
Size distribution	STEM, TEM, SEM,	FFF, HDC, SEC	UC, CFUF	SP-ICPMS	

	AFM, STM			
Dissolution		Dialysis, CFUF		Voltammetry, diffusive gradients in thin films
Speciation		SEC-ICP-MS	XAS, XRD	Titration
Structure	STEM, TEM, SEM, AFM, STM		XRD, SANS	
Surface charge		CE		Zeta potential
Surface chemistry	AEM, CFM		XPS, SERS	

(Note: The abbreviations for the instrumentations presented in this table are provided in the abbreviations section of this thesis)

2.7 Summary

This review provides information about the chronological development of nanotechnology, terminologies and current gaps in international standards for nanotechnology, different types of nanomaterials, methods of nanoparticles synthesis, transition towards green nanotechnology, green synthesis of gold nanoparticles and characterization techniques for nanoparticle analysis. The concepts of green chemistry and green engineering along with green nanotechnology are expected to grow, influencing scientists and engineers worldwide.

CONNECTING STATEMENT TO CHAPTER III

As mentioned in the review of literature, there is currently a transition towards green nanotechnology, and **Chapter III** describes the green synthesis of gold nanoparticles from grapes and by-products. The experiments and interpretation of results were performed by Ms. Krishnaswamy with the guidance of Dr. Orsat, while Dr. Hojatollah Vali (Facility for Electron Microscopy Research, McGill University) helped with TEM imaging. This work was published in the *Journal of Food Engineering* in 2014.

Krishnaswamy K, Vali H, Orsat V. Value-adding to grape waste: Green synthesis of gold nanoparticles. **Journal of Food Engineering**. 2014, 142, 210-220.

A part of this chapter was presented in the following conference

1. K. Krishnaswamy* & V. Orsat. Green synthesis of gold nanoparticles (AuNP) from grape waste: value addition to agricultural waste. (CSC 2013) 96th Canadian Chemistry Conference & Exhibition, May 26 -30, 2013, Quebec, QC, CA (**Best Oral Presentation Award**)
2. K. Krishnaswamy*, V. Orsat and H. Vali. Biogenic precipitation of nano-gold particles using plant extracts. *Conférence NanoQuébec 2012. Hyatt Regency, Montréal. (Poster presentation)*

CHAPTER III

VALUE-ADDING TO GRAPE WASTE: GREEN SYNTHESIS OF GOLD NANOPARTICLES

3.1 Abstract

In this study we report the potential use of food waste such as grape skin, stalk and seeds obtained after grape processing to produce gold nanoparticles (AuNP). The gold nanoparticles were synthesized according to the rules of green chemistry and integrating the goals of green nanotechnology. Results from the present work establish that AuNP were synthesized in a single step method using water at room temperature. The growth of AuNP was instantaneous within 5 minutes and was found to be highly stabilised. Thus produced AuNP were characterised using UV-Vis spectrophotometer, high resolution transmission electron microscope (HR-TEM) and energy-dispersive X-ray spectroscopy (EDX). The mean particle size for the green synthesized gold nanoparticles from grape waste ranged from 20 -25 nm. Furthermore, a central composite design was used to determine the influences of the concentrations of catechin (0.5, 1, 1.5 mM) and HAuCl_4 (0.5, 1, 1.5 mM), and of temperature (10, 25, 45 °C) on the green synthesis of AuNP. Their interactions were determined by response surface methodology (RSM).

Keywords: Grapes; High resolution transmission electron microscope (HR-TEM); Response surface method; Catechin; Gold nanoparticles.

3.2 Introduction

Synthesizing novel nanoparticles based on the concept of green nanotechnology is gaining momentum. Researchers in nanotechnology are looking for greener alternatives to synthesis nanoparticles. Green nanotechnology integrates the principles of green chemistry and green engineering to produce eco-friendly, safe, nanoparticles that do not use toxic chemicals in their synthesis protocol (Castro et al., 2011; McKenzie & Hutchison, 2004; Philip, 2009). The progressive development of ‘nanotechnology’ towards ‘green nanotechnology’ is shown in Figure 3.1.

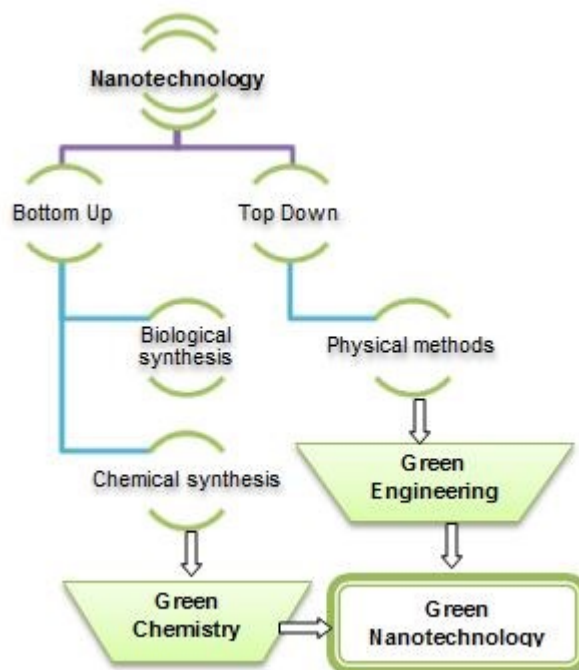


Figure 3.1 Flow chart showing the progressive transition towards green nanotechnology

The production of nanoparticles of noble metals, such as gold nanoparticles (AuNP), is of great interest due to their unique characteristics. Manipulations of their

size and shape produces unique properties which have potential applications in semiconductors (Schmid & Corain, 2003) and spectroscopy (Mulvaney, 1996), and in biomedical applications such as drug delivery (Mahal et al., 2013; Paciotti et al., 2004; Singh et al., 2013), tissue/tumor imaging (Jain et al., 2006) and cancer therapy (Peng et al., 2009). Current chemical and physical methods for the synthesis of AuNP use hazardous compounds such as hydrazine, sodium borohydride, and dimethyl formamide (DMF) as reducing agents, and may also require the use of expensive instruments. These methods produce AuNP efficiently, however downstream processing to separate them from the toxic substances is expensive and time consuming. Presence of even a small trace of hazardous compounds makes these AuNP incompatible for biomedical applications.

On the other hand, waste management represents an important challenge in the agri-food based industries. It demands an integrated approach in the context of recycling, reuse and recovery (Pfaltzgraff et al., 2013). Grape (*Vitis vinifera L.*) is one of the world's largest fruit crop with a global production of 68 million tonnes (2009) of which, 38 million tonnes are processed. Annually around to 2.5 million tonnes of grape waste are generated (FAOSTAT, 2012). This huge challenge in the management of grape waste must be addressed.

Since 2000, the synthesis of nanoparticles using bacteria (Kalishwaralal et al., 2009), fungus (Du et al., 2011; Gade et al., 2010) and plant extracts such as rose (Ghoreishi et al., 2011), tea (Nune et al., 2009), honey (Philip, 2009), lemongrass leaf (Shankar et al., 2005), tansy fruit (Dubey et al., 2010) etc. for nanoparticle synthesis are under intense exploration (Nadagouda et al., 2009). This can be a viable substitute to the

conventional physico-chemical methods of synthesizing nanoparticles (Karn, 2008; Schmidt, 2007; Schwarz, 2009).

In the present study, the use of agricultural wastes materials such as grape seed, grape skin and grape stalk was investigated individually for the production of gold nanoparticles. Earlier studies have used grape wine and grape pomace extract to reduce gold nanoparticles using 50 W of microwave power (Baruwati & Varma, 2009). But in this study we have isolated individual components of grape pomace like the grape seed, skin and stalk and have found that individual components have the potential to form gold nanoparticles without much agglomeration in water at room temperature, following the principles of green engineering. Recent studies have shown remarkable *in-vitro* stability and affinity of gold nanoparticles synthesized from grapes towards human breast cancer cells (HBL-100) biocompatibility (Amarnath et al., 2011). Grapes and grape wastes like seed, skin and stalk contain proanthocyanidins. Proanthocyanidins are a rich source of natural antioxidants and have many health benefits such as protection against cardiovascular disease and radiation (Castillo et al., 2000), prevention of cataract (Yamakoshi et al., 2002), anti-hyperglycemic effects (Pinent et al., 2004), protection against oxidative DNA damage in mouse brain cells (Guo et al., 2007), and neuroprotective effects by crossing the blood-brain barrier (Prasain et al., 2009).

In this paper we report a simple, cost-effective procedure to produce gold nanoparticles that are stable with extended shelf life. Recent reports have shown an increased use of water as the solvent in chemical reactions instead of organic solvents (Li & Chen, 2006). The water dispersible nature of gold nanoparticles from grape byproducts

along with their inherent health benefits can revolutionize the impact of nanotechnology on drug/ nutraceutical delivery.

Flavan -3-ols are the most complex subclass of flavonoids ranging from the simple monomer catechin to oligomeric and polymeric proanthocyanidins (Crozier et al., 2008). The plant matrix (grape seed, skin and stalk) used was too complex to identify individual compounds responsible for the bio-reduction, hence catechin, a simple monomeric unit of proanthocyanidins, a powerful polyphenolic compound present in grapes was used as a reference compound to study its influence on the green synthesis of AuNP. The use of catechin would thus be a first step to help us understand the mechanism of formation of gold nanoparticles from grape products.

In this study, the response surface method (RSM) was used to assess the relationship between green synthesized AuNP and independent variables such as the concentration of catechin, the concentration of hydrogen tetrachloroaurate (III), and process temperature. Central composite design, the most widely used approach of RSM (Myers et al., 2009), was employed to determine the effect of our operating variables since it is highly efficient, providing sufficient information on the effect of process variables for process optimization with a reduced number of total experimental runs.

3.3 Materials and Methods

3.3.1 Sample preparation –Synthesis of AuNP using grapes seed, skin and stalk

The seed, skin, and stalk of grapes were freshly collected and washed with deionised water. Grape skins and stalks were cut finely while whole grape seeds were used. For each biomaterial, three grams were mixed with 50 ml deionised water and were heated at 60°C for 2 min (Figure 3.2). Heating leads to the rupture of plant cells and aids in the release of intra-cellular materials into the solution. The clear supernatant was cooled to room temperature and filtered using 11µm Whatman filter paper (Whatman filter paper, Grade 1). Hydrogen tetrachloroaurate ($\text{HAuCl}_4 \cdot 3\text{H}_2\text{O}$) was obtained from Sigma-Aldrich Chemicals Co., (St. Louis, MO), and 1 mM HAuCl_4 solution was prepared using deionised water. Five ml of each plant extract was added to 12 ml of HAuCl_4 solution and the total reaction volume was made up to 30 ml by addition of deionised water.

3.3.2 Synthesis of AuNP using catechin

(+) Catechin hydrate was obtained from Sigma Aldrich Chemicals Co., (St. Louis, MO). The effects of three different concentrations (0.5, 1, 1.5 mM) of catechin on the synthesis of AuNP at three different concentrations (0.5, 1, 1.5 mM) of HAuCl_4 at 10°C, 25°C, and 40 °C was investigated.

3.3.3 Apparatus and measurements

The maximum surface plasmon resonance (SPR) was measured by wave scan from 400 to 800 nm range using a UV-Vis spectrophotometer (Ultrospec 2100 pro, Biochrom Ltd., Cambridge, UK). The time of addition of plant extract or catechin solution to the

HAuCl₄ solution was considered to be the start of the reaction. The colour of the HAuCl₄ changed from light yellow to pink (Figure 3.2), which indicated the formation of AuNP.

A drop of the sample solution was applied to a carbon coated TEM grid. The sample was allowed to stand for 1 min on the TEM grid and excess solution was carefully removed using Whatman grade 1 filter paper. This allows the formation a thin film of sample on the TEM grid. The sample was left at room temperature until a dried film was obtained. Transmission electron microscopy (TEM) analyses were performed using a FEI Tecnai 12 TEM equipped with an AMT XR-80C CCD Camera System (FEI Company, Oregon, USA) operated at 120 kV. Images were analyzed with TEM image analysis platform and the mean diameter was calculated from the measurements of at least 50 particles from the series of experiments. Each experiment was performed three times. The TEM images of AuNP were selected from one of the replicate samples.

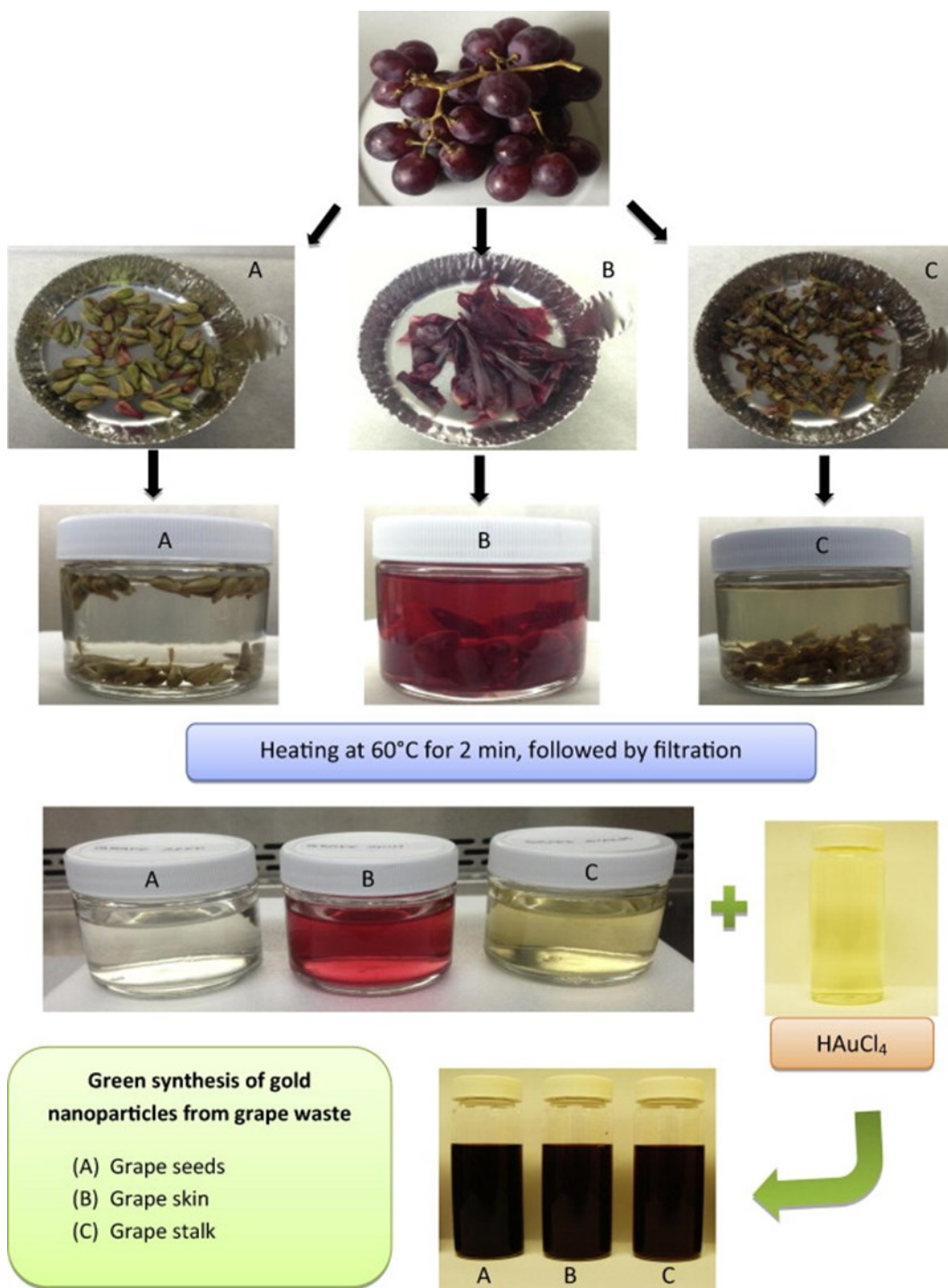


Figure 3.2 Schematic flow diagram for the green synthesis of gold nanoparticles from grape waste, A) grape seed; B) grape skin; C) grape stalk

The elemental analysis of chemical constituents were determined by energy-dispersive X-ray spectroscopy (EDX) using FEI Tecnai G² F20 operated at 200 kV with a Cryo-S/TEM Gatan Ultrascan 4000 4k x 4k CCD Camera System, Model 895 with EDAX Genesis EDS (FEI Company, Oregon, USA). Olympus LEXT OLS4000 3D laser microscope was used to capture three dimensional images. A drop of gold nanoparticles solution was smeared on a glass slide and was used to view the green synthesized gold nanoparticles under the microscope.

3.3.4 Statistical design

A face centered central composite design with 8 factorial points, 6 axial points, and 6 center points, which totals 20 experimental runs was used to fit the second order polynomial model shown in Equation 1.

$$Y = \beta_0 + \sum_{i=1}^3 \beta_i X_i + \sum_{i=1}^3 \beta_{ii} X_i^2 + \sum_{i=1}^2 \sum_{j=i+1}^3 \beta_{ij} X_i X_j \quad (\text{Eq. 3.1})$$

Where Y is the predicted response, β_0 is the regression coefficient for the intercept (a constant), β_i is the coefficient for the linear effect, β_{ii} is the coefficient for the quadratic effect, β_{ij} is the coefficient for the interaction effect, and X_i and X_j are independent variables.

In the study using catechin for the bioreduction of AuNP, the null hypothesis (H_0) assumed that the linear, quadratic and bilinear effects of the independent variables had no effect on the green synthesis of AuNP. While the alternative hypothesis (H_1) assumed that at least one of the linear, quadratic and bilinear effects of the independent variables had an effect on the green synthesis of AuNP. The hypothesis along with the coded values and uncoded values used are given in Table 3.1 and Table 3.2.

Table 3.1 Null and alternative hypothesis to study the effect of linear, quadratic and bilinear interactions of the variables

	Null	Alternative
Linear effect	$H_{01} : \sum_{i=1}^3 \beta_i X_i = 0$	$H_{11} : \sum_{i=1}^3 \beta_i X_i \neq 0$
Quadratic effect	$H_{02} : \sum_{i=1}^3 \beta_{ii} X_i^2 = 0$	$H_{12} : \sum_{i=1}^3 \beta_{ii} X_i^2 \neq 0$
Bilinear effect	$H_{03} : \sum_{i=1}^2 \sum_{j=i+1}^3 \beta_{ij} X_i X_j = 0$	$H_{13} : \sum_{i=1}^2 \sum_{j=i+1}^3 \beta_{ij} X_i X_j \neq 0$

Table 3.2 Code levels for independent variables in central composite design for the green synthesis of AuNP

Independent variables				Coded levels		
				-1	0	1
Conc. of Catechin (mM)	X1	0.5	1	1.5		
Conc. of reducing agent (mM)	X2	0.5	1	1.5		
Temperature (°C)	X3	10	25	40		

SAS software version 9.2 (SAS Institute Inc., Cary, NC) was used for the statistical analysis of the results to generate the response surface plots for the quadratic models. ChemBioDraw Ultra version 12.0.2 and ChemBio3D (CambridgeSoft, PerkinElmer, Massachusetts, USA) were used to draw and model the chemical structures.

3.4 Results and discussion

In the schematic flow diagram shown in Figure 3.2, it can be clearly seen that after the filtration process, the grape seed extract (GSE) was completely colourless, but the grape skin extract (GSK) showed a pink colour due to the presence of the colouring

pigments present in the skin. The grape stalk extract (GST) had a pale yellow colouration. When the grape extracts solutions were mixed with the HAuCl_4 solution, appearance of ruby red color was observed within 5 minutes.

The wavelength for grape skin extract showed a maximum absorbance at 515 nm initially, even after 12 hours, the maximum absorbance was found to be at the same wavelength. The presence of anthocyanin, which is a water soluble colouring pigment present in vacuoles of grape skin cells, contributes to the excitation at 515nm. There was no significant increase in the absorbance over the wavelength from 400-800 nm for grape seed, grape skin extracts and for the HAuCl_4 solution. Similar trend of absorbance pattern was obtained for the extracts when monitored over a period of 12 hours (Figure 3.3).

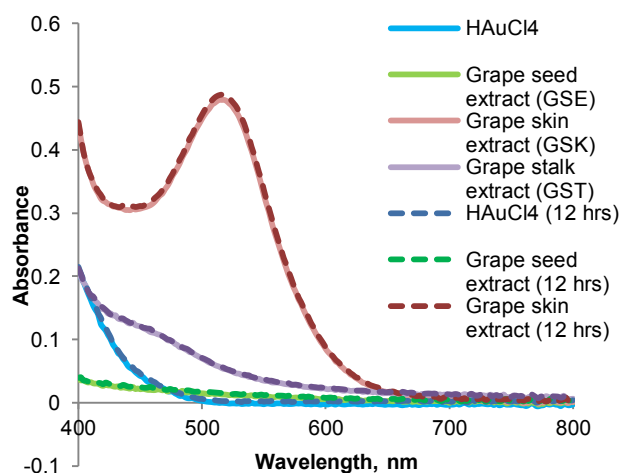


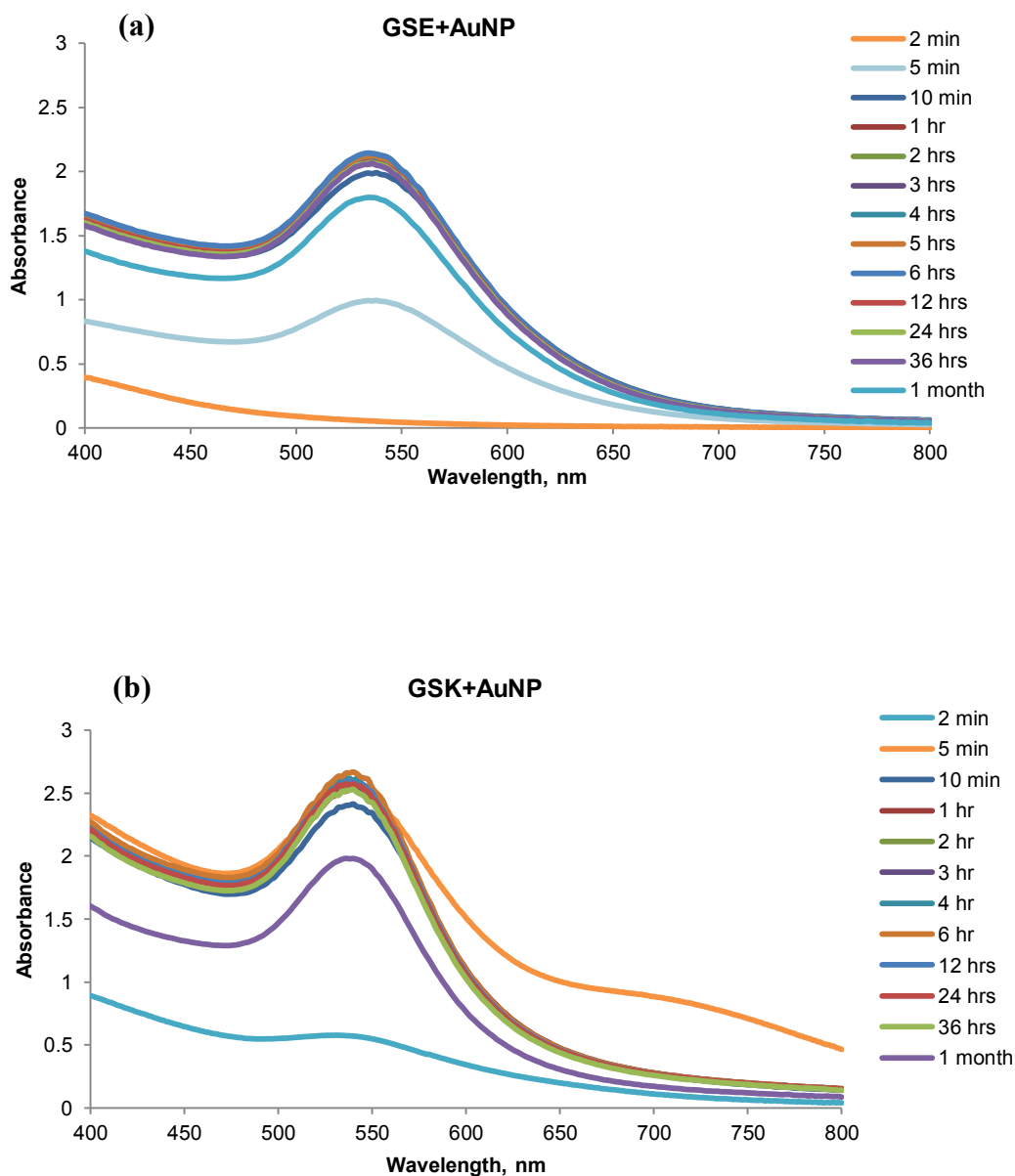
Figure 3.3 Changes in the absorbance of the grape seed, skin, stalk extracts and HAuCl_4 solution over time

This indicates that the grape extracts did not have a significant change in colour and absorbance pattern over the period of time tested. The colour of the plant extract did not change significantly when stored under refrigerated conditions for a week. Storing the plant extracts at room temperature resulted however in darkening and colour change of the extracts. Thus the extracts used for the synthesis of gold nanoparticles were prepared fresh for this experiment. The pH of the fresh grape seed extract was about 6.1, while the pH of grape skin extract and grape stalk extract was about 4.5 and 4.6 respectively. The pH of the grape extracts was measured after 12 hrs and there was no substantial change.

The appearance of a pink-ruby red colour indicating the formation of gold nanoparticles is due to surface plasmon resonance. Figure 3.4(a) shows the UV-Vis spectra recorded as a function of time of the reaction between HAuCl_4 and grape seed extract. The maximum surface plasmon resonance for gold nanoparticles obtained from grape seed extract (GSE+AuNP) was at 536 nm. UV-Vis spectra recorded at 2 minutes just after the addition of HAuCl_4 solution, was similar to that of GSE. At 5 minutes the spectra showed a progressing peak, while after 10 minutes the absorbance was 1.992 at 536 nm. The maximum UV-Vis absorbance was at 536 nm wavelength for 36 hours and gradually decreased after a month due to agglomeration. GSE+AuNP solution was found to be stable for about a year.

The UV-Vis spectra recorded as a function of time of reaction between HAuCl_4 and grape skin extracts (GSK+AuNP), given in Figure 3.4(b), shows a different trend. The spectra recorded at 2 min had increased intensity of absorbance when compared to GSK (Figure 3.3). Within 5 min, the absorbance increased rapidly at 536 nm and had maximum absorbance from 536-538nm for about 36 hours. The agglomeration of

GSK+AuNP was comparatively more than that of GSE+AuNP after 1 month. The UV-absorbance spectra for grape stalk extract synthesized gold nanoparticles (GST+AuNP) shown in Figure 3.4(c) follows a similar trend to that of grape seed extract. The maximum surface plasmon resonance for GST+AuNP was also between 536-538 nm.



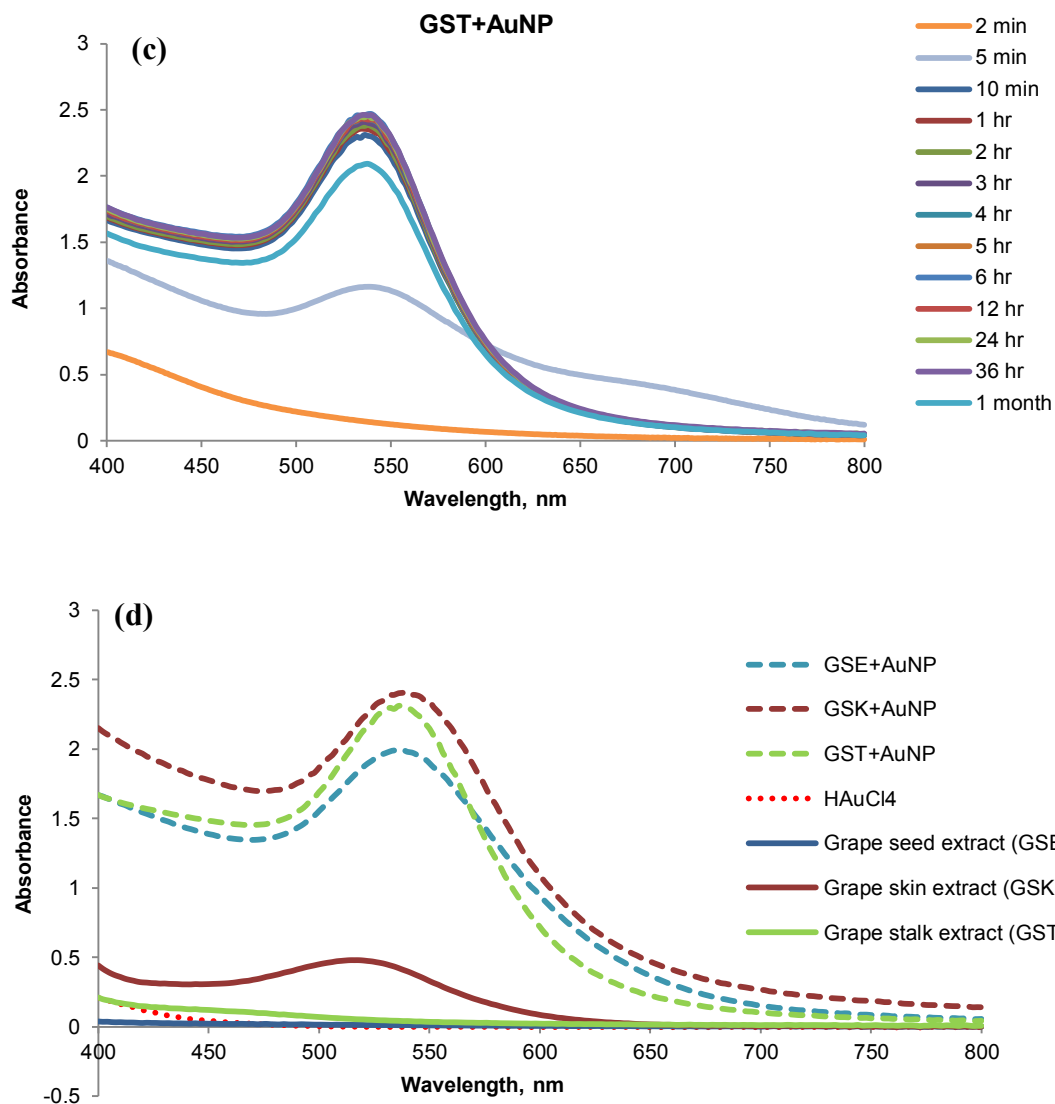


Figure 3.4 UV-Visible spectra recorded as a function of time of reaction between HAuCl_4 and grape extracts. (a) grape seed extract synthesized gold nanoparticles (GSE+AuNP), (b) grape skin extract synthesized gold nanoparticles (GSK+AuNP), (c) grape stalk extract synthesized gold nanoparticles (GST+AuNP), (d) comparing the absorbance of grape extracts before the addition of HAuCl_4 and after the formation of gold nanoparticles

Figure 3.4(d) compares the absorbance of freshly prepared GSE, GSK and GST with the spectra of grape extract mediated synthesis of gold nanoparticles recorded at 10 min. Upon the addition of the HAuCl_4 to the grape extracts, it was found that the appearance of pink ruby-red colour indicating the formation of gold nanoparticles was first observed in grape skin extract (pH= 4.5), followed by grape stalk extract (pH= 4.6) and then by the grape seed extract (pH= 6.1). All these visual observations were made within 5 minutes after the addition of the HAuCl_4 solution. The acidic conditions of GSK and GST might be favourable for the formation of gold nanoparticles when compared to GSE. Thus, pH of the plant extracts might play a vital role in the formation of gold nanoparticles. But in this study the natural pH of the grape extracts were maintained for the green synthesis of gold nanoparticles. Further studies changing the pH of the plant extracts and synthesising gold nanoparticles will be of interest in future.

We can see from the flow diagram (Figure 3.2), that the color of the grape skin extract was light wine color due to the presence of anthocyanin pigments present in the grape skin, and grape stalk exhibited pale yellow color, which is likely due to the presence of colored pigments and tannins. This can be spectrally shown from Figure 3.3 which presents the maximum excitation wavelength for grape extracts without the addition of HAuCl_4 (i.e. prior to the formation of AuNP). Figure 3.3 shows the grape skin had greater absorbance followed by grape stalk. The interaction of the colored tannins present in grape skin and stalk with the HAuCl_4 might lead to the trend seen in Fig. 3.4b and Fig. 3.4c at 5 min. As we have seen, the first few minutes are critical for nucleation and formation of gold nanoparticles. Once they are stabilized, the grape extract synthesized AuNP exhibit a similar trend over the range of wavelength from 400-800 nm.

The spectral properties from previously published data for pigmented tannins has maximum absorption wavelength from 535 to 540 nm, this may vary according to grape variety and other climatic factors (Kennedy et al., 2001). The other factors that might contribute to this may be the nature and concentration of the anthocyanidins, and their secondary structures formed during equilibrium (Bueno et al., 2012).

Haiss et al. (2007) reported that the surface plasmon resonance (SPR) peak for gold nanoparticles was clearly visible between 520 and 580 nm (Haiss et al., 2007). The average particle size ranged from 10 to 100 nm for gold nanoparticles produced by *Bacillus licheniformis* (Kalishwaralal et al., 2009). In our study we report the formation of gold nanoparticles within 5 min using grape seed, skin and stalk extracts. This is an important result as green synthesized gold nanoparticles from grape waste could compete favourably with chemical synthesis methods following green nanotechnology approach.

The transmission electron microscopy (TEM) results indicate the presence of spherical to quasi-spherical shaped gold nanoparticles synthesized from GSE+AuNP, GSK+AuNP and GST+AuNP. The average size of the gold nanoparticles produced ranged from 20 to 25 nm in diameter. Figures 3.5(a, b, c) present the TEM images of grape extracts synthesized gold nanoparticles (AuNP) with a size distribution graph (scale bars = 100 nm). The statistical data from the TEM image analysis for GSE+AuNP, GSK+AuNP and GST+AuNP is summarised in Table 3.3.

Table 3.3 Summary of TEM image analysis with particle size for the grape waste synthesized gold nanoparticles.

S. No	Grape wastes	Mean Size (nm)	Std. Dev (±)	Min. size (nm)	Max. size (nm)	UV λ_{max} (nm)
1.	GSE+AuNP	21.5	8.6	3.4	39.9	536
2.	GSK+AuNP	20.2	5.7	7.3	37.4	536
3.	GST+AuNP	24.8	5.5	15.0	39.4	538

Comparing our results with Baruwati & Varma (2009), spherical size gold nanoparticles similar to the micrographs shown in Figure 3.5 a,b,c were formed. Du et al. (2011) reported bioreduction of gold nanoparticles by *Penicillium sp.* by extracellular biosynthesis with a maximum UV-Vis absorbance at 545 nm for spherical gold nanoparticles of 30-50 nm (Du et al., 2011). Nadagouda et al. (2009) synthesized green gold nanoparticles using biodegradable plant surfactants such as VeruSOL-3, and observed particles ranging from 20 nm to 1 μm in size with various geometrical structures such as spheres, prisms, rods, and hexagons (Nadagouda et al., 2009). Strong and West (2011) reported maximum absorption for gold nanoparticles for wavelengths ranging from 520 to 575 nm, with smaller particles absorbing at lower wavelengths (Strong & West, 2011).

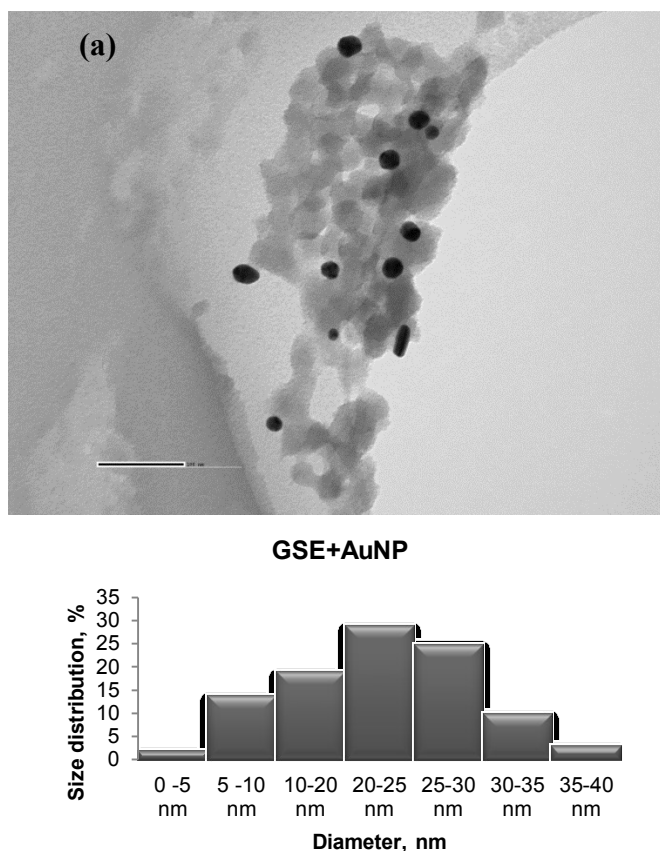


Figure 3.5 (a) TEM image of grape seed extract synthesized gold nanoparticles (GSE+AuNP) with size distribution graph (scale bars = 100 nm)

Similar relationship was observed when studying the results obtained from TEM and UV-Vis spectra. Gold nanoparticles produced from grape seed and grape skin were small quasi- nearly spherical particles with uniform distributed diameters of 20 to 21 nm, which corresponded to maximum adsorption at a wavelength of 536 nm. Nanoparticles produced using grape stalk had similar quasi spherical structure with a diameter of 24 nm which had a maximum adsorption at wavelength of 538 nm. Thus maximum wavelength (λ_{max}) due to surface plasmon resonance and size of nanoparticles can be related to each other.

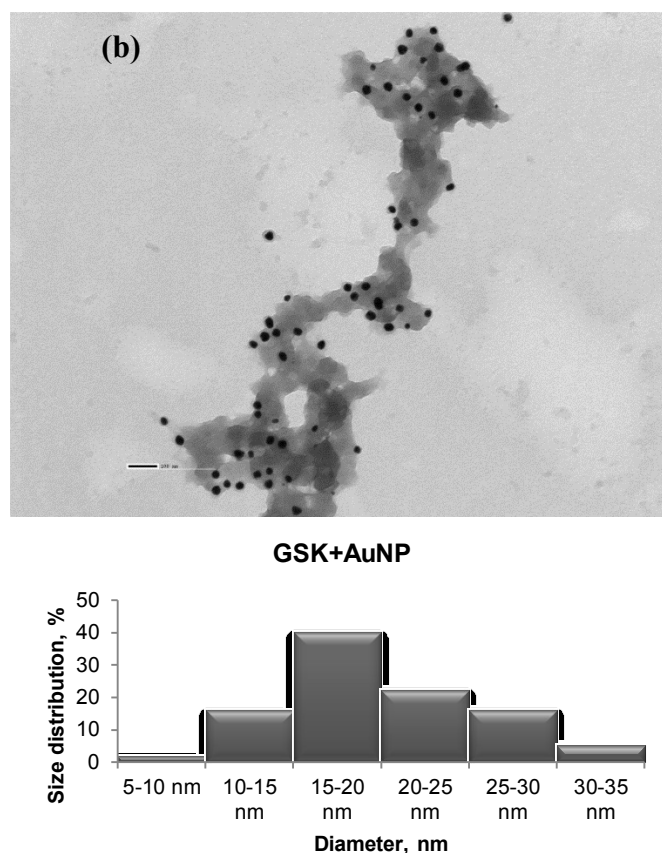


Figure 3.5 (b) TEM image of grape skin extract synthesized gold nanoparticles (GSK+AuNP) with size distribution graph (scale bars = 100 nm)

A thin layer of plant material was observed around the AuNP that were produced using grape seed, skin and stalk extracts (Figure 3.5 (a,b,c)). The morphology of gold nanoparticles produced by GSE, GSK and GST were nearly quasi-spherical in shape. The TEM grid containing GST+AuNP was subjected to energy-dispersive X-ray spectroscopy (EDX) to determine the elemental constituents using a high resolution transmission electron microscope (HRTEM).

The HRTEM image (Figure 3.6(a)) of grape stalk mediated AuNP clearly shows the atomic structure of gold nanoparticles with lattice fringes. The EDX results of this analysis are given in Figure 3.6(b) and show the elemental peaks of gold present in the sample. The image of GST+AuNP obtained from 3D laser microscope shown in Figure 3.6(c) also indicated a thin film of organic grape matrix within which the gold nanoparticles were embedded. This grape matrix which is present in grape seed, skin and stalk might act as nucleation sites for the growth of gold nanoparticles providing stabilization.

Nune et al. (2009) produced gold nanoparticles by reducing sodium tetrachloroaurate (NaAuCl_4) with Darjeeling tea leaves within 30 minutes. They reported that the catechin present in tea leaves acts as a reducing and stabilizing agent, and reported that epicatechin and epigallocatechin, also present in tea, can act only as reducing agents thus requiring an additional substance, such as gum Arabic, for stabilization (Nune et al., 2009). Proanthocyanidins present in grape seed, skin and stalk are made up of simple monomeric units of catechin and epicatechin. It consists of phenolic flavan-3-ol nucleus as the fundamental structural unit which is similar to the catechin present in tea leaves.

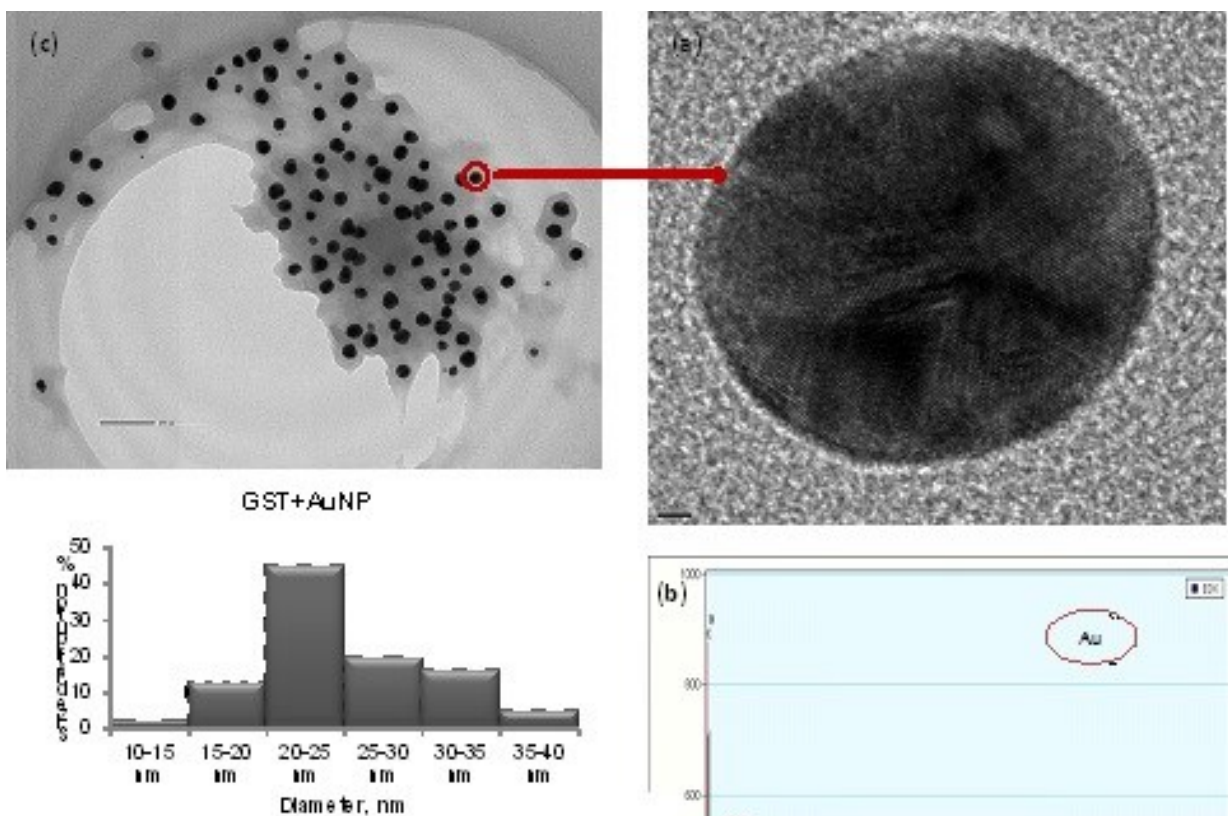
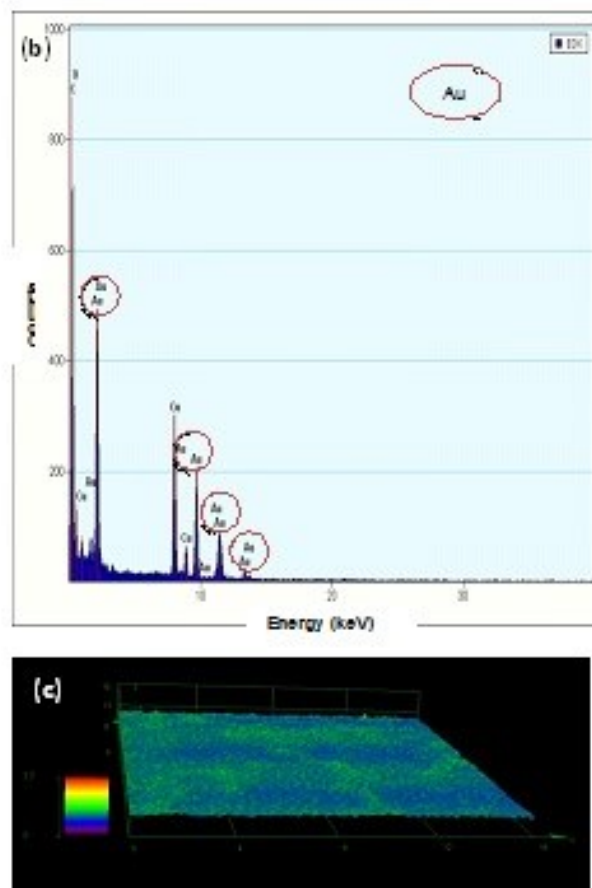


Figure 3.5c TEM image of grape stalk extract synthesised gold nanoparticles (GST+AuNP) with size distribution graph (scale bars = 100 nm).

Figure 3.6 (a) HRTEM image of grape stalk extract synthesized AuNP showing atomic structures (scale bar = 2 nm), **(b)** corresponding EDX plot GST+ AuNP showing the elemental peak for gold, **(c)** image of GST+AuNP obtained from 3D laser microscope showing a thin film of grape matrix over gold nanoparticles.



Grape seeds, skin and stalk have high content of polyphenolic compounds such as catechin, epicatechin, anthocyanidin, proanthocyanidin and condensed tannins which can be the potential compounds responsible for reducing and stabilizing the gold

nanoparticles. To study the mechanism of nanoparticle formation in such a complex and intricate system (grape matrix) is difficult. Therefore, catechin being the monomeric unit of polyphenols present in grape matrix was taken as a representative sample for further studies.

Table 3.4 Composition of phenolic compounds present in seed, stalk, skin in Merlot variety (Souquet et al., 2000).

	% gallate	% EGC	% EC	% CAT	mg Tannins / kg crop
G.Skin	5.16	22.69	67.20	4.96	1605.0
G.Seeds	32.45	-	54.36	13.19	2323.5
G.Stems	15.55	2.44	67.66	14.35	221.3

Where, EGC: (-) epigallocatechin, EC: (-) epicatechin, CAT: (+) catechin

Grape seed, stalk and skin have phenolic components in varying concentrations. The composition of phenolic compounds present in seed, stalk, skin in Merlot variety is provided in Table 3.4 (Souquet et al., 2000). This varies for different cultivars, climatic conditions, geographic locations, agricultural practices, etc. Tannin or proanthocyanidin is a major compound present in grape products. Proanthocyanidin is a complex polymer made up of simple units of catechin and epicatechin, belonging to flavan-3-ols.

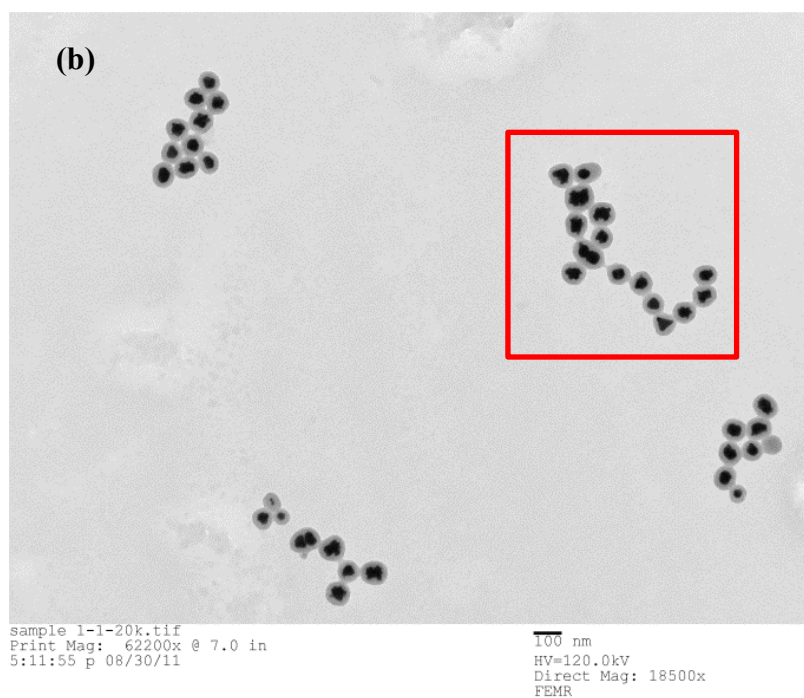
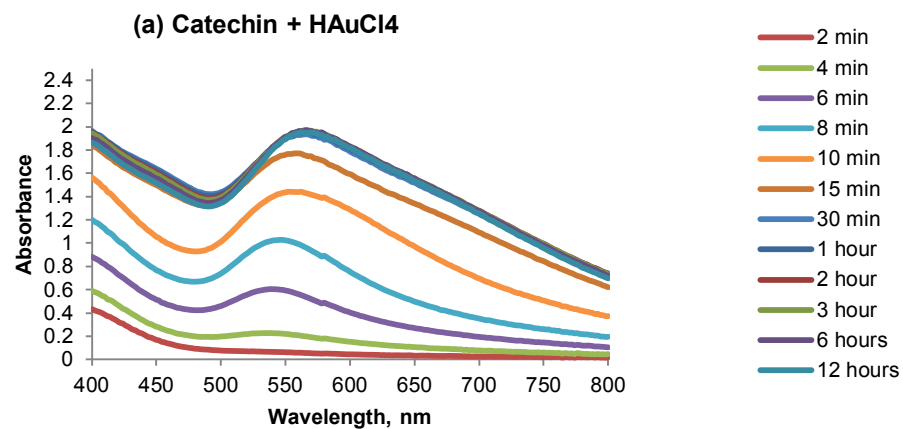


Figure 3.7 (a) UV-Vis spectra shows the reaction of catechin with HAuCl₄ solution over period of time, (b) TEM image of catechin synthesized gold nanoparticles

Hence in our preliminary studies, experiments were conducted with certain phenolic compounds with different concentrations and varying solvents like ethanol to water. It was found that catechin in water represented a similar structure from TEM micrographs with plasmon resonance peak at 550 nm from UV-Vis spectra (Figure 3.7(a)). Figure 3.7(b) shows the TEM image of catechin reduced gold nanoparticles, where the highlighted portion present in the square, is part of the magnified image provided in Figure 3.9. Based on these results we used catechin, a monomeric unit of the phenolic proanthocyanidin present in grapes as a sample representative for our study.

3.4.1 RSM for green synthesis of AuNP using catechin

Response surface regression models (RSM) were fitted to the absorbance value at 4 min for all the 20 combinations of central composite face centered experimental runs at 560 nm and are presented in Table 3.5. The ANOVA of the quadratic regression model for green synthesized AuNP by catechin is given in Table 3.6. The model obtained was significant with a *p*-value of 0.0069, and with an R^2 value of 84.83%. From the ANOVA table the model was found to be significant. The parameter estimates of the model with a *p* value less than 0.05 were significant. The linear effects of concentration of catechin and temperature were also found to be significant.

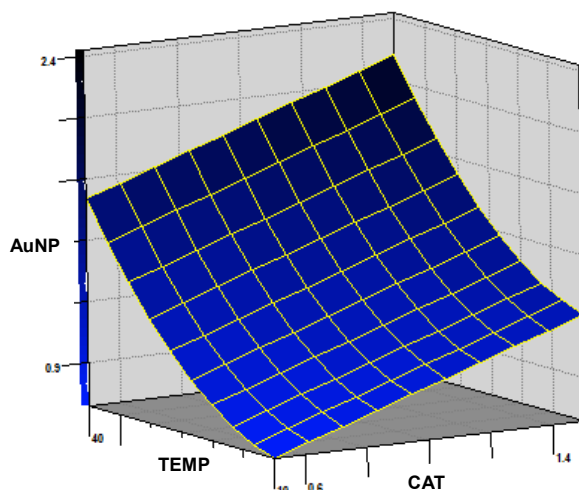


Figure 3.8 Response surface plot representing the effect of catechin and temperature on the green synthesis of gold nanoparticles using catechin

From the parameter estimates, the bilinear terms of concentration of catechin and HAuCl_4 solution, and the bilinear terms concentration of HAuCl_4 and temperature were found to have an influence on the synthesis of gold nanoparticles. Figure 3.8 presents the surface plots showing the interaction of concentration of catechin and temperature on the green synthesis of AuNP. As temperature and the concentration of catechin increase there is an increase in the rate of synthesis of the gold nanoparticles. With a lower concentration of HAuCl_4 , as the temperature increases, the rate of AuNP synthesis remains constant for 10-25 °C then gradually increases. A decrease in the rate of AuNP synthesis was found at lower temperature and higher concentration of HAuCl_4 .

Table 3.5 Uncoded values and their corresponding response for face centered central composite design.

Run	CAT (X1)	HAuCl ₄ (X2)	TEMP (X3)	Y=mX+c	R ²	A ₄
R1	1	1	25	y = 0.0065x + 0.0838	0.9284	1.593
R2	1	1	25	y = 0.0063x + 0.1306	0.9329	1.567
R3	0.5	1	25	y = 0.0059x - 0.5393	0.8972	0.463
R4	1	1.5	25	y = 0.0044x - 0.6949	0.6300	0.325
R5	1	1	25	y = 0.0063x + 0.115	0.9335	1.571
R6	1.5	1	25	y = 0.0058x + 0.4797	0.8700	1.842
R7	1	1	25	y = 0.006x + 0.2339	0.9308	1.481
R8	1.5	0.5	40	y = 0.0196x + 1.9869	0.6750	1.578
R9	1	0.5	25	y = 0.0066x + 1.5302	0.8330	1.521
R10	1	1	40	y = 0.0058x - 0.0493	0.9572	2.556
R11	0.5	0.5	40	y = 0.0054x - 0.3601	0.9685	1.811
R12	0.5	0.5	10	y = 0.005x - 0.1654	0.9641	1.365
R13	0.5	1.5	10	y = 0.0074x - 0.1832	0.7357	0.134
R14	1.5	0.5	10	y = 0.0064x + 1.4686	0.7795	1.199
R15	1.5	1.5	10	y = 0.0034x - 0.4818	0.9611	1.040
R16	1	1	10	y = 0.006x + 0.3446	0.9238	1.111
R17	0.5	1.5	40	y = 0.0063x + 0.2411	0.8014	1.915
R18	1	1	25	y = 0.006x + 0.187	0.9260	1.531
R19	1	1	25	y = 0.0054x + 0.1503	0.9071	1.508
R20	1.5	1.5	40	y = 0.01x - 0.2344	0.8483	2.862

A₄ = absorbance at 4 mins after the onset of the reaction; Y= negative Ln (Absorbance); X= time of reaction in seconds; c= constant.

It was found that when an equal concentration of catechin (1 mM) and HAuCl₄ (1 mM) was used at room temperature (25°C) , the reaction occurred within one minute, the reaction rate then gradually increased fitting a straight regression line with R² = 0.9284. In Run 8, when the temperature was increased to 40 °C with an increase in catechin concentration, the reaction was nearly instantaneous, occurring within 190 s (3.1 min). The absorbance measured in the UV-Vis spectra was greater than 3. It was

interesting to note that even with an increase or a decrease in temperature, (Runs 10, 11, 12, 15, and 16) if the concentrations of catechin and HAuCl₄ were equal, the reaction proceeded with an R² value greater than 0.9. In Run 4 and Run 13, where the concentration of HAuCl₄ was twice the concentration of the catechin, the reaction did not occur until an initial lag period of 0 to 300 s, and once the reaction started it was rapid. All these observations clearly indicate the bilinear relationships between catechin and HAuCl₄ concentrations and between HAuCl₄ concentration and temperature.

Table 3.6 ANOVA table for green synthesis of gold nanoparticles from catechin.

Source	DF	Estimate	Std error	SS	MS	F	Pr > F
CAT	1	0.2833	0.110997	0.802589	0.802589	6.514395	0.0287 *
HAUCL4	1	-0.1198	0.110997	0.14352	0.14352	1.164916	0.3058
TEMP	1	0.5873	0.110997	3.449213	3.449213	27.99632	0.0004 *
CAT*CAT	1	-0.148364	0.211662	0.060532	0.060532	0.491325	0.4993
CAT*HAUCL4	1	0.2815	0.124098	0.633938	0.633938	5.145502	0.0467 *
CAT*TEMP	1	-0.00325	0.124098	0.000084	0.000084	0.000686	0.9796
HAUCL4*HAUCL4	1	-0.377864	0.211662	0.392648	0.392648	3.187013	0.1045
HAUCL4*TEMP	1	0.34725	0.124098	0.964661	0.964661	7.829886	0.0189 *
TEMP*TEMP	1	0.5326364	0.211662	0.780179	0.780179	6.332501	0.0306 *

The intricate complexity of biological systems present in nature, many a times, are non-linear or have curvature that might not necessarily fit into a second order polynomial model. In order to fit the data and accommodate the effect of curvature, higher order polynomial models can be used (Baş & Boyacı, 2007). Thus, based on the present analysis, it was found that the quadratic effect of temperature and the bilinear effects of

all the three independent factors were significant and had a major effect on the synthesis of gold nanoparticles.

3.4.2 Mechanism for green synthesis of gold nanoparticles by catechin

The understanding of the mechanism of green synthesis of gold nanoparticles by biological material is still in its infancy; hence more investigation is required. Leiva et al. (2009) postulated that although the mechanism of gold reduction reaction is not fully understood, it might occur due to the presence of the –OH group present in the reducing agent (Leiva et al., 2009). Thus the –OH group present in the catechin molecule might be the factor required to successfully reduce gold salts.

Shankar et al. (2003) reported the rapid reduction of chloroaurate ions to stable gold nanoparticles using a geranium leaf–fungus, *Colletotrichum sp.*, which produced a variety of particulate shapes including rods, flat sheets, spheres and triangles. They also mentioned that the terpenoids in geranium leaves, and polypeptides/ enzymes of *Colletotrichum sp.* might act as reducing and capping agents (Shankar et al., 2003). Kalishwaralal et al. (2009) reported that proteins, organic acids and polysaccharides secreted by bacteria could facilitate bio-reduction of gold nanoparticles. They also reported that the initial gold nanoparticles that were formed were thermodynamically unstable due to insufficient capping material which might have led to linear assemblies driven by Brownian motion and short-range interaction (Kalishwaralal et al., 2009).

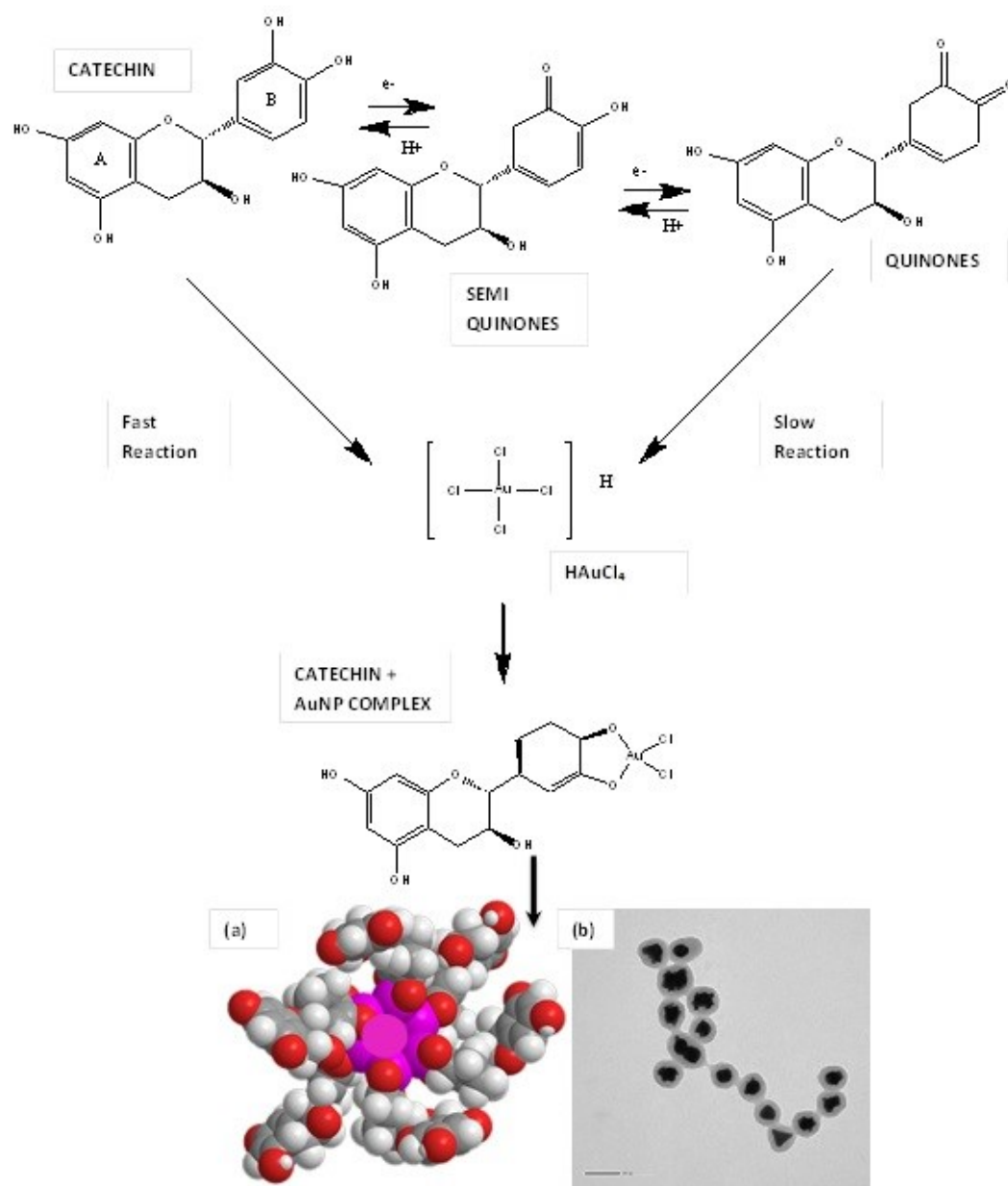


Figure 3.9 Schematic process flow for green synthesis of AuNP by catechin; reduction of catechin to quinone and generation of gold atoms by forming catechin+AuNP complex, (a) pictorial representation of gold nanoparticles surrounded by catechin molecule, (b) TEM image of catechin+AuNP showing a clear layer of catechin surrounding the gold nanoparticles (scale bars = 100 nm)

A single plant cell can be considered as a huge nanofactory or nanoreactor containing various cell organelles, proteins and other secondary metabolites that can interact in the formation of gold nanoparticles. Thus from our study using catechin, a single basic monomer molecule present in grape, through RSM and using TEM images, we have conceptualized a model which is illustrated in the schematic presented in Figure 3.9. The health benefits of catechin have received considerable attention and catechin can be used as a food supplement to provide antioxidant effects both by scavenging free radicals and through metal chelation.

Catechin acts like a bidentate ligand and the protonation state of the catechol moiety on the B-ring plays a significant role in metal chelation and the scavenging activity of catechin. The initial step of oxidation occurs on the B-ring due to partial deprotonation which leads to the transformation of *o*-phenols to *o*-quinones, a fundamental step in browning. *o*-Quinones are highly reactive species that form dimers and subsequently polymers due to prolonged autoxidation with other polyphenolic molecules (Torreggiani et al., 2008). The addition of H₂AuCl₄ solution to the catechin solution resulted in the maximum surface plasmon resonance at 560 nm within 5 min which corresponds to gold nanoparticles. This indicates that there was an interaction between the metal and the catechin, which acted as a bidentate ligand.

From the TEM images obtained for catechin synthesized AuNP (Figure 3.9(b)), a clear layer of catechin was observed around the AuNP. This layer might act as the nucleation factor and lead to self-assembly of gold atoms to gold nano crystals. Most of the reports available for chemical synthesis of gold nanoparticles are based on the reduction of Au(III) to Au(0) by sodium citrate and sodium borohydride as reducing

agents. Stabilizing or capping agents are added to the aqueous solution to prevent uncontrolled aggregation into larger particles (Genç et al., 2011). However, in our case, the plant matrix itself acts as a reducing and stabilizing agent with an added advantage of providing control of size and shape of the AuNP being formed. This provides the evidence for the possibility of using grape seed, skin, and stalk for green synthesis of gold nanoparticles at a lower cost and in an ecofriendly manner.

The fact that this reaction is taking place within few minutes is very interesting. As the time scale for nucleation, formation of nanoparticles and stabilization is at a very small time span, it becomes very difficult to elucidate the mechanism clearly. Many scientists in this field are trying to figure out a solution to this challenging question. When a biological material is involved in the process it really becomes difficult to pin down to one pathway. A review article by Durán et al. (2011) explains various approaches that might lead to formation of the nanoparticles and at the conclusion the authors clearly mentioned that a lot of work has to be done in this area to understand the mechanisms.

3.5 Conclusion

We have reported a simple single step eco-friendly method to produce gold nanoparticles surrounded by plant matrix which acts as a capping or stabilizing agent. Gold nanoparticles embedded within polymer matrices have gained much attention, since they can be easily tailored to have optical, electrical, catalytic and physical properties of interest. The results of this study support the concept of synthesizing gold nanoparticles by the polyphenolic compounds present in grape seed, skin and stalk. Such a method for synthesizing AuNP will be an added advantage, and other food waste materials rich in

polyphenols can be potentially converted into a high value nanoparticle. This might open ways to explore other naturally available food compounds present in the flavonoids family for synthesizing gold nanoparticles using green nanotechnology.

Thus produced gold nanoparticles from grapes seeds, skin, stalk and catechin can find potential application as biocompatible gold nanoparticles for use in medical application, in molecular imaging, and in cancer therapy. This can open windows to future novel multifunctional green nanomaterials.

CONNECTING STATEMENT TO CHAPTER IV

Results from Chapter III highlighted that gold nanoparticles can be synthesized using grape waste. This has led to the exploration of other waste materials for gold nanoparticle synthesis. For this purpose the large source of naturally occurring biomass which collects during the Canadian fall season, such as the shedding of maple leaves and pine needles was considered.

Chapter IV explores the potential of synthesising gold nanoparticles from pine needle and maple leaf extracts. The experiments and results interpretation were performed by Ms. Krishnaswamy under the guidance of Dr. Orsat. The results of this chapter were published in the journal *Industrial Crops and Products* in 2015.

1. Krishnaswamy K and Orsat V. Insight into the nanodielectric properties of gold nanoparticles synthesized from maple leaf and pine needle extracts. **Industrial Crops and Products**. 2015, 66, 131-136.

CHAPTER IV

GREEN SYNTHESIS OF GOLD NANOPARTICLES FROM MAPLE LEAF AND PINE NEEDLE EXTRACTS

4.1 Abstract

This study reports on the use of maple leaf (*Acer saccharum*) and pine needle (*Pinus strobus*) extracts for the green synthesis of gold nanoparticles (AuNP). The gold nanoparticles were formed within 10 minutes using distilled water as the solvent following green nanotechnology approach. This is the first study reporting the use of maple leaves and pine needles for synthesizing gold nanoparticles. Characterization using transmission electron microscope (TEM) indicated the presence of quasi-spherical to triangular prisms of AuNP; nanodielectric properties were studied using dielectric spectroscopy which provides information about dielectric constant (ϵ') and dielectric loss factor (ϵ''); thermal properties of the nanoparticle solution were studied using a differential scanning calorimeter (DSC). This information, on the physical characterization of green synthesized AuNP, will be useful in designing applications for hyperthermal treatments using radiofrequency waves and for microwave based tumor therapy.

Keywords: Green nanotechnology; Maple leaf; Pine; Nanodielectrics; Transmission electron microscope (TEM); Differential scanning calorimeter (DSC).

4.2 Introduction

Efficient use of natural resources and the development of innovative green synthesis methods are key to sustainable advancements in nanotechnology. Green nanoscience integrates nanotechnology with the emerging field of green chemistry for developing greener products, processes and applications (McKenzie & Hutchison, 2004). The last decade has seen a tremendous growth in the use of biomaterials for the synthesis of nanoparticles and in particular gold nanoparticles as carriers for targeted drug delivery. Using a green chemistry approach for the synthesis of nanoparticles is competitively and environmentally a better solution than using harmful chemicals as reducing agents or surfactants.

In this study, we report the use of plant materials, namely maple leaves and pine needles for the green synthesis of gold nanoparticles. The maple tree being deciduous sheds off its leaves during the fall season; which is generally considered as a domestic waste product and is at best used for composting. This paper proposes an alternative use for this biomass. This is the first study stating that maple leaves and pine needles can be used as prospective bio-reducing agents to produce gold nanoparticles. Thus formed gold nanoparticles are considered eco-friendly as they do not use toxic chemicals during their synthesis and can be better substitutes to chemically synthesized gold nanoparticles in a variety of applications.

Song and Kim (2009) studied the biological synthesis of silver nanoparticles using five different plant leaves extract such as Pine (*Pinus desiflora*), Persimmon (*Diopyros kaki*), Ginkgo (*Ginko biloba*), Magnolia (*Magnolia kobus*) and Platanus (*Platanus orientalis*). They found that there was rapid reduction of silver nanoparticles

using magnolia leaf broth within 11 min at 95°C. A very recent report by Vivekanandhan et al. (2013) stated the use of maple leaf extract for the functionalization of ZnO powders with silver nanoparticles. There are a growing number of reports available in the literature for the reduction of gold nanoparticles by different plant materials, but till date there is no data available demonstrating the use of maple leaves and pine needles for the synthesis of gold nanoparticles following a green chemistry approach along with their physical characterization.

“Nanodielectrics” is the study of dielectric phenomena of nanoscale materials and fabrication of structures, devices and systems that have novel dielectric properties because of their nanometric size (Cao et al., 2004; Lewis, 1994). The concepts of nanodielectrics were mentioned in the landmark theoretical paper by Lewis (1994) that went unnoticed until the experimental works published by an eminent UK/US team in 2002 (Nelson et al., 2002). Since then, there is an increase in the reports being published in the field of nanodielectrics (Fothergill, 2007; Green & Vaughan, 2008). Dielectric spectroscopy involves the study of a material’s response to an applied electric field. The dielectric data provides information on how materials react to an applied electromagnetic field. This information will be of great use for the development of a variety of applications, such as new semiconductor devices, identification of new electrical insulators, for cancer detection since cancer cells have different permittivity than healthy cells, for monitoring chemical reactions, etc.

4.3 Experimental details

The maple leaves and pine needles were collected between 8 and 9 am in mid-July on the Macdonald campus, McGill University, Ste-Anne-de-Bellevue, Canada. During this period the maple leaves are generally green in color. Three grams of each plant material were weighed, cut into fine pieces and were placed individually into two Erlenmeyer flasks containing 50 ml of deionized water. The flasks were heated at 60°C for 2 min, the extracts were cooled to room temperature and filtered using 11 µm pore size Whatman filter paper (Grade 1). The above mentioned steps were completed within 30 min of sample collection from the trees to avoid any post-harvest degradation of chemical compounds present in the plant matrix.

Hydrogen tetrachloroaurate ($\text{HAuCl}_4 \cdot 3\text{H}_2\text{O}$) was obtained from Sigma-Aldrich Chemicals Co., (St. Louis, MO), and 1 mM HAuCl_4 solution was prepared using deionized water. Five ml of each plant extract was added to 12 ml of HAuCl_4 solution and the total reaction volume was made up to 30 ml by addition of deionized water.

UV-Visible spectrophotometer (Ultrospec 2100 pro, Biochrom Ltd., Cambridge, UK) was used for this study. The maple leaf and pine needle extract synthesized AuNP were analyzed through a transmission electron microscope (TEM) by placing a drop of the sample solution on a carbon coated TEM grid. Transmission electron microscopy (TEM) analyses were performed using a FEI Tecnai 12 TEM equipped with an AMT XR-80C CCD Camera System (FEI Company, Oregon, USA) which was operated at 120 kV.

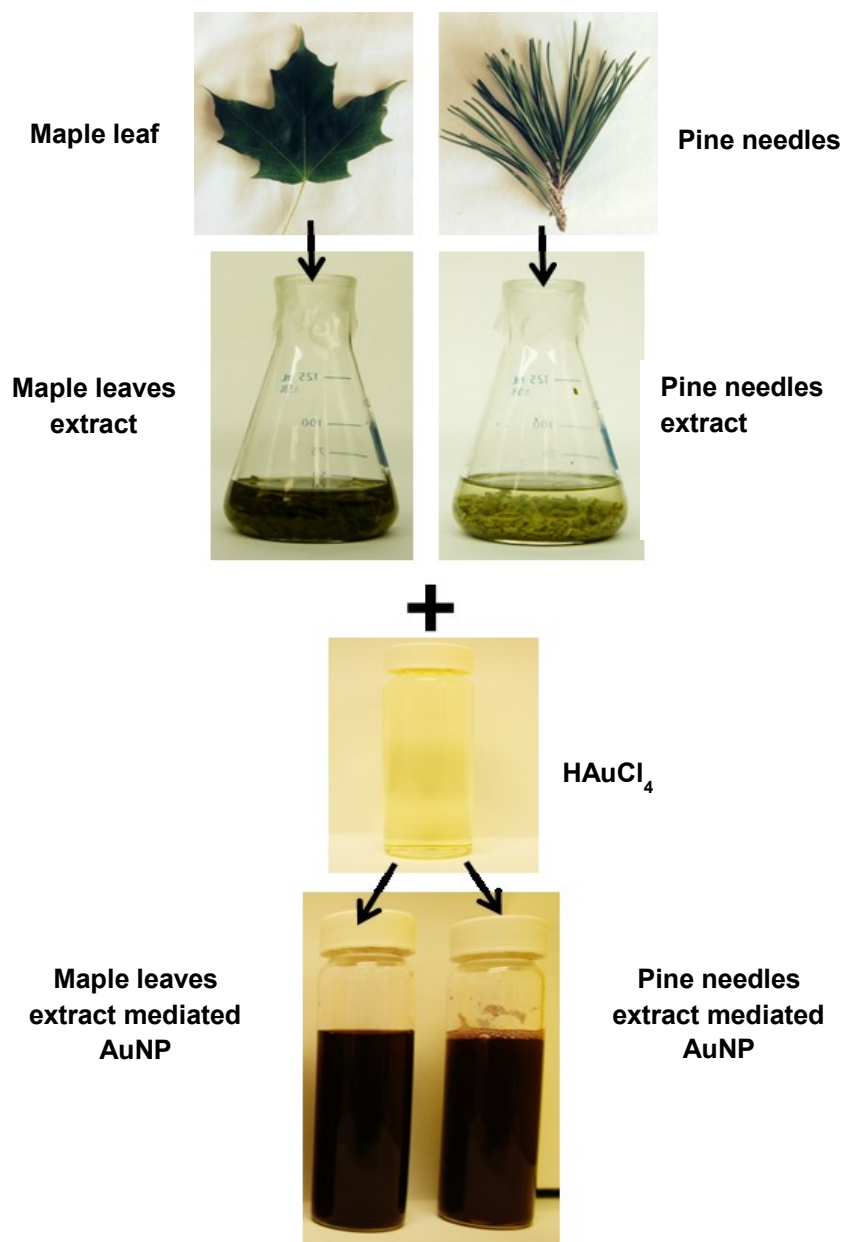


Figure 4.1 Schematic flow diagram for green synthesis of gold nanoparticles mediated through maple leaf and pine needle extracts

The dielectric measurements were performed using an open ended coaxial probe, ideal for measuring liquids. A network analyzer (Agilent S Parameter Network Analyzer, 8722ES, Agilent Technologies, USA) with slim form probe was used to record the dielectric data. The probe was immersed into the solution containing the gold nanoparticles. The broadband frequency range from 200 MHz to 20 GHz was selected for this study.

4.4 Results and discussion

The maple leaf and pine needle extracts were green in color following filtration. Upon the addition of the HAuCl_4 solution to each of the plant extracts, appearance of a ruby red color was observed within 10 minutes (Figure 4.1). This indicated the formation of gold nanoparticles. Figure 4.2(a) shows the UV-visible spectra for the maple leaf extract reduced gold nanoparticles indicating a maximum absorbance at 534 nm when analyzed with a UV-Visible spectrophotometer.

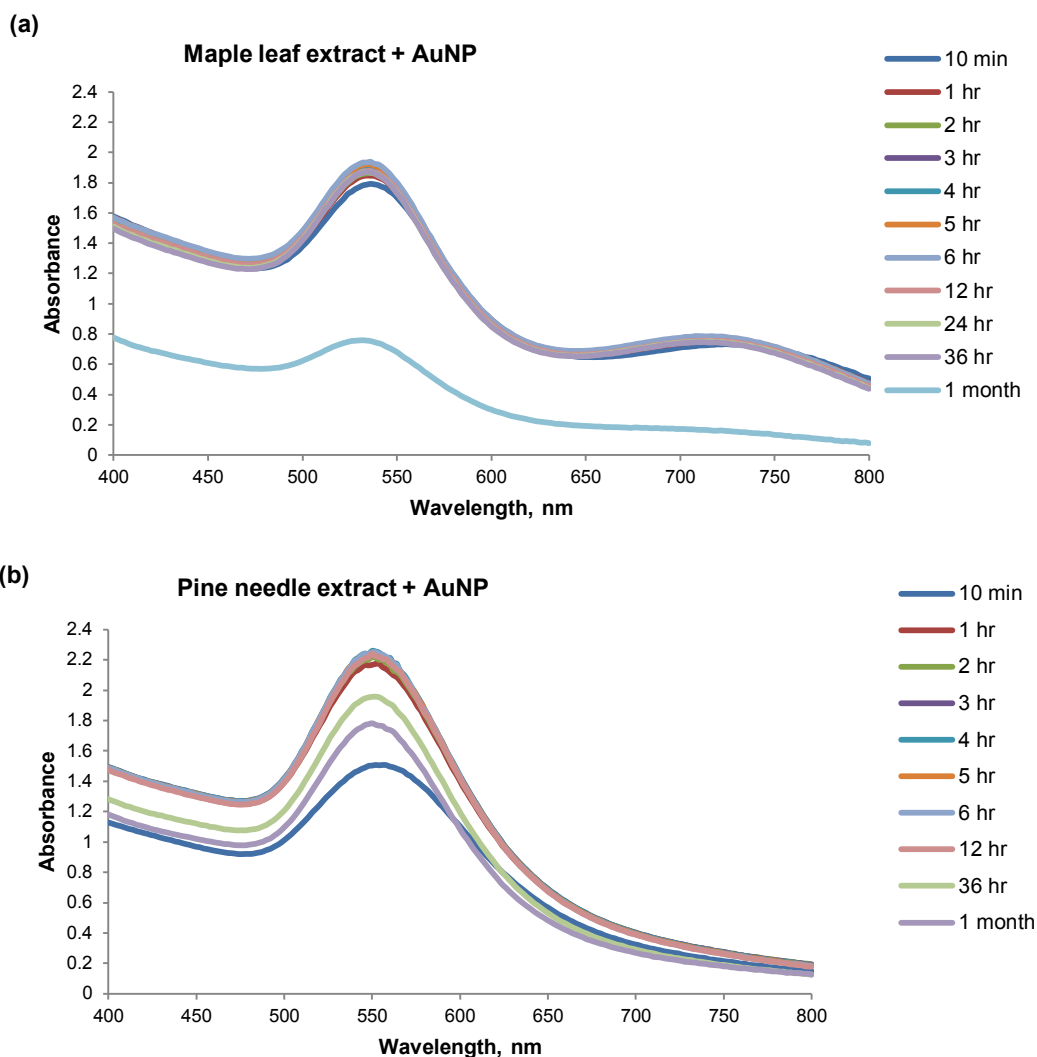


Figure 4.2 UV-Visible spectra recorded as a function of time of reaction between HAuCl_4 and plant extracts (a) maple leaf extract; (b) pine needle extract

The UV-Visible spectra obtained for maple leaf extract reduced gold nanoparticles after a period of one month storage showed a decrease in the absorbance from 1.792 to 0.779 at 532 nm. Settling of gold nanoparticles was observed at the bottom of the bottle, this might be due to the agglomeration of gold nanoparticles synthesized by maple leaf extract. The pine needle extract-synthesized gold nanoparticles showed a maximum absorbance at 552 nm within first 10 min as can be seen in its UV-visible spectra shown in Figure 4.2(b). The AuNP solution containing pine extract remained the

same without significant agglomeration after one month storage when compared to maple leaf extract.

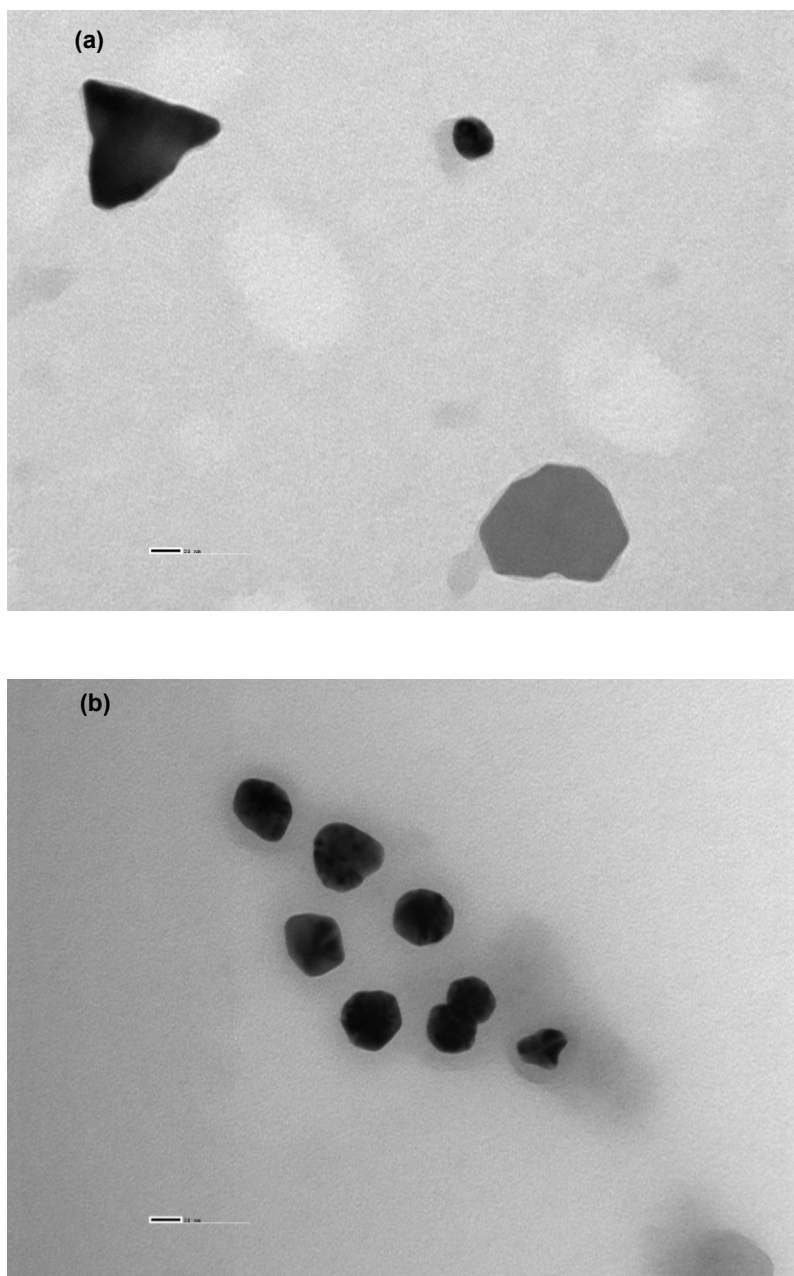


Figure 4.3 TEM micrograph (scale bars = 20 nm) of gold nanoparticles synthesized using (a) maple leaf extract; (b) pine needle extract

The transition electron microscope (TEM) results indicate the presence of spherical to triangular prism of gold nanoparticles synthesized by maple leaf extract as shown in Figure 4.3(a). The TEM images of pine needles extract mediated AuNP showed the presence of spherical to quasi-spherical shaped gold nanoparticles shown in Figure 4.3(b). A distinctive layer of the organic plant material was found surrounding the pine needle extract AuNP which was absent in the maple leaf extract AuNP. The pine needle mediated AuNP under observation have shown to be stable for a year without much agglomeration. This is an interesting result as this naturally available plant source has the potential not only to reduce the gold nanoparticle but also act as a stabilizing agent.

It can be clearly seen that beautiful triangular prism of gold nanoparticles were produced by the maple leaves extract (Figure 4.3(a)). The shape of the nanoparticle plays a significant role in modulating the electronic properties of nanoscale materials. Shankar et al. (2004) reported gold nanotriangles synthesized using lemongrass extracts having high anisotropic electron transport. Synthesizing metal nanotriangles often requires elaborate time consuming transformations from spherical to triangular prism. But we have found a simple single step method to produce gold nanotriangles using maple leaf extracts. Such gold nanotriangles produced through a green chemistry approach can be used as conductive tips in scanning tunneling microscopes. Gold nanotriangles have the potential to absorb a large amount of near infrared rays (NIR), modulating optical properties and can be used for hyperthermia treatments of tumors (Shankar et al., 2004), for antibacterial and antifungal activity (Smitha & Gopchandran, 2013) and to increase the surface enhanced Raman scattering (SERS) properties. Thus further studies are required by varying the concentration of the maple leaf extract and controlling other

parameters such as time and temperature to have a more precise control over the size and shape of the produced gold nanoparticles.

A clear organic layer was found surrounding the quasi spherical gold nanoparticles synthesized using the pine extract (Figure 4.3 (b)), which provided stabilization to the gold nanoparticles. The mechanism, responsible for the reduction to nanoparticles by plant mediated methods, is still unclear as a single plant cell itself is a complex nanosystem. Recent reports have mentioned that the phenolic compounds present in the plant matrix might act as reducing agents for the formation of nanoparticles. Pine needles contain a high amount of condensed tannins such as polymeric and oligomeric proanthocyanidins made up of flavan-3-ol units (Weber et al., 2006). Similarly maple leaves also contain hydrolysable and condensed tannins (Baldwin et al., 1987). Therefore we hypothesize that the phenolic compounds present in maple leaves and pine needles might be responsible for the successful reducing of the gold nanoparticles. Currently, further studies are conducted by our group to identify the phenolic compounds responsible for the bioreduction of gold nanoparticles.

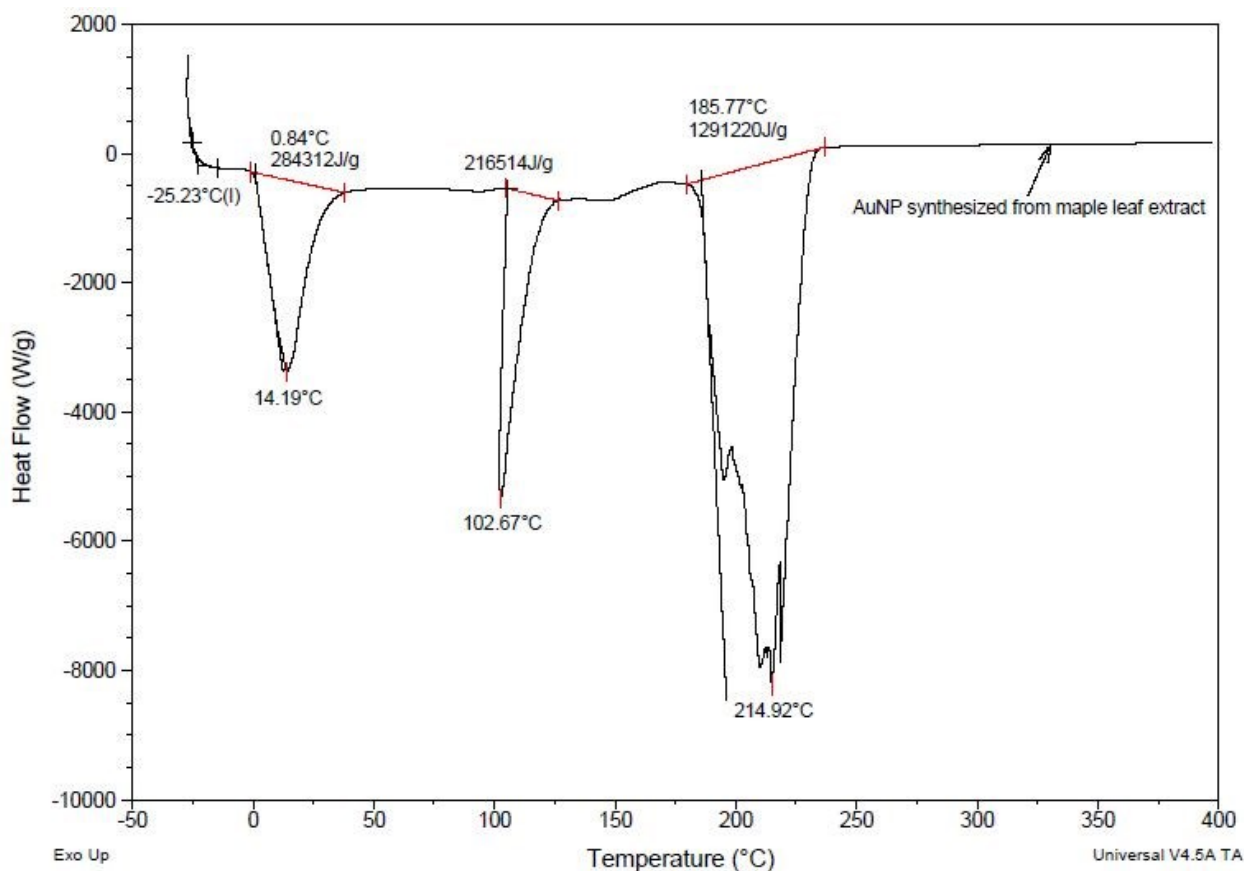


Figure 4.4 DSC thermographs obtained for gold nanoparticles synthesized using maple leaf extract

The analysis of the thermal properties of the nanoparticle solutions synthesized from maple leaf and pine needle extracts showed an interesting behavior. Presently there is no report in the literature on the thermal properties of gold nanoparticles synthesized from maple leaf and pine needle extracts. The experiments were conducted from a temperature range of -30 °C to 400 °C with a heating rate of 10 °C/ min. The DSC thermograph for gold nanoparticles synthesized using maple leaf extract is shown in Figure 4.4. From the thermograph obtained from maple leaves it can be seen that the onset of the initial crystallization phase occurred near -30 °C and while the glass transition temperature (T_g) occurred at -25.23 °C. The onset melting temperature (T_m)

was at 0.84 °C indicating the phase change from solid to liquid phase with the heat capacity of 284.31 kJ/g. The steep peak at 102.67 °C might be due to hydrated molecules present in the plant matrix and the final decomposition peak for the gold nanoparticles synthesized from maple leaf was at 214.92 °C with a considerable heat capacity of 1291.22 kJ/g.

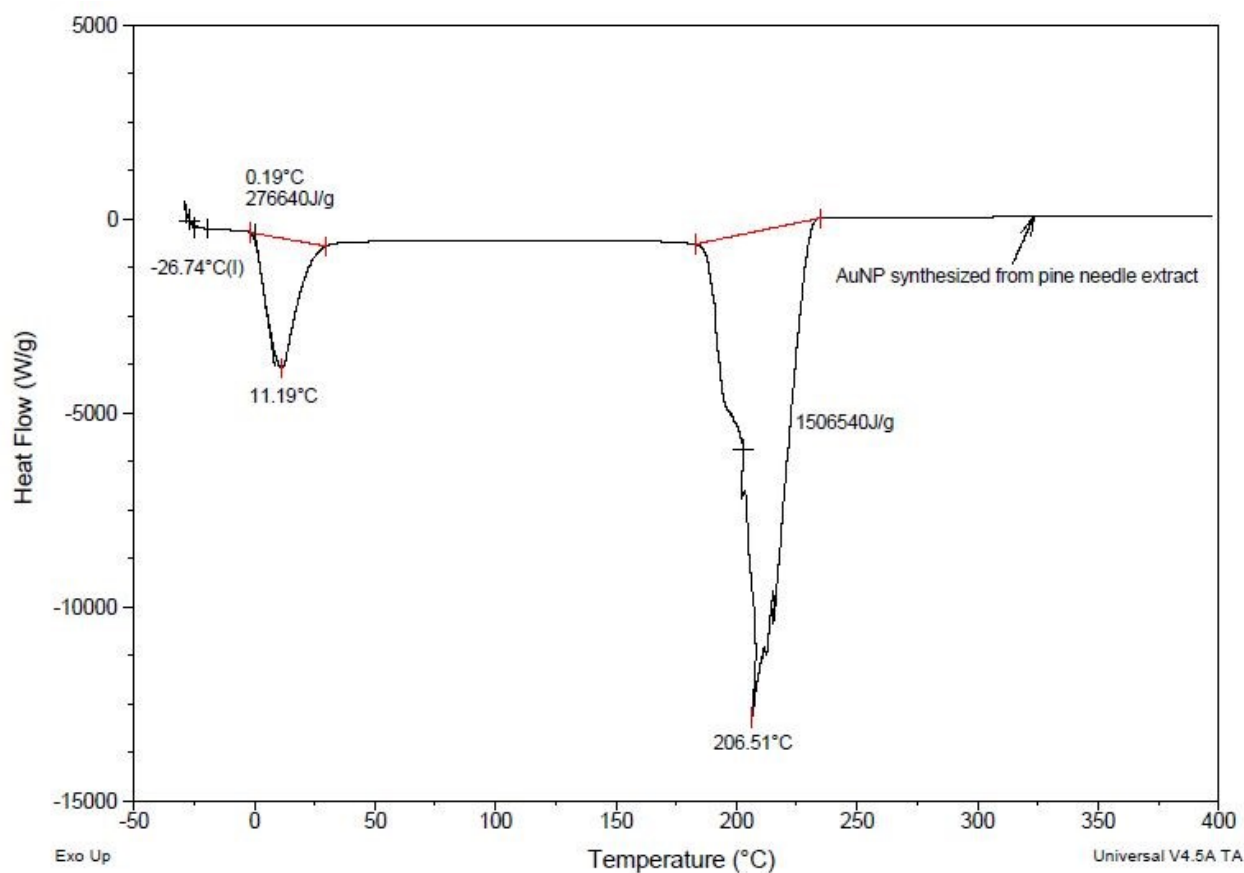


Figure 4.5 DSC thermographs obtained for gold nanoparticles synthesized using pine needle extract

Figure 4.5 presents the DSC thermograph for gold nanoparticles synthesized from pine needle extract. The glass transition temperature was at -26.74 °C followed by the melting onset temperature at 0.19 °C with the heat capacity of 276.64 kJ/g. The final decomposition peak for gold nanoparticles synthesized from pine needle extract was at 206.51 °C with a heat capacity of 1506.54 kJ/g. The temperature of decomposition for the gold nanoparticles from both the plant mediated synthesis were 10 °C apart with pine mediated AuNP having higher heat capacity.

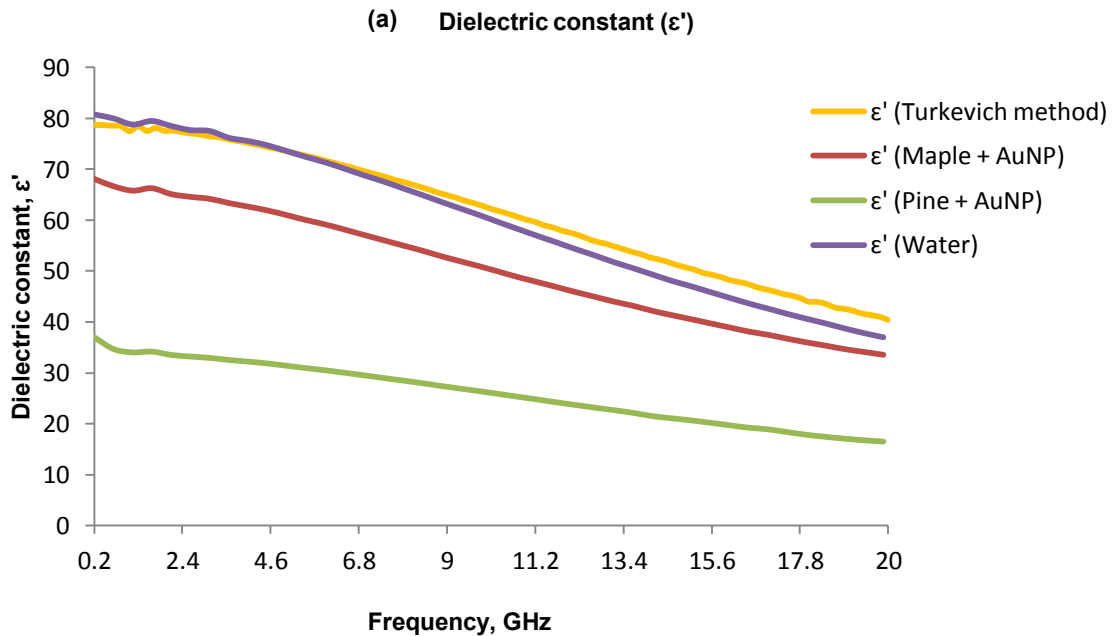
Dielectric spectroscopic measurements are fast and non-destructive with no specific requirements for sample preparation. In this study, the broadband frequency range from 200 MHz to 20 GHz was selected as the dielectric properties of a material vary with frequency. The selected frequency range falls between the very high radio frequency (RF, 30-300 MHz) and ultra-high frequency (300-3000 MHz) in the microwave region (Orsat, 2010). With the selected frequency range the applied energy travels down through the cable, into the open ended coaxial probe, the field fringes out into the material and how it reflects back depends upon the inherent properties of the material. From the measured reflected data we can calculate the complex permittivity (ϵ^*) with real (ϵ') and imaginary parts (ϵ'').

$$\epsilon^* = \epsilon' - j\epsilon'' \text{ (farads/meter)} \quad (\text{Eq. 4.1})$$

The dielectric constant (ϵ') is the material's ability to store electrical energy and the dielectric loss factor (ϵ'') is the material's ability to dissipate electrical energy. The loss tangent or dissipation factor ($\tan \delta = \epsilon''/\epsilon'$) is related to the material's ability to penetrate and dissipate electrical energy as heat. The measurements were obtained at $20 \pm 3^\circ\text{C}$.

Pure water has a high dielectric constant (ϵ') of 80.4 at 20°C due to the presence of dipole moments that cause polarization. Under the influence of an applied electric field, water tends to easily polarize. The presence of H^+ and OH^- ions in water leads to effective electrical conduction. Knowledge of a material's dielectric property can help determine its molecular structure. A change in molecular structure can lead to a change in dielectric properties. A dielectric material (host material) containing filler particles with sizes of 10- 100 nm (nanoparticles) in a well dispersed state constitutes a nanodielectric system. The host materials can be solids, liquids or polymers in which nanoparticles are dispersed. In our case the host material are plant extracts in water, with the synthesized gold nanoparticles in suspension. The green synthesized nanofluids using plant extract were compared with the gold nanoparticles synthesized using Turkevich method. Chlorauric acid solution (95 ml) was heated to 100°C and 5 ml of 1% sodium citrate solution was added to boiling solution with good mechanical stirring. Deep wine red colour gold nanoparticles were formed. The results from the electron microscopic study reported spherical particles and this method is considered as a standard method due its high reproducibility (Li et al., 2011; Turkevich et al., 1951).

The pine needle and maple leaf extracts mediated gold nanoparticle solutions exhibited dielectric constant values lower than water which decreased slowly with an increase in frequency in the considered frequency range (Figure 6 (a)). The ϵ' for maple leaf extract mediated AuNP ranged from 68.11 to 33.55 for the selected frequency of 200 MHz - 20 GHz. The ϵ' for pine needles mediated AuNP ranged from 37.01 to 16.50 for the selected frequency range, which is much less compared to the ϵ' for pure water. It is interesting to note that the dielectric properties of gold nanoparticles synthesized using the Turkevich method was similar to the dielectric properties of water from 200 MHz to 6.5 GHz and from 6.5 GHz to 20 GHz the dielectric constant was slightly more than that of water. The dielectric constant for AuNP by Turkevich method ranged from 78.71 to 40.41 and for water it ranged from 80.77 to 36.99 over the frequency range of 200 MHz - 20 GHz.



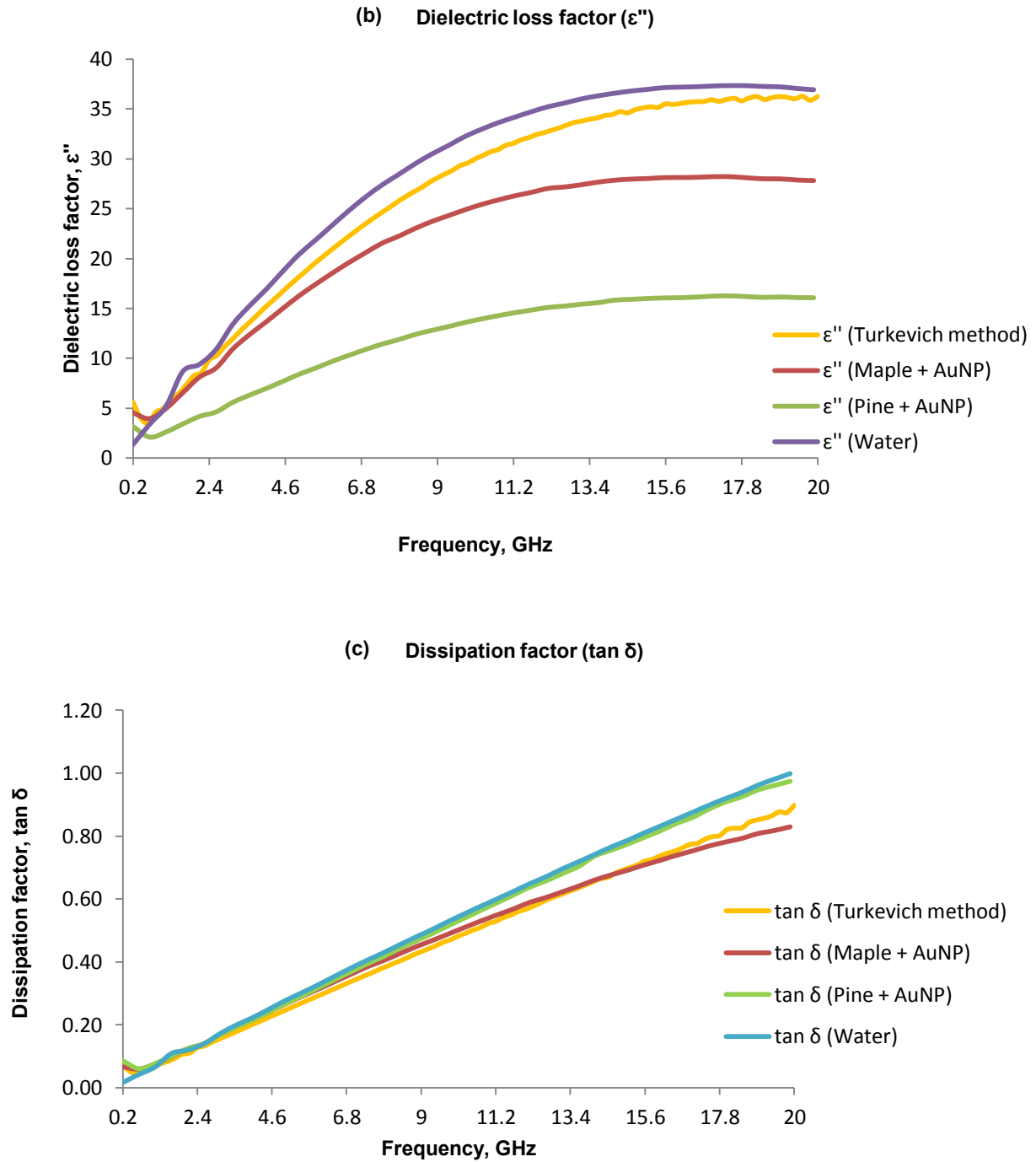


Figure 4.6 Graph showing (a) dielectric constant (ϵ'); (b) dielectric loss factor (ϵ''); (c) dissipation factor ($\tan \delta$) for gold nanofluids from plant extracts and from the Turkevich method over the frequency range from 200 MHz to 20 GHz

The dielectric loss factor (ϵ'') determines the ease with which a material can be heated by an applied electromagnetic energy field. High values of ϵ'' lead to desirable volumetric heating and low values of ϵ'' indicate the material's transparency to the incoming energy.

From Figure 4.6(b), it can be seen that the dielectric loss factor (ϵ'') increases with an increase in frequency (200 MHz - 20 GHz). The gold nanoparticle solution exhibited a similar trend to water with lower dielectric loss factor. The ϵ'' values for maple + AuNP ranged from 4.52 to 27.82 and ϵ'' values for pine + AuNP ranged from 3.15 to 16.07 for the selected frequency range. It was found that the dielectric loss factor for the AuNP synthesized using the Turkevich method was higher than that of pine and maple extract synthesized AuNP ranging from 5.60 to 36.26.

The loss tangent ($\tan \delta$) values for maple + AuNP ranged from 0.06 to 0.83; and for AuNP synthesized using the Turkevich method ranged from 0.07 to 0.89 for the selected frequency of 200 MHz - 20 GHz. The $\tan \delta$ values for pine + AuNP ranged from 0.08 to 0.97 for the selected frequency range. Figure 4.6(c) shows that there was an increase in the dissipation factor with an increase in frequency. It is exciting to see that pine + AuNP solution exhibited lower ϵ' and ϵ'' values compared to water, but for the dissipation factor ($\tan \delta$), the trend was similar to that of water. This shows that the pine + AuNP solution has better heat dissipation properties when compared to maple synthesized AuNP solution and AuNP solution synthesized by the Turkevich method. The dielectric data obtained from this study is additional information complimentary to the gold nanoparticles research to date as it has been found that the behavior of nanofluids synthesized using water as a solvent has similar properties as that of water.

This makes these green synthesized gold nanoparticles to be an excellent material to be used in microwave environment for heating applications. As far as the literature is concerned, there is no report till date stating the use of maple leaves for the synthesis of a gold nanoparticle along with its characterization. There are many factors such as seasonal variation, leaf age, leaf canopy, variation due to genotype; geographical locations, etc. which might have an effect on the secondary metabolites produced by the plants. It would be interesting to study the effect of these individual factors on the plant materials and how these affect the formation of gold nanoparticles. This will provide interesting results, related to green synthesized gold nanoparticles with varying size, shape, structure, all having enormous potential for a variety of application related developments.

4.5 Conclusions

This is the first study reporting that gold nanoparticles can be synthesized using maple leaf and pine needle extracts following the principles of green chemistry. To our knowledge this is the first report on the nanodielectric properties of green synthesized gold nanoparticles using maple leaf extract and pine needle extract comparing with the Turkevich method. These properties will be useful in the development of better tools for various biomedical applications such as the hyperthermal treatment of cancer, tissue/tumor imaging, etc. We strongly believe that such studies will open new avenues for more research on nanodielectrics and plant based synthesis of AuNP through a green nanotechnology approach.

CONNECTING STATEMENT TO CHAPTER V

Results from Chapter III and IV, have proven that gold nanoparticles can be synthesized from grape waste, maple leaves and pine needles. The understanding of the mechanisms involved in the synthesis of nanoparticles is in its infancy and represents challenging questions that many researchers in this field are trying to address. As the plant matrix is a complex system composed of multiple compounds that may be too numerous to help in understanding the mechanism, a representative compound, catechin present in grapes and pine needles, was selected for further study. **Chapter V** deals with the gold nanofluidic solutions synthesized from catechin. The experiments and results interpretation were performed by Ms. Krishnaswamy under the guidance of Dr. Orsat. The results of this chapter were published in the *Journal of Experimental Nanoscience* in 2015.

1. Krishnaswamy, K. and V. Orsat, Gold nanofluids synthesised using antioxidant catechin, its characterisation and studies on nucleation. **Journal of Experimental Nanoscience**. 2015, DOI: 10.1080/17458080.2015.1061217.

Part of this chapter will be presented in the forthcoming conference, 12th International Congress on Engineering and Food (IFEC12), in June 2015, Quebec City, Quebec, Canada.

CHAPTER V

GOLD NANOFLUIDS SYNTHESIZED USING CATECHIN AND THEIR CHARACTERISATION

5.1 Abstract

Nanofluids are a new class of fluids where nano-sized solid particles (AuNP) are dispersed in a liquid medium. This study aims to experimentally investigate the production of gold nanofluids using catechin, a polyphenolic compound. The characterization of the green synthesized nanoparticles using UV-Visible spectrophotometry, differential scanning calorimetry (DSC), dielectric spectroscopy, and transmission electron microscopy (TEM), attempts to generate information to understand the properties of green synthesized gold nanofluids. Four nanofluids were prepared by varying their concentrations between catechin and tannic acid to form AuNP in water. The gold nanofluids exhibited interesting thermal, surface plasmon resonance (SPR) and dielectric properties. The formation of the gold nanoparticles was studied using two different methods using transmission electron microscopy and they exhibited interesting growth patterns within 1 minute. These results are significant as they shed light on the importance of the onset of AuNP formation.

Keywords: Green nanotechnology; Nanodielectrics; Transmission electron microscope (TEM); Differential scanning calorimeter (DSC).

5.2 Introduction

Nanofluids are nanoscale colloidal suspensions having a two-phase system (solid phase containing condensed nanomaterial and a liquid phase). Nanofluids (*nano particle fluid* suspension) are engineered by suspending nanoparticles in aqueous or organic medium (Choi, 2009; Das et al., 2008; Puliti et al., 2011). Nanofluid technology has seen a progressive development over the past decade and Eijkel and Van Den Berg (2005) stated that the study of the fundamental properties of the nanofluids will facilitate untapped possibilities for nanofluidic applications. Nanofluids can be produced by two methods, a two-step production method and a single-step production method. The two-step method is the most commonly used method for preparing nanofluids. Physical methods of particulate formation, such as inert-gas condensation, thermal spray, and ball milling are used to produce nanomaterials in a dry powder form as the first processing step. Then the nanosized powders are dispersed in a fluid (organic or aqueous medium) by intensive magnetic force agitation, ultra-sonication, high shear mixing, and homogenization as a second processing step (Yu & Xie, 2012; Zhu et al., 2000).

As the nanopowder synthesis methods have already been scaled up to industrial production levels, the two-step method is the most widely used nanofluid synthesis procedure. Many researchers purchase commercially available nanoparticles in powder form and mix them with the base fluid with the potential addition of a surfactant (Choi, 2009). The most important issue facing the two-step method is the stability of the nanofluids. The high surface area and surface activity of the nanoparticles lead to aggregation and instability of the suspension in nanofluids. Thus the nanofluid research

community is searching for alternative techniques for developing stable nanofluids using a one-step method.

The single-step method involves chemical synthesis methods, where simultaneous formation and dispersion of nanoparticles occur within the host fluid. Water, oil, acetone, decene and ethylene glycol are some of the commonly used base fluids. The unit operations such as drying, storage, transportation and dispersion of nanoparticles which are required in the two-step method are reduced in the single-step method. Thus increasing the stability of the nanofluids and minimizing particulate agglomeration (Li et al., 2009). Some of the stabilizers used in the single-step method are tri-*n*-octylphosphine oxide (Guo et al., 2001), oleic acid (Hyeon et al., 2001), dodecane thiol (Taleb et al., 1997), cetyltrimethyl ammonium – bromide (Jana et al., 2001), thiols (Brust et al., 1994), etc. The concentration and composition of the stabilizers vary depending upon different synthesis protocols. The most important disadvantage encountered in the single-step method for nanofluids synthesis is the presence of residual stabilizers in the nanofluids due to incomplete reactions. It is difficult to eliminate and purify the nanofluids from such impurities (Yu & Xie, 2012).

The study of colloidal suspensions with micron sized particles has been in existence since way before the nanotechnological era, but their size posed significant corrosion problems in engineering applications (Puliti et al., 2011). Rapid settling of millimeter or micrometer sized particles in fluid suspension is also a major problem. Such particles are not applicable for microsystems as they can clog the microfluidic channels. The uniform dispersion and stable suspension of nanoparticles in the host fluids can be a

solution to this problem. Table 5.1 below shows the stability results obtained when comparing microparticles and nanoparticles as adapted from Das et al. (2008).

Table 5.1 Benefits of nanofluids containing nanoparticles versus microparticles (Das et al., 2008)

Properties	Microparticles	Nanoparticles
Stability	Settle	Stable
Surface/volume ratio	1	1,000 times larger than microparticles
Clog in microchannel	Yes	No
Erosion / abrasion of microchannels	Yes	No

The previously described two-step production and single-step production methods either use toxic chemicals in their synthesis protocols or might require high energy consuming equipment. Recent concerns and challenges facing nanotechnology are demanding the manufacturing of safe, less toxic, less energy consuming nanoparticles. Looking forward, it is prudent to reason and develop green nanofluids by choosing safe nanoparticles with less toxic chemicals. Choi (2009) stated that low-cost, high-volume production of green nanofluids would be one of the most challenging future research directions. Hence in order to address the above mentioned issues, this study aims to use catechin, a polyphenolic compound present in various agricultural waste materials such as grape seed, skin, stalk, pine needles, etc., for successful synthesis of green gold nanofluids.

5.3 Materials and methods

5.3.1 Sample preparation

Chloroauric acid trihydrate ($\text{HAuCl}_4 \cdot 3\text{H}_2\text{O}$), catechin and tannic acid were obtained from Sigma-Aldrich. One mM concentration of catechin, tannic acid and HAuCl_4 solutions were prepared with deionized water. Four different nanofluids containing gold nanoparticle were prepared as shown in Figure 5.1, and details of the composition are provided in Table 5.2.

Table 5.2 Composition of four different nanofluids synthesized using catechin (CAT) and tannic acid (TAE)

Sample Code	AuNP Nanofluids	Catechin (ml)	Tannic acid (ml)	HAuCl_4 (ml)	Total reaction volume (ml)	Temp (°C)
A	TAE + AuNP	-	5	5	10	25
B	1:1 CAT: TAE + AuNP	2.5	2.5	5	10	25
C	1:4 CAT: TAE + AuNP	1	4	5	10	25
D	CAT + AuNP	5	-	5	10	25

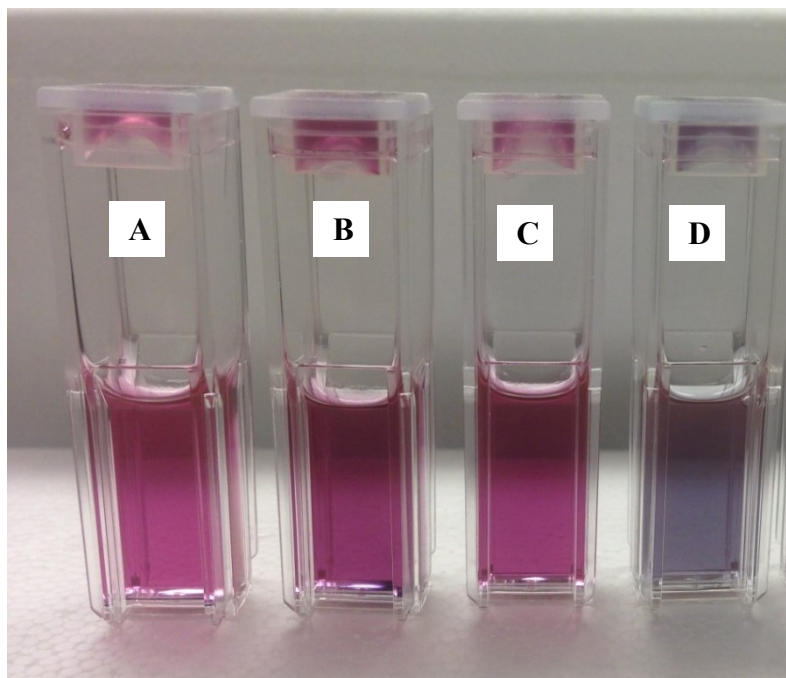


Figure 5.1 Green nanofluids containing gold nanoparticles

5.3.2 UV-Vis Spectrophotometer

UV-visible spectra were recorded using a spectrophotometer (Ultrospec 2100 pro, Biochrom Ltd., Cambridge, England). The time of addition of the HAuCl_4 solution to the polyphenol solution was considered as the start of the reaction. The colour change from the light yellow colour of HAuCl_4 to pink indicates the formation of gold nanoparticles. The synthesis of gold nanoparticles was monitored by periodic sampling of the nanoparticle solution using the wavescan mode of Ultrospec 2100 pro spectrophotometer from 400 – 800 nm wavelengths with medium scan and a step size of 1 nm.

5.3.3 Differential Scanning Calorimeter

The thermal properties such as specific heat, melting and boiling point of the gold nanofluids were studied using a differential scanning calorimeter (DSC Q-100 V9.8 built 296, TA Instruments, Texas, USA). Sample solutions containing gold nanoparticles (500 μ l) were centrifuged at 8000 rpm for 4 min. The AuNP particles were collected and 20 μ l of the AuNP particles were placed in small aluminum pans. The sample pans were hermetically sealed. The samples were made to cover the entire bottom surface of the pan to ensure good thermal contact. Care was taken to prevent over filling of the pan. Nitrogen was used as the purge gas as it is inert in nature. The rate of flow of nitrogen was 50 ml/min. Indium was used for calibration. The system was equilibrated at -20 $^{\circ}$ C, with ramp increase in temperature at 10 $^{\circ}$ C/min up to 400 $^{\circ}$ C. Reproducibility was checked by running samples in triplicates. TA Universal Analysis V4.5A software was used for processing the obtained data.

5.3.4 Dielectric spectroscopy

The interactions of nanoparticles with microwave energy can be determined by studying the dielectric properties of the nanofluids. Dielectric spectroscopy measurements consist of a dielectric probe and a network analyser to measure the dielectric properties that a material possesses at the microwave frequency of interest (Liao et al., 2001). The dielectric constant (ϵ') is an indicator of a material's capacity to store energy. The dielectric loss factor (ϵ'') is an indicator of the material's ability to convert the absorbed microwave energy into heat. The loss factor, $\tan \delta = \epsilon'' / \epsilon'$, is an overall indicator representing the microwave heating capacity of the material. In order to determine the microwave heating ability of the gold nanoparticles, the dielectric properties were measured for the green AuNP nanofluids.

5.3.5 Transmission electron microscopy

A drop of the nanofluid sample was added on carbon coated TEM grids. The solution on the TEM grid was allowed to stand for 1 min and the extra solution was carefully removed by using filter paper to form a thin film. The sample was left at room temperature until a dried film was obtained. Transmission electron microscopy (TEM) analyses were performed using FEI Tecnai G² F20 Cryo-S/TEM operated at 200 kV with Gatan Ultrascan 4k x 4k Digital (CCD) Camera System.

5.4 Results and discussion

5.4.1 Thermal properties of nanofluids

Experimental results on the specific heats of nanofluids are very limited and recently this property is gaining importance for designing new products and applications (Puliti et al., 2011). This study aims to provide experimental data on the specific heat of nanofluids containing gold nanoparticles.

The differential scanning calorimeter (DSC) is a useful instrument to determine the thermal transition of a material associated with heat flow as a function of time and temperature. Qualitative and quantitative data on the endothermic (heat absorption) and exothermic (heat evolution) processes of a material, during phase changes, can be obtained using a DSC thermogram. The DSC curve provides the fingerprint about the thermal behavior of a compound under analysis. The peaks are observed by a characteristic shift from the base line either up or down. The area under the peak is proportional to the amount of heat developed during a reaction. From the DSC curves, enthalpies of transitions are computed by integrating the peak corresponding to the given transition.

In DSC peak integration, the sample size is used to normalize the area under the peak and to obtain the experimental heat in joules per gram. On the y-axis the heat units are expressed in watts per gram while the x-axis is expressed as a function of both time and temperature. For engineering applications, knowledge of both time and temperature dependency is important hence in this study the thermal properties of the AuNP nanofluids are expressed as a function of both parameters. The thermal behaviour of the nanofluids was monitored over a range of temperatures from -20 °C to 400°C with an increase in temperature programmed at 10 °C/min.

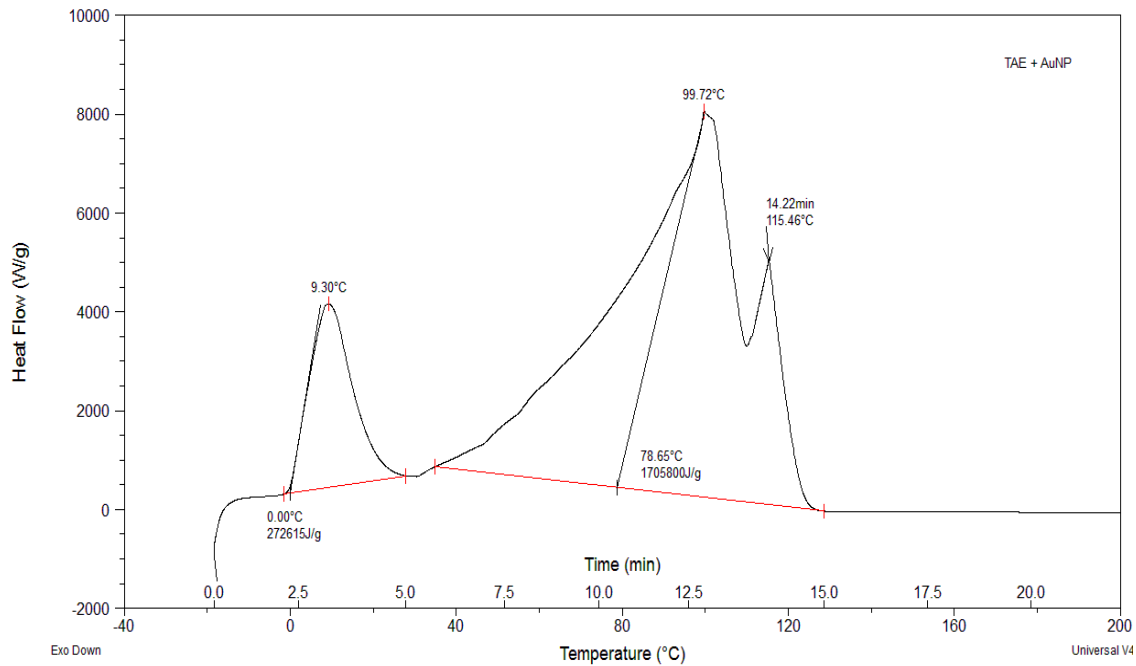


Figure 5.2 DSC thermogram for TAE +AuNP nanofluid (sample A)

The DSC thermogram presented in Figure 5.2 (TAE + AuNP) shows a sharp melting endothermic peak with an onset melting temperature at zero degrees Celsius. The peak maximum was at $9.30^{\circ}\text{C} \pm 0.39^{\circ}\text{C}$ with the peak onset at 0°C , stating the

conversion of solid phase to liquid phase. The specific heat (C_p) of the system during this transition is $272.62 \text{ kJ/g} \pm 13.93 \text{ kJ/g}$. Figure 5.2, shows the appearance of a broad transition for the TAE + AuNP nanofluids with an onset temperature at $78.65 \text{ }^\circ\text{C} \pm 8.01 \text{ }^\circ\text{C}$ and the peak maximum was obtained at $99.72 \text{ }^\circ\text{C} \pm 1.96 \text{ }^\circ\text{C}$, which can be related to the phase change from liquid to vapour state. The interesting fact during this transition is the broad transition time and the C_p required during this transition which is $1705.80 \text{ kJ/g} \pm 60.83 \text{ kJ/g}$. A secondary shoulder peak of the broad thermal transition was obtained around 14 min at $115.46 \text{ }^\circ\text{C}$.

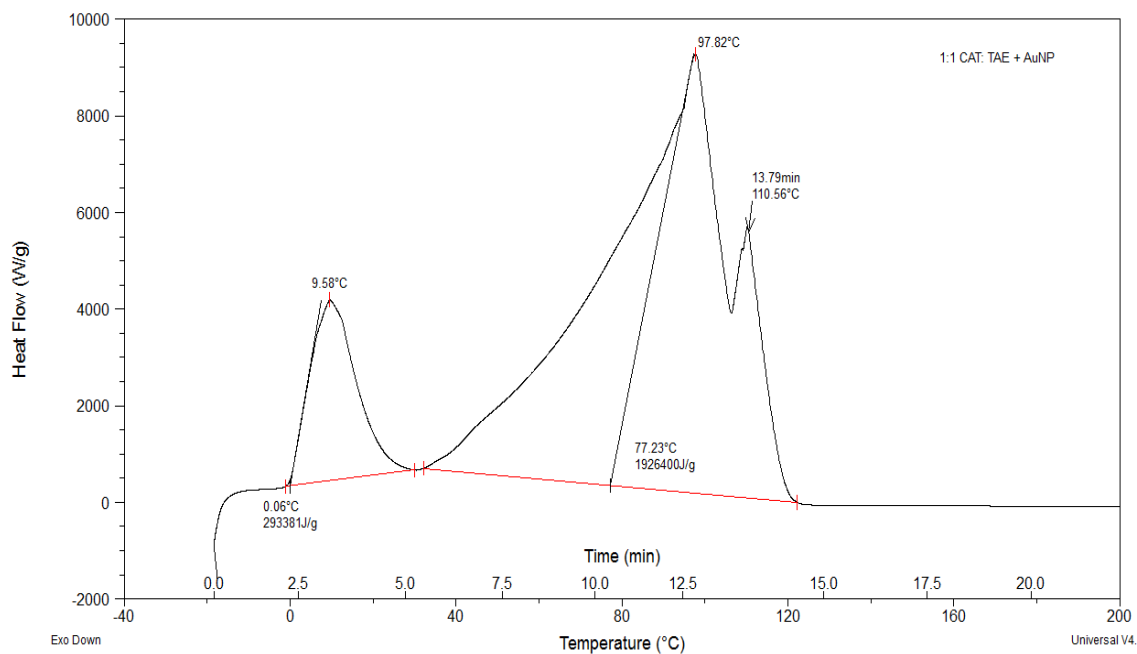


Figure 5.3 DSC thermogram for 1:1 CAT: TAE + AuNP nanofluid (sample B)

A similar trend for the DSC thermogram was obtained for the nanofluids synthesized using 1: 1 CAT : TAE + AuNP. Figure 5.3 shows a melting endothermic peak with an onset melting temperature at zero degrees Celsius. The peak maximum was

at $9.68^{\circ}\text{C} \pm 5.59^{\circ}\text{C}$ with the peak onset at 0°C , stating the conversion of solid phase to liquid phase. The specific heat (C_p) of the system during this transition is $289.74 \text{ kJ/g} \pm 5.15 \text{ kJ/g}$. A broad thermal transition for the 1:1 CAT: TAE + AuNP nanofluids occurred with an onset temperature at $76.63^{\circ}\text{C} \pm 0.86^{\circ}\text{C}$ and the peak maximum was obtained at $97.55^{\circ}\text{C} \pm 0.38^{\circ}\text{C}$, where the C_p required during this transition was $1911.34 \text{ kJ/g} \pm 21.31 \text{ kJ/g}$ along with a secondary peak around 14 min at 110.56°C .

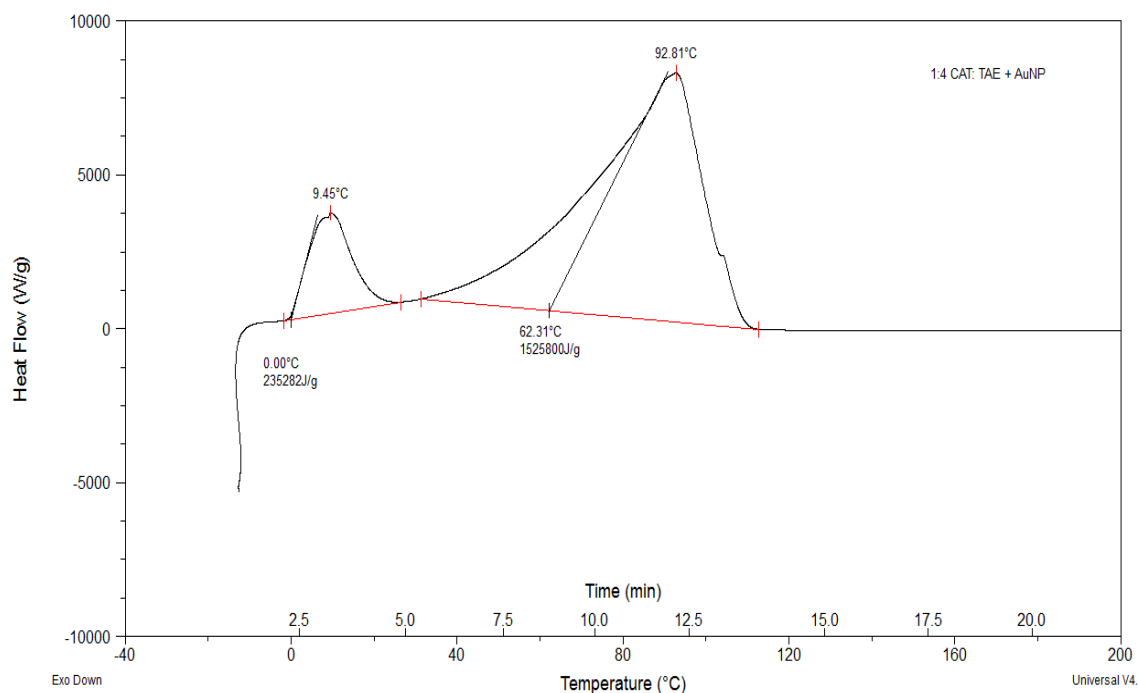


Figure 5.4 DSC thermogram for 1:4 CAT: TAE + AuNP nanofluid (sample C)

In the DSC thermogram for 1:4 CAT:TAE + AuNP nanofluid (Figure 5.4), a large portion of the exothermic crystallisation process can be seen around -20°C followed by a melting endothermic peak as the temperature rises. The peak maximum was at $8.94^{\circ}\text{C} \pm 0.45^{\circ}\text{C}$ with the peak onset at 0°C , stating the conversion of solid phase to liquid phase. The specific heat (C_p) of the system during this transition was $250.43 \text{ kJ/g} \pm$

15.81 kJ/g. Figure 5.4 shows the appearance of a broad transition for the TAE + AuNP nanofluids with an onset temperature at $63.85\text{ }^{\circ}\text{C} \pm 2.17\text{ }^{\circ}\text{C}$ and the peak maximum was obtained at $94.58\text{ }^{\circ}\text{C} \pm 2.50\text{ }^{\circ}\text{C}$, and the C_p required during this transition was $1689.03\text{ kJ/g} \pm 95.25\text{ kJ/g}$ which is relatively lower than for the other nanofluids. The interesting thermal behaviour of 1:4 CAT:TAE + AuNP nanofluid is illustrated in the lower onset endothermic temperature for the first and the second peak, relatively lower C_p for both the thermal transitions, and disappearance of the secondary shoulder peak.

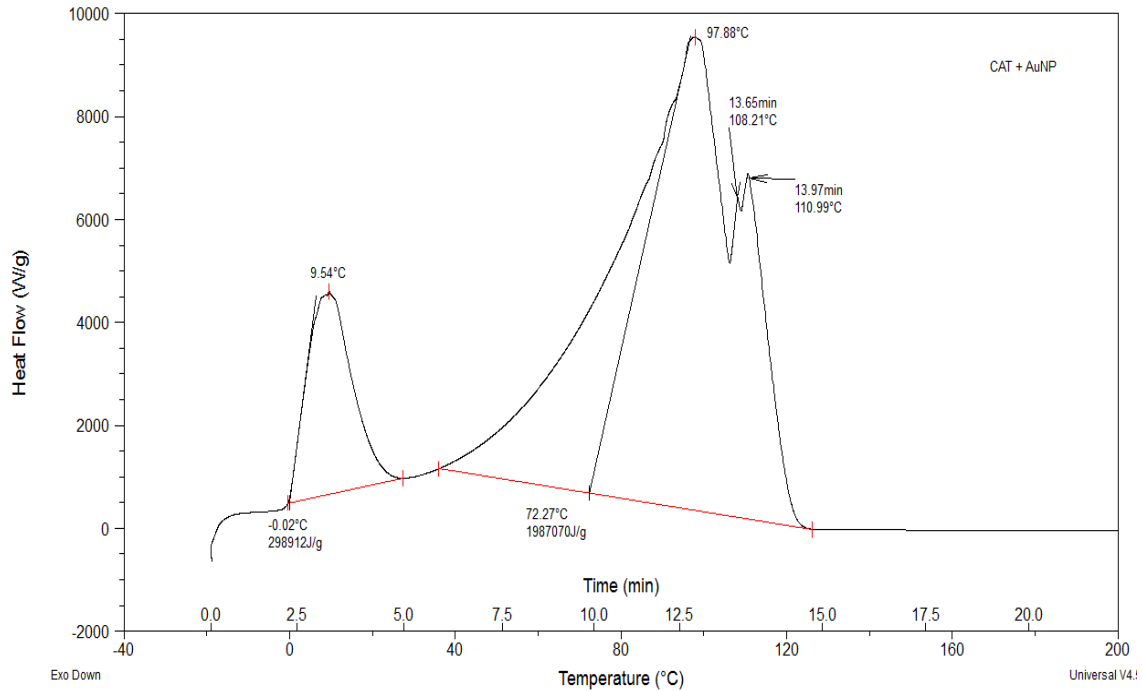


Figure 5.5 DSC thermogram for CAT + AuNP nanofluid (sample D)

Figure 5.5 shows the DSC thermogram for CAT+ AuNP, with a sharp melting endothermic peak with an onset melting temperature at -0.02°C and the peak maximum was at $9.53^{\circ}\text{C} \pm 0.55\text{ }^{\circ}\text{C}$ stating the conversion of solid phase to liquid phase. The specific heat (C_p) of the system during this transition is comparatively higher to other nanofluids in this study, $297.00\text{ kJ/g} \pm 2.70\text{ kJ/g}$. The broad thermal transition for CAT +

AuNP nanofluids occurred with an onset temperature at $74.41\text{ }^{\circ}\text{C} \pm 8.44\text{ }^{\circ}\text{C}$ and the peak maximum was obtained at $96.90^{\circ}\text{C} \pm 0.90\text{ }^{\circ}\text{C}$, and the C_p required during this transition was $1944.76\text{ kJ/g} \pm 77.49\text{ kJ/g}$. The CAT+AuNP nanofluid has interesting thermal properties as the specific heat for both the thermal transition were comparatively higher than for the other nanofluids, and the occurrence of two secondary shoulder peaks at 13 min at 108.21 and $110.99\text{ }^{\circ}\text{C}$. Figure 5.6, shows the overlay of the DSC thermographs of all the four green synthesized gold nanofluids for visual comparison of their thermal behaviours. The overlay figure presented in Figure 5.6 clearly indicates the disappearance of the secondary peak for 1:4 CAT:TAE + AuNP nanofluids, the reason for such a behaviour will be explained while discussing further results.

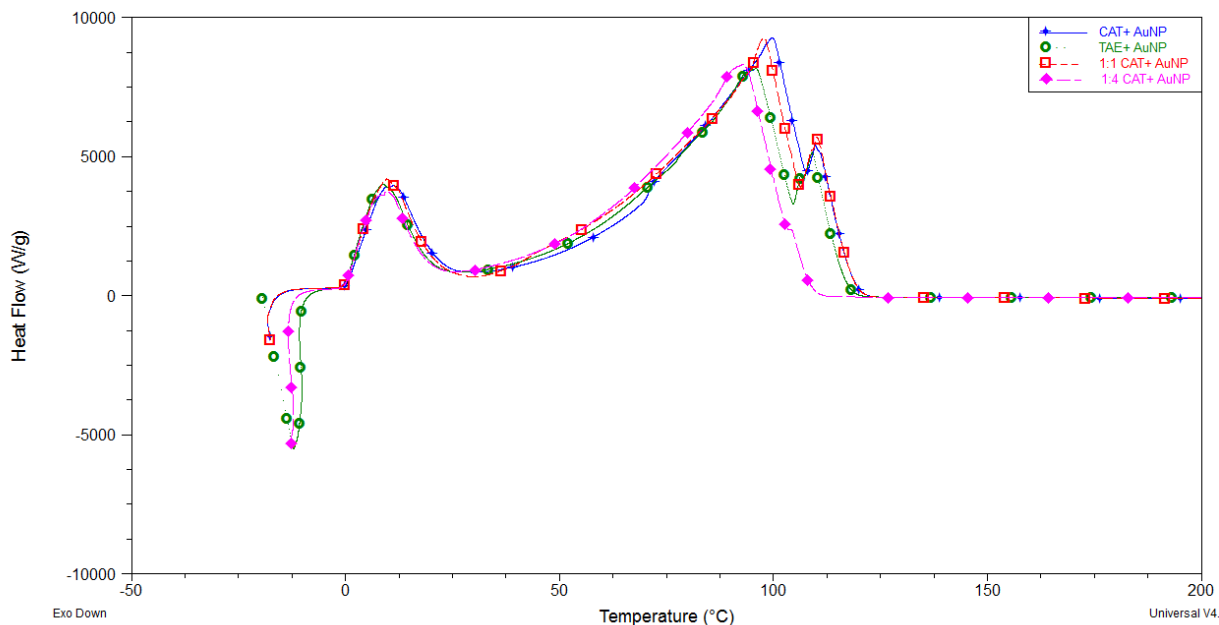


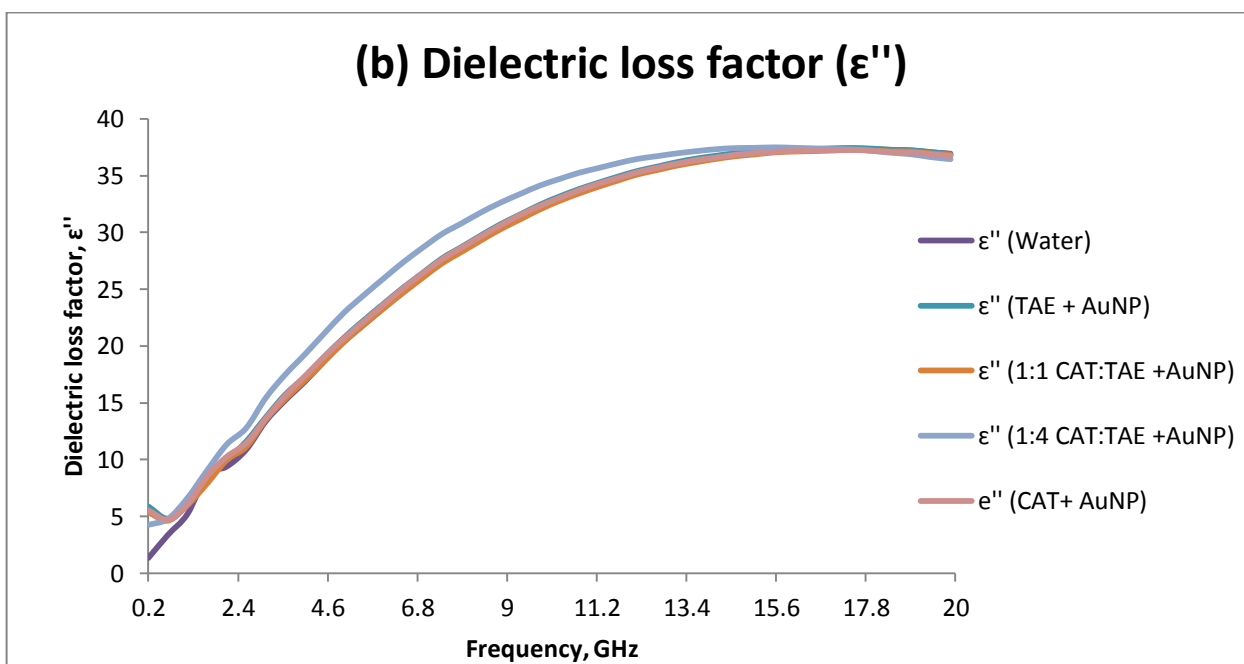
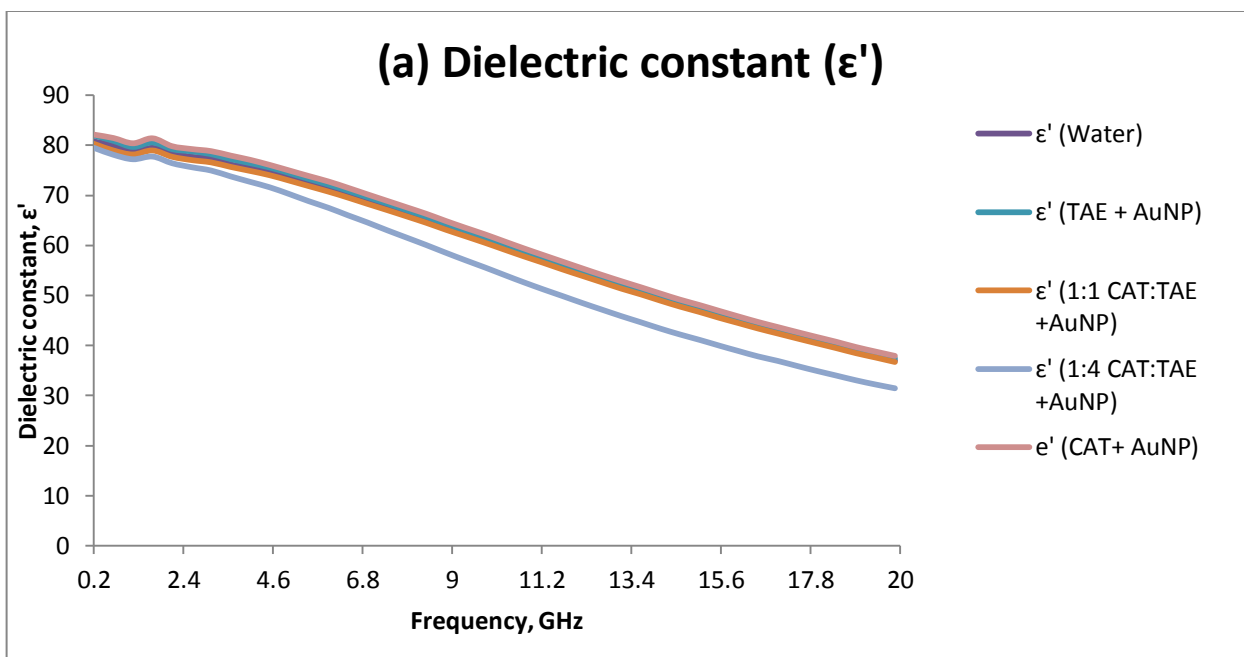
Figure 5.6 Overlay of DSC thermographs for the four different green synthesized AuNP nanofluids

The recent literature on nanofluids states that nanofluids have higher thermal conductivity than the base fluids. Vajjha and Das (2009) experimentally found an

increase in thermal conductivity of three nanofluids containing aluminum oxide, copper oxide and zinc oxide in a base fluid of (60:40) ethylene glycol and water mixture compared to base fluid. Shin and Banerjee (2011) reported anomalous enhancement of specific heat (14.5 % increase) of SiO_2 /chloride nanofluid prepared from barium chloride, sodium chloride, calcium chloride and lithium chloride along with silicon dioxide. Dudda and Shin (2013) studied the specific heat capacity using DSC for four different nanomaterials containing binary nitrate salt (NaNO_3 and KNO_3) and found that the specific heat capacity was enhanced with an increase in nanoparticle size. The results obtained in the present study are significant and have shown an increase in the specific heat capacity of the green synthesized nanofluids containing AuNP. The surface atoms of the nanoparticles have high specific surface energy compared to the bulk material, this might be responsible for the enhancement of specific heat in the nanofluids (Shin & Banerjee, 2011). Puliti et al. (2011) stated that literature containing experimental data for specific heat of nanofluids is limited. More research has to focus on understanding the specific heat of nanofluids as knowledge about specific heat plays a fundamental role in optimizing many engineering applications.

5.4.2 Dielectric properties of nanofluids

The dielectric properties of nanofluids containing AuNP were studied over a broad frequency range from 200 MHz to 20 GHz. This range was selected to evaluate the dielectric constant (ϵ'), dielectric loss factor (ϵ'') and dissipation factor ($\tan \delta$) for the AuNP nanofluids.



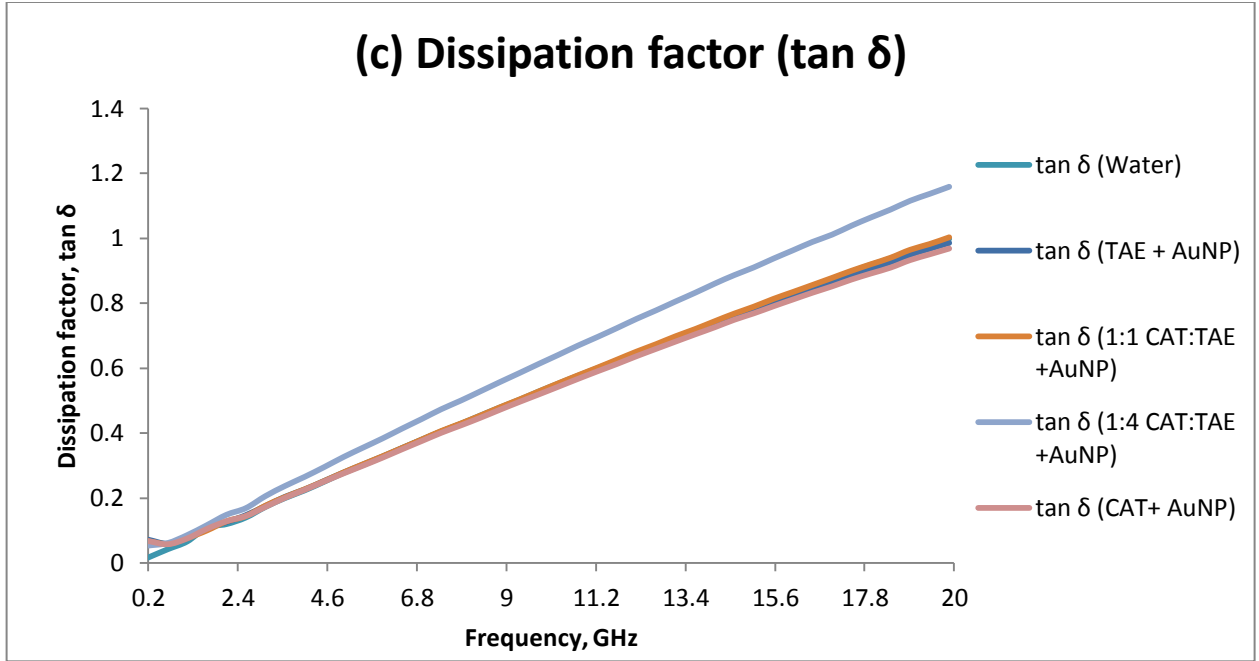


Figure 5.7 Dielectric properties of green synthesized AuNP nanofluids, (a) Dielectric constant (ϵ'); (b) Dielectric loss factor (ϵ''); (c) Dissipation factor ($\tan \delta$)

During the experimentation, it was found that introducing the nanofluids to the microwave environment led to volumetric heating of the nanofluids. This might be due to the direct coupling of the electromagnetic field with the polar and ionic components present in the nanofluids. Therefore, this study was conducted to understand the dielectric properties of gold nanoparticles in water and their interactions with the microwave energy.

From the dielectric properties data we can calculate the complex permittivity (ϵ^*) with real (ϵ') and imaginary parts (ϵ'') which describes the interactions of the electromagnetic waves with the nanofluids.

$$\epsilon^* = \epsilon' - j\epsilon'' \text{ (farads/meter)} \quad (\text{Eq. 5.1})$$

The dielectric constant (ϵ') is the real part of the complex dielectric permittivity, and is the measure of the material's ability to store microwave energy. The dielectric loss factor (ϵ'') is the imaginary component of the complex dielectric permittivity and represents the material's ability to dissipate microwave energy. The loss tangent or dissipation factor ($\tan \delta = \epsilon''/\epsilon'$) is related to the material's ability to penetrate and dissipate electrical energy as heat. The volumetric heating of the microwaves is influenced by the penetration depth, and the lower the frequency, the higher is the penetration depth (Meda et al., 2005; Routray & Orsat, 2013; Venkatesh & Raghavan, 2004). The dielectric properties of the AuNP nanofluids are presented in Figure 5.7. The nanofluids TAE + AuNP, 1:1 CAT:TAE + AuNP and CAT+ AuNP followed a similar trend exhibiting analogous dielectric properties to that of water. The ϵ' for TAE+ AuNP for the selected frequency of 200 MHz to 20 GHz ranged from 81.97 ± 0.32 to 37.43 ± 0.18 ; ϵ' for 1:1 CAT: TAE ranged from 80.30 ± 0.62 to 36.71 ± 0.22 ; ϵ' for CAT + AuNP ranged from 82.14 ± 0.27 to 37.93 ± 0.06 for 200 MHz to 20 GHz. The ϵ' for 1:4 CAT : TAE for the selected frequency ranged from 79.51 ± 0.31 to 31.45 ± 0.23 , which is slightly lower than that of the other nanofluids. The results obtained from this study show an interesting trend for 1:4 CAT:TAE + AuNP, when compared to the other AuNP nanofluids for ϵ' , ϵ'' and $\tan \delta$. It is interesting to note that the $\tan \delta$ for 1:4 CAT: TAE was higher than that of the other nanofluids ranging from 0.06 ± 0.01 to 1.16 ± 0.01 for 200 MHz to 20 GHz.

5.4.3 Interpretation of TEM micrographs

It can be seen from the TEM images for TAE + AuNP (Figure 5.8), that different shapes like spherical, rhomboidal and triangular prisms of AuNP were formed. There was no presence of an organic layer surrounding the gold nanoparticles.

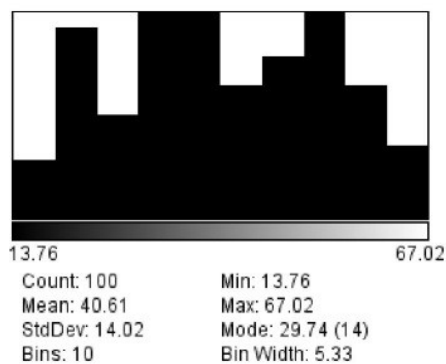
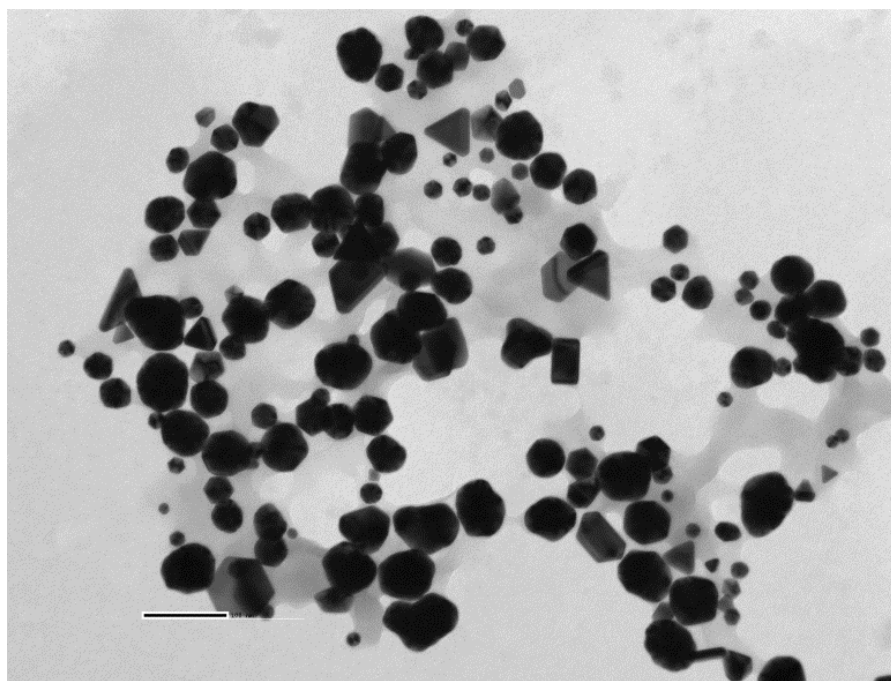


Figure 5.8 TEM micrograph of gold nanoparticles synthesized by TAE + AuNP

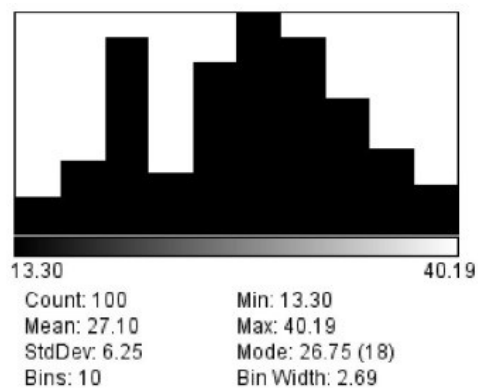
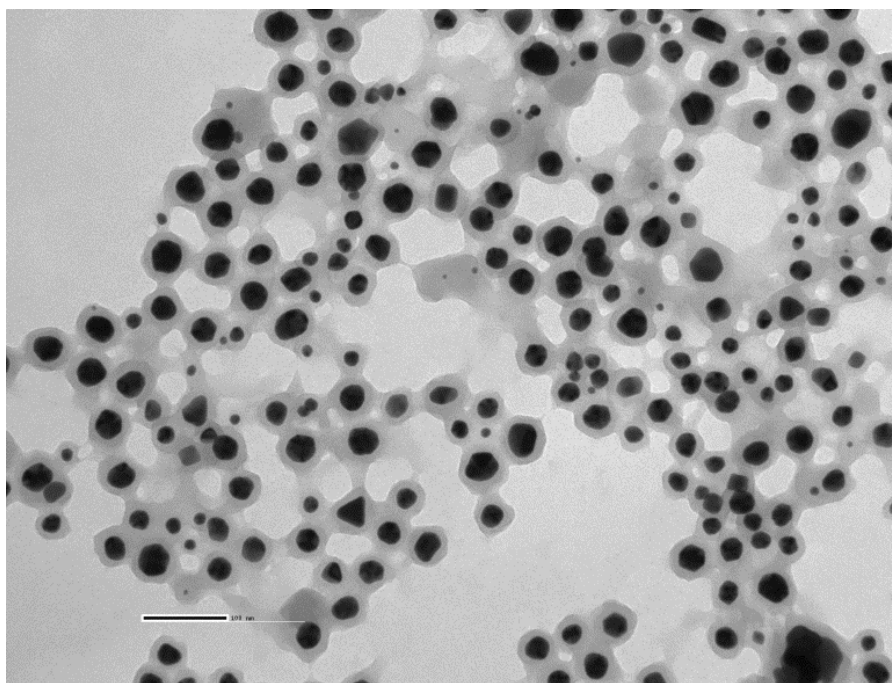


Figure 5.9 TEM micrograph of gold nanoparticles synthesized by 1:1 TAE: CAT + AuNP

Nearly spherical shaped AuNP were synthesized by 1:1 tannic acid and catechin solution. It can be seen from Figure 5.9, that the gold nanoparticles are surrounded by an organic layer. The formed spherical gold nanoparticles were varying in size. From Figure 5.10, it can be seen that a dense layer of organic material is surrounding the gold nanoparticle synthesized using 1:4 TAE:CAT + AuNP. This is interesting as structural formation obtained is different from other gold nanoparticles.

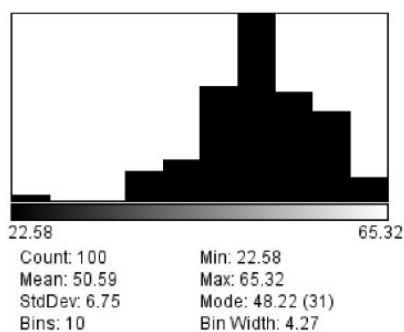
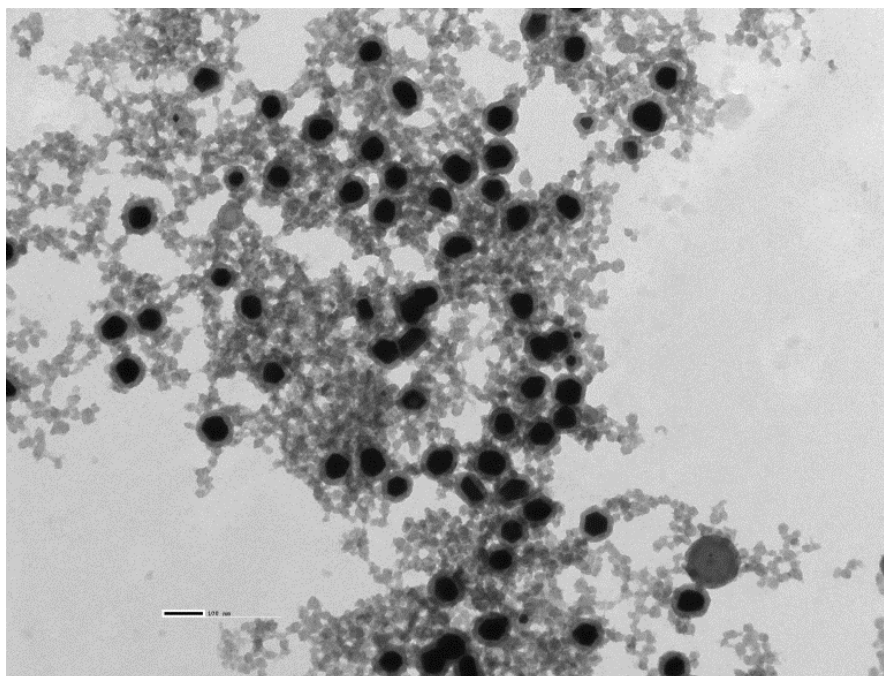


Figure 5.10 TEM micrograph of gold nanoparticles synthesized by 1:4 CAT: TAE + AuNP

The reason for the formation of the organic layer can be due to the interaction between catechin and tannic acid that might have led to the formation of a complex chain surrounding the nanoparticles. It should also be noted that the results obtained for 1:4 CAT:TAE + AuNP from the DSC study and the dielectric properties study showed a different trend compared to the other three nanoparticle systems. Based on the observations from the TEM images, we put forward that the interaction between AuNP and the polyphenolic chain from catechin and tannic acid complex could be a probable

reason for the difference in properties. This could also be the reason for the disappearance of the secondary endothermic peak from the DSC thermogram in Figure 5.4 and the increase in the dissipation factor shown in Figure 5.7(c).

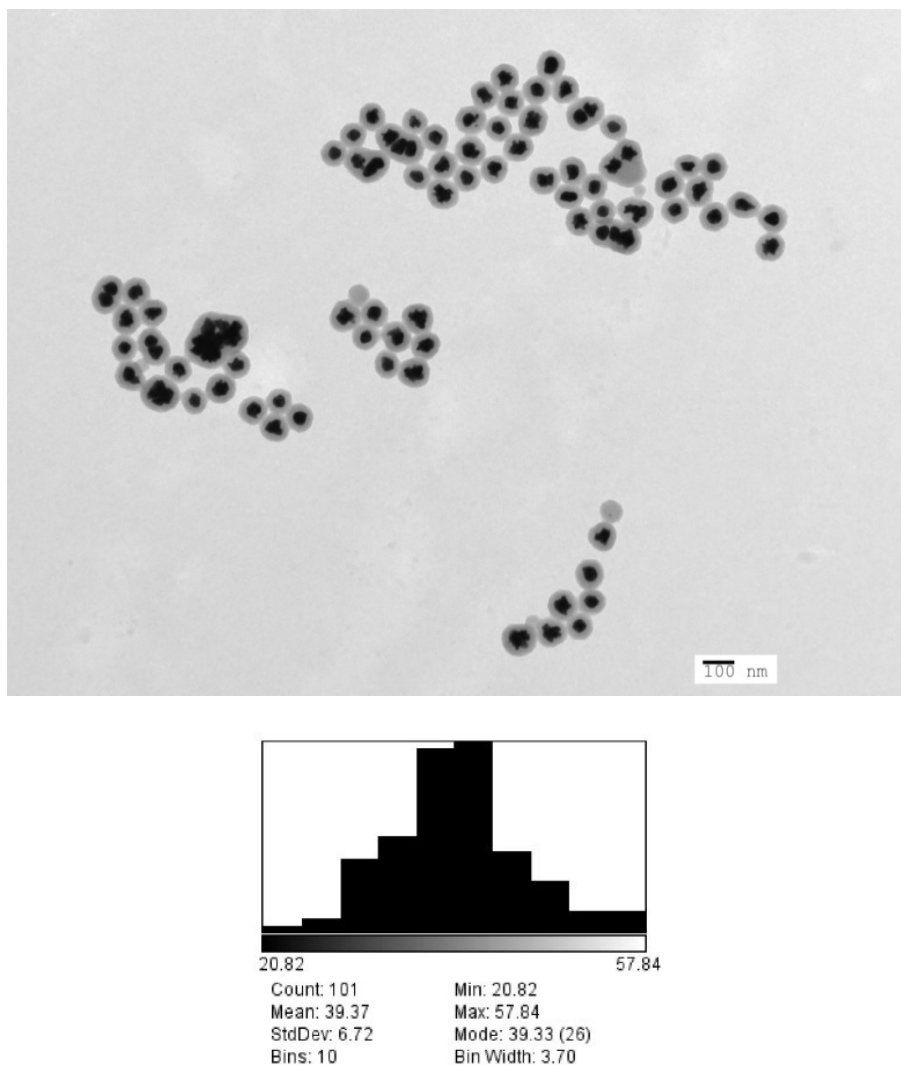


Figure 5.11 TEM micrograph of gold nanoparticles synthesized by CAT + AuNP, indicating clear encapsulation of gold nanoparticles by catechin layer (core and shell form)

The gold nanoparticles synthesized using catechin show a unique pattern from the TEM image (Figure 5.11). A uniform layer of organic matter is found surrounding the gold nanoparticles. From the image it can be seen that the gold nanoparticles, if assumed to be quasi spherical in shape, are encapsulated by a spherical organic layer. This forms a core and shell pattern, where AuNP is found in the core and the catechin layer is the shell. Table 5.3 shows the particle size distribution of AuNP in nanofluids.

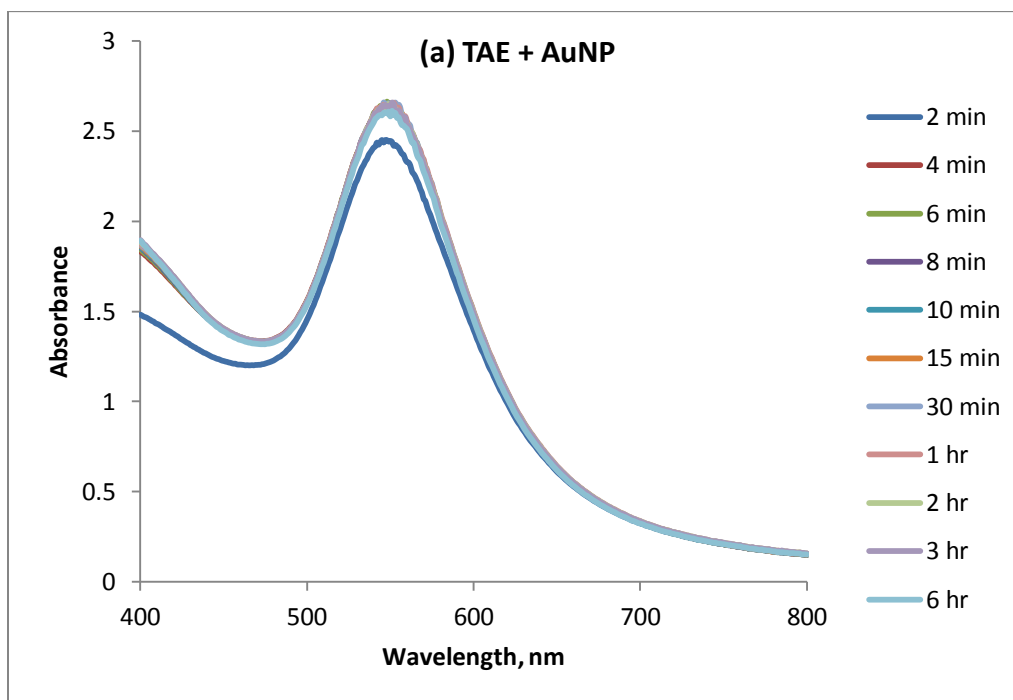
Table 5.3 Particle size analysis of AuNP size in nanofluids

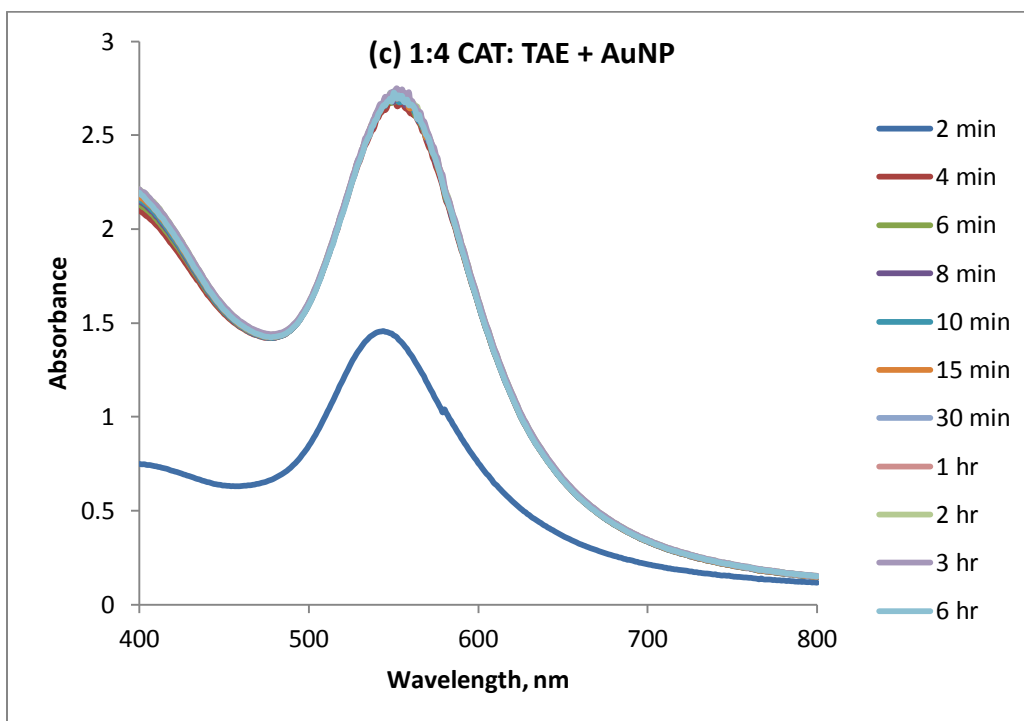
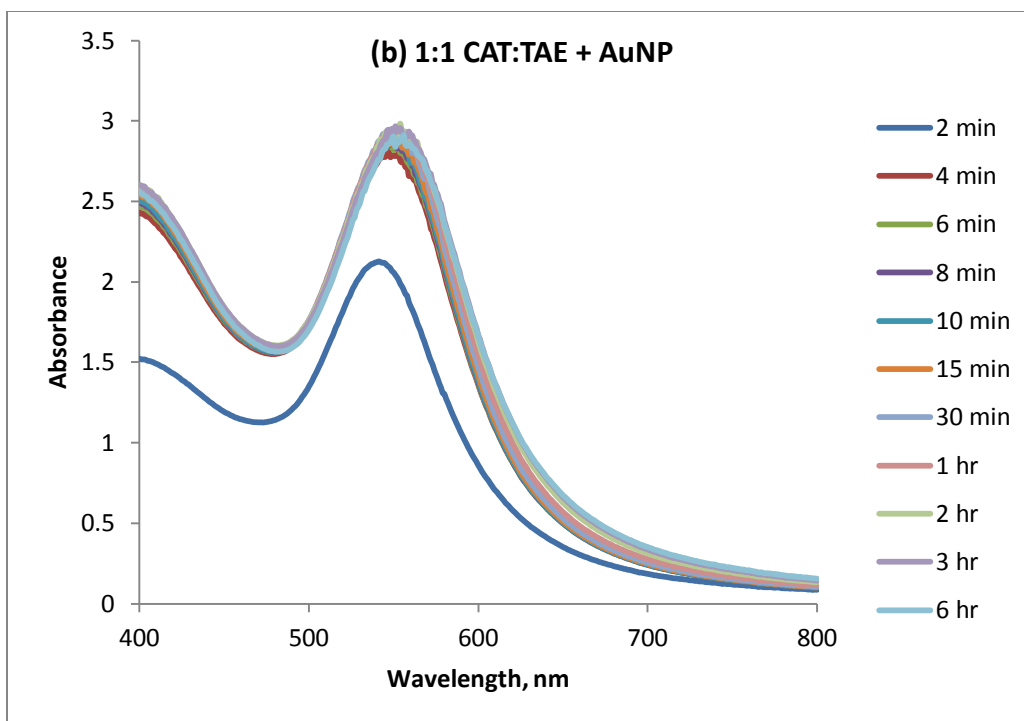
S. No.	AuNP Nanofluids	Min. (nm)	Max. (nm)	Mean (nm)	Std. dev. (\pm)	Particle shape	UV-Vis λ_{\max} (nm)
1.	TAE AuNP +	13.8	67.0	40.6	14.0	Triangles, rectangle-inclined, polygon, spherical, quasi-spherical	550
2.	1:1 CAT: TAE AuNP +	13.3	40.2	27.1	6.2	Mostly spherical to quasi-spherical (thin layer)	552
3.	1:4 CAT: TAE AuNP +	22.6	65.3	50.6	6.8	Mostly spherical to quasi-spherical (thick layer)	550
4.	CAT AuNP +	20.8	57.8	39.4	6.7	Quasi- spherical (core-shell type encapsulation)	560

5.4.4 Spectral properties of nanofluids

The results from UV-Vis spectra provide information about the surface plasmon resonance (SPR) for the gold nanoparticles in solution. The AuNP solutions were scanned over a wavelength from 400 nm to 800 nm on medium scan with peak table on and step size of 1.0 nm interval. The addition of HAuCl_4 to the reaction medium was taken as the initial start of the reaction and the solutions were monitored over a period of 6 hours. Figure 5.12 (a) shows the surface plasmon resonance (SPR) for tannic acid synthesized

AuNP. The λ_{max} was found to be at 550 nm with rapid synthesis of AuNP. Figure 5.12 (b) shows the surface plasmon resonance (SPR) for 1:1 CAT: TAE synthesized AuNP. The λ_{max} was found to be at 552 nm with rapid synthesis of AuNP. It can be seen that within 2 minutes after the onset of the reaction the SPR peak was found around 540 nm with absorbance around 2.122 and by 4 minutes there was an increase in absorbance. The similar trend was obtained over the time period of observation with SPR peak ranging from 546 nm to 552 nm.





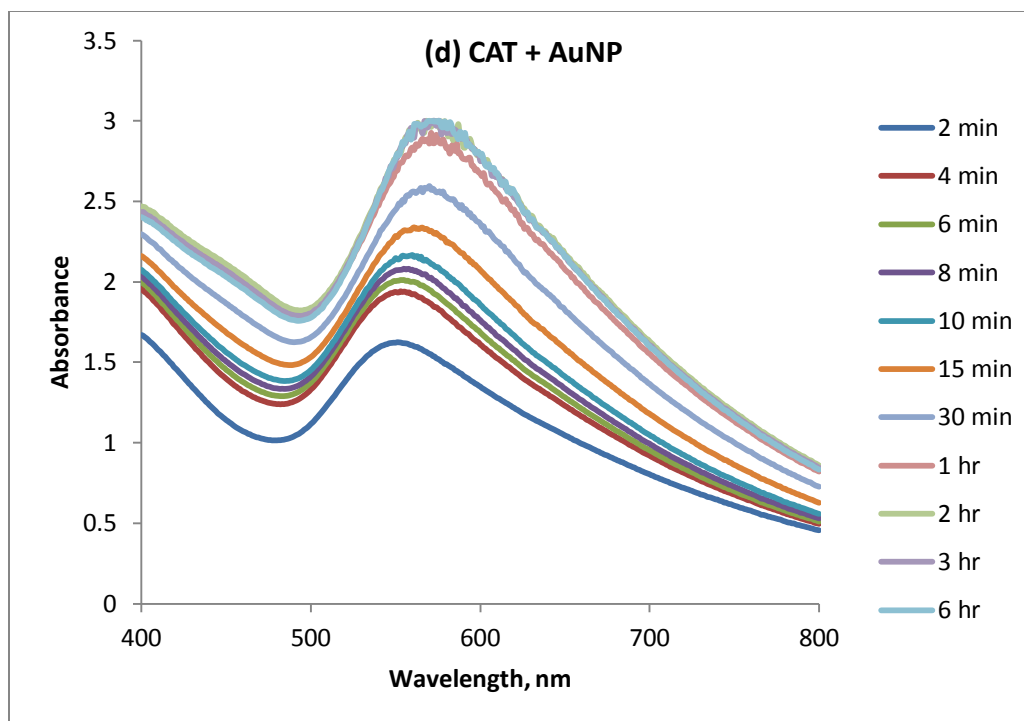


Figure 5.12 UV- Vis spectra for gold nanofluids with SPR Peak, (a) TAE+AuNP; (b) 1:1 CAT:TAE+AuNP; (c) 1:4 CAT: TAE+AuNP; (d) CAT+AuNP

The SPR peak over the wavelengths from 400 nm to 800 nm for 1:4 CAT: TAE synthesized AuNP is provided in Figure 5.12 (c). It can be seen that within 2 minutes after the onset of the reaction the SPR peak was found around 538 nm with absorbance around 1.438. The absorbance signals obtained for 1:4 CAT: TAE synthesized AuNP were lower than those obtained for 1:1 CAT: TAE synthesized AuNP. Within 4 minutes there was an increase in absorbance with complete overlapping of the curves obtained from 4 minutes to 6 hours of observation. The λ_{max} for 1:4 CAT: TAE synthesized AuNP was found to be at 550 nm.

Figure 5.12 (d) shows the SPR peak absorbance for catechin synthesized AuNP over the wavelength of 400 nm to 800 nm. The figure shows a progressive increase of absorbance over the time period. Initially the first SPR peak appeared at 547 nm with absorbance of 1.620 by 2 minutes, followed by increase in absorbance from 1.620 to 1.930 at 547 nm for 4 min. There was a gradual increase in the absorbance along with an increase in the SPR peaks from 6 min to 30 min. The increase in time, SPR wavelength and absorbance for CAT + AuNP are 6 min, 550 nm, 2.005; 8 min, 552 nm, 2.074; 10 min, 554 nm, 2.163; 15 min, 560 nm, 2.334; 30 min, 560 nm, 2.561. The λ_{max} for CAT synthesized AuNP was found to be at 560 nm.

5.4.5 Studies on nucleation of AuNP

From the results obtained from the TEM images, it can be clearly seen that the catechin synthesized AuNP had uniform layer of catechin encapsulating the gold nanoparticles when compared to the other AuNP synthesized methods. The TEM image of catechin synthesized AuNP, shown in Figure 5.11, clearly indicates an even encapsulation of gold nanoparticles by the catechin molecules. This is an interesting and intriguing result; hence catechin (CAT) was used as a reference compound for AuNP synthesis for further studies.

Correspondingly, a simple experiment was conducted to understand the mechanism of nucleation and growth of gold nanoparticles. Catechin solution (1 mM) and HAuCl₄ solution (1mM) at room temperature (25°C) were used in the nucleation and growth study. The reaction between catechin and HAuCl₄ solutions took place in a glass vial to form AuNP.

(a) CAT on grid: Five μl of catechin solution was smeared on the carbon coated TEM grids and was allowed to stand for 1 min. Excess solution was carefully removed using filter paper. The catechin solution was air dried to form a thin film. 5 μl of HAuCl_4 solution was added to the TEM grid coated with dried catechin solution, and the reaction was allowed to occur for 1 min.

After 1 min, the excess HAuCl_4 solution was removed from the TEM grid by blotting with filter paper and the sample was analyzed by the FEI Tecnai 12 TEM given in Figure 5.13. From the TEM image, it can be seen that gold nanoparticles have started to nucleate within 1 minute of the start of the reaction. The nucleation of AuNP has occurred instantaneously and the visibility of AuNP can be seen in areas having more catechin. The region containing catechin aiding the growth of AuNP is highlighted in Figure 5.13.



Figure 5.13 TEM image of Catechin on grid for CAT+AuNP Nanofluid

(b) Reaction on grid: Five μl of catechin solution and 5 μl of HAuCl_4 solution were added directly on the TEM grid, and allowed to stand for 1 min. The excess solution was removed with filter paper and air dried to form a thin film which was analyzed with FEI Tecnai 12 TEM. Figure 5.14 shows the AuNP synthesized using reaction on grid method. It can be seen that the reaction was instantaneous, the presence of water plays an interesting role in assisting the instant nucleation and formation of gold nanoparticles. This is an exciting result signifying that the formation of AuNP could be rapid in an

aqueous medium as the image obtained reveals the formation of AuNP within 1 min of reaction time.

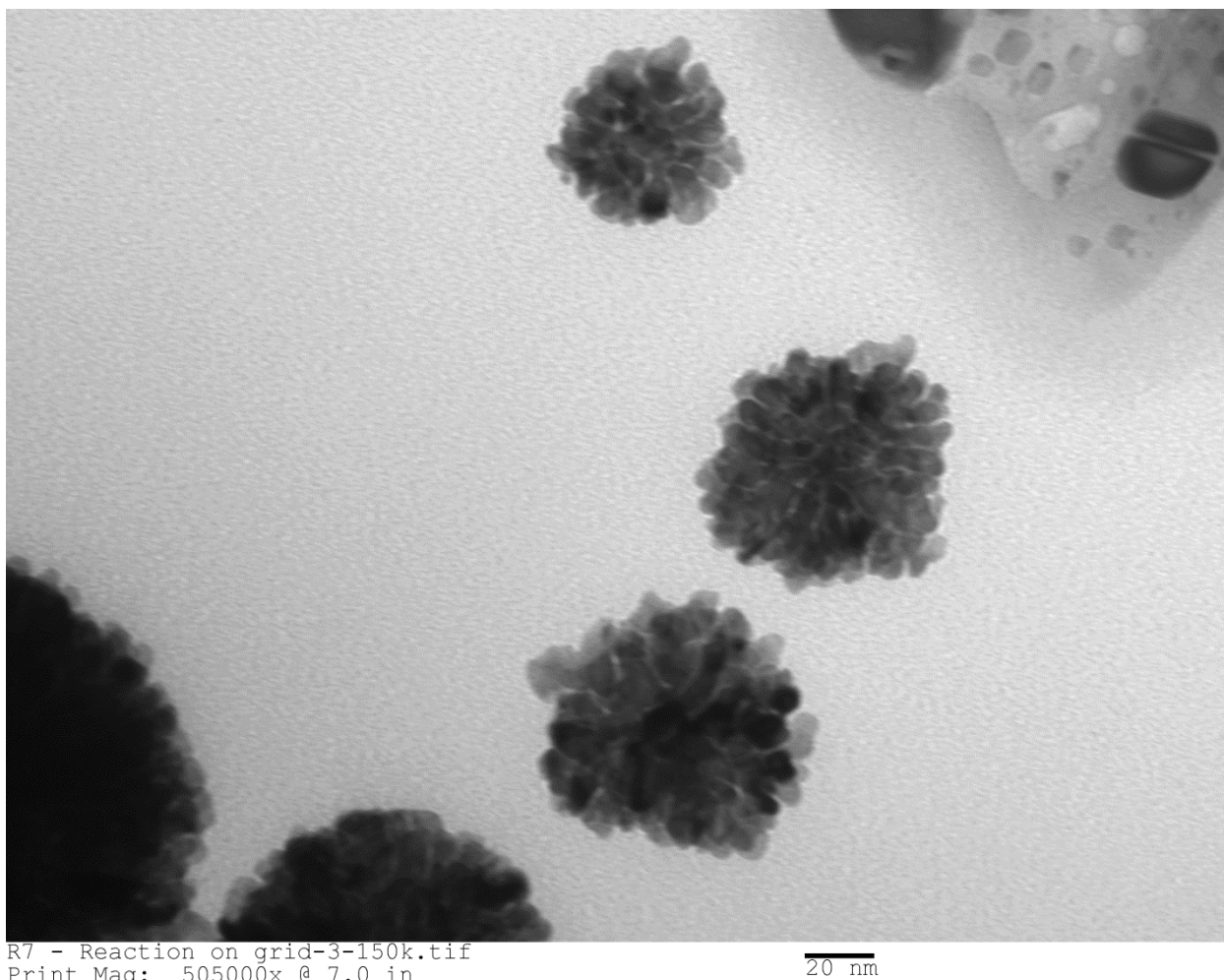


Figure 5.14 TEM image of reaction on grid for CAT+AuNP nanofluid

Both catechin on grid and reaction on grid techniques provide an insight into the formation of AuNP. These two methods show the interesting phenomenon of formation of AuNP, further research is required to understand the factors aiding the formation of AuNP which would facilitate further manipulation, control and optimization of the size of AuNP for suitable and targeted end applications.

5.5 Conclusion

Nanofluids were prepared by varying their concentrations between catechin and tannic acid to form AuNP using water as the base fluid. Interesting thermal, dielectric and spectral properties were obtained for the green synthesized gold nanofluids. The TEM images of catechin synthesized AuNP show nearly perfect encapsulation as core and shell. This is an exciting result as this system can be used as carrier for drug delivery and also as a contrast agent providing signals in detection applications. The results obtained from this study point out the potential of manufacturing green synthesized AuNP nanofluids which can have a wider scope of application as functional materials. The nanofluids market in heat transfer applications alone is estimated to be over 2 billion dollars / year (Puliti et al., 2011). Nanofluids containing nanoparticles can be used for the design of new biosensors to assess the quality and safety of food materials (Warriner et al., 2014). Engineering applications of a special nanofluid system are rarely reported as investigations on different nanofluids system are still at the experimental stage (Li et al., 2009). Thus further advances in nanofluids will create new opportunities to enhance the properties of conventional materials and will add new dimensions and potential for innovation to future applications.

CONNECTING STATEMENT TO CHAPTER VI

In **Chapter VI**, attempts are made to make an organic–inorganic hybrid vehicle for drug delivery system. A *top-down approach* for polymeric nanoparticles synthesis method is adopted in this study. The gold nanoparticle synthesized from catechin, which was explained in the previous chapter is used for encapsulation into maltodextrin as the carrier. Three encapsulation methods are studied with three different concentrations of maltodextrin.

The protocols and experimental design were developed and the experiments were performed by Ms. Krishnaswamy under the guidance of Dr. Orsat. The results from this chapter have been organized in a manuscript to be submitted for publication in the *Journal of Controlled Release*.

A part of this chapter was presented in the following conference

1. K. Krishnaswamy* & V. Orsat. Microwave and lyophilisation techniques for encapsulation of green synthesized gold nanoparticles. IUFoST 17th World Congress of Food Science and Technology & Expo. August 17-21, 2014, Montreal, QC, Canada.

(Poster presentation)

2. K. Krishnaswamy* & V. Orsat. Studies on encapsulation and characterization of green synthesized gold nanoparticles. ASABE and CSBE | SCGAB Annual International Meeting. July 13-16, 2014, Montreal, QC, Canada. **(Oral presentation)**

CHAPTER VI

SYNTHESIS AND CHARACTERISATION OF GOLD NANOPARTICLES ENCAPSULATED IN MALTODEXTRIN MATRIX

6.1 Abstract

The present study aims at developing a polymeric functional food delivery system containing gold nanoparticles. Encapsulation techniques such as freeze drying encapsulation (FE) and microwave assisted encapsulation (ME) were compared with simple encapsulation method (SE). Encapsulated powders containing gold nanoparticles (AuNP) were synthesized by a green nanotechnology approach. The AuNP encapsulated powders were characterised using a differential scanning calorimeter (DSC), Fourier transform infrared spectroscopy (FTIR), scanning electron microscope (SEM), and particle size analyser. A full factorial experimental design was used to study the influence of maltodextrin concentration on the response of AuNP loading, encapsulation efficiency and yield. The yield of AuNP encapsulated maltodextrin powder by microwave assisted encapsulation was comparatively more than that of simple encapsulation and freeze drying encapsulation while the results obtained for AuNP loading were interestingly different. It can be seen from the SEM micrographs that the morphological structure for freeze drying encapsulation showed an encapsulated spherical shaped structure while microwave assisted encapsulation led to complexation of AuNP into the maltodextrin matrix. The FTIR spectra's for all the three encapsulation methods confirm the presence of the AuNP in the maltodextrin matrix.

Key words: Catechin, Freeze drying encapsulation, Microwave assisted encapsulation.

6.2 Introduction

The delivery of bioactive compounds to specific sites is important in designing drug delivery systems for therapeutics as well as for delivery of vitamins, antioxidants and functional food ingredients. The delivery systems in pharma and cosmetics industries use tailor made synthetic materials with specific properties such as specific dissolution properties. Such synthetic materials in general are not ‘food grade’ and often set limitations to be used in food delivery systems (Shimoni, 2008). Designing new delivery vehicles using food grade materials and having improved encapsulation properties is a challenging task. This study aims at developing new delivery systems to encapsulate gold nanoparticles using food grade maltodextrin.

Polymeric nanoparticles may be either nanospheres or nanocapsules, and for nanoencapsulation of drugs the diameter can range from 1 to 1000 nm (Reis et al., 2006). In the ‘top-down’ approach to produce nanoparticles, structures are generated by breaking up bulk materials, while the ‘bottom-up’ approach allows for self-assembly of molecules and these are the two currently used strategic approaches to produce nanoparticles (Chen et al., 2006).

Nanoparticles are synthesized from pre-formed polymers in the ‘top-down’ method including solvent emulsification–evaporation (Emulsion evaporation method), solvent emulsification - diffusion (Emulsion diffusion method), coacervation and nanoprecipitation (Solvent displacement method). Emulsification of the organic solution of a polymer in an aqueous phase is followed by the evaporation of the organic solvent which takes place in emulsion evaporation method. The nature of the active compound determines whether single emulsion oil-in-water (o/w) or water-in-oil (w/o) and double emulsion water-oil-

water (w/o/w) are used for nanoencapsulation (Sabliov & Astete, 2008). The active compound is dispersed in an organic volatile solvent like dichloromethane and ethyl acetate in which the preformed synthetic polymer such as poly (D, L-lactide-co-glycolide) is dissolved. The organic phase is emulsified into an aqueous phase in presence of stabilizers like poly(vinyl alcohol), didecyl dimethyl ammonium bromide under high speed stirring, microfluidisation or probe sonication to yield emulsions. The organic solvent is evaporated at normal or reduced pressure and the nanoparticles are collected by centrifugation (Bilati et al., 2005).

In solvent emulsification - diffusion (Emulsion diffusion method) the polymer is dissolved in a partly water miscible organic phase, like benzyl alcohol, propylene carbonate, and ethyl acetate. Surfactants like anionic sodium dodecyl sulfate (SDS), non-ionic polyvinyl alcohol (PVA) or cationic didecyl dimethyl ammonium bromide (DMAB) are used to emulsify the organic phase into an aqueous phase under constant stirring. Blended matrix of PLGA and polyoxyethelene derivatives copolymers have also been used in emulsion diffusion method (Csaba et al., 2005; Sabliov & Astete, 2008). Time required for emulsification, rate of stirring, type of organic solvent and polymer properties influence the final properties of the resulting nanoparticles (Cegnar et al., 2004).

In nanoprecipitation (Solvent displacement method) the active compound and the polymer are dissolved in a polar solvent miscible with water such as acetonitrile, acetone, ethanol or methanol. The organic phase is added drop by drop into the aqueous phase containing surfactant under mild stirring. Nanoparticle formation is by rapid solvent diffusion, the nanoparticle suspension can be concentrated or evaporated under reduced

pressure and purified by centrifugation (Galindo-Rodríguez et al., 2005; Sabliov & Astete, 2008).

Emulsion polymerization, interfacial polymerization, interfacial polycondensation and molecular inclusion use monomers as their starting point and come under the 'bottom-up' process to produce polymeric nanoparticles. In emulsion polymerization, an aqueous phase of monomer is dissolved into a continuous aqueous solution that requires neither surfactants nor emulsifiers. The monomer molecule dissolved in a continuous aqueous phase collides with an initiator molecule that might be a free radical or ion. Polymerization can also be initiated by high energy source such as γ -radiation, ultraviolet or strong visible light (Reis et al., 2006; Vauthier et al., 2003). Poly(alkylcyanoacrylates) were used to produce polyacrylamide nanospheres for medical application using this method (Vauthier et al., 2003).

Poly(ethylcyanoacrylate) encapsulating insulin (<500 nm) (Radwan & Aboul-Enein, 2002) , poly(butylcyanoacrylate) encapsulating progesterone (250 nm) (Li et al., 1986), poly(isobutylcyanoacrylate) (40-80 nm) and poly(isohexylcyanoacrylate) (30 – 80 nm) encapsulating ampicillin (Seijo et al., 1990), are some of the encapsulated materials using emulsion polymerization method. This method is becoming less important as it requires toxic organic solvents such as cyclohexane (ICH, class 2), n-pentane (ICH, class 3) and toluene (ICH, class 2) and toxic surfactants, monomers, initiators that are subsequently eliminated from the formed nanoparticles (Reis et al., 2006).

Interfacial polymerization was used to encapsulate insulin (~151 nm) in poly(ethyl 2-cyanoacrylate) (Watanasirichaikul et al., 2000), Poly(isobutylcyanoacrylate) was used to encapsulate darodipine (150 nm) (Hubert et al., 1991) and calcitonin (1000-2000 nm) (Lowe & Temple, 1994). There are recent reviews on nanoencapsulation as delivery systems (Fathi et al., 2014; Liu et al., 2008; Mishra et al., 2010; Reis et al., 2006; Sabliov & Astete, 2008; Vrignaud et al., 2011), which will shed light on the available methods for producing nanoparticles.

As mentioned earlier, the use of toxic chemicals in the synthesis of nanoparticles makes such techniques unsuitable for use in food delivery systems. There is thus a need for developing new techniques for forming nanoparticles focused on functional food delivery systems using naturally available polymers. Pertaining to the above mentioned issue, this study addresses the design of new delivery systems containing gold nanoparticles using food grade maltodextrin. The gold nanoparticles act as signaling agents in developing delivery vehicles. Three encapsulation methods such as microwave assisted encapsulation (ME) and freeze drying encapsulation (FE) and simple encapsulation (SE) were investigated using three different concentrations of maltodextrin. The specific aim of this study is to develop delivery systems using water without using other solvents or surfactants following a green nanotechnology approach.

6.3 Materials and methods

6.3.1 Materials

Maltodextrin, catechin, $\text{HAuCl}_4 \cdot 3\text{H}_2\text{O}$ were purchased from Sigma-Aldrich Co., Canada. Maltodextrin is made of chains of D-glucose units linked by α (1 \rightarrow 4) glycosidic bonds $[\text{C}_{6n}\text{H}_{(10n+2)}\text{O}_{(5n+1)}]$, where ($n=3$ to 20). The molecular weight varies based on the number of glucose chains. The maltodextrin used in this study has dextrose equivalent (DE) of 4.0 to 7.0.

All chemicals were used without further purification. Distilled water with resistivity of 18.2 $\text{M}\Omega\cdot\text{cm}$ was obtained from a Millipore system (Simplicity 185). All glassware used for the experiment was cleaned and dried in hot air oven at 105°C for 12 hours prior to use. The solvent used throughout this study is distilled water.

6.3.2 Preparation of gold nanoparticles

The gold nanoparticles were synthesized using 1 mM catechin (Mw: 290.27 g/mol) with 1mM $\text{HAuCl}_4 \cdot 3\text{H}_2\text{O}$ (Mw: 393.83 g/mol). The solution was allowed to react for 20 min and was used for the encapsulation study. The prepared stock solution was kept in the dark to protect against light effects.

6.3.3 Encapsulation methods

Maltodextrin was mixed with distilled water heated at 50°C for 15 min with constant magnetic stirring at 1000 rpm to make an aqueous solution. This method was used for making three different concentrations of maltodextrin solutions (0.5, 1 and 1.5 M).

The prepared gold nanoparticles solution was dispersed into the aqueous maltodextrin solutions at three different concentrations. The resulting mixture was stirred for 15 min using a magnetic stirrer at 1000 rpm. For simple inclusion encapsulation (SE), the samples were placed in 5mL porcelain crucibles (24 x 20 x 1.8mm; Fisher Scientific) and dried in a shaker-incubator at 25 ± 2 °C with 100 rpm (Benchmark, Incu-Shaker Mini) for 48 hours. For freeze encapsulation/ lyophilisation encapsulation (FE), the prepared samples were frozen at -20 °C and then lyophilized at -47 °C for 24 hours. For microwave assisted encapsulation (ME), the samples were placed in 5mL porcelain crucibles (24 x 20 x 1.8mm; Fisher Scientific) and heated with maximum incident microwave power of 200 W with an intermittent pause for the microwave cycle duration every 30 sec. The temperature was maintained at 80°C for encapsulation of AuNP in the maltodextrin matrix. The solution was microwave heated for 40 min for 0.5 M concentration, 100 min for 1M concentration and 140 min for 1.5 M concentration to produce the encapsulated powder.

The encapsulated powder from all the three methods were ground using a pestle and mortar for 5 minutes to ensure the lumps formed during the encapsulation process were broken. All the encapsulated powders were stored at -20° C until further use.

6.3.4 AuNP loading, encapsulation efficiency and yield

Quantification of AuNP loading into the maltodextrin matrix, encapsulation efficiency and yield of the encapsulated powder were calculated based on (Ankrum et al., 2014) with certain modifications adapted for gold nanoparticles.

$$\text{AuNP loading} = \frac{(C_R \times V_R)}{M_{EP}} \quad (\text{Eq. 6.1})$$

$$\text{Encapsulation efficiency} = \left(\left[\frac{(C_R \times V_R)}{M_{EP}} \right] / \left[\frac{M_{NP}}{(M_{NP} + M_{MD})} \right] \right) \quad (\text{Eq. 6.2})$$

$$\text{Yield \%} = \left(\frac{\text{Final weight after encapsulation}}{\text{Initial weight before encapsulation}} \right) \times 100 \quad (\text{Eq. 6.3})$$

Where,

C_R = AuNP concentration of the release medium (mg/ μ l)

V_R = volume of the release medium (μ l) = 2000 μ l

M_{EP} = mass of the encapsulated powder (mg) = 2 mg

C_R = AuNP concentration of the release medium (mg/ μ l)

M_{NP} = mass of the AuNP (mg/ μ l)

M_{MD} = mass of the maltodextrin (mg/ μ l)

(Assumption: Concentration of AuNP in the release medium is considered to be equal to mass of the nanoparticle, as the mass of AuNP was very little and negligible)

6.3.5 Particle size analysis

The particle size of the AuNP encapsulated powder was measured using a DelsaTM Nano C Particle Analyzer (Beckman Coulter, CA, U.S.A). The samples were prepared in an Eppendorf tube, where 0.10 g of the AuNP encapsulated powder was mixed with 1.5 ml of deionized water and sonicated for 5 min. The resulting solution was transferred to 1 cm path length plastic cuvette. Deionized water (0.5 ml) was used to rinse the

Eppendorf tube and to make up the total volume to 2 ml in the cuvette for particle size analysis. Scattering angle of 165.0° , with a pinhole set to $50\ \mu\text{m}$, and refractive index of 1.3328 at a temperature of 25°C for 70 continuous accumulation times were used for this study as recommended by the equipment manufacturer Beckman Coulter. The samples were replicated thrice ($n=3$).

6.3.6 Differential Scanning Calorimeter

The thermal properties of the AuNP encapsulated powder were studied using a differential scanning calorimeter (DSC Q-100 V9.8 built 296, TA Instruments, Texas, USA). Nine combinations of AuNP encapsulated maltodextrin powder obtained from 3 encapsulation methods with 3 different concentrations of maltodextrin were selected, and 5 mg ($\pm 0.5\ \text{mg}$) of each powder sample was placed in small aluminum pans. The sample pans were hermetically sealed. The samples were prepared to cover the entire bottom surface of the pan to ensure good thermal contact. Care was taken to prevent over filling of the pan. Nitrogen was used as the purge gas as it is inert in nature. The rate of flow of nitrogen was 50 ml/min. Indium was used for calibration. The thermal process was monitored from 0 to 400°C , with ramping up at $10\ ^\circ\text{C}/\text{min}$. Reproducibility was checked by running the sample in triplicates. TA Universal Analysis V4.5A software was used for processing the data.

6.3.7 Scanning Electron Microscopy

The SEM images were obtained from an Olympus TM3000 scanning electron microscope. The experiment was conducted with a field emission at 5 kV. A small amount of the sample was spread on double adhesive carbon tabs (Carbon Tabs, 25mm dia, Canemco-Marivac, Canada) and mounted on the metal stub for measurement.

6.3.8 Fourier Transform Infrared Spectroscopy

FTIR measurements were carried out on a Thermo Scientific Nicolet iS5. Attenuated total reflectance (ATR) method was used to collect the spectra using iD5 ATR with diamond crystal. A small amount of sample was placed on the ATR platform, care was taken to ensure that the sample covers the surface of the diamond crystal completely and that there is proper contact between the sample powder and the diamond crystal. All spectra were averaged from 32 scans and collected in absorbance mode at 4 cm^{-1} spectral resolution through the $4000\text{--}600\text{ cm}^{-1}$ range. To eliminate possible equipment drift, the environmental spectrum which includes water vapour and carbon dioxide was collected as background before every spectral collection of the sample.

6.3.9 Statistical analysis

A 3×3 full factorial design was used for this study, where different concentrations of maltodextrin were used for encapsulation of gold nanoparticles. Microwave assisted encapsulation was compared with freeze drying encapsulation and simple encapsulation method. The experiments were conducted in triplicate and the difference was considered significant at $p < 0.05$.

6.4 Results and discussion

6.4.1 Results from the statistical analysis

The experimental results such as yield %, AuNP loading, encapsulation efficiency and particle size obtained for the three encapsulation technique simple encapsulation (SE), freeze drying encapsulation (FE) and microwave assisted encapsulation (ME) for three different maltodextrin concentrations are listed in Table 6.1.

The regression plot for the % yield response for different encapsulation methods as a function of maltodextrin concentration is shown in Figure 6.1.

Table 6.1 Full factorial design for the encapsulation of AuNP into a maltodextrin matrix

RUNS	MD	ENCAP. METHOD	YIELD %	AuNP LOADING	ENCAP. EFF	PARTICLE DIA. (um)
1	0.5	SE	79.63	0.3603	45.90	1.195
2	0.5	FE	71.88	0.3111	45.85	1.174
3	0.5	ME	83.82	1.025	46.57	1.366
4	1	SE	82.61	0.4493	45.99	1.334
5	1	FE	76.02	0.4288	45.97	1.633
6	1	ME	86.07	0.5040	46.04	1.361
7	1.5	SE	82.63	0.6217	46.16	2.319
8	1.5	FE	77.38	0.5602	46.10	2.116
9	1.5	ME	90.65	0.2950	45.83	1.037
10	0.5	SE	79.19	0.3768	45.92	1.172
11	0.5	FE	71.76	0.2864	45.83	0.930
12	0.5	ME	79.8	1.020	46.56	2.071
13	1	SE	81.07	0.4698	46.01	1.454
14	1	FE	75.06	0.4479	45.99	1.982
15	1	ME	85.36	0.4530	45.99	1.141
16	1.5	SE	85.06	0.6573	46.20	2.655
17	1.5	FE	76.92	0.5656	46.11	2.359
18	1.5	ME	88.78	0.3080	45.85	1.685
19	0.5	SE	78.53	0.3795	45.92	1.441
20	0.5	FE	71.7	0.3124	45.85	0.868
21	0.5	ME	80.1	1.010	46.55	1.613
22	1	SE	82.45	0.4999	46.04	1.733
23	1	FE	75.41	0.4370	45.98	2.262
24	1	ME	85.97	0.5030	46.04	1.316
25	1.5	SE	82.96	0.5136	46.05	1.864
26	1.5	FE	76.83	0.5492	46.09	2.220
27	1.5	ME	87.43	0.2780	45.82	1.220

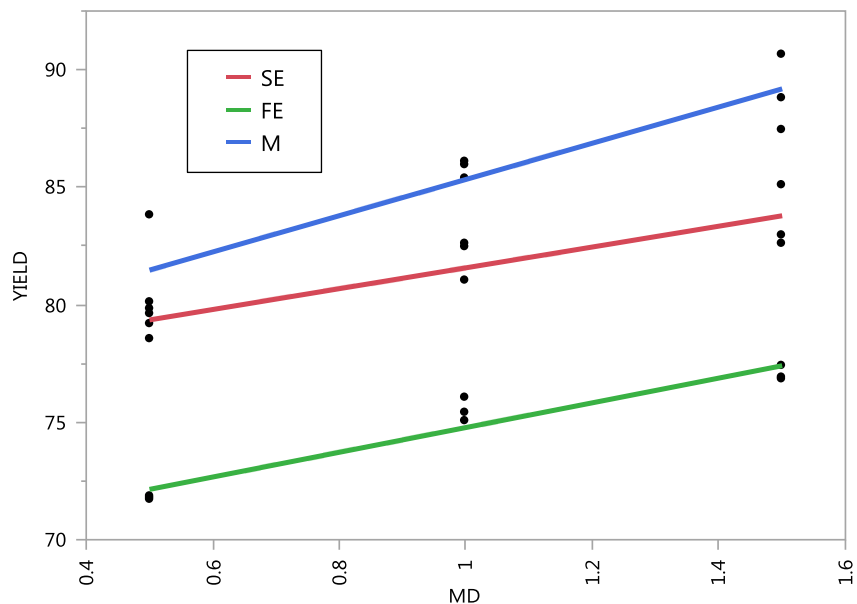


Figure 6.1 Plot showing the effect of different encapsulation methods on the % yield for encapsulation of AuNP into maltodextrin (MD)

The concentration of maltodextrin is plotted on the x-axis, and it is clearly seen that the yield for the encapsulated powder increased with the increase in maltodextrin concentration for all the three encapsulation methods. The LS means for AuNP % yield is 81.57 % for SE, 74.77 % for FE and 85.33 % for ME respectively with a standard error of 0.37 %. The maximum yield was obtained for microwave assisted encapsulation and the minimum yield was obtained with the freeze drying encapsulation method. This can be related to the fact that after freeze drying the encapsulated powder obtained was light, less dense in structure and very porous. This might have led to possible losses of the AuNP during the freeze drying process and handling. On the other hand with microwave assisted encapsulation, the product formed was dense, solid, with an amorphous crystals structure (Abbasi & Rahimi, 2008). The encapsulated powder stayed intact within the 5mL porcelain crucibles, a pestle and mortar was used to grind the solid into powder form.

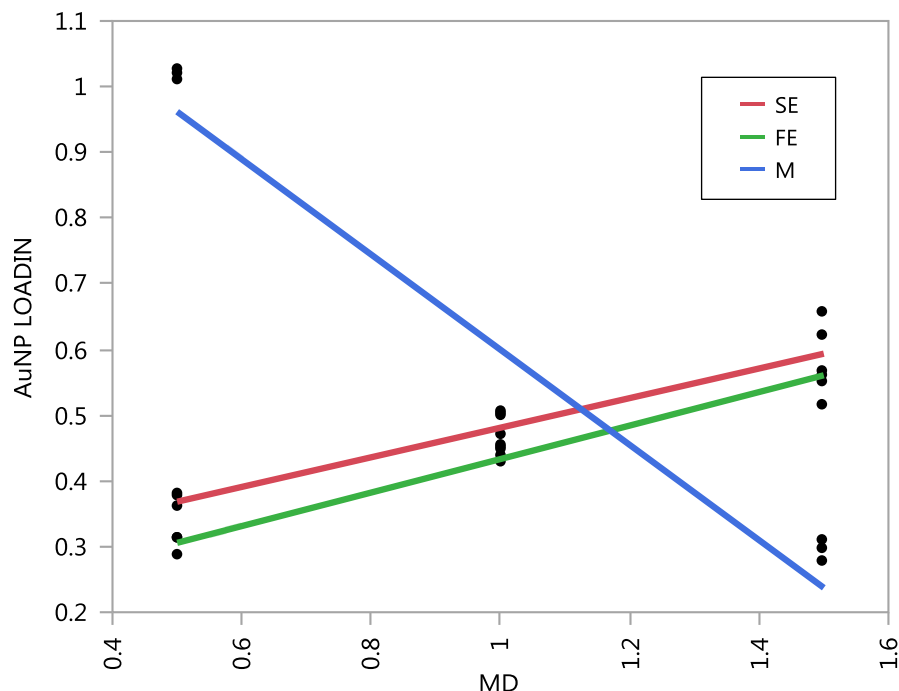


Figure 6.2 Plot showing the effect of different encapsulation method on AuNP loading into maltodextrin (MD)

It can be seen from Figure 6.2, for gold nanoparticles loading into maltodextrin matrix, that with an increase in concentration of maltodextrin there was an increase in the AuNP loading for freeze drying and simple encapsulation methods. This trend was reversed in the case of the microwave assisted encapsulation method, where with an increase in concentration of maltodextrin, there was a decrease in the release of AuNP from the maltodextrin matrix. It should be noted that the amount of AuNP added was kept constant while varying the concentration of maltodextrin for all the encapsulation methods. So with the increase in the concentration of maltodextrin, the AuNP was strongly entrapped within the matrix during microwave encapsulation. Thus in microwave encapsulation of AuNP into the maltodextrin, an increase in concentration of maltodextrin controls the release of AuNP from its matrix, showing strong entrapment within the matrix.

From an application point of view, this will be an interesting feature to consider while designing intelligent packaging materials.

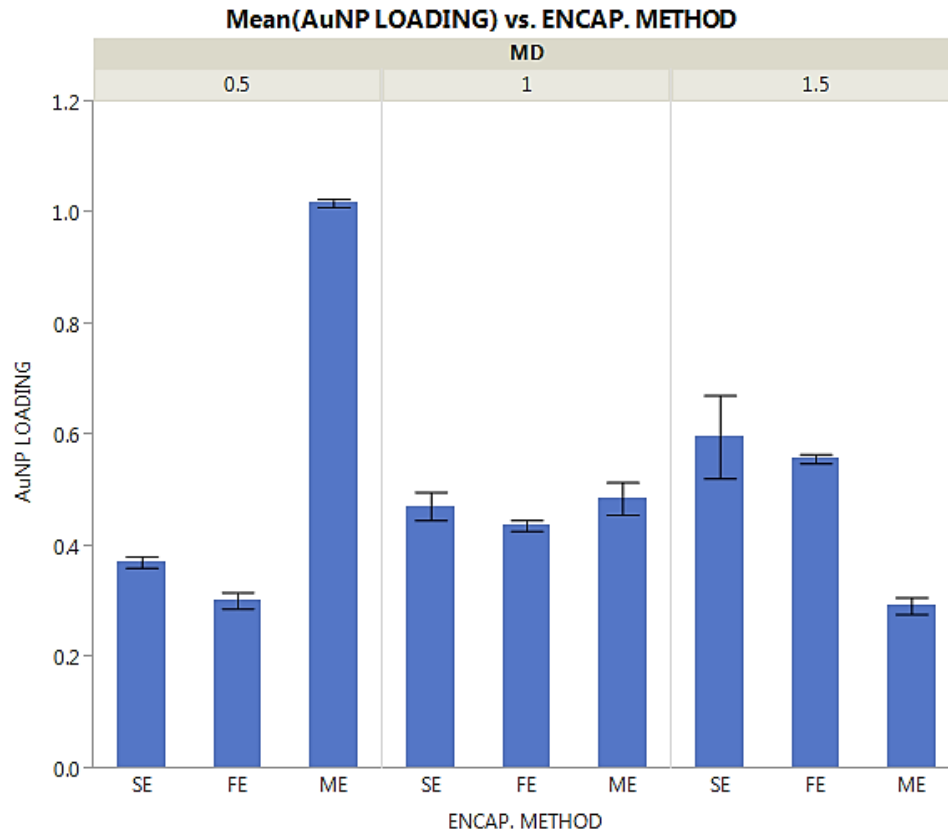


Figure 6.3 Graph showing the effect of AuNP loading for different encapsulation methods

Figure 6.3 provides the mean of AuNP loading with the three encapsulation methods as compared with three maltodextrin concentrations, while the standard deviations are provided as error bars. It can be seen that the gold nanoparticles loading for the 1M maltodextrin concentration yield did not have much difference compared to the 0.5 M and 1.5 M concentrations.

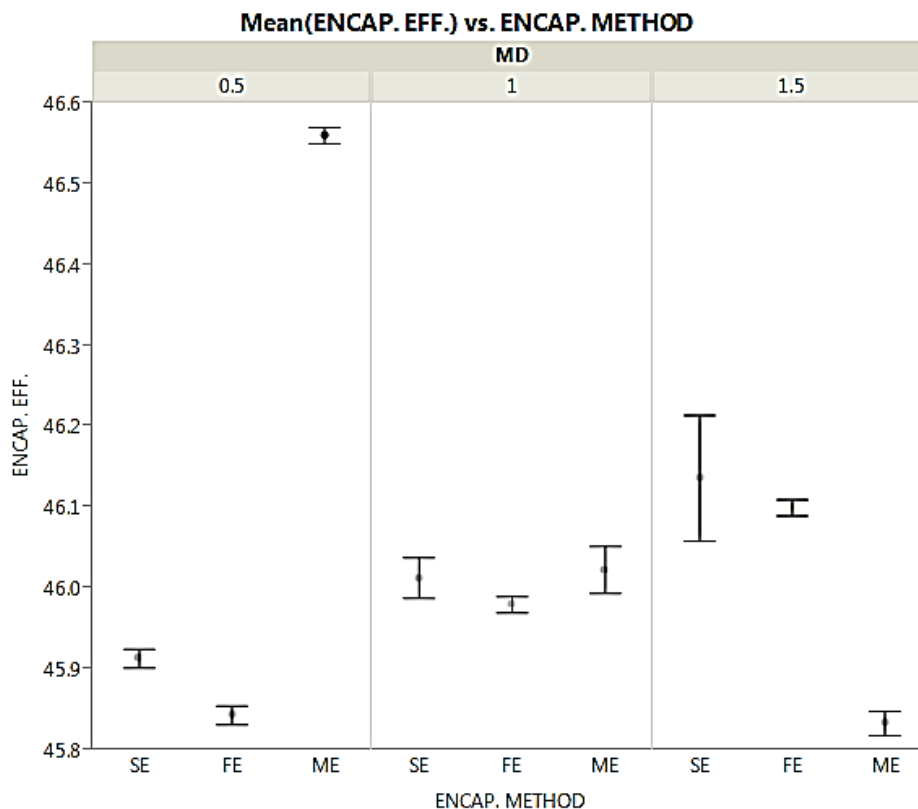


Figure 6.4 Grid showing the mean of encapsulation efficiency for the three encapsulation methods for the three different concentrations along with the std. deviation error bar

The encapsulation efficiency presented in Figure 6.4 of gold nanoparticles into maltodextrin matrix was similar to the AuNP loading plot shown in Figure 6.2. With an increase in concentration of maltodextrin, there was an increase in the encapsulation efficiency for both the freeze drying and simple encapsulation methods, whereas there was a decrease in the encapsulation efficiency for the microwave assisted encapsulation method. From Figure 6.4, it can be seen for 1M concentration of maltodextrin, for all the three encapsulation methods, that there was less variation of the mean value and less std. deviation within the group, when compared to 0.5 and 1.5 M concentrations. Based on

this, the 1 M concentration was found to be optimum with less deviation about the mean for the three encapsulation methods.

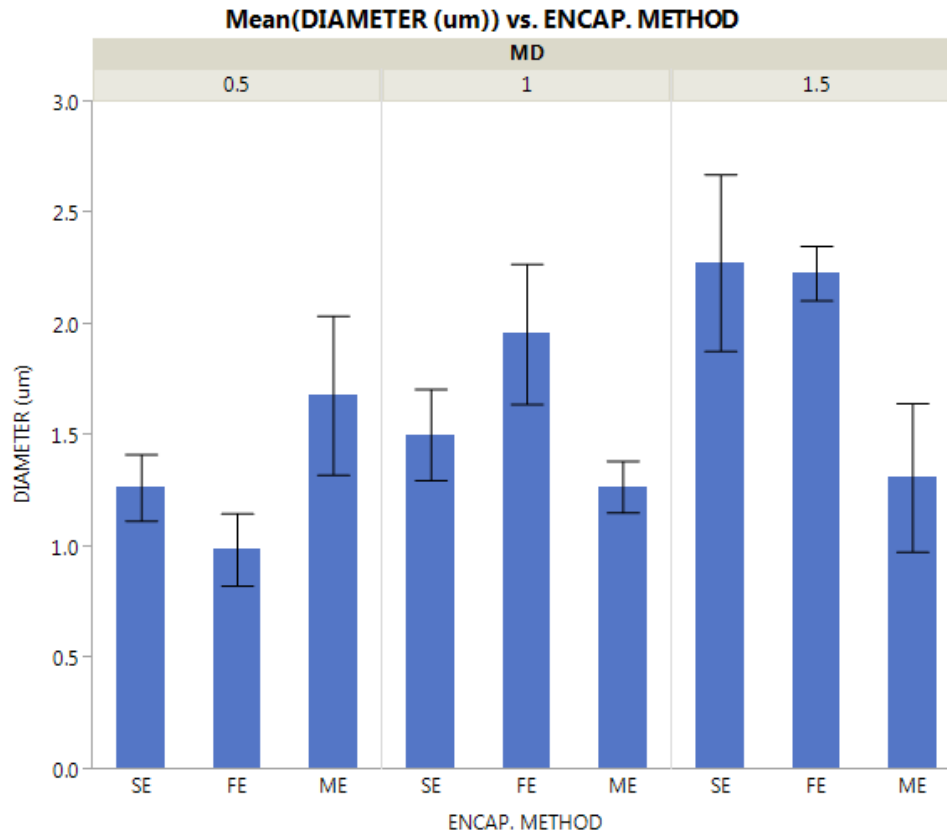


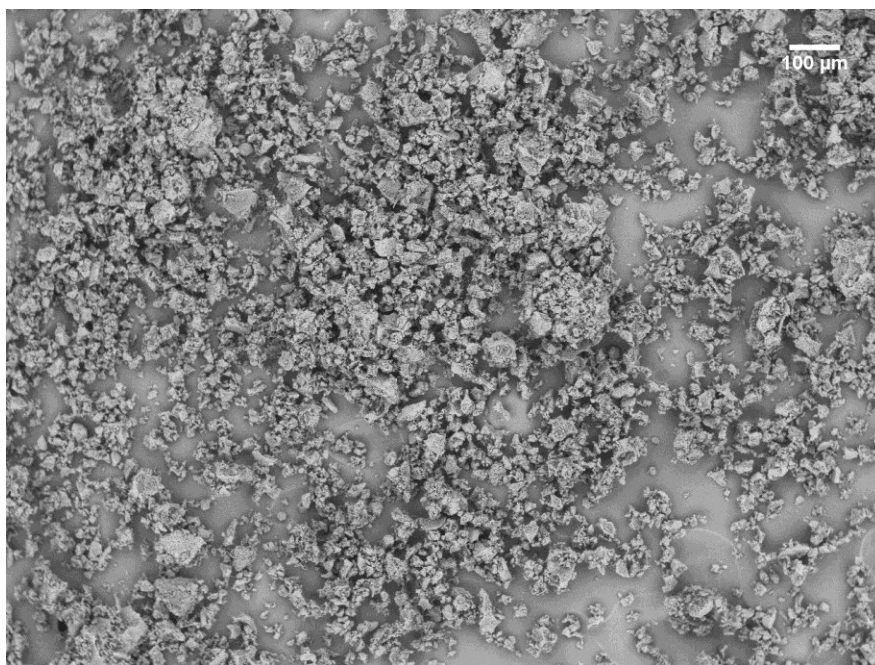
Figure 6.5 Graph representing the mean diameter of the encapsulated powder using the three encapsulation methods SE, FE and ME

From Figure 6.5, it can be seen that with the increase in the concentration of the maltodextrin, the diameter of the particle increased for simple encapsulation and freeze drying encapsulation, whereas in the case of microwave assisted encapsulation a reverse trend was obtained. The reason for such behaviour will be provided in the next section while discussing the SEM images of the microencapsulated powders containing nanoparticles.

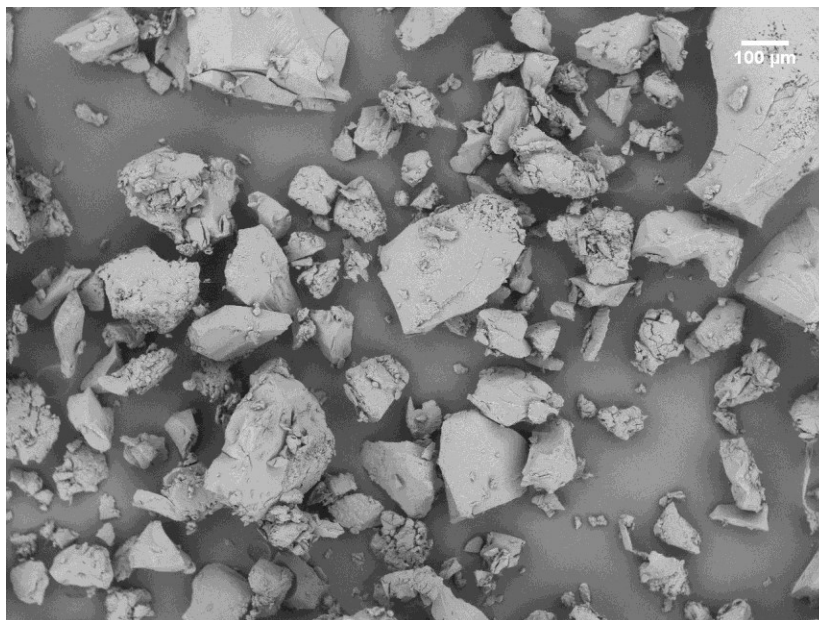
6.4.2 Interpretation of SEM images

The difference in structural morphology was observed among the three different encapsulation methods. The SEM images of the microencapsulated powder from 0.5M, 1M and 1.5 M concentrations for an individual encapsulation method resembled the same. Hence the discussion in this section will focus on the structural morphology obtained from the three encapsulation methods such as simple encapsulation (SE), freeze drying encapsulation (FE) and microwave assisted encapsulation (ME) method.

Figure 6.6 shows the SEM micrograph of AuNP encapsulated powder at 100 x magnification, it can be clearly seen that the size of the encapsulated powder by freeze drying method and simple encapsulation method were comparatively smaller than the size of the particle obtained from the microwave assisted encapsulation method.



a) Lyophilisation encapsulation (FE) , magnification 100 x



b) Microwave assisted encapsulation (ME) , magnification 100 x



c) Simple encapsulation (SE) , magnification 100 x

Figure 6.6 SEM micrograph of AuNP encapsulated powder at 100 x magnification.

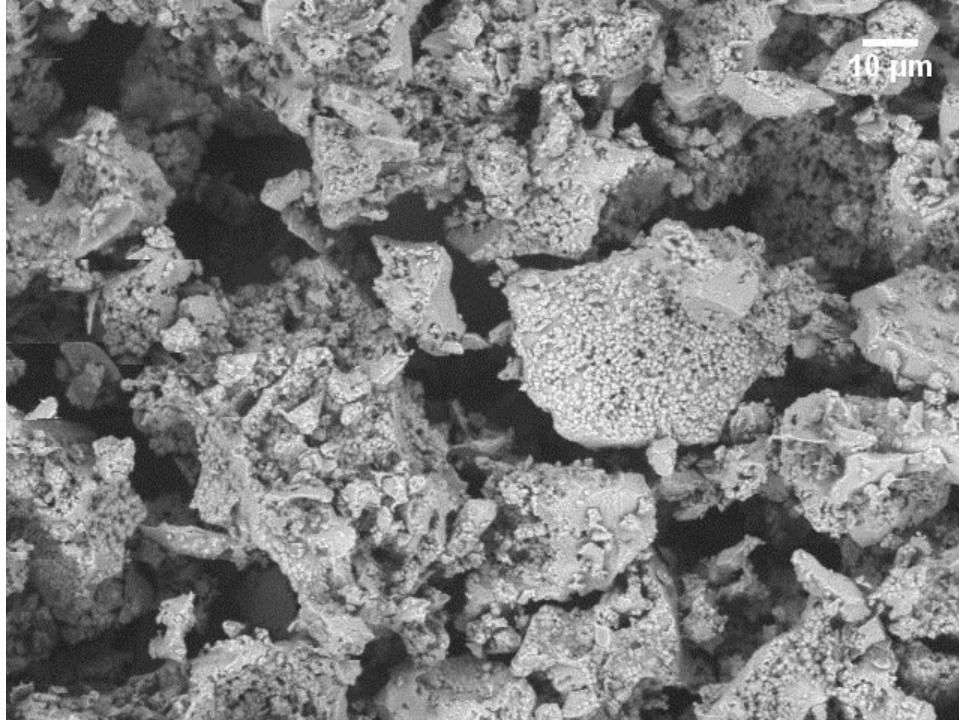
a) FE; b) ME; c) SE

The surface morphology of the encapsulated powder could be clearly seen with an increase in magnification at 1000x shown in Figure 6.7. Small capsules were seen on the surface of powders obtained by freeze drying encapsulation, the surface was smooth with respect to powders obtained by microwave assisted encapsulation method, presence of pores were seen on the surface of the powders obtained from the simple encapsulation method.

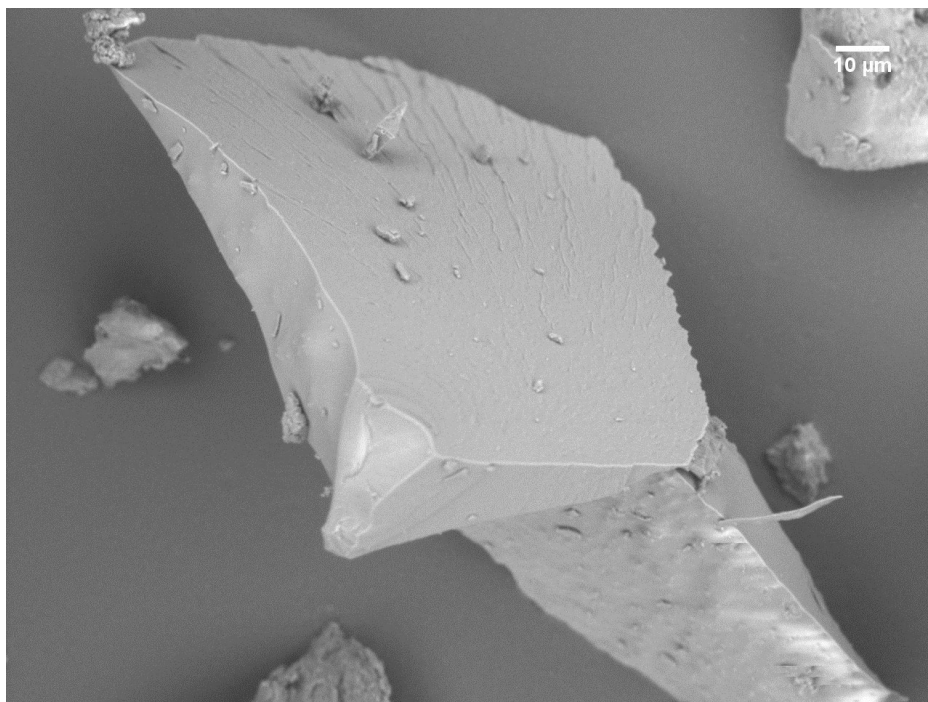
The surface morphology of microwave encapsulated powder was interesting; in order to examine the surface closely, the image was magnified to 2000x (Figure 6.8) and was compared with the SEM image of FE powder at 2000x, it can be seen that the FE powder had small spherical structures and was porous, while the ME powder had a dense, smooth surface. Even the cross section of the ME powder did not show the presence of pores which is an interesting feature. In microwave encapsulation of AuNP into maltodextrin matrix, increase in concentration of maltodextrin can be negatively correlated to release of AuNP, showing strong entrapment within the matrix.

The reason for significant difference in the structure of the microwave assisted encapsulation powder when compared to freeze drying encapsulation and simple encapsulation might be due to the internal heating phenomenon associated with the microwave energy (Clark et al., 2000). The sample containing the maltodextrin and AuNP, is placed within a small crucible inside a microwave system. The microwave heating results in heating up of the core followed by the surface providing a dense matrix of AuNP encapsulated powder. Thus the microwave encapsulated powder did not have pores when observed with scanning electron microscope. Interactions of gold nanoparticles in maltodextrin matrix and its reaction to microwave energy create this

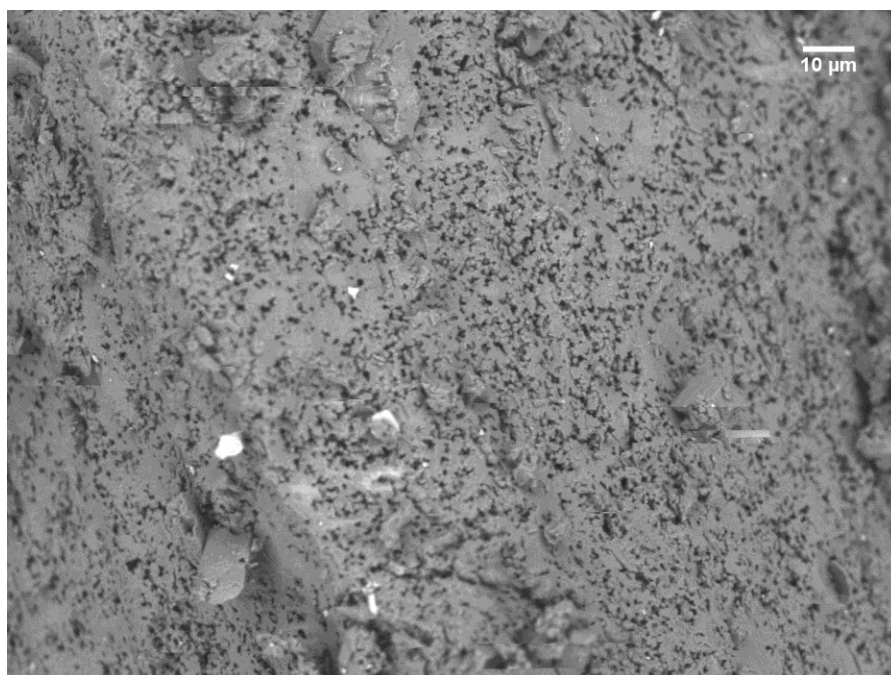
interesting surface morphology. The reasons for such surface morphology are unknown and need to be studied further.



a) Freeze drying encapsulation (FE) , magnification 1000 x



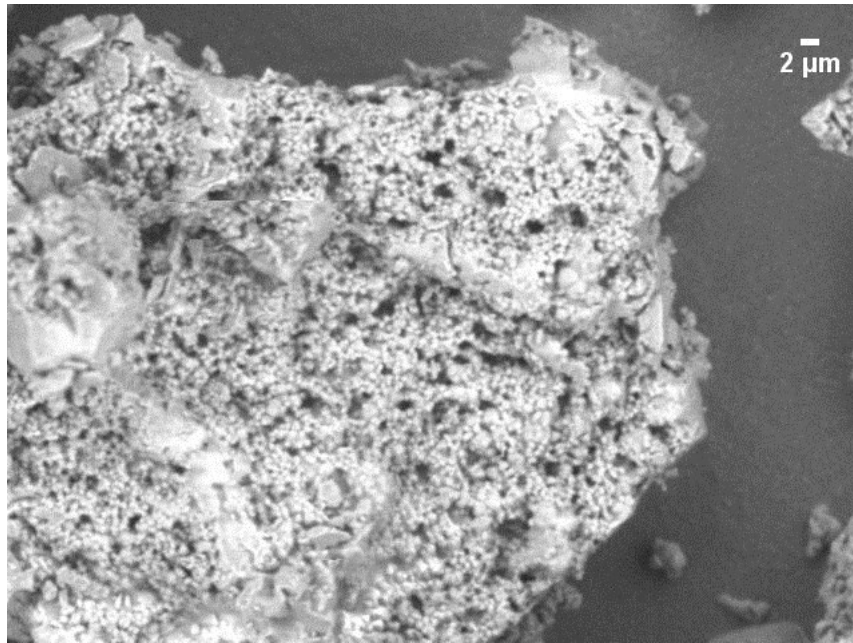
b) Microwave assisted encapsulation (ME) , magnification 1000 x



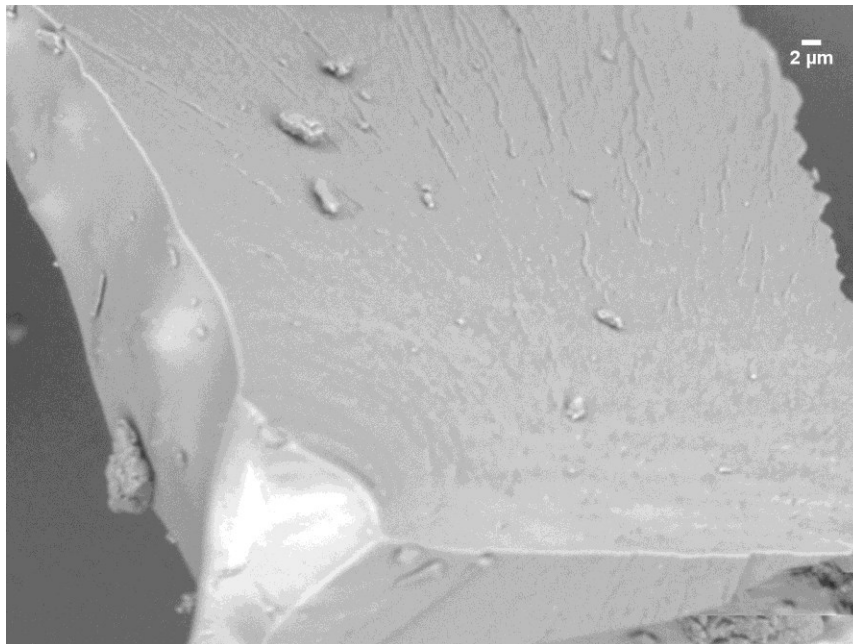
c) Simple encapsulation (SE) , magnification 1000 x

Figure 6.7 SEM micrograph of AuNP encapsulated powder at 1000 x magnification.

a) FE; b) ME; c) SE



Freeze drying encapsulation (FE) , magnification 2000 x



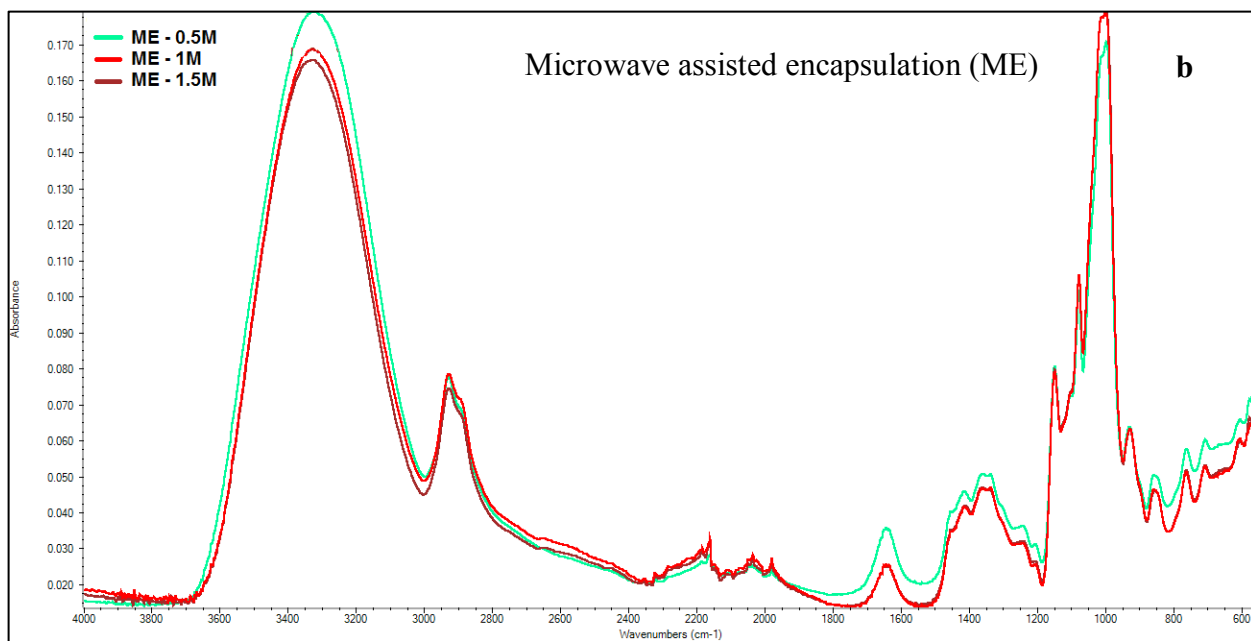
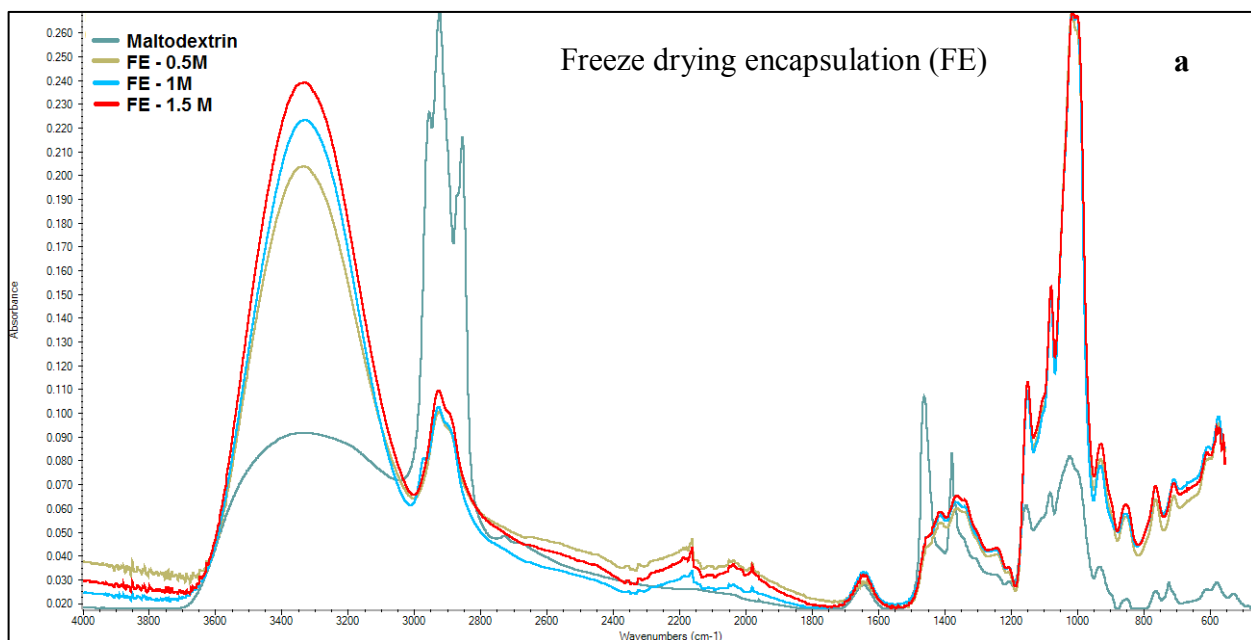
Microwave assisted encapsulation (ME) , magnification 2000 x

Figure 6.8 Comparing the SEM micrographs for freeze drying and microwave assisted encapsulation methods

6.4.3 Conformation of functional groups from FTIR spectra

FTIR analysis was used to identify the functional groups and for structural characterisation of AuNP encapsulated maltodextrin powders produced by the three encapsulation methods. The presence of the broad absorbance peak at 3332 cm^{-1} corresponds to the hydroxyl functional group in alcohols and phenolic compounds (Song et al., 2009). It can be seen from Figure 6.9(a) that the peak at 3324.68 cm^{-1} for pure maltodextrin was medium and after the encapsulation process the peak intensified to a broad peak for all the three encapsulation methods, freeze drying encapsulation (FE) 3331.55 cm^{-1} , microwave assisted encapsulation (ME) 3331.43 cm^{-1} and simple encapsulation methods (SE) 3332.30 cm^{-1} .

The presence of strong alkyl C-H stretching vibrations of methyl groups present at 2923.56 cm^{-1} and 2854.13 cm^{-1} was shifted to medium C-H stretching in all the FTIR spectra after the encapsulation process. The peak at 2854.13 cm^{-1} in pure maltodextrin was completely reduced and only the peaks at 2925.13 cm^{-1} (FE); 2928.48 cm^{-1} (ME); 2926.84 cm^{-1} (SE) were present after encapsulation for all the three concentrations. In Figure 6.9, we can see the presence of some peaks from 2350 to 2100 cm^{-1} for all the encapsulated powders which is absent in maltodextrin alone which might be due to the vibrations of the $\text{C}\equiv\text{C}$ of the alkynes group. The medium peak at 1459.85 cm^{-1} present in maltodextrin was reduced in the encapsulated powders, however there was the presence of peaks at 1409.85 cm^{-1} (FE), 1416.17 cm^{-1} (ME) and 1410.84 cm^{-1} (SE) around the same region, and this can be attributed to the stretching of the C-H bonds of the alkane group.



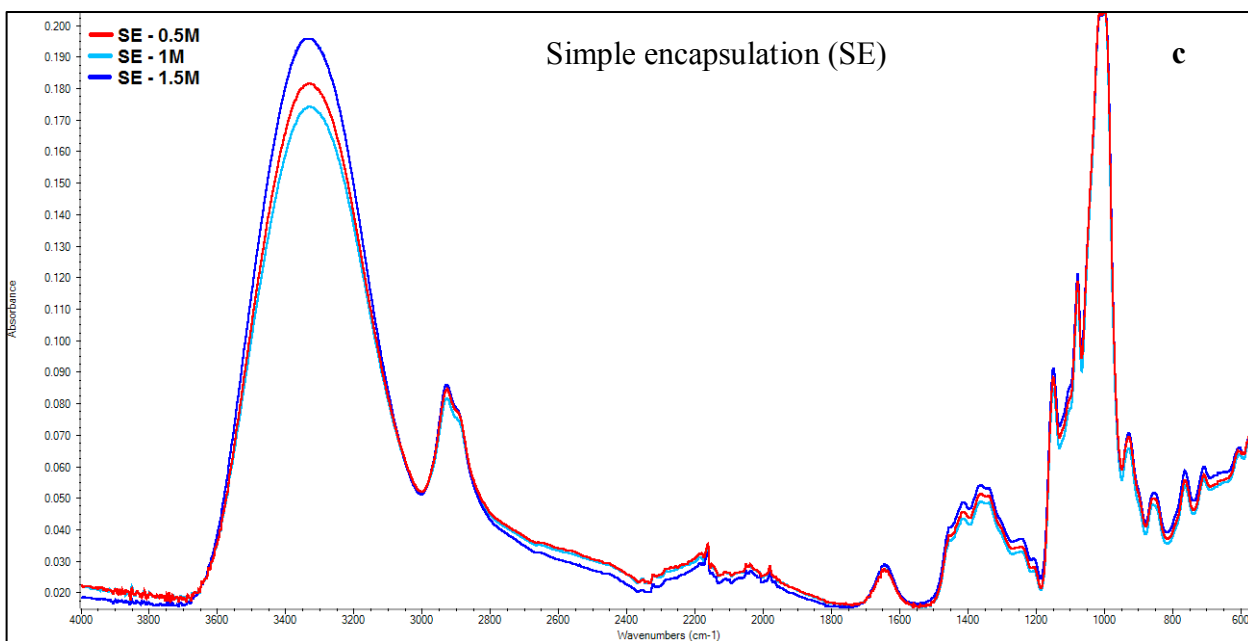


Figure 6.9 FTIR spectra for AuNP encapsulated powders for the three concentrations by a) Freeze drying encapsulation (FE); b) Microwave assisted encapsulation (ME); c) Simple encapsulation (SE)

The presence of the absorption peaks at (FE) 1077.16 cm^{-1} , (ME) 1076.91 cm^{-1} and (SE) 1077.09 cm^{-1} are present in the AuNP encapsulated powders and are absent in pure maltodextrin. This is similar to the FTIR peak at 1077 cm^{-1} obtained for gold nanoparticles obtained from *Cinnamomum camphora* leaf (Huang et al., 2007). A recent study (Kuppusamy et al., 2014) states that the presence of absorption peaks from 797.20 to 850.40 cm^{-1} indicates the presence of R-CH groups which are responsible for the reduction of Au^{III} into Au^0 . When comparing the FTIR spectra for AuNP encapsulated powders and pure maltodextrin, the presence of absorption peaks at 849.25 cm^{-1} for FE, 857.12 cm^{-1} for ME and 852.05 cm^{-1} for SE, are completely absent in the case of pure maltodextrin. These IR peaks can be related to the gold nanoparticles absorption peaks

from the literature, the occurrence of this peak in the AuNP encapsulated powder which is absent in pure maltodextrin indicates the change in the chemical nature of maltodextrin after encapsulation with gold nanoparticles.

6.4.4 Thermal analysis using differential scanning calorimeter (DSC)

6.4.4.1 DSC results for AuNP powder by freeze drying encapsulation method

The DSC thermal profile for the AuNP encapsulated maltodextrin powder was investigated from 0°C to 400°C. From the DSC thermograph for AuNP encapsulated maltodextrin powder (0.5M) using freeze drying method, the first endothermic peak was found with an onset temperature at 59.12 ± 1.04 °C and the peak maximum was at 115.78 ± 0.59 °C and a heat capacity of 162.97 ± 1.19 J/g. This endothermic transition took place at 7.5 min after the start of the thermal heating with ramping up at every 10 °C/min.

The first exothermic peak occurred at an onset of 263.40 ± 0.38 °C and a peak maximum at 266.93 ± 0.41 °C with a smaller heat capacity of 3.07 ± 0.46 J/g. Small shoulder peak appeared around 272.00 °C which appeared in all three replicates. The last thermal decomposition occurred with an onset temperature of 273.79 ± 1.39 °C and a peak maximum at 276.07 ± 1.64 °C with c_p of 9.75 ± 2.02 J/g around 16 min.

Figure 6.10 presents the DSC thermograph for AuNP encapsulated maltodextrin powder (1M) using freeze drying technique. The first exothermic peak occurred with an onset temperature of 20.32 ± 0.26 °C with a lower heat capacity of 4.28 ± 0.87 J/g and a peak maximum of 21.58 ± 0.23 °C. The first endothermic peak occurred with an onset temperature of 72.73 ± 3.43 °C with heat capacity of 173.05 ± 7.14 J/g and the peak maximum of 121.35 ± 3.50 °C at 10 min.

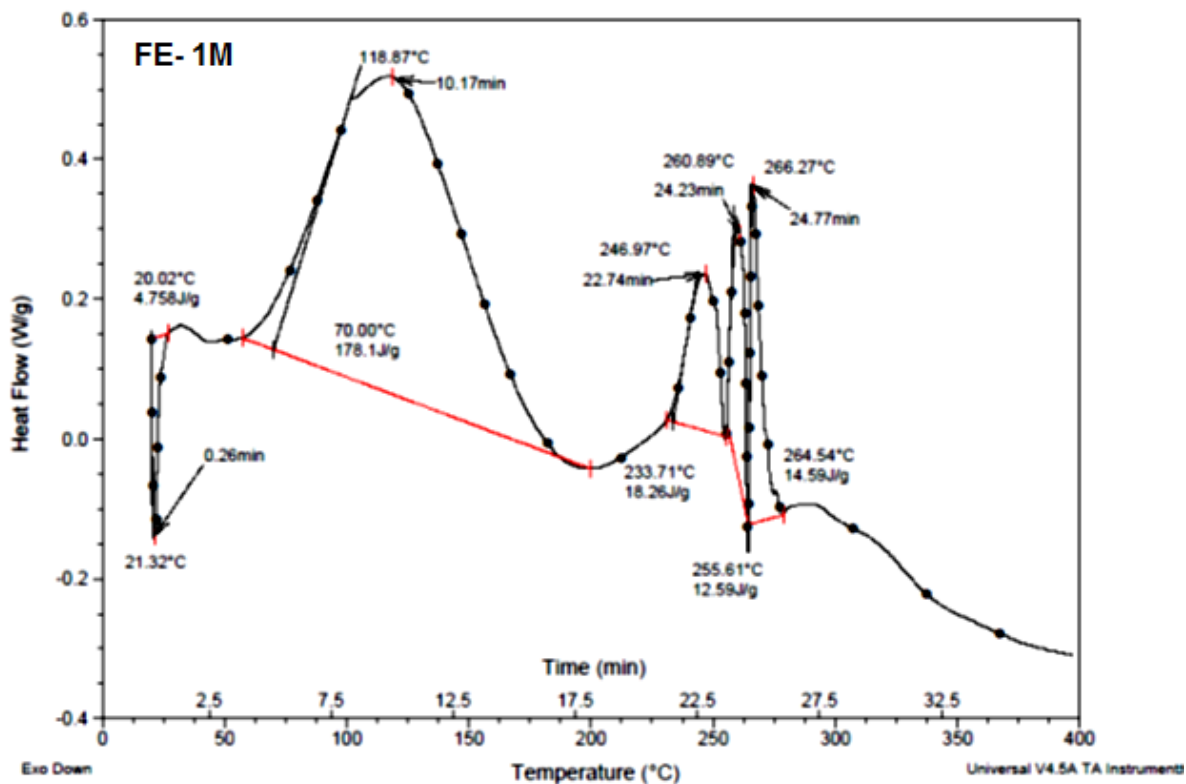


Figure 6.10 DSC thermograph for AuNP encapsulated maltodextrin powder by freeze drying encapsulation method (1M)

The second endothermic peak occurred at 233.23 ± 0.47 °C with comparatively lower heat capacity of 17.82 ± 0.63 J/g with respect to the first endothermic peak and a peak maximum at 247.36 ± 2.26 °C. From Figure 6.10 it can be seen that three endothermic peaks occurred between 22 to 24 min of the heating cycle. The fourth endothermic peak occurred with an onset temperature of 256.86 ± 3.63 °C and peaked maximum at 261.79 ± 3.61 °C with a c_p of 11.14 ± 1.64 J/g at 24 min. The last endothermic decomposition peak was found at 24 min, with onset temperature at 262.96 ± 2.23 °C and peak maximum at 264.66 ± 2.28 °C with a heat capacity of 14.07 ± 0.74 J/g.

Similar trend was found for (FE – 1.5 M) AuNP encapsulated powder obtained from freeze drying method with slight difference in the thermal transition temperatures. The first exothermic peak occurred with an onset temperature of 20.50 ± 0.02 °C and peak maximum at 21.71 ± 0.06 °C with 3.98 ± 0.41 J/g (cP). The first endothermic peak obtained for 1.5 M maltodextrin containing AuNP was slightly lower to the endothermic peak obtained for 1 M maltodextrin containing AuNP. The onset temperature was at 57.25 ± 0.37 °C and the peak maximum was at 103.56 ± 0.59 °C with the heat capacity of 168.10 ± 2.12 J/g. Even the time of the first endothermic peak decomposition was at 8 min compared to that of 10 min in case of 1M maltodextrin containing AuNP.

The second endothermic peak was at 232.42 ± 1.89 °C onset temperature and 250.10 ± 0.51 °C peak maximum with 33.40 ± 2.28 J/g heat capacity. The third peak occurred at 261.34 ± 0.75 °C onset temperature and peak maximum at 265.61 ± 0.33 °C with c_p of 7.94 ± 0.14 J/g. The fourth peak occurred at 268.48 ± 0.68 °C onset temperature and peak maximum of 270.57 ± 1.05 °C with c_p of 9.91 ± 0.53 J/g. The second, third and fourth endothermic peaks occurred between 23 to 25 min.

In the case of FE-0.5M the last thermal decomposition occurred around 16 min whereas in the case of FE- 1M and FE – 1.5M the last thermal decomposition occurred between 24 to 25 min. Thus the latter two compositions have more thermal stability compared to FE- 0.5M. When comparing between FE- 1M and FE- 1.5 M, though they both follow similar thermal decomposition profiles, the first endothermic decomposition peak for FE-1M occurred at 10 min with maximum peak temperature of 121.35 °C compared to the first endothermic decomposition peak temperature of 103.56 °C for FE- 1.5 M at 8 min. Therefore a higher time and temperature combination is required for the

thermal decomposition of AuNP encapsulated 1M maltodextrin by freeze drying technique.

6.4.4.2 DSC results for AuNP powder by microwave assisted encapsulation method

The first exothermic peak for AuNP encapsulated in maltodextrin (0.5M) by microwave assisted encapsulation method occurred at 21.78 ± 0.01 °C peak maximum temperature with a heat capacity of 2.01 ± 0.05 J/g. The first endothermic peak had an onset temperature at 76.38 ± 3.71 °C and a peak maximum at 129.16 ± 1.20 °C with heat capacity of 136.90 ± 3.11 J/g. This thermal transition occurred at 11 min.

The second endothermic peak occurred at 229.91 ± 0.56 °C with c_p of 24.80 ± 3.95 J/g with its peak maximum temperature at 244.88 ± 2.18 °C at 23 min. The presence of an endothermic peak between 22 and 24 min was found to be not as prominent as those obtained in the DSC thermograph for AuNP encapsulated powders by freeze drying method. The third endothermic peak was sharp with an onset temperature at 260.94 ± 0.25 °C and a peak maximum temperature of 262.84 ± 0.16 °C with heat capacity of 17.23 ± 3.63 J/g. The last thermal transitions took place at 24 min.

Figure 6.11 shows the DSC thermograph for AuNP encapsulated powder (1M) using microwave assisted encapsulation method. From the figure it can be seen that the first thermal exothermic transition took place from an onset temperature of 20.67 °C and a peak maximum of 21.76 ± 0.01 °C and heat capacity of 1.89 ± 0.18 J/g.

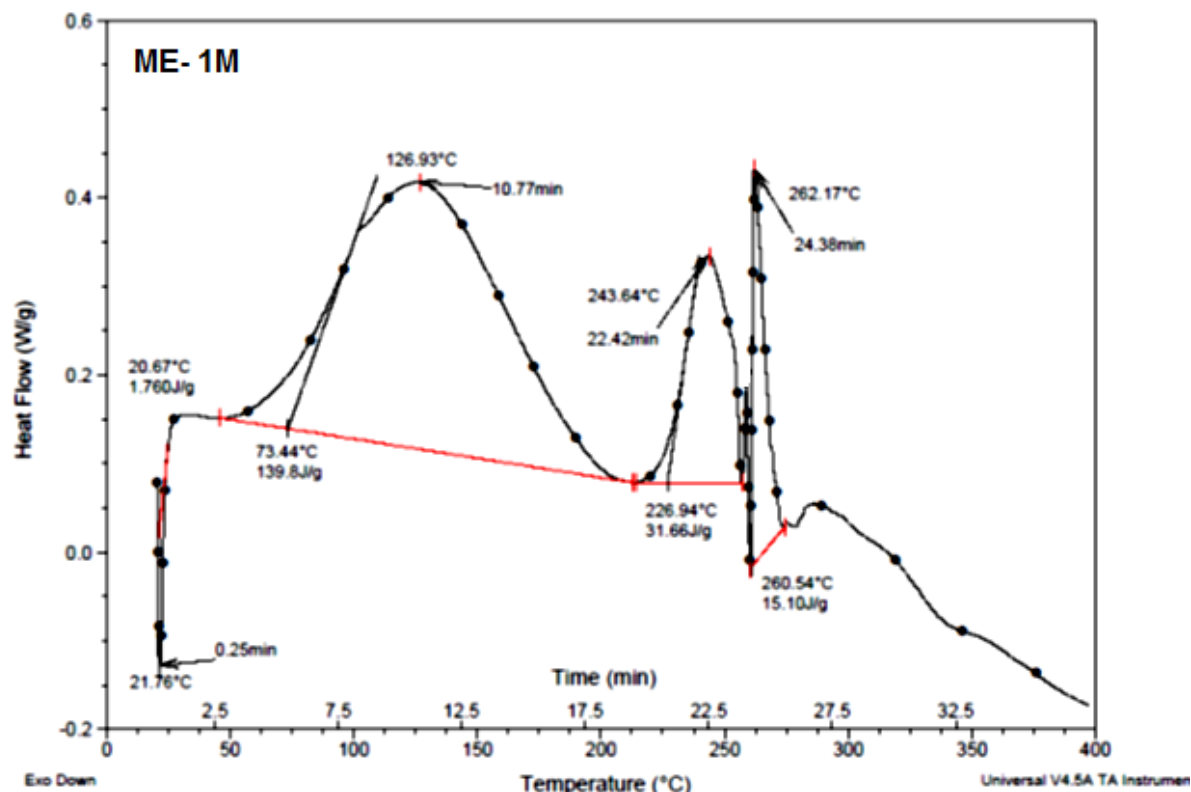


Figure 6.11 DSC thermograph for AuNP encapsulated powder by microwave assisted encapsulation method (1M)

Following a steady increase in temperature of 10 °C/min, the first endothermic peak occurred with an onset temperature of 76.22 ± 3.93 °C and peak maximum of 127.71 ± 1.10 °C and heat capacity of 136.75 ± 4.31 J/g at 11 min. The second endothermic peak had an onset at 228.92 ± 2.80 °C and a peak maximum temperature of 246.13 ± 3.51 °C with heat capacity of 34.65 ± 4.23 J/g at 22 min. The onset temperature for the third endothermic peak was at 264.73 ± 5.93 °C and maximum peak temperature of 266.07 ± 5.52 °C with heat capacity of 11.50 ± 5.09 J/g at 24 min.

The DSC thermograph for (1.5 M) maltodextrin containing AuNP has an exothermic peak with a heat capacity of 2.54 ± 0.54 J/g having an onset temperature at

20.57 \pm 0.05 $^{\circ}\text{C}$ and peak maximum at 21.72 \pm 0.08 $^{\circ}\text{C}$. The first endothermic peak occurred with an onset temperature of 63.77 \pm 3.42 $^{\circ}\text{C}$ and a peak maximum at 120.39 \pm 4.99 $^{\circ}\text{C}$ with heat capacity of 125.10 \pm 6.51 J/g at 11 min. The second endothermic peak occurred with an onset temperature of 224.88 \pm 6.92 $^{\circ}\text{C}$ and peak maximum of 247.53 \pm 0.45 $^{\circ}\text{C}$ with heat capacity of 34.78 \pm 5.73 J/g at 23 min. The third endothermic peak had a heat capacity of 15.89 \pm 4.89 J/g with onset temperature of 257.97 \pm 5.98 $^{\circ}\text{C}$ and peak maximum temperature of 259.79 \pm 5.89 $^{\circ}\text{C}$ at 24 min.

6.4.4.3 DSC results for AuNP powder by simple encapsulation method

The DSC thermograph for AuNP encapsulated maltodextrin (0.5M) by simple encapsulation method has an exothermic peak maximum at 21.63 \pm 0.20 $^{\circ}\text{C}$ with heat capacity of 5.59 \pm 0.67 J/g. The first endothermic peak occurred at 56.74 \pm 4.89 $^{\circ}\text{C}$ onset temperature and a peak maximum of 108.93 \pm 3.79 $^{\circ}\text{C}$ with a heat capacity of 177.30 \pm 0.28 J/g at 9 min. The second endothermic peak had a peak maximum at 249.52 \pm 2.78 $^{\circ}\text{C}$ at an onset temperature of 225.39 \pm 0.52 $^{\circ}\text{C}$ with heat capacity of 27.18 \pm 2.69 J/g at 23 min.

The intermediate peak between 23 min and 25 min was prominent similar to that of DSC thermographs obtained for freeze drying method. The third endothermic peak occurred at an onset temperature of 258.79 \pm 1.99 $^{\circ}\text{C}$ and a peak maximum of 263.67 \pm 1.58 $^{\circ}\text{C}$ with heat capacity of 15.36 \pm 0.66 J/g at 24 min. The last thermal decomposition occurred at 25 min with an onset temperature of 268.43 \pm 2.11 $^{\circ}\text{C}$ and peak maximum of 270.56 \pm 2.88 $^{\circ}\text{C}$ with c_p of 9.64 \pm 2.00 J/g.

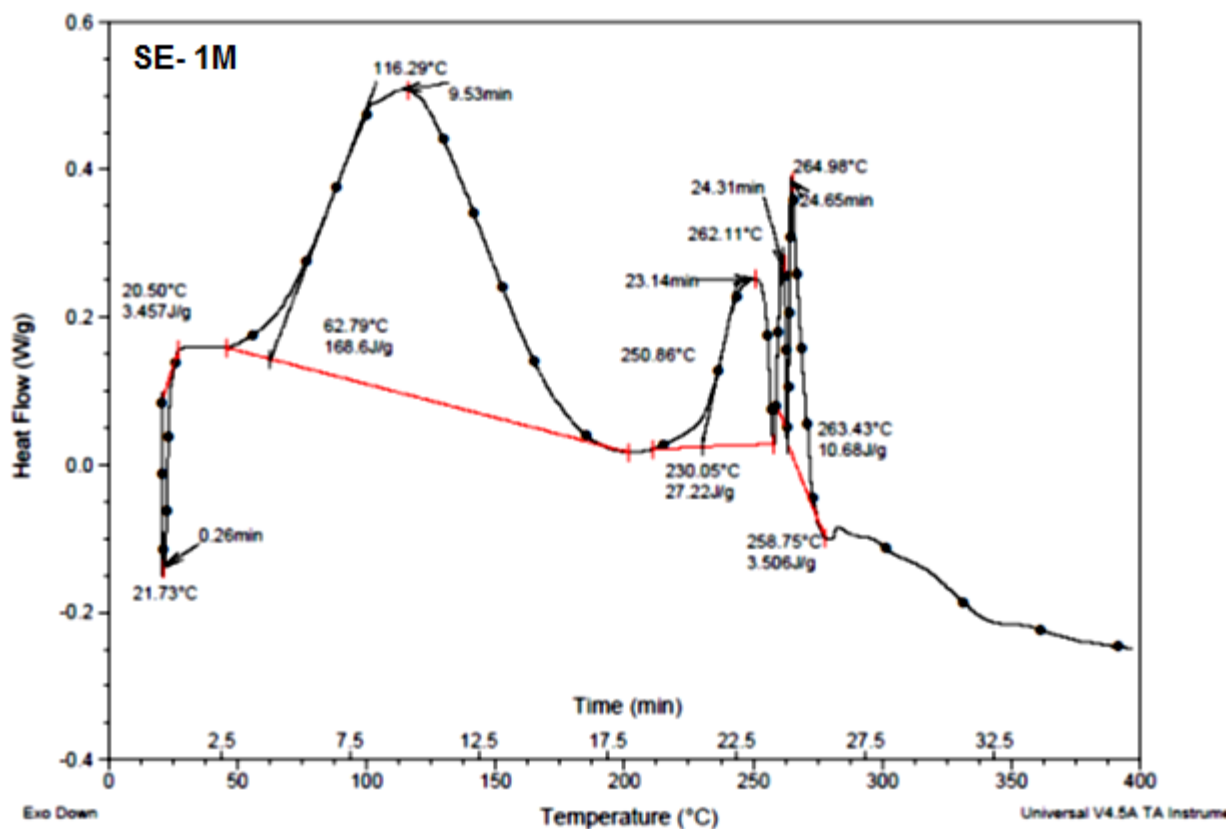


Figure 6.12 DSC thermograph for AuNP encapsulated powder by simple encapsulation method (1M)

The DSC thermograph for AuNP encapsulated maltodextrin (1M) is shown in Figure 6.12, from which can be seen the occurrence of the exothermic peak maximum at 21.74 ± 0.01 °C and a peak onset temperature 20.48 ± 0.03 °C with heat capacity of 3.23 ± 0.32 J/g. The first endothermic peak had an onset temperature of 61.49 ± 1.84 °C and peak maximum of 113.95 ± 3.31 °C with c_p of 169.55 ± 1.34 J/g at 9 min.

The second endothermic transition occurred at an onset of 227.66 ± 3.38 °C and peak maximum temperature of 251.11 ± 0.35 °C with heat capacity of 26.25 ± 1.37 J/g at 23 min. The third endothermic peak onset temperature was at 258.07 ± 0.97 °C and

maximum peak temperature was at 262.33 ± 0.31 °C with heat capacity of 3.25 ± 0.36 J/g. The fourth endothermic transition took place with an onset temperature of 265.19 ± 2.48 °C and reached a maximum temperature of 266.75 ± 2.50 °C and heat capacity of 10.35 ± 0.47 J/g. The last two thermal transitions occurred at 24 min.

The DSC thermograph for (1.5M) maltodextrin containing AuNP had the exothermic peak maximum at 21.82 ± 0.09 °C with heat capacity of 5.03 ± 0.03 J/g. The first endothermic peak occurred with an onset temperature of 72.68 ± 8.59 °C and a peak maximum of 118.65 ± 7.16 °C with heat capacity of 158.10 ± 4.53 J/g at 10 min.

The onset temperature for the second endothermic peak was at 232.12 ± 0.75 °C and peak maximum at 252.28 ± 0.95 °C with heat capacity of 25.43 ± 4.29 J/g at 23 min. The third endothermic peak had onset temperature of 260.10 ± 2.89 °C and peak maximum of 264.40 ± 2.38 °C with heat capacity of 7.47 ± 2.06 J/g at 24 min. The fourth endothermic peak had an onset temperature of 266.04 ± 2.20 °C and peak maximum of 267.94 ± 2.69 °C with heat capacity of 11.80 ± 2.73 J/g at 25 min.

Thus the thermal properties of AuNP encapsulated powder in maltodextrin has been characterised by DSC. The representation of the time and temperature combination in the thermal analysis data will be useful information for designing and developing new applications. The characterization of nanomaterials in this study adds information to the current literature database. This information is important as different nanomaterials show different thermal and structural properties. The thermal properties of maltodextrin encapsulated AuNP powder obtained from microwave assisted encapsulation and freeze drying encapsulation exhibited similar trends during thermal decomposition. However,

comparing the SEM images of maltodextrin encapsulated AuNP powders produced by these two methods, reveals completely different surface morphologies. The reasons for such changes need further investigation.

6.5 Conclusion:

The results from this study show that the gold nanoparticles can be successfully incorporated into a food grade polymer matrix using just water as the solvent. The results from the encapsulation efficiency and AuNP loading study for 1M concentration of maltodextrin showed relatively few differences for the three methods when compared to 0.5M and 1.5M concentrations. The AuNP encapsulated powders were characterised using a particle size analyzer, differential scanning calorimeter (DSC), spectral properties using Fourier transform infrared spectroscopy (FTIR), UV-Vis spectrophotometer and structural morphology using a scanning electron microscope (SEM). The SEM micrographs revealed that microcapsules were obtained from freeze drying encapsulation, whereas microwave assisted encapsulation resulted in the complexation of the gold nanoparticles within the polymer matrix. The fundamental understanding of how microwave interacts with the gold nanoparticles and maltodextrin will be a key to unlock avenues for future application. The results obtained from this study are significant as they demonstrate that gold nanoparticles can be incorporated into maltodextrin using simple methods with water as the solvent. By developing such new encapsulation protocols the use of toxic chemicals for synthesizing nanoparticles can be eventually avoided.

CONNECTING STATEMENT TO CHAPTER VII

In Chapter VI, it was demonstrated that gold nanoparticles can be incorporated into a maltodextrin matrix which is a linear polysaccharide by a top-down approach. This chapter explores the ***bottom-up approach*** for polymeric nanoparticle synthesis. **Chapter VII** looks at the possibility of incorporating gold nanoparticles (AuNP) into cyclic structures such as beta cyclodextrin (BCD). The encapsulation of AuNP in BCD complex was studied using three encapsulation methods.

The protocols were developed and the experiments were conducted by Ms. Krishnaswamy under the guidance of Dr. Orsat. This study is under preparation for publication in the *Journal of Nanoparticle Research*.

CHAPTER VII

BETA-CYCLODEXTRIN ENCAPSULATED GOLD NANOPARTICLES USING GREEN NANOTECHNOLOGY APPROACH

7.1 Abstract

The formation of supramolecular complex between beta-cyclodextrin (BCD) and catechin synthesized gold nanoparticles (AuNP) is investigated in this study by comparing with three encapsulation methods such as molecular inclusion encapsulation (MIB), lyophilisation encapsulation (FEB) and microwave assisted encapsulation (MEB). The AuNP encapsulated powders were characterised using differential scanning calorimetry (DSC), Fourier transform infrared spectroscopy (FTIR), scanning electron microscopy (SEM) and particle size analysis. Shorter reaction time was required for the complexation of gold nanoparticles into beta-cyclodextrin (BCD) using microwave assisted encapsulation. High desirability value was obtained for AuNP + BCD powders obtained from lyophilisation encapsulation method when comparing yield %, AuNP loading, AuNP encapsulation efficiency and particle size with the other methods. The morphological results from SEM revealed an interesting structure for the AuNP encapsulated BCD powder obtained by the three encapsulation methods. The SEM images from the lyophilisation encapsulation method showed spherical globular morphology with a particle size of about 1 μm containing gold nanoparticles.

Key words: Catechin, Freeze drying, gold nanoparticles, nano-encapsulation, SEM, DSC, FTIR.

7.2 Introduction

Cyclodextrins (CD) are cyclic oligomers of α -D-glucopyranose produced from starch degradation by cyclodextrin glucanotransferase (CGTase) enzyme resulting in intramolecular transglycosylation reaction. Supra molecular self- assembly of bioactive compounds can be achieved by cyclodextrin due to their unique structure. The structure of first generation or parent cyclodextrins are α -cyclodextrins (α - CD), β -cyclodextrins (β - CD) and γ -cyclodextrins (γ - CD) is provided in Figure 7.1. It has a truncated cone structure like a torus with a hydrophilic outer surface and a hydrophobic inner cavity (Astray et al., 2009; Szejtli, 1998). The cyclic structure of CD is due to the formation of a link among glucopyranose of dextrin through glycosidic oxygen bridges of α (1,4) bonds (Figure 7.2).

The first generation or parent cyclodextrins such as α -cyclodextrins (α - CD), β -cyclodextrins (β - CD) and γ -cyclodextrins (γ - CD) consist of six, seven and eight α (1,4)- linked glycosyl units. Cyclodextrin is a torus molecule (doughnut-shaped) with a hydrophobic internal cavity and a hydrophilic external cavity which enhances the entrapment of the guest molecule either wholly or partially without the formation of a covalent bond (Del Valle, 2004; Szejtli, 1998). The main properties of cyclodextrins are given in Table 7.1.

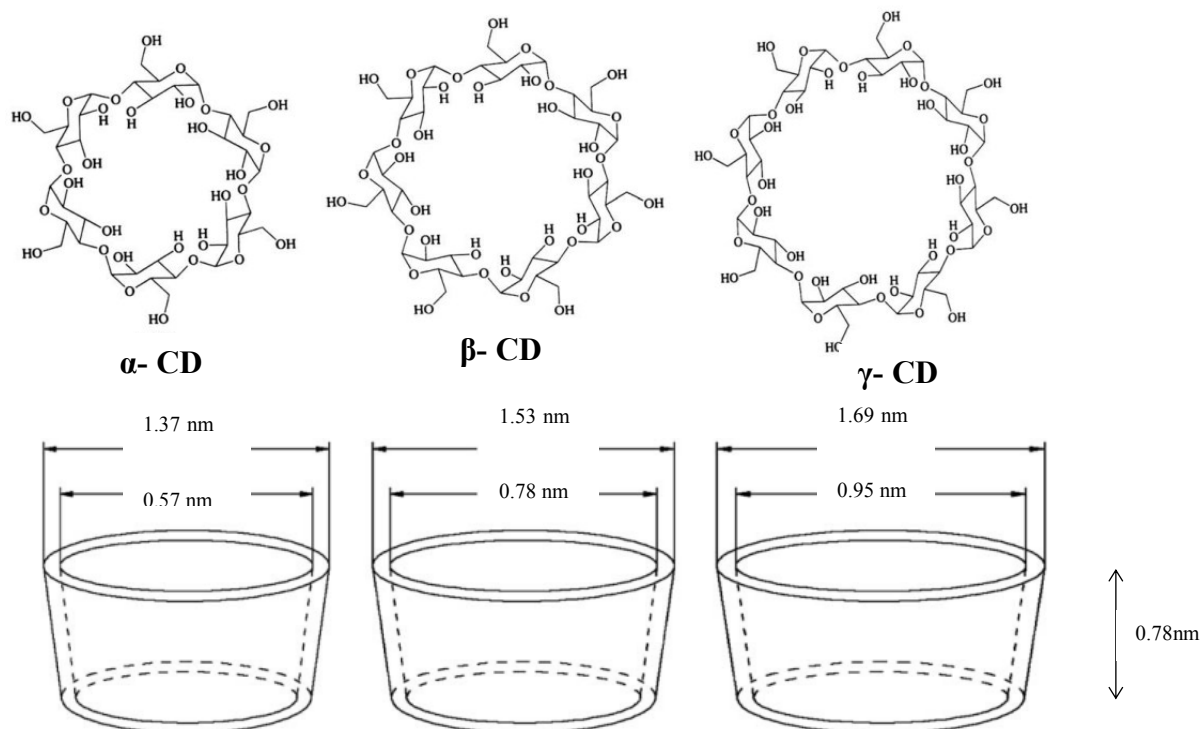


Figure 7.1 Chemical structure and approximate geometric dimensions of α -cyclodextrins (α - CD), β -cyclodextrins (β - CD) and γ -cyclodextrins (γ - CD) (Astray et al., 2009)

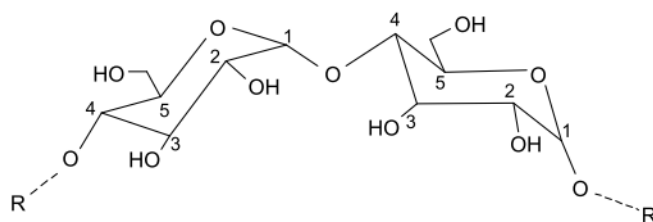


Figure 7.2 Glycosidic oxygen bridge α (1,4) bond formation between two molecules of glucopyranose (Astray et al., 2009)

Cyclodextrins are empty capsules with a certain molecular size that can take in a variety of host molecules within their cavity. The resulting complex is called “inclusion complex”. The “guest” molecule (inner core) forms an inclusion complex either totally or

partially with the “host” molecule (outer core). The cyclodextrin molecule has a hydrophilic outside that can dissolve in water and the inner apolar cavity provides a hydrophobic matrix creating a “micro heterogeneous environment” (Astray et al., 2009; Szejtli, 1998).

Inclusion of a guest molecule into the cyclodextrin cavity takes place due to substitution of water by a less polar guest. The forces which bind the guest and cyclodextrin molecules together are a combination of Van der Waals forces, hydrophobic interactions and hydrogen bonds (Del Valle, 2004).

Table 7.1 Properties of different cyclodextrins (Del Valle, 2004)

Property	α - Cyclodextrin	β - Cyclodextrin	γ - Cyclodextrin
No. of glucopyranose unit	6	7	8
Molecular weight (g/mol)	972	1135	1297
Solubility in water at 25 ⁰ C (% w/v)	14.5	1.85	23.2
Outer diameter (Å)	14.6	15.4	17.5
Cavity diameter (Å)	4.7 – 5.3	6.0 – 6.5	7.5 – 8.3
Height of torus Å	7.9	7.9	7.9
Cavity volume Å ³	174	262	427

Cyclodextrins are widely used in pharmaceutical applications (Loftsson & Duchêne, 2007) as drug delivery systems (Machín et al., 2012) for controlled drug release (Hirayama & Uekama, 1999) and in cosmetics (Buschmann & Schollmeyer, 2002) as most of the drugs are poorly soluble in water, sensitive to oxidation, light and thermal decomposition (Szejtli, 1998; Szenté & Szejtli, 2004). They are used in the food industry

as food additives, for elimination of undesired taste, stabilization of flavors, removal of undesired compounds, to avoid microbiological contamination and to encapsulate plant bioactive compounds (Astray et al., 2010; Augustin & Hemar, 2009; Pinho et al., 2014).

Cyclodextrins functionalised graphene-gold nanoparticles have been demonstrated to be highly sensitive biosensors (Xue et al., 2015), and the inclusion of gold-silver core in beta-cyclodextrin has been shown to enhance surface enhanced Raman scattering (SERS) (Pande et al., 2007). Cyclodextrin capped gold nanoparticles for non-covalent encapsulation of chemotherapeutic drug β – Lapachone was studied by HeeáKook et al., (2009) which exhibits superior activity against cancer cells in breast, lung and prostate tissues. These AuNP were functionalised with compounds like α -methoxy- ω -mercapto-poly(ethylene glycol) and α -succinimidyl propionate- ω -lipoic acid-poly(ethylene glycol) (HeeáKook et al., 2009) which might be toxic. Anticancer drug methotrexate was complexed with beta-cyclodextrin bearing gold glyconanoparticles for site specific drug delivery of compounds like bisalkyltetra (ethylene glycol) disulfide following complex synthesis protocols (Aykaç et al., 2013). There is a need to develop simple synthesis protocols for complexation of beta-cyclodextrin.

Beta-cyclodextrin is a FDA (Food and Drug Administration) approved highly biocompatible molecule obtained from starch degradation (Pinho et al., 2014). This study aims to form complexation of gold nanoparticles synthesized using catechin into a beta-cyclodextrin cavity following a simple, non-complicated protocol, using water as the solvent. Three encapsulation methods such as molecular inclusion encapsulation (MIB), lyophilisation encapsulation (FEB) and microwave assisted encapsulation (MEB) were investigated for the complexation of AuNP into beta-cyclodextrin.

7.3 Materials and methods

7.3.1 Materials

Beta-cyclodextrin (BCD), catechin, $\text{HAuCl}_4 \cdot 3\text{H}_2\text{O}$ were purchased from Sigma-Aldrich Co. (Canada). All chemicals were used without further purification. Distilled water with resistivity of $18.2 \text{ M}\Omega\cdot\text{cm}$ was obtained from Millipore system (Simplicity 185). All glassware used for the experiment was cleaned and dried in a hot air oven at 105°C for 12 hours prior to use.

7.3.2 Preparation of gold nanoparticles

The gold nanoparticles were synthesized using 1 mM catechin (Mw: 290.27 g/mol) with 1mM $\text{HAuCl}_4 \cdot 3\text{H}_2\text{O}$ (Mw: 393.83 g/mol). The solution was allowed to react for 20 min and was used for the encapsulation study. The prepared stock solution was kept in the dark to protect against light.

7.3.3 Encapsulation methods

For encapsulation of BCD+AuNP complex, 11.35 g of BCD (1M) was mixed with 20 ml double distilled water at $50 \pm 1^\circ\text{C}$. A magnetic stirrer was introduced into the beaker to aid in complete mixing of BCD. The gold nanoparticle solution was taken in a 5ml syringe (PrecisionGlide[®] Needle, 25 G $1\frac{1}{2}$), and was added drop by drop into the beaker containing the aqueous solution of BCD. A ratio (1:1) of guest molecule (catechin synthesized AuNP) with host molecule (beta-cyclodextrin) was used for molecular inclusion (Pinho et al., 2014; Szejtli, 1998). The solutions were allowed to mix with constant stirring at 200 rpm for 1 hour.

The prepared gold nanoparticles solution was dispersed into aqueous beta-cyclodextrin solutions of three different concentrations. The resulting mixture was stirred

for 15 min using a magnetic stirrer at 1000 rpm. For molecular inclusion encapsulation (MIB) of AuNP within BCD, the samples were placed in 5mL porcelain crucibles (24 x 20 x 1.8mm; Fisher Scientific) and dried in shaker cum incubator at 25 ± 2 °C with 100 rpm (Benchmark, Incu-Shaker Mini) for 48 hours. For freeze encapsulation/lyophilisation encapsulation (FEB), the prepared samples were frozen at -20 °C and then lyophilized at -47 °C for 24 hours. For microwave assisted encapsulation (MEB), the samples were placed in 5mL porcelain crucibles (24 x 20 x 1.8mm; Fisher Scientific) and heated with maximum incident microwave power of 200 W for 30 min with microwave ON/OFF cycle for every 30 sec. The temperature was maintained at 80°C for encapsulation of AuNP in the beta-cyclodextrin matrix (Puglisi et al., 2012).

The encapsulated powder from all the three methods were ground using a pestle and mortar for 5 minutes to ensure the lumps formed during the encapsulation process were broken and the sample powder was uniform. All the encapsulated powders were stored at -20° C until further use.

7.3.4 AuNP loading, Encapsulation efficiency and Yield %

Quantification of AuNP loading into beta-cyclodextrin cavity, encapsulation efficiency and yield% of the encapsulated powder were calculated based on the study of Ankrum et al., (2014) with certain modifications adapted for gold nanoparticles.

$$\text{AuNP loading} = \frac{(C_R \times V_R)}{M_{EP}} \quad (\text{Eq. 7.1})$$

$$\text{Encapsulation efficiency} = \left(\left[\frac{(C_R \times V_R)}{M_{EP}} \right] / \left[\frac{M_{NP}}{(M_{NP} + M_{BD})} \right] \right) \quad (\text{Eq. 7.2})$$

$$\text{Yield \%} = \left(\frac{\text{Final weight after encapsulation}}{\text{Initial weight before encapsulation}} \right) \times 100 \quad (\text{Eq. 7.3})$$

Where,

C_R = AuNP concentration of the release medium (mg/ μ l)

V_R = volume of the release medium (μ l) = 2000 μ l

M_{EP} = mass of the encapsulated powder (mg) = 20 mg

C_R = AuNP concentration of the release medium (mg/ μ l)

M_{NP} = mass of the AuNP (mg/ μ l)

M_{BD} = mass of the beta-cyclodextrin (mg/ μ l)

7.3.5 Particle size analysis

The particle size of the AuNP encapsulated powder was measured using a DelsaTM Nano C Particle Analyzer (Beckman Coulter, CA, U.S.A). The samples were prepared in an Eppendorf tube, where 0.10 g of the AuNP encapsulated powder was mixed with 1.5 ml of deionized water and sonicated for 5 min. The resulting solution was transferred to a 1 cm path length plastic cuvette. Deionized water (0.5 ml) was used to rinse the Eppendorf tube and to make up the total volume to 2 ml in the cuvette for particle size analysis. Scattering angle of 165.0°, with a pinhole set to 50 μ m, and refractive index of 1.3328 at a temperature of 25°C for 70 continuous accumulation times were used for this study. The samples were replicated thrice (n=3).

7.3.6 Differential Scanning Calorimeter

The thermal properties of the AuNP encapsulated powder was studied using a differential scanning calorimeter (DSC Q-100 V9.8 built 296, TA Instruments, Texas, USA). Triplicate samples of AuNP + BCD encapsulated powders obtained by the three encapsulation methods were selected and 5 mg (± 0.5 mg) of each powder was placed in small aluminum pans. The sample pans were hermetically sealed. The samples were made to cover the entire bottom surface of the pan to ensure good thermal contact. Care was taken to prevent over filling of the pan.

Nitrogen was used as the purge gas as it is inert in nature. The rate of flow of nitrogen was 50 ml/min. Indium was used for calibration. The thermal process was monitored from 0 to 400°C, with ramping up at 10 °C/min. Reproducibility was checked by running the sample in triplicates. TA Universal Analysis V4.5A software was used for processing the data.

7.3.7 Scanning Electron Microscopy

The SEM images were obtained from Olympus TM3000 scanning electron microscope. The experiment was conducted with a field emission at 5 kV. A small amount of the sample was spread on a double adhesive carbon tab (Carbon Tabs, 25mm dia, Canemco-Marivac, Canada) and mounted on the metal stub.

7.3.8 Fourier Transform Infrared Spectroscopy

FTIR measurements were carried out using a Thermo Scientific Nicolet iS5. Attenuated total reflectance (ATR) method was used to collect the spectra using iD5 ATR with diamond crystal. A small amount of the AuNP + BCD powder was placed on the ATR platform, and care was taken to ensure that the sample covered the surface of the

diamond crystal completely and that there was proper contact between the sample powder and the diamond crystal.

All spectra were averaged from 32 scans and collected in absorbance mode at 4 cm⁻¹ spectral resolution from 4000- 600 cm⁻¹ range. To eliminate the possible equipment drift, the environmental spectrum which includes water vapour and carbon dioxide was collected as background before every spectral collection of each sample.

7.3.9 Statistical analysis

One-way ANOVA was used for this study. Microwave assisted encapsulation was compared with lyophilisation encapsulation and molecular inclusion encapsulation method. The experiments were conducted in triplicates and the difference was considered significant at $p < 0.05$.

7.4 Results and discussion

7.4.1 Interpretation of UV-Visible spectra for surface plasmon resonance (SPR)

In order to find the maximum wavelength for surface plasmon resonance (SPR) for the different concentrations of AuNP, a UV-Vis spectra scan was taken from 400-900 nm, with medium scan speed and step up size for every 1.0 nm as shown in Figure 7.3. The increase in the nanoparticle concentration for every 100 µl and the subsequent increase in the SPR peak can be clearly seen from Figure 7.3. The maximum SPR peak value was absorbed at 560 nm wavelength based on which a standard curve with different concentrations of gold nanoparticles was plotted as shown in Figure 7.4, where the regression values will be useful for estimating the concentration of gold nanoparticles entrapped into beta-cyclodextrin.

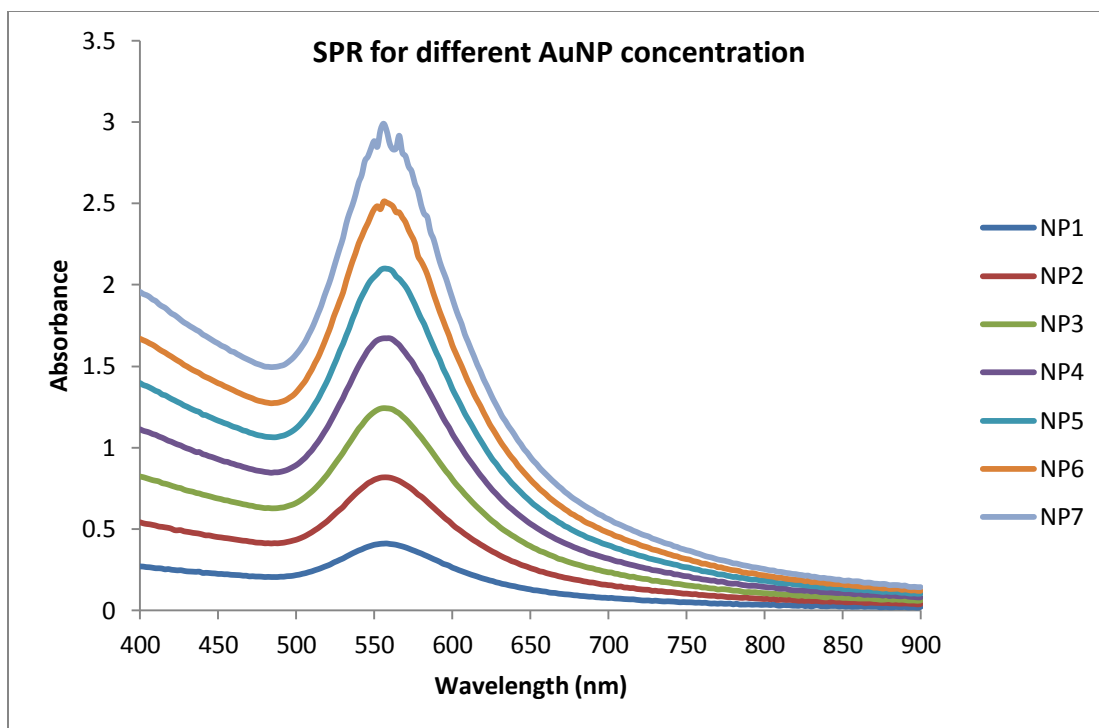


Figure 7.3 Surface plasmon resonance (SPR) plots for different concentrations of gold nanoparticles

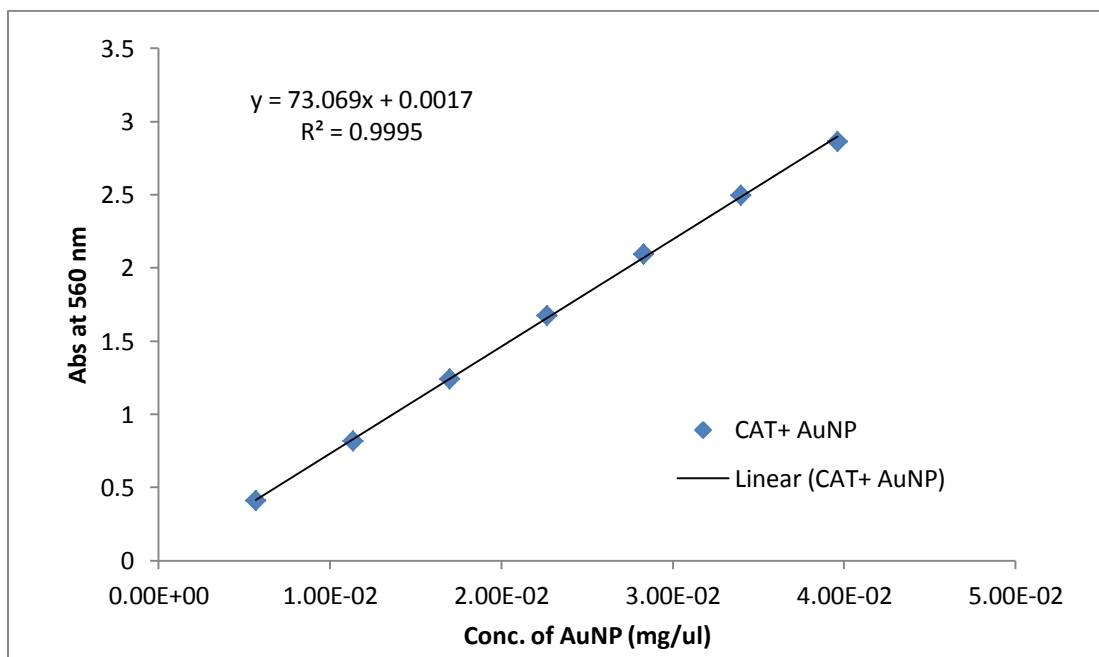


Figure 7.4 Standard curve obtained for different concentration of gold nanoparticles

Figure 7.5 shows the UV-Vis spectra for AuNP encapsulated beta-cyclodextrin (BCD) powder dissolved in water. The SPR wavelength was scanned from 400 nm to 800 nm, with medium scan speed and step up size for every 1.0 nm. Pure beta-cyclodextrin powder did not have any peak around 560 nm, but the gold nanoparticles encapsulated powder obtained by all the three encapsulation methods showed excitation around 560 nm. This indicated the encapsulation of gold nanoparticles into the beta-cyclodextrin complex.

The release of AuNP into the release medium (water) from the BCD complex was high in both the cases of encapsulation by molecular inclusion method (MIB) and lyophilisation method (FEB); but the release of AuNP from BCD complex was relatively less for microwave assisted encapsulation method (MEB).

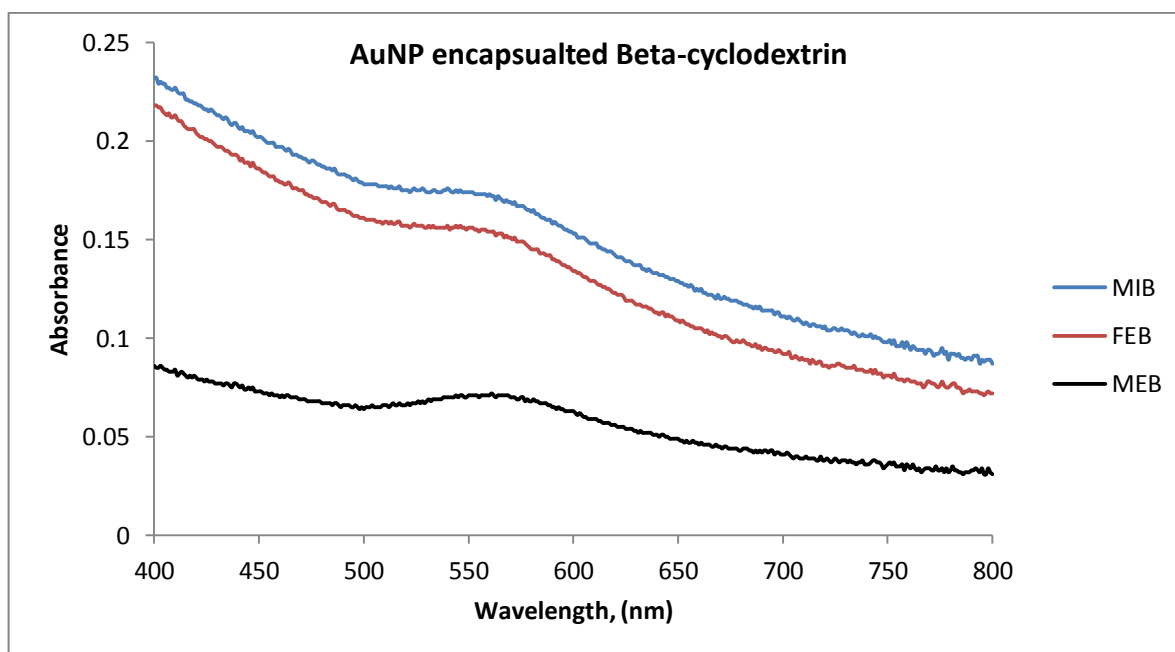


Figure 7.5 Surface plasmon resonance (SPR) plots for encapsulation of gold nanoparticles into beta-cyclodextrin complex

7.4.2 Results from statistical analysis

The experimental results such as yield %, AuNP loading, encapsulation efficiency and particle size obtained for the three encapsulation techniques such as molecular inclusion in beta-cyclodextrin (MIB), lyophilisation encapsulation (FEB) and microwave assisted encapsulation (MEB) are listed in Table 7.2.

The desirability function (D) is an important criterion when multiple responses are considered to measure the outcome of a method (Bezerra et al., 2008; Krishnaswamy et al., 2013). The prediction profiler along with the desirability function are provided in Figure 7.6.

Table 7.2 Encapsulation properties of AuNP encapsulated beta-cyclodextrin complex

Encapsulation method	Yield %	AuNP loading	AuNP encapsulation efficiency	Particle diameter (μm)
MIB	84.81	0.2303	45.77	1.763
	84.02	0.2344	45.77	1.922
	84.88	0.2495	45.79	1.723
FEB	85.92	0.2016	45.74	0.905
	85.89	0.2084	45.75	1.343
	85.98	0.2139	45.75	1.311
MEB	84.02	0.0921	45.63	1.713
	82.79	0.0948	45.63	1.466
	85.01	0.0976	45.64	2.042

The prediction profiler consists of a plot matrix of the individual responses that are to be maximized or minimized. The row at the bottom of the plot matrix containing the response is dedicated to the desirability function. The overall desirability is measured from 0 to 1 on the desirability scale provided to the left of the plot matrix.

The numerical value besides the word desirability on the vertical axis is the geometric mean of the desirability measures for the responses (JMP[®], Version 11. SAS Institute Inc., Cary, NC). The aim of this analysis is to maximize overall desirability value by maximizing the yield %, AuNP loading and AuNP encapsulation efficiency responses and to minimize the particle diameter.

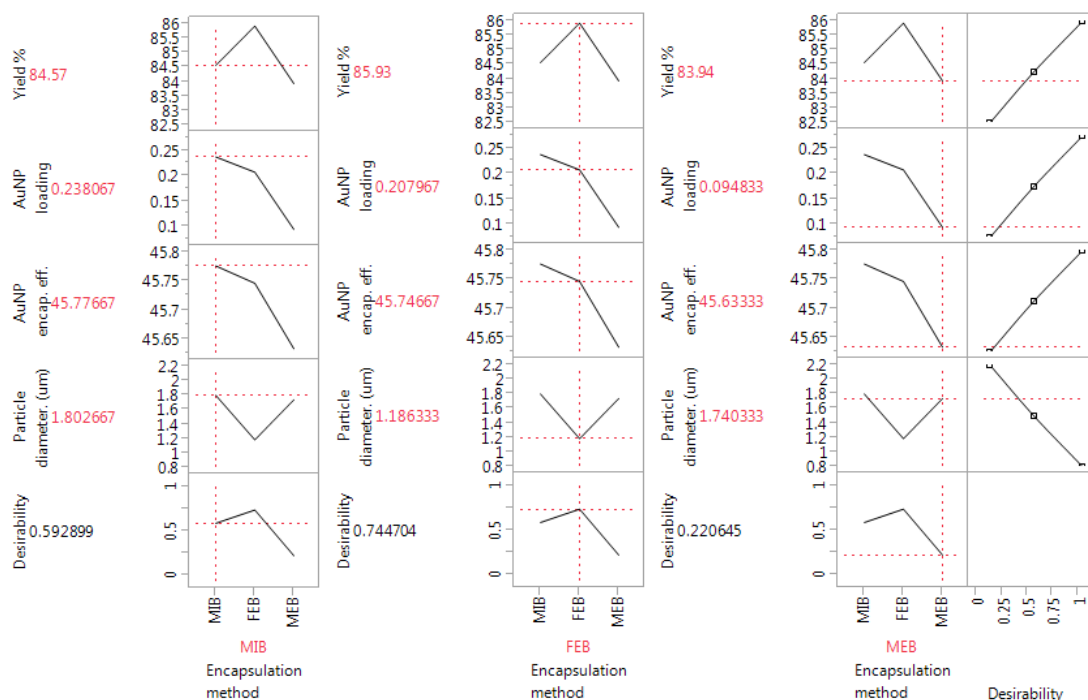


Figure 7.6 Prediction profiler plot showing the desirability functions for the three encapsulation methods

The geometric mean of yield %, AuNP loading, AuNP encapsulation efficiency and particle diameter is provided in the prediction profiler along with its desirability function. For the molecular inclusion method (MIB) the overall desirability (D) value was 0.5929, the overall desirability value for the lyophilisation encapsulation method (FEB) was 0.7447 and the D value for microwave assisted encapsulation was 0.2206. It can be

seen that the maximum desirability value was found for the (FEB) lyophilisation encapsulation method.

7.4.3 Thermal analysis using differential scanning calorimetry (DSC)

The DSC thermographs for AuNP encapsulated beta-cyclodextrin powder for the three encapsulation methods MIB, FEB and MEB were investigated from 0°C to 400°C. Figure 7.7 presents the DSC thermograph of AuNP encapsulated in beta-cyclodextrin by molecular inclusion method. In Figure 7.7 the presence of an exothermic peak maximum can be seen at 21.90 ± 0.19 °C with heat capacity of 1.57 ± 0.16 J/g. With the increase in temperature, with a ramping up at 10 °C/min, the first endothermic peak occurred with an onset temperature of 107.75 ± 4.60 °C and the peak maximum of 137.26 ± 2.44 °C.

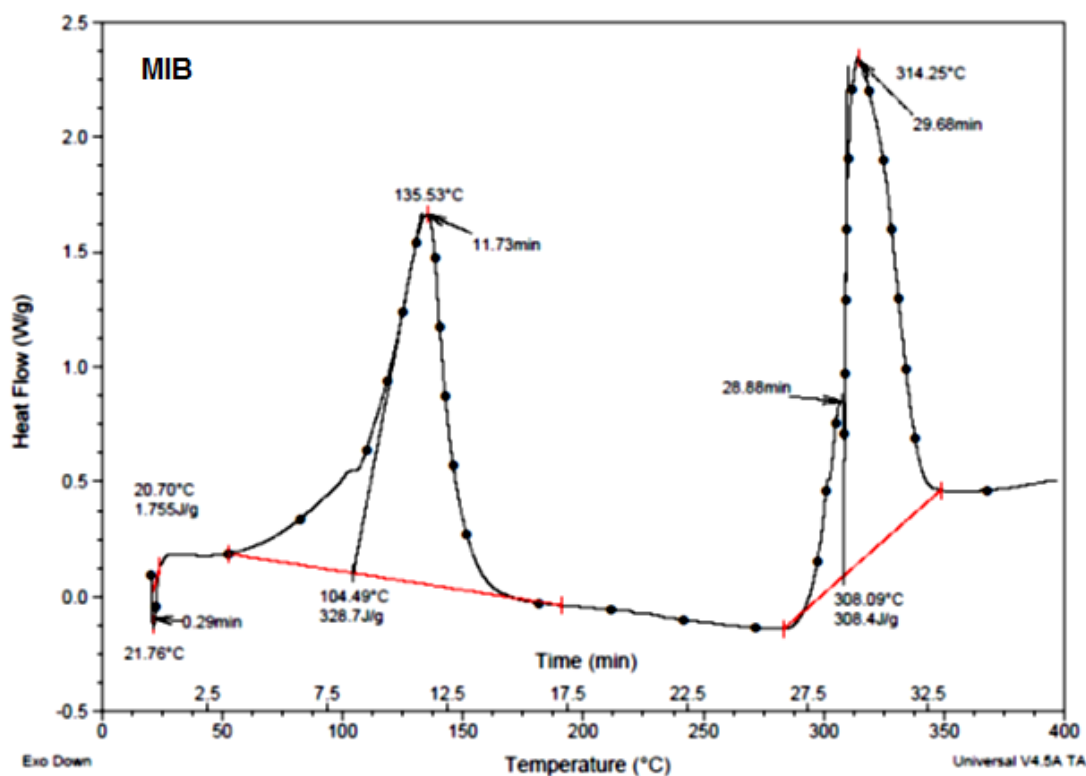


Figure 7.7 DSC thermograph for AuNP encapsulated beta-cyclodextrin powder produced by molecular inclusion method (MIB)

The heat capacity for this thermal transition was high with 324.67 ± 3.71 J/g at 12 min. The last endothermic thermal decomposition occurred at an onset temperature of 307.60 ± 0.70 °C and peak maximum of 313.86 ± 2.91 °C with heat capacity of 309.43 ± 1.46 J/g at 30 min.

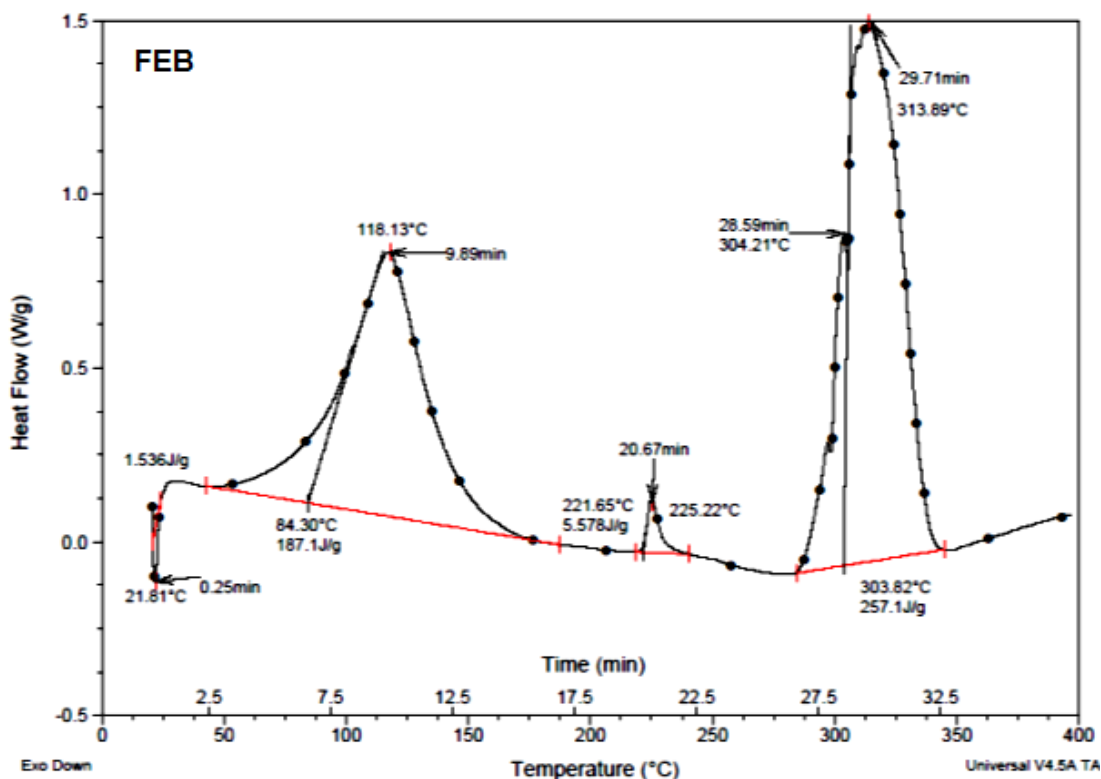


Figure 7.8 DSC thermograph for AuNP encapsulated beta-cyclodextrin powder produced by lyophilisation encapsulation method (FEB)

The DSC thermograph for AuNP encapsulated in beta-cyclodextrin by lyophilisation method is shown in Figure 7.8. The exothermic peak maximum was at 21.81 ± 0.05 °C with heat capacity of 2.33 ± 0.70 J/g. The first endothermic peak had an onset temperature at 83.13 ± 1.65 °C and a peak maximum of 115.99 ± 3.03 °C with a heat capacity of 191.05 ± 5.59 J/g at 10 min.

It Figure 7.8, the presence of a small endothermic peak onset can be clearly seen at 221.51 ± 0.34 °C and peak maximum of 225.02 ± 0.58 °C with the heat capacity of 5.37 ± 1.27 J/g at 20 min. This peak might be an outcome indicating proper encapsulation of AuNP into the beta-cyclodextrin complex. The last thermal endothermic decomposition peak occurred with an onset temperature of 304.89 ± 0.96 °C and the peak maximum of 313.10 ± 2.10 °C with a heat capacity of 259.20 ± 2.97 J/g at 30 min.

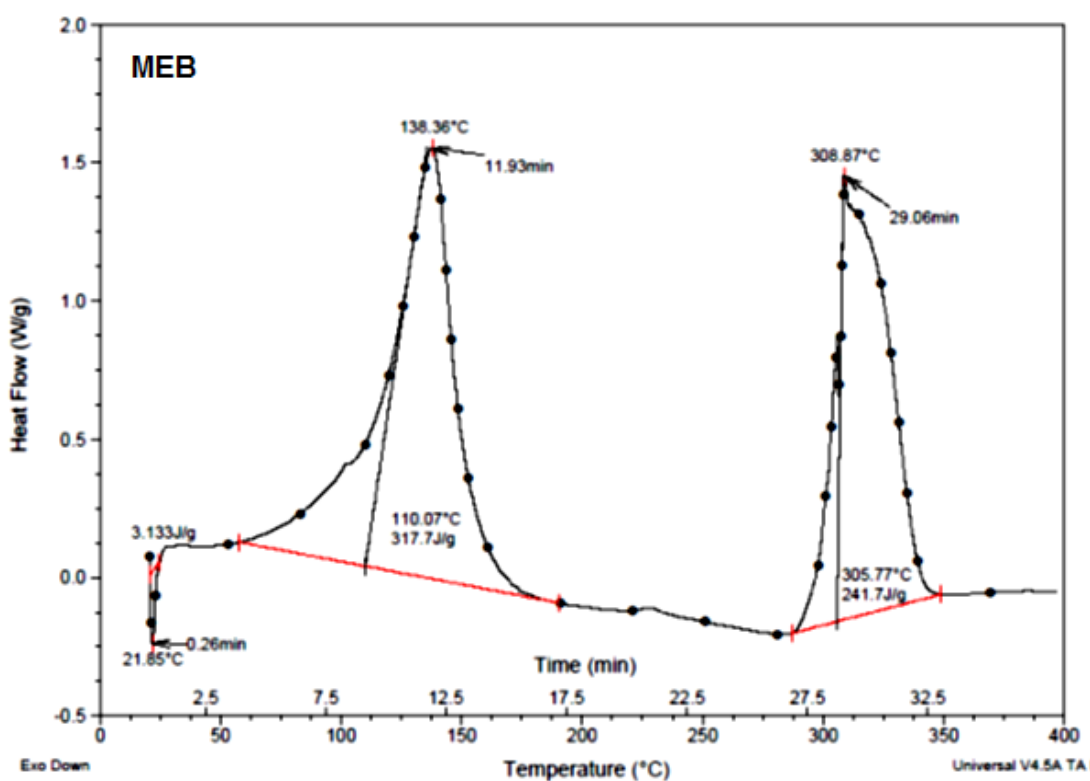


Figure 7.9 DSC thermograph for AuNP encapsulated beta-cyclodextrin powder produced by microwave assisted encapsulation method (MEB)

The DSC results of AuNP encapsulated in beta-cyclodextrin by microwave assisted encapsulation method are shown in Figure 7.9. The exothermic peak maximum was at 21.80 ± 0.04 °C with a heat capacity of 3.13 ± 0.69 J/g. The first endothermic

transition had an onset at 102.09 ± 11.29 °C and a peak maximum temperature at 136.71 ± 8.33 °C with a heat capacity of 313.10 ± 6.51 J/g at 11 min.

The last endothermic peak occurred with an onset temperature of 307.37 ± 1.42 °C and a peak maximum of 312.28 ± 4.39 °C. This thermal transition occurred at 30 min with the heat capacity of 250.37 ± 8.65 J/g.

In a study related to inclusion of vanilin into beta-cyclodextrin, the DSC thermogram for pure BCD showed an endothermic peak at 175 °C (Karathanos et al., 2007) where the scan rate was 10 °C/min between 70 to 230 °C. In our study the range of the investigation was from 0 to 400 °C with the same scan rate of 10°C/min. Due to the broader temperature range, it was possible to observe the endothermic peak around 310 °C for catechin synthesized AuNP + BCD inclusion complex by all the three encapsulation methods.

Namazi and Heydari (2014) studied the DSC thermograms of BCD based dendrimers loaded with naproxen and naltrexone as guest molecules for a temperature range from 20 to 350 °C with the scanning rate of 10°C/min. They were able to obtain an endothermic peak for BCD complex around 320 °C due to its thermal decomposition (Namazi & Heydari, 2014).

When a guest molecule forms complexation with the BCD, there is a shift in the melting, boiling and sublimation points or disappearance of certain peaks (Li & Xu, 2010). Li and Xu (2010) also reported that the grinding method had better inclusion efficiency than co-evaporation method. They were able to see shift in the peak temperature with a change in grinding time. The shift in the peak temperature for the

three encapsulation methods might be due to the difference in the inclusion complex formation and interaction between AuNP and BCD cavity.

The presence of the small endothermic peak at 225 °C around 20 min was found for all the three replicates for AuNP encapsulated powder by FEB method. The overlay of the DSC thermograph for FEB samples is provided in Figure 7.10(a). The occurrence of this small endothermic peak in FEB method is an interesting phenomenon. This endothermic peak was absent in both molecular inclusion method (MIB) and microwave encapsulation method (MEB).

The overlay of the DSC thermograph for AuNP encapsulated powder obtained from microwave assisted encapsulation method (MEB) is provided in Figure 7.10(b). The prominence of an endothermic peak at 225°C present for FEB powders was absent in all the three replicates of AuNP+BCD powders produced by MEB method. The reason for such behaviour is clearly not understood and further investigation is required to understand the reason for such a pattern.

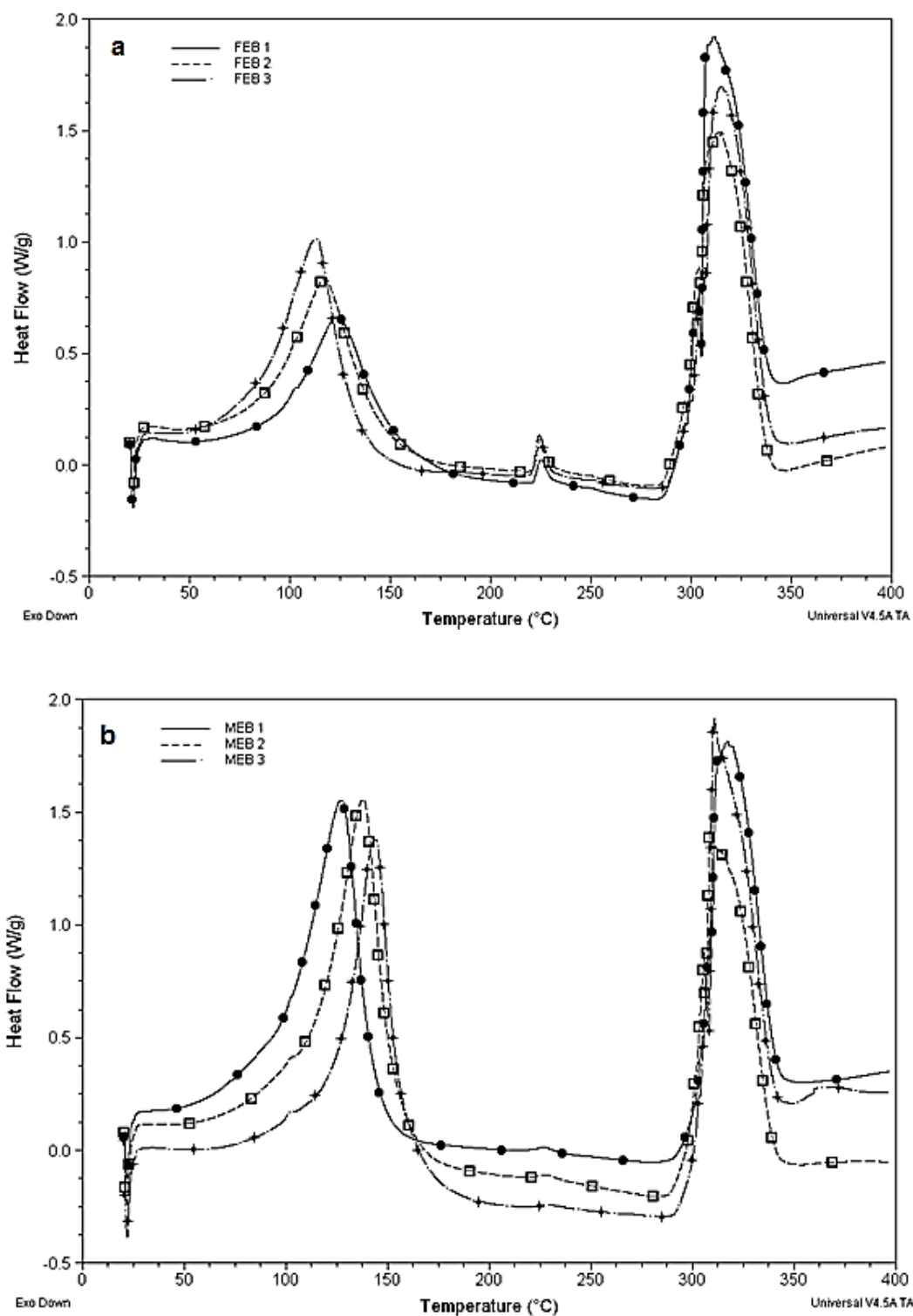


Figure 7.10 Overlay of DSC thermograph of (a) lyophilisation encapsulation method (FEB); (b) microwave assisted encapsulation method (MEB)

7.4.4 Functional groups conformation using FTIR spectra

Changes in the characteristic bands of the pure host with new spectroscopic bands are due to vibrations of atoms or groups due to host-guest interactions (Stražišar et al., 2008). Figure 7.11 shows the overlay of FTIR spectra for AuNP encapsulated beta-cyclodextrin powder by microwave assisted encapsulation (MEB); molecular inclusion method (MIB); lyophilisation encapsulation (FEB) along with FTIR spectra for beta-cyclodextrin alone. The FTIR spectrum shows the interaction between BCD and the guest molecule (AuNP) by the modification of the spectral properties after encapsulation.

The IR peak at 3343.96 cm^{-1} present in pure BCD was shifted to 3311.51 cm^{-1} for MEB and 3316.70 cm^{-1} for MIB. The peak shift for FEB was relatively less compared to the other two methods and was at 3332.92 cm^{-1} . This peak is assigned to the stretching of the O-H groups in alcohols and O-H groups in the aromatic ring of phenols. The strong peaks for BCD at 2954.41 cm^{-1} , 2923.56 cm^{-1} and 2854.13 cm^{-1} diminished to single medium peak around $2924 \pm 1\text{ cm}^{-1}$ after encapsulation which is due to medium stretching of the C-H bonds. Certain peaks appeared between 2350 to 2035 cm^{-1} for all the encapsulated powder which was completely absent in the pure BCD (Stancanelli et al., 2008). H-O-H bending was observed in the AuNP encapsulated BCD powder at 1644.13 cm^{-1} for MEB, 1650.87 cm^{-1} for MIB and 1650.99 cm^{-1} , 1644.14 cm^{-1} for FEB. The absorbance around 1650 cm^{-1} was relatively high for MEB and MIB whereas the FTIR spectrum for FEB was similar to that of BCD.

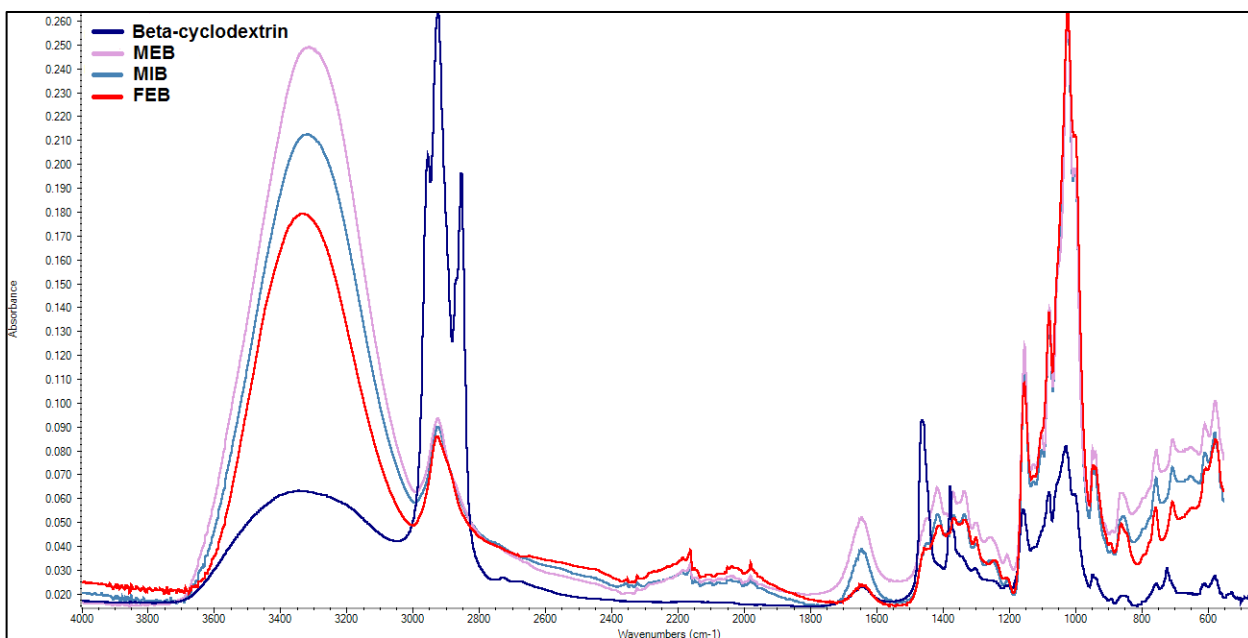


Figure 7.11 FTIR spectra for AuNP encapsulated beta-cyclodextrin powder by microwave assisted encapsulation (MEB); molecular inclusion method (MIB); lyophilisation encapsulation (FEB) overlay with FTIR spectra for pure beta-cyclodextrin

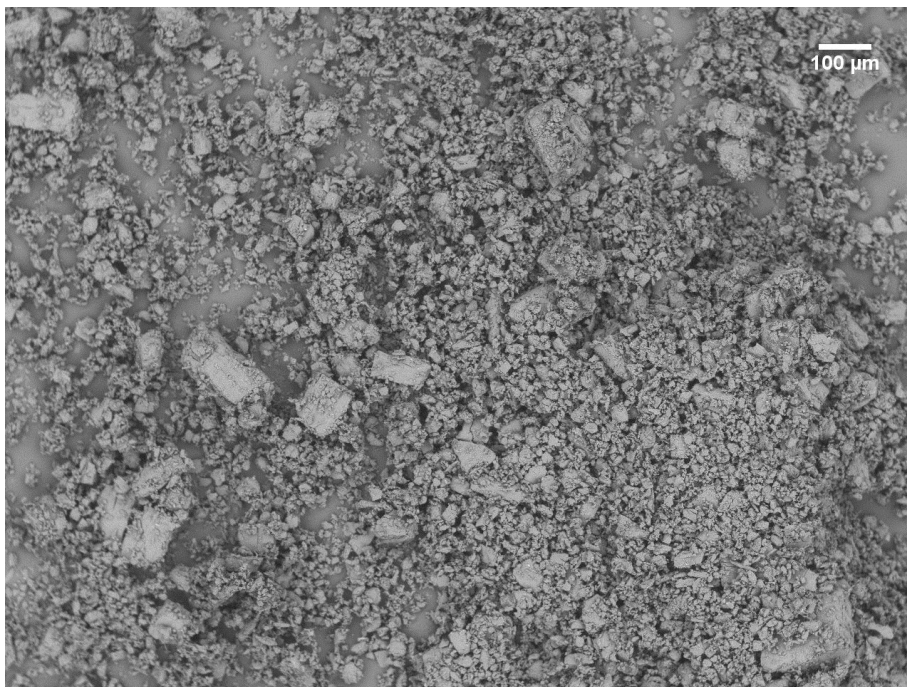
It can be seen from Figure 7.11, that the sharp peaks at 1461.78 cm^{-1} and 1376.93 cm^{-1} for BCD were relatively reduced and slightly shifted in the case of the encapsulated powder, which is assigned to the C-H stretching of the alkanes group. There is an increase in the absorbance of IR peak at 1152 cm^{-1} and 1125 cm^{-1} for the AuNP + BCD encapsulated powder compared to BCD alone which can be assigned to the C-O stretching of the COOH groups and C-O-C bending respectively.

A single broad peak centered at 1077 cm^{-1} along with the presence of peaks at 945 cm^{-1} , 890 cm^{-1} , 860 cm^{-1} in the fingerprint region were observed for the AuNP + BCD encapsulated powder. The presence of a single peak at 721.25 cm^{-1} for BCD occurred as two peaks in the AuNP + BCD encapsulated powder at 755 cm^{-1} and 705 cm^{-1} .

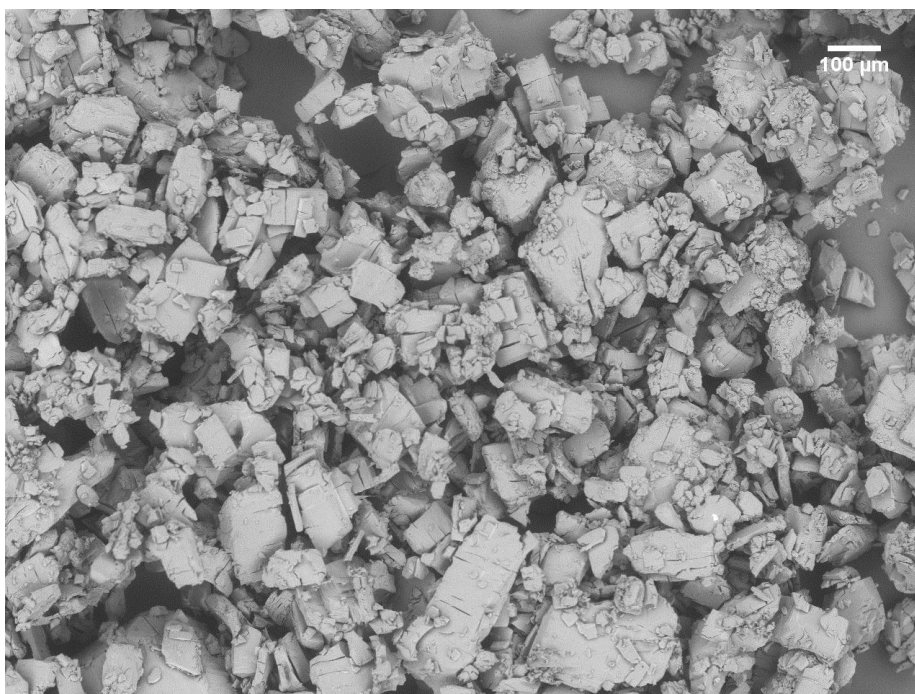
There is an increase in the absorbance of bands occurring between 800 – 1400 cm⁻¹ for AuNP + BCD encapsulated powder compared to BCD which was assigned to C-O, C-C, C-O-C stretching, and the deformation vibration (ν) of ν C-O, ν C-C, ν C-O-C. This increase might be due to van der Waals interaction between the BCD and guest molecule (AuNP) (Bonenfant et al., 2009).

7.4.5 Interpretation of SEM micrographs

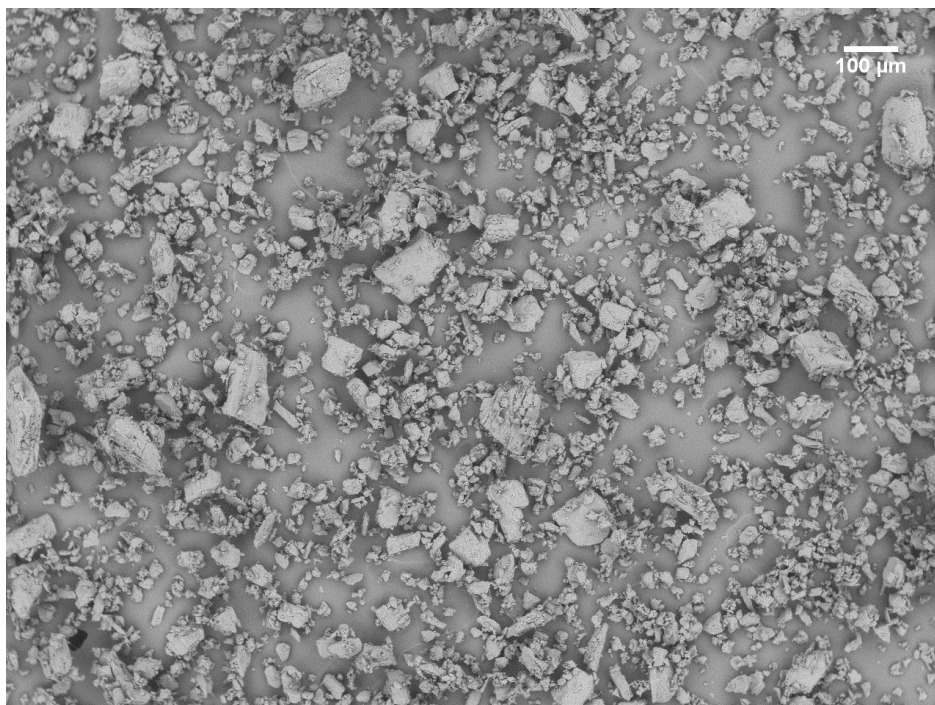
Figure 7.12 presents SEM micrographs of AuNP + BCD encapsulated powder at 100 x magnification for the three methods of encapsulation, and it can be clearly seen that the sizes of the encapsulated powder by lyophilisation encapsulation method (FEB) and molecular inclusion method (MIB) were comparatively smaller than the size of the particles obtained for microwave assisted encapsulation method (MEB).



(a) Lyophilisation encapsulation within BCD matrix (FEB), magnification 100 x



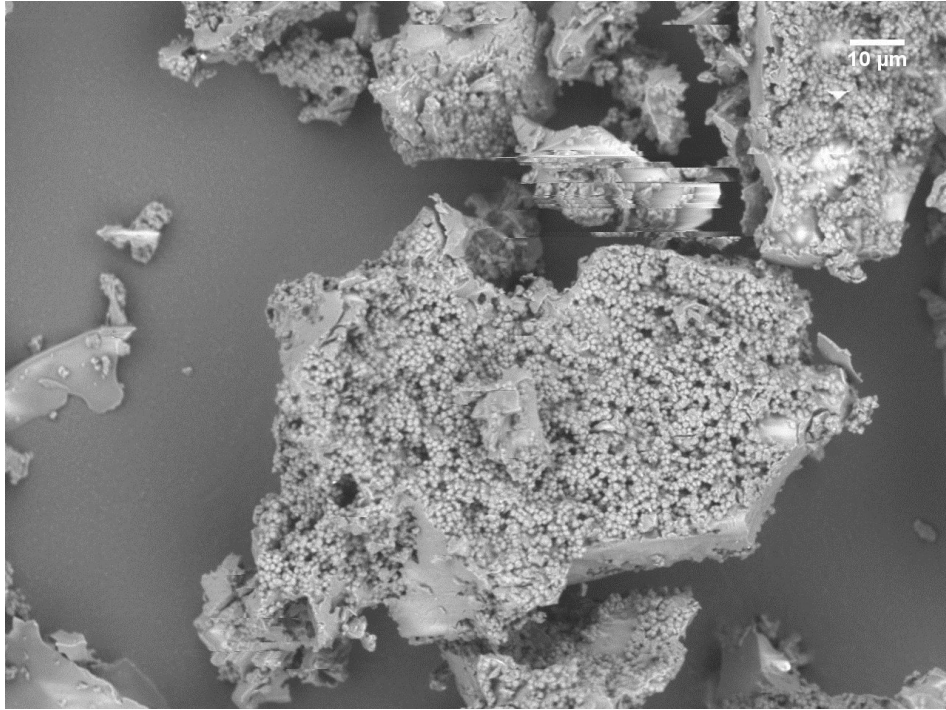
(b) Microwave assisted encapsulation within BCD matrix (MEB), magnification 100x



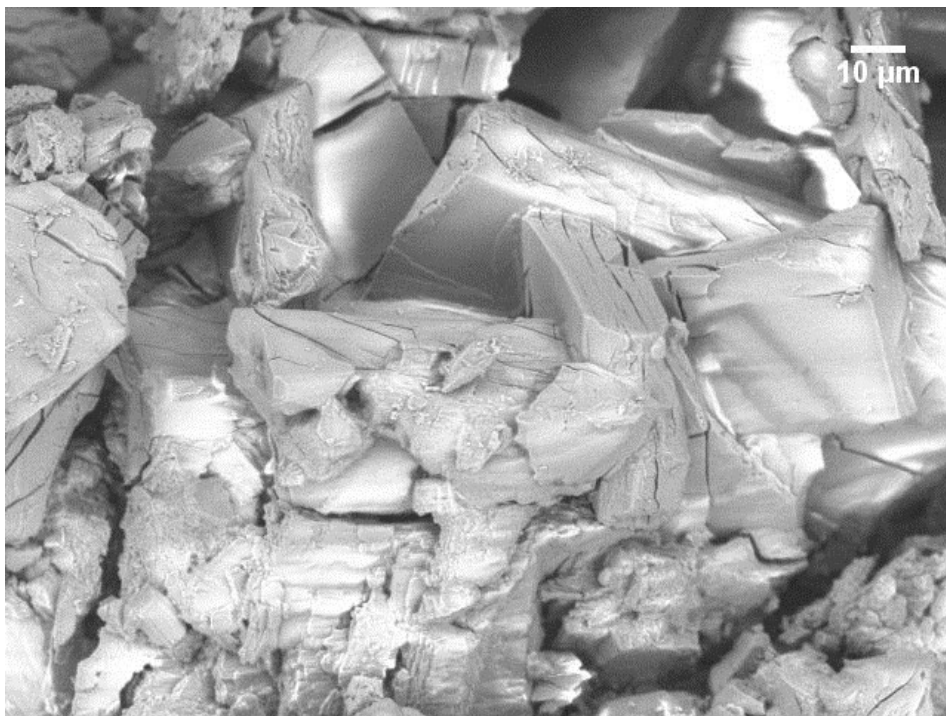
(c) Molecular inclusion encapsulation within BCD matrix (MIB), magnification 100 x

Figure 7.12 SEM micrograph of AuNP encapsulated powder obtained from beta-cyclodextrin at 100 x magnification. a) FEB; b) MEB; c) MIB

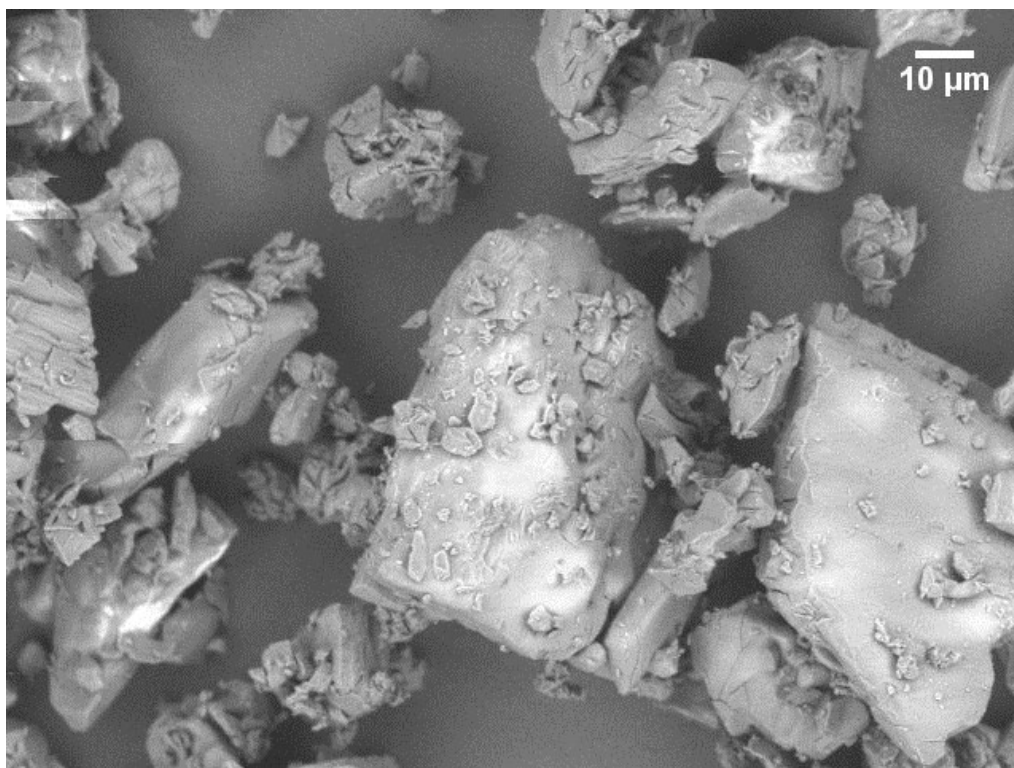
The surface morphology of the encapsulated powders could be clearly seen with an increase in magnification at 1000x shown in Figure 7.13. Small capsules were seen on the surface of powders obtained by lyophilisation encapsulation (FEB), the surface was smooth with respect to powders obtained by microwave assisted encapsulation method (MEB). The molecular inclusion method (MIB) produced irregular shaped particles having a smooth surface.



(a) Lyophilisation encapsulation (FEB), magnification 1000 x



(b) Microwave assisted encapsulation (MEB), magnification 1000 x

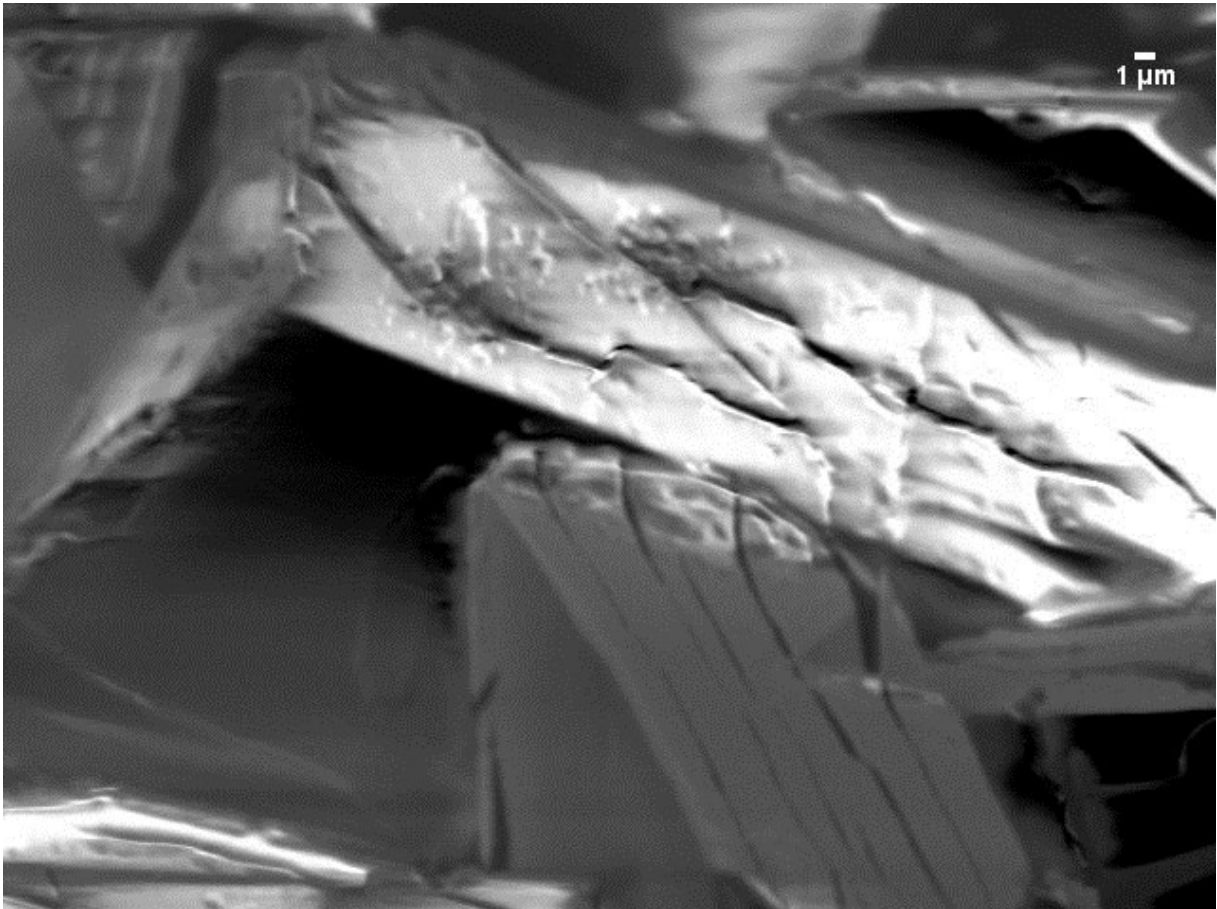


(c) Molecular inclusion encapsulation (MIB), magnification 1000 x

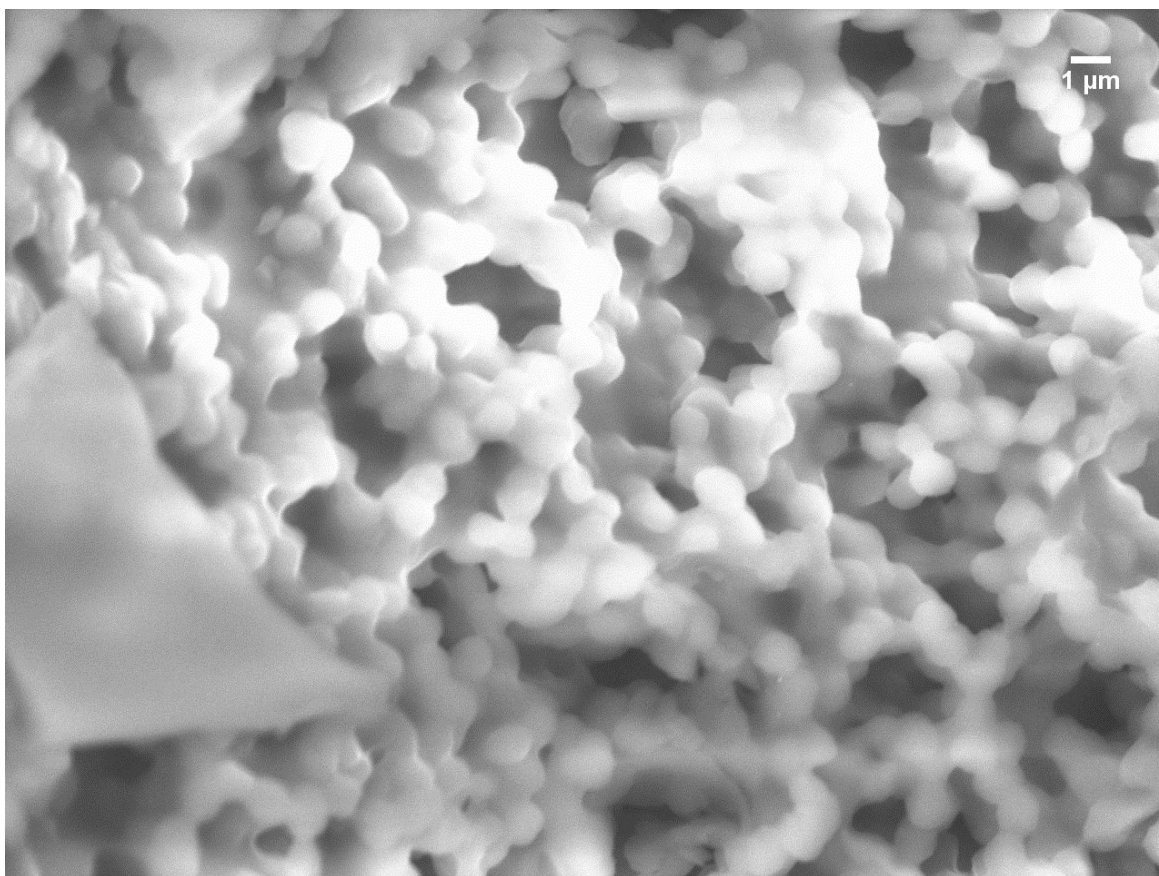
Figure 7.13 SEM micrograph of AuNP encapsulated powder obtained from beta-cyclodextrin at 1000 x magnification. a) FEB; b) MEB; c) MIB

The surface morphology of the powder obtained from lyophilisation encapsulation method (FEB) was interesting; in order to examine the surface closely the image was magnified to 6000x (Figure 7.14) and was compared with the SEM image of MEB powder at 3000x. It can be seen that the FEB powder had small spherical structures, while the MEB powder had a dense, smooth surface.

The internal heating phenomenon associated with the microwave energy might be the reason for the formation of the smooth surface for the microwave assisted encapsulation powder when compared to lyophilisation encapsulation (Clark et al., 2000).



Microwave assisted encapsulation (MEB), magnification 3000 x



Lyophilisation encapsulation (FEB), magnification 6000 x

Figure 7.14 Comparing the SEM micrographs for microwave assisted encapsulation and lyophilisation encapsulation of AuNP within beta-cyclodextrin cavity

In order to clearly see the encapsulation of AuNP into BCD, the SEM image of the FEB powder was further magnified to a maximum of 20,000 x magnification. Uniform spherical encapsulated particles were seen using this magnified SEM image. The SEM micrograph of FEB powder showed the presence of uniform, spherical shaped structures of 1 μm in diameter size. This supports that the lyophilisation method (FEB) provides better encapsulation of AuNP into beta-cyclodextrin.

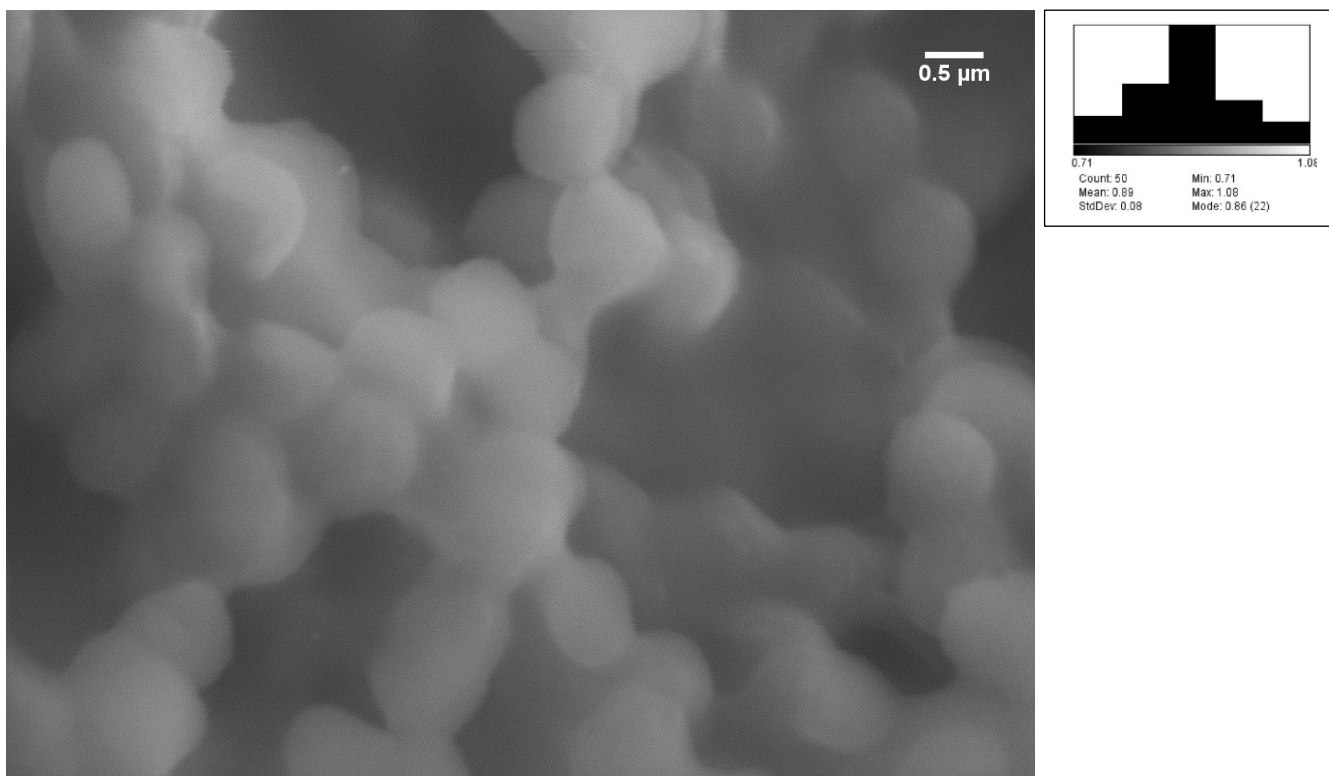


Figure 7.15 SEM micrograph of AuNP encapsulated in beta-cyclodextrin powder obtained from lyophilisation encapsulation method at 20,000 x magnification

7.5 Conclusion

It was found that gold nanoparticles (AuNP) synthesized using catechin can be successfully incorporated within the BCD cavity to form inclusion complex. This study proves that molecular level encapsulation of AuNP into beta-cyclodextrin can be achieved by all three encapsulation methods. The powder obtained from lyophilisation encapsulation method (FEB) showed higher desirability value compared to the microwave assisted encapsulation (MEB) and molecular inclusion encapsulation (MIB). The structural morphology of FEB powder produced uniform spherical shaped particles, while the surface morphology of MEB was smooth and dense. The results obtained from

both lyophilisation method and microwave assisted encapsulation method are interesting, and has aided in creating a unique class of AuNP encapsulated nanomaterials.

CONNECTING STATEMENT TO CHAPTER VIII

Chapter VIII deals with the potential applications of the synthesized gold nanoparticles and encapsulated powders. The advancement in nanotechnology has been predicted for an increase in economic growth. Interdisciplinary collaborations are required for defining newer applications of nanoparticles. Better understanding and knowledge about nanotechnology is the need of the hour to tap into the potential of this new technology and intensify the commercialization opportunities. This chapter provides information about the potential applications of nanoparticles in the agro-food sector. This chapter also shines a light on thinking about sustainable nanotechnology approaches.

CHAPTER VIII

CURRENT STATUS, TRENDS AND APPLICATIONS OF NANOTECHNOLOGY

8.1 Current status of nanotechnology

There is a worldwide investment in nanotechnology as it is predicted to be a major driving force for future economic development. Government funding for nanotechnology related research and development has increased over the past two decades. In 2009, nanotechnology generated products were worth quarter trillion dollars worldwide, of which 91\$ billion dollars worth of products were found in the US market (Roco, 2011). This section provides information about the budget allotted by the governments to increase R&D activity in the nanotechnology sector. Private industries invest a huge amount in R&D related to nanotechnology research; the data related to such industrial investments are however not covered in this section.

8.1.1 National Nanotechnology Initiatives (NNI) and budget allotted for R&D in nanotechnology

With the initiation of the National Nanotechnology Initiative (NNI) involving multiagency, the US federal funding for the fiscal year 2001, was US\$ 497 billion and made NNI as a top science and technology priority. The main objective of this initiative was to facilitate academia, private sector, industries, state and federal government to form a broad alliance to work together to develop nanoscience and nanoengineering sectors to reap the potential social and economic benefits of nanotechnology. This funding to NNI has increased over the past decade, to increase research and development (R&D),

establishing interdisciplinary research centers and accelerating technology transfer to the private sector.

The five major federal agencies funded by the NNI initiative in 2000 were, the National Science Foundation (NSF), Department of Energy (DOE), National Aeronautics and Space Administration (NASA), National Institute of Standards and Technology (NIST) and the Environmental Protection Agency (EPA). The NNI members increased to 25 Federal departments and agencies in 2010 (Bhushan, 2010; Roco & Bainbridge, 2005).

The main reasons for beginning NNI were to fill the major fundamental knowledge gaps in understanding the matter at nanoscale, and in turn anticipate novel applications from nanotechnology. With the initiation of NNI, other nations announced coherent R&D programs in nanotechnology: Japan (April 2001), Korea (July 2001), the European Community (March 2002), Germany (May 2002), China (2002), Taiwan (September 2002). However, NNI is the largest program with the cumulative funding nearly \$21 billion since the inception of NNI in 2001 including the funding for 2015 (NNI Fiscal Year 2015 Budget).

Table 8.1 shows six key indicators which will help to portray the value of the investment, science breakthrough through publications, patent applications and development in the field of nanotechnology. The overall average growth rate worldwide related to nanotechnology is approximately 25 % from 2000-2008. This will increase in the future (Roco, 2011).

Table 8.1 Six key indicators of nanotechnology development in the world and the United States (Roco, 2011)

World/US/	People Primary workforce	SCI papers	Patent applications	Final products market	R&D funding public + private	Venture capital
2000	~60,000	18,085	1,197	~\$30 B	~\$1.2 B	~\$0.21 B
(actual)	/25,000/	/5,342/	/405/	/\$13 B/	/\$0.37 B/	/\$0.17 B/
2008	~400,00	70,287	12,776	~\$200 B	~\$15 B	~\$1.4 B
(actual)	/150,000/	/15,000/	/ 3,729 /	/\$80 B/	/\$3.7 B/	/\$1.17 B/
2000–2008	~25%	~18%	~35%	~25%	~35%	~30%
average growth						
2015	~2,000,000			~1,000 B		
(2000 estimate ^b)	/800,000/			/\$400 B/		
2020	~6,000,000			~\$3,000 B		
(extrapolation)	/2,000,000/			/\$1,000 B/		

(Note: The global figures are provided in bold text in Table 8.1; U.S. figures are indicated in gray)

8.1.2 NNI investments by Program Component Areas for 2015

The NNI Strategic Plan, 2014 has indicated new Program Component Areas (PCA) for 2015. PCA provide an organizational framework for categorizing NNI activities. The PCA are revised regularly which is considered critical to achieve NNIs goal and vision.

The Figure 8.1 provides the percentage distribution of funds for the 5 categories highlighted in the 2015 NNI framework. Sustainable Nanomanufacturing is a key area of investment which involves design of scalable sustainable nanomaterials, process and measurement technologies (<http://www.nano.gov/nni-pca>).

The key areas that are focused in PCA of NNI 2015 are mentioned below,

1. “Nanotechnology Signature Initiatives

-Nanotechnology for Solar Energy Collection and Conversion

-Sustainable Nanomanufacturing

-Nanoelectronics for 2020 and Beyond

-Nanotechnology Knowledge Infrastructure

-Nanotechnology for Sensors and Sensors for Nanotechnology

2. Foundational Research

3. Nanotechnology-Enabled Applications, Devices, and Systems

4. Research Infrastructure and Instrumentation

5. Environment, Health, and Safety”

2015 NNI Investments by PCA

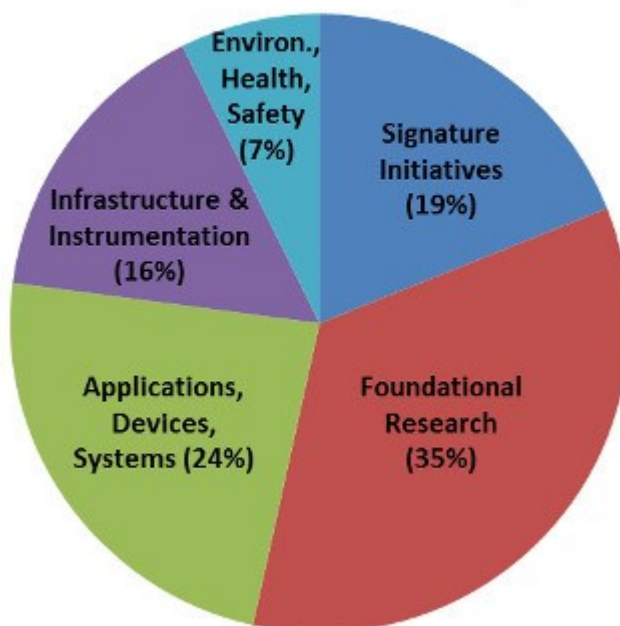


Figure 8.1 Highlighted Program Component Areas (PCA) for NNI investment in 2015 (<http://nano.gov/node/1128>).

The Nanotechnology Signature Initiative serves as a bridging category across multiple federal agencies. It focuses on foundational research and nanotechnology-enabled applications. This category currently spotlights 5 topical areas comprising nanotechnology for solar energy collection and conversion contributing to the future energy needs. The two thrust areas in the sustainable nanomanufacturing subcategory emphasize the design of scalable and sustainable nanomaterials and improving nanomanufacturing measurement technologies. The nanotechnology for sensors subcategory focuses on developing and improving new nanomaterials based sensors to overcome the barriers associated with conventional sensors and to develop devices to detect and identify engineered nanomaterials (ENMs). This will be valuable to assess the impact of ENMs on human health and environment.

Elucidation of scientific principles related to nanoscale structures, processes and mechanisms is the key area of focus in the Foundation Research category. The Applications, Devices and Systems category focuses on creating nanometrology standards and nanoscale reference materials for scale-up. Establishment of research facilities, developing next generation instrumentation for characterization and developing educational curricula and a skilled workforce is addressed by the Infrastructure and Instrumentation category. EHS category is dedicated to R&D related to nanotechnology risk assessment and management (<http://www.nano.gov/nni-pca>).

8.1.3 Position of Canada in R&D related to nanotechnology

The funding for R&D in nanotechnology in Canada is provided by the federal government through its major research funding agencies such as Natural Sciences and Engineering Research Council (NSERC), Canadian Institute for Health Research (CHIR), National Research Council (NRC) and the Canada Foundation for Innovation (CFI) along with provincial funding from the provinces. NanoAlberta, NanoQuebec, Nanotechnology Network of Ontario and the British Columbia Nanotechnology Alliance are some of the nanotechnology frameworks from the provinces (Fitzgibbons & McNiven, 2006; Tahmooresnejad et al., 2015).

The National Institute for Nanotechnology (NINT) is the hub for nanotechnology R&D in Canada. It is located in Edmonton, Alberta, with a \$52.2 million multiple lab facility for nanotechnology research. It was established in 2001 as a partnership of the National Research Council of Canada and University of Alberta (NINT, 2015).

8.2 Gold nanoparticles: current status and application

The interesting properties of gold nanoparticles have attracted scientists working in both theoretical and experimental fields. The absorption and scattering properties of gold nanoparticles have applications in biological imaging; they can effectively act as image contrast agent for biological and cell imaging applications. Therapeutic photothermal applications are based on the optical properties of gold nanoparticles (Jain et al., 2006).

The gold nanoparticles have wide range of applications in DNA-AuNP assemblies, AuNP enhanced immuno sensors, electrochemical sensors, catalysis, nonlinear optics (Daniel & Astruc, 2004; Guo & Wang, 2007; Warriner et al., 2014; Zeng et al., 2011).

Manipulations of size and shape of gold nanoparticles produce unique properties which have potential applications in semiconductors (Schmid & Corain, 2003) and spectroscopy (Mulvaney, 1996), and in biomedical applications such as drug delivery (Mahal et al., 2013; Paciotti et al., 2004; Singh et al., 2013), cancer therapy (Peng et al., 2009), contrast agents for X-rays and hyperthermia (Sperling et al., 2008). With increases in the development of gold nanoparticles and multi-disciplinary collaborations there will be discoveries of newer applications for gold nanoparticles.

The top 12 countries in the world that have contributed to research on gold nanoparticles are presented in Figure 8.2. From the figure it can be clearly seen that the US and China have each reported over 9000 documents related to gold nanoparticles followed by Japan, India and Germany. A total of 1475 patents applications were found in Scopus search for gold nanoparticles as of March, 2015. The major disciplines under which the large number of patents were filed and/or obtained were chemical engineering, chemistry, and material science, physics followed by other engineering, biochemistry, molecular biology and microbiology with relatively fewer patents in environmental science (Figure 8.3).

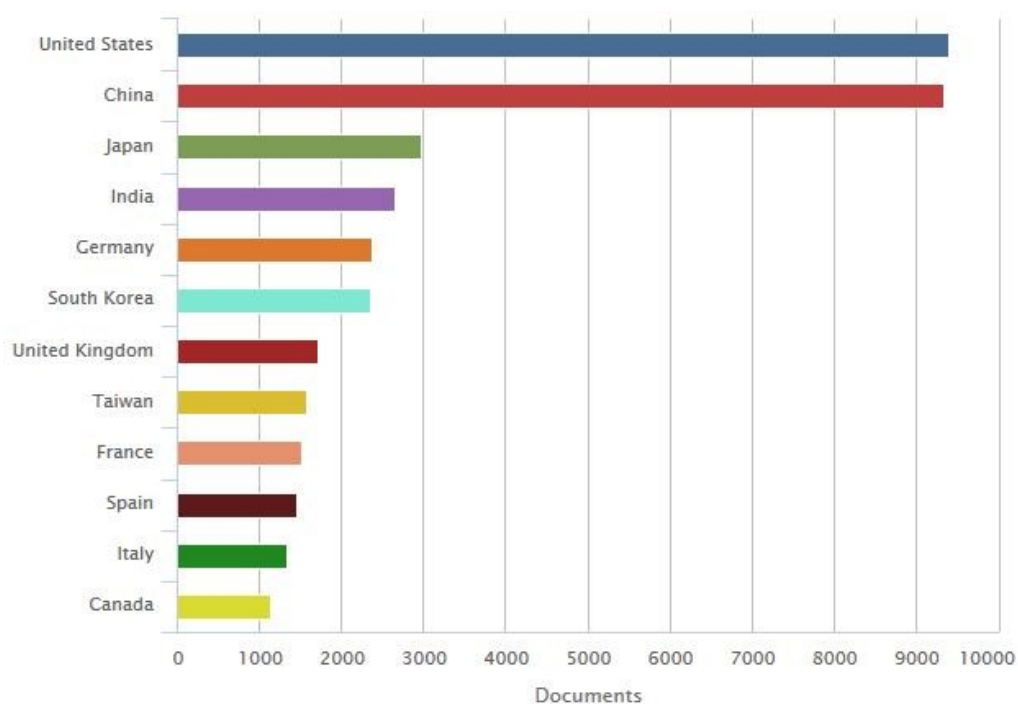


Figure 8.2 Top 12 countries with high contribution of documents in research related to gold nanoparticles (Data retrieved from Scopus, April, 2015 with the search term ‘gold nanoparticles’)

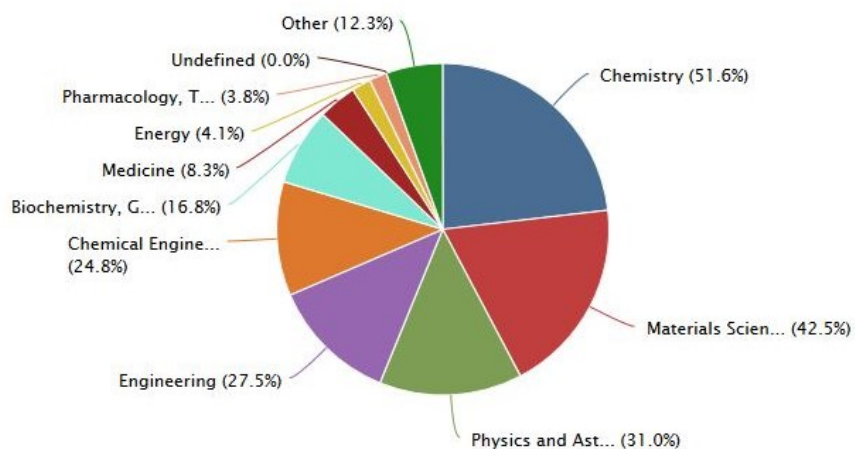


Figure 8.3 Patent applications filed / obtained for gold nanoparticles in various disciplines (Data retrieved from Scopus, April 2015 with the patent search term ‘gold nanoparticles’)

8.3 General applications of nanotechnology in agro-food systems

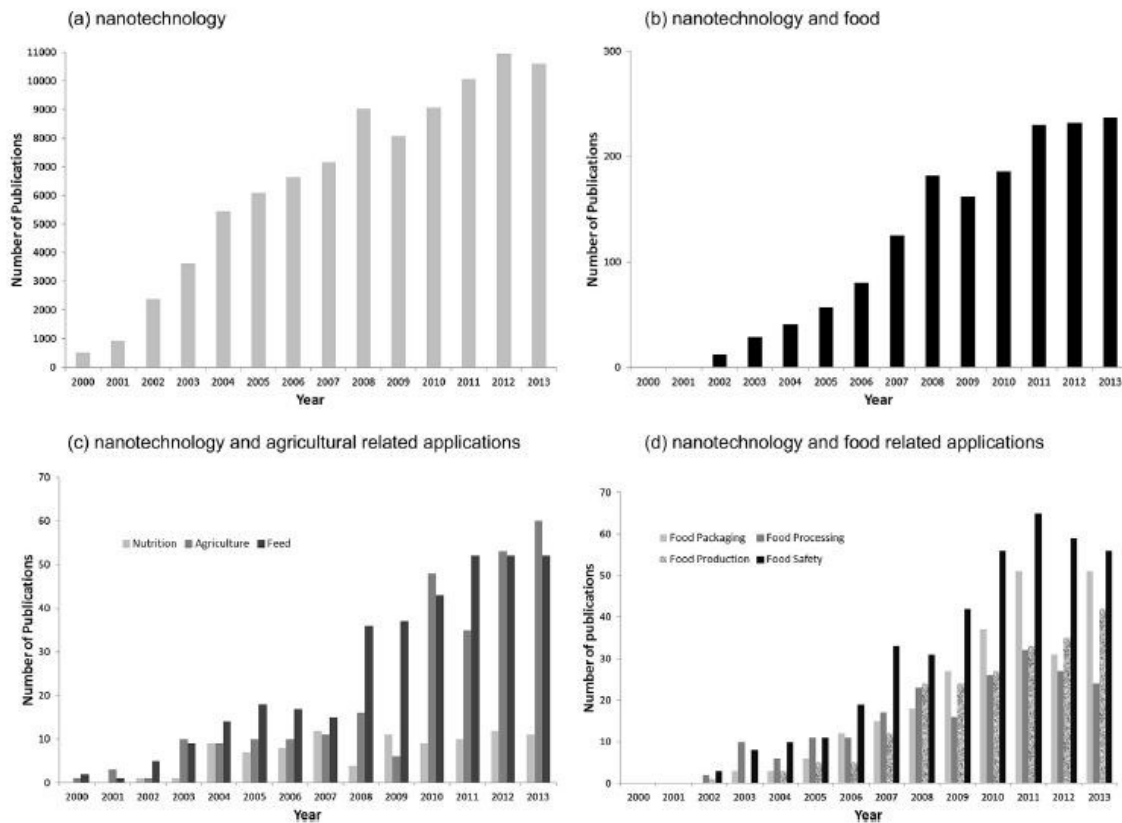


Figure 8.4 Number of nanotechnology publications per year in the Scopus database using the key terms as indicated (a) nanotechnology (b) nanotechnology and food (c) nanotechnology and agricultural related applications (d) nanotechnology and food related applications (Handford et al., 2014)

The application of nanotechnology is a relatively new concept in the agri-food sector when compared to other disciplines. The number of publications related to nanotechnology and food is now growing rapidly as illustrated in Figure 8.4 and Table 8.2. The major reasons for such late adoption of nanotechnology in agro-food systems are due to a lack of unifying regulations and product guidelines, product labelling, and potential consumer health risk (Coles & Frewer, 2013). However, there is a heavy investment by the large scale food companies and agricultural manufacturers in nanotechnology R&D.

Table 8.2 Application of nanotechnology in agro-food industry

	Product	Nano-component	Function of nanocomponent	Commercial status	Further information	Reference
Delivery systems	Syngenta KARATE ZEON®	Not disclosed	Controlled release of insecticide lambda-cyhalothrin used on food crops	Commercially available	Increased efficacy, water solubility, crop adherence, triggered release	www.syngenta.com
	Lypo-Spheric™	Liposomes	Triggers collagen production Protects	Commercially available	Vitamin C, B Complex Vitamins	http://www.livonlabs.com/
Carbon nanotubes	Bayer - Baytubes™	Carbon nanotube	Enhances the properties of aluminum: nearly as strong as steel	Commercially available	Special mechanical, electrical and thermal properties	http://www.materialscience.bayer.com/
Nanomaterials	Nansulate® Translucent High Heat	Nanosize structures dispersed in acrylic latex coating	Excellent thermal insulation, sustainable moisture resistant coating	Commercially available	Food processing equipment application: heat exchangers, boilers, steam pipeline insulation	http://www.nansulate.com/
Complex nanomaterials	OilFresh®	Not disclosed	Nanoceramic inserts for deep fat fryers	Commercially available	This product has been authorized by the FDA in the US and NSF International.	http://www.oilfresh.com/of1000.html
Nanosized nutrients/foods	Unilever-low fat ice cream.	Not disclosed	Product design compensates for the loss in creaminess due to fat reduction	Research stage	Uniform sized emulsion	

This Table is inspired by Cushen et al. (2012) modified and updated with applications related to this chapter.

Table 8.3 Summary of current and projected applications of nanotechnology in the food production chain (Rossi et al., 2014)

Nanotechnology	Application	Function
Agricultural production		
Nanosensors	Nanosprays	Binding and coloring micro-organisms;
	Hand-held devices	Detection of contaminants, mycotoxins and microorganism
Nano-sized additives	Organic or inorganic nano-sized additives for feed applications, including removal of toxins in feed	Various (including nutritional additives) with lesser amounts needed for a specific function
Nanopesticides	Nano-emulsions, encapsulates	Increased efficacy and water solubility
	Triggered release nano-encapsulates	Triggered (local) release
Other nanosized agrochemicals	Nano-sized fertilisers, biocides, veterinary medicines	Improved delivery of agrochemicals in the field, better efficacy, better control of application/dose, less use of solvents in agricultural spraying.
Food processing		
Processed nano-structured or nano-textured food products	Nanoemulsions, micelles	Use of less fat and emulsifiers, stable emulsions, better tasting food products
Nano-sized additives	Organic or inorganic nano-sized additives for food and health-food applications	Various, but lesser amounts would be needed for a function or a taste attribute, better dispersability may also occur
Nanoencapsulates	Nano-carrier systems in the form of liposomes or biopolymer-based nano-encapsulated substances	Providing protective barriers, flavor and taste masking, controlled release, and better dispersability for water-insoluble food ingredients and additives
Nutritional supplements and nutraceuticals	Nano-ingredients and additives	Enhanced absorption and bioavailability of nano-sized ingredients in the body
	Nano-carrier systems for delivery of nutrients	
Nanofilters	Nanofiltration (e.g., porous silica, regenerated cellulose membranes)	Filtration of water and removal of some undesired components in food, such as bitter taste in some plant extracts
FCMs, food storage and handling		
Nanocomposites	Incorporating nanoparticles	Improving strength of materials,

Nano-coatings	into a polymer to form a composite Incorporating nanomaterials onto the packaging surface	durability, barrier properties, biodegradation Improving barrier properties
‘Active’ FCMs	Incorporating active nanoparticles with intentional release into- and consequent effect on the packaged food	Oxygen scavenging, prevention of growth of pathogens
‘Intelligent’ packaging materials	Incorporating nanosensors for food labelling	Detection of food deterioration, monitoring storage conditions
Surface biocides	Incorporating nanoparticles (Ag, ZnO, MgO) on surfaces	Antimicrobial coating for refrigerators, storage containers, equipment for food processing, handling and preparation

8.4 Potential applications of nanomaterials synthesized in this PhD study

There are two types of nanomaterials synthesized in this PhD study. The nanomaterials from Chapters III, IV and V resulted in gold nanoparticles in aqueous form. This solution can have a wide range of application in nanofluidic systems and as well as being used as a contrast agent in imaging. The optical properties of the synthesized gold nanoparticles are interesting and could be further investigated to be applied in developing sensors. The gold nanoparticles synthesized using catechin were encapsulated by a nearly spherical layer of organic material. This surface modification of gold nanoparticles can be utilized to attach other bio-active compounds to the surface of the nanoparticles and can be used as a metallic delivery system of bio-active compounds.

The nanomaterials produced based on methods in Chapters VI and VII, resulted in an organic – inorganic hybrid delivery system in powder form. This makes handling of the synthesized powder nanomaterial convenient. The powders obtained from freeze drying can be used for food delivery system. The gold nanoparticles present in the

encapsulated sphere can provide signals due to surface plasmon resonance (SPR). This would be helpful to design a delivery vehicle for targeted delivery of nutrients. As the carrier material alone does not provide SPR signals, it is difficult to track the movement of encapsulated compounds in biological system. The presence of gold nanoparticles in the carrier matrix increases the SPR signals of the carrier delivery system that can be targeted and traced. The powders produced using microwave assisted encapsulation method had interesting surface morphology; this might find applications in design of packaging materials. The presence of gold nanoparticles in the packaging material can lead to the development of intelligent packaging materials.

8.5 Nanotechnology benefits, risk and challenges

The development of nanotechnology and nanomaterials has led to new challenges, especially understanding and managing the health risks associated with nanoproducts. The scientific data related to the health effects on consumers and workers exposed to nanomaterials are largely unavailable as new nanomaterials are being developed. In parallel there is extensive research on toxicological studies of nanomaterials in progress. The results of these studies will be helpful in developing guidelines for handling and about the health benefits and risks of nanomaterials (Hatto, 2009; Murashov & Howard, 2009; Murashov & Howard, 2008; NIOSH, 2006).

8.5.1 Scientific gaps in knowledge

The current gaps in knowledge that has to be addressed related to nanotechnology are mentioned in this section (Handford et al., 2014).

- Need for clear, uniform definitions of nanomaterials and nanotechnology which is currently lacking. A comprehensive international standard for nanotechnology has to be developed.
- Instrumentation, characterization techniques and analysis methods have to be developed specific to nanomaterials. The methods developed for one type of nanomaterials may not hold for another, so a large database comprising methodology has to be developed. This information must be updated and revised as and when new nanomaterials are discovered.
- Toxicological studies of nanomaterials, their interactions with human body and environment has to be accessed. The adsorption, distribution, metabolism and elimination profiles of nanomaterials are unclear. As currently there is a lack of risk assessment data, and guidance for risk management while handling nanomaterials.
- Creating awareness about nanotechnology in consumers and the public. Implementation of nano-education programs in schools and educational institutions.

8.6 Sustainable gold nanoparticles

Gold is a unique element used by various civilizations of the world and has occupied an important place in the history of mankind for over 7000 years (Gimeno & Laguna, 2003). Gold symbolized immortality by the alchemists as it was the only metal that did not corrode (Kauffman, 1985a). They used *aurum potable* or portable gold as medicine and consumed it internally as a cure for ailments (Brust & Kiely, 2002; Kauffman, 1985a). The Chinese used gold in their traditional medicine (Kauffman,

1985b; Leicester, 1971). It has been known that gold was considered the elixir of life in many ancient civilizations. Historical references of the past indicate that gold nanoparticles were used in ancient Indian medicinal systems of Ayurveda and Siddha. The chemical inertness of gold towards atoms and molecules has made gold the noblest of all metals (Hammer & Norskov, 1995). It is time to look back and determine the health benefits of green synthesized gold nanoparticles for useful applications.

Our ancient wisdom of learning from nature might be the key to sustainable nanomaterials. Nature has perfected the art of nanoscale synthesis over billions of years. More observations are required and better instrumentations should be developed to understand the complex phenomenon occurring at the nanoscale. Once this understanding is reached, we will be able comprehend the compounds present in the agricultural waste materials and their interactions that play a vital role to initiate the synthesis of gold nanoparticles.

CHAPTER IX

SUMMARY AND CONTRIBUTIONS TO KNOWLEDGE

9.1 Summary

Developing new methods for sustainable synthesis of nanomaterials can be considered as the future building blocks for developments in nanotechnology. In this PhD study, nanomaterials were synthesised following a green nanotechnology approach. Two types of nanomaterials were synthesised in this study, first being gold nanoparticles in aqueous form and the second being gold nanoparticles encapsulated in polymer matrix to form a powder. In search for greener alternatives to produce nanoparticles, agricultural waste materials were used in this study to synthesize gold nanoparticles, in turn adding value to waste.

Gold nanoparticles (AuNP) were synthesized using agricultural waste materials such as grape seed, skin and stalk in Chapter III. It was found that gold nanoparticles could be produced within 5 minutes without any addition of stabilising agents. The synthesised gold nanoparticles were characterised using UV-Vis spectrophotometer, high resolution transmission electron microscope (HR-TEM) and energy-dispersive X-ray spectroscopy (EDX). The average size of the gold nanoparticles synthesized using grape seed (GSE+AuNP), grape skin (GSK+AuNP) and grape stalk (GST+AuNP) ranged from 20-25 nm from TEM analysis. This study provided inspiration to explore other agricultural waste materials for gold nanoparticles synthesis.

There is huge amount of waste generated from shedding of maple leaves and pine needles during the fall season in Canada. Chapter IV explored the potentials of using maple leaf and pine needle extracts to synthesize gold nanoparticles. Characterization using TEM revealed the presence of quasi- spherical to triangular shaped gold nanoparticles. This is the first scientific report stating that gold nanoparticles could be synthesized using maple leaf extract.

As the plant matrix is a complex system, a representative polyphenolic compound present in grape seed, skin, and stalk was selected for further investigation. The dispersion of nanoparticles in liquid medium led to a new class of fluids called nanofluids. In Chapter V, four nanofluids were formed by varying the concentration of catechin (CAT) and tannic acid (TAE). Gold nanoparticles synthesized using tannic acid (TAE+AuNP) showed triangular, polygon and quasi-spherical structures. The AuNP synthesized using 1:1 and 1:4 ratio of catechin and tannic acid produced mostly spherical to quasi-spherical gold nanoparticles with a network of organic layer surrounding the AuNP. The gold nanoparticles synthesised using catechin (CAT+AuNP) showed quasi-spherical shape with perfect encapsulation by an organic layer. This structural morphology is similar to core-shell type, where the core consists of gold nanoparticles and the shell is made up of catechin. The summary of the green synthesized gold nanoparticles is provided in Figure 9.1.

A new top-down approach has been developed to form polymeric nanoparticles containing gold nanoparticles. Most of the top-down methods like emulsion evaporation, emulsion diffusion, coacervation either require emulsifiers or organic solvents to form polymeric nanoparticles.

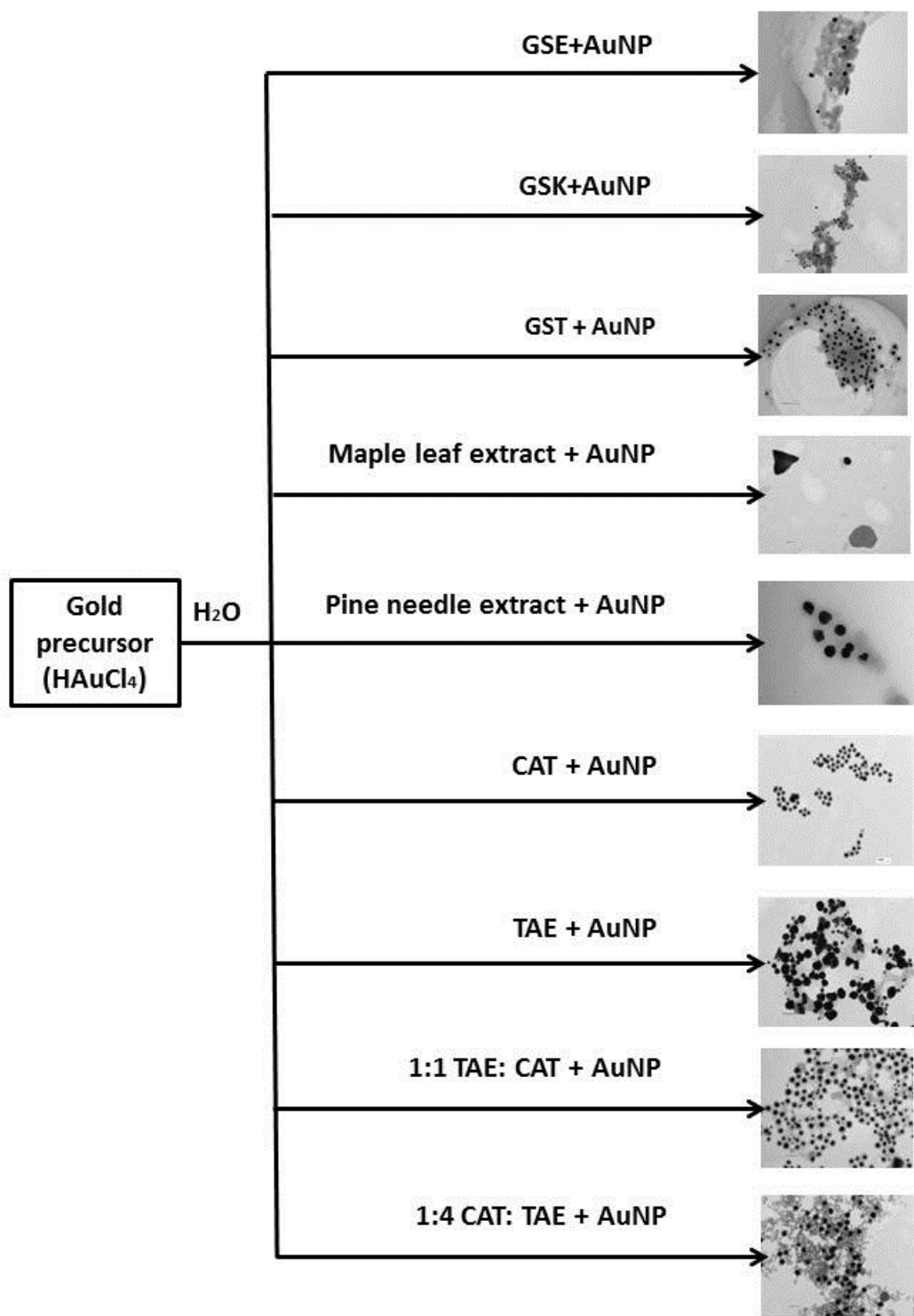


Figure 9.1 Summary of green synthesized gold nanoparticles (AuNP)

In nanoprecipitation both the polymer and the drug is dissolved in a polar or water miscible organic solvent such as acetone, acetonitrile, ethanol or methanol and added drop-wise into an aqueous solution of surfactant. The solvent is removed under reduced pressure by evaporation (Sabliov & Astete, 2008).

The method used in Chapter VI is a modified nanoprecipitation method, where instead of using a water miscible organic solvent, just water is used in the encapsulation process. The use of surfactant in the synthesis protocol was eliminated and the water was evaporated using simple conventional drying, freeze drying and by microwave heating. This is first report stating the formation of AuNP encapsulated powder into maltodextrin matrix without any organic solvent, emulsifiers or surfactant. This method was designed keeping in mind the green nanotechnology approach.

Bottom-up approach using beta-cyclodextrin to form inclusion complex with AuNP was investigated in Chapter VII. Three encapsulation methods were studied for inclusion formation namely, molecular inclusion encapsulation (MIB), lyophilisation encapsulation (FEB) and microwave assisted encapsulation (MEB). The nanomaterials containing gold nanoparticles in polymer matrix obtained from both studies (Chapters VI and VII) were characterized using differential scanning calorimetry (DSC), Fourier transform infrared spectroscopy (FTIR), particle size analysis and scanning electron microscopy (SEM). Interesting surface morphology was observed in the case of synthesized nanomaterials obtained from different encapsulation methods. The summary of nanomaterials containing gold nanoparticles in polymer matrix is provided in Figure 9.2. The overall summary of this PhD study is provided in Figure 9.3.

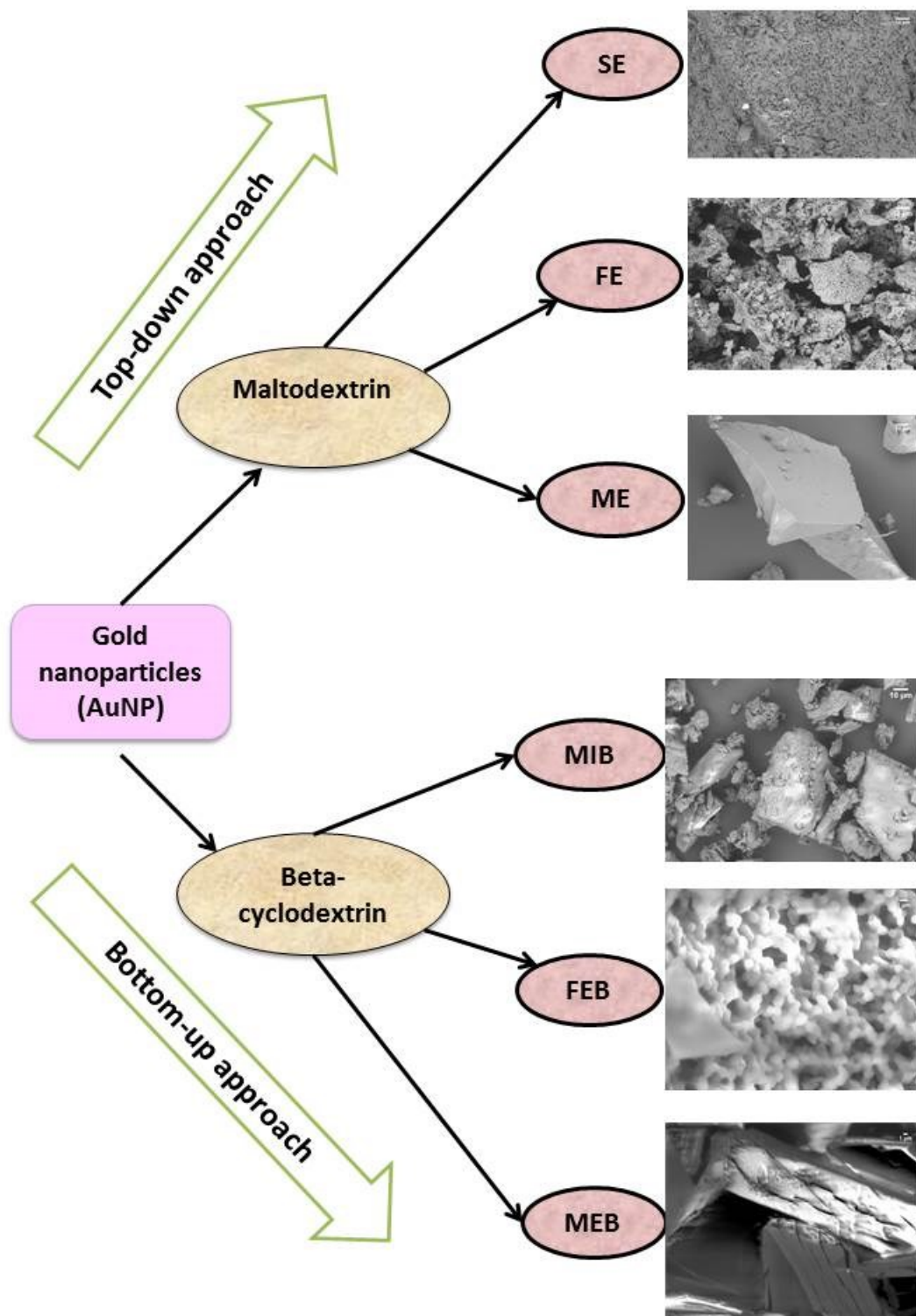


Figure 9.2 Summary of encapsulation of gold nanoparticles (AuNP)

8.2 Contributions to knowledge

1. This PhD study proves that gold nanoparticles can be produced using agricultural waste materials like grape seed, grape skin and grape stalk.
2. This is the first scientific report stating the use of maple leaf extract for the synthesis of gold nanoparticles.
3. Single step gold nanoparticles synthesis methods (9 methods) have been developed and characterized to produce eco-friendly gold nanoparticles without the use of surfactants or stabilising agents.
4. A new method of top-down approach for nanomaterial synthesis incorporating gold nanoparticles into maltodextrin matrix has been developed by using simple encapsulation (SE), freeze drying encapsulation (FE) and microwave assisted encapsulation method (ME) and characterized.
5. Bottom-up approach for inclusion of gold nanoparticles into beta-cyclodextrin cavity by molecular inclusion method (MIB), lyophilisation encapsulation (FEB) and microwave assisted encapsulation (MEB) was developed and characterized. This study reports interesting surface morphology of nanomaterials that can be used for different applications.
6. Nanomaterials containing gold nanoparticles in a polymer matrix were synthesised. Six different AuNP encapsulated powders were produced and characterized.
7. A green nanotechnology approach was adopted and followed throughout this PhD study affirming its possible use in the production of nanomaterials.

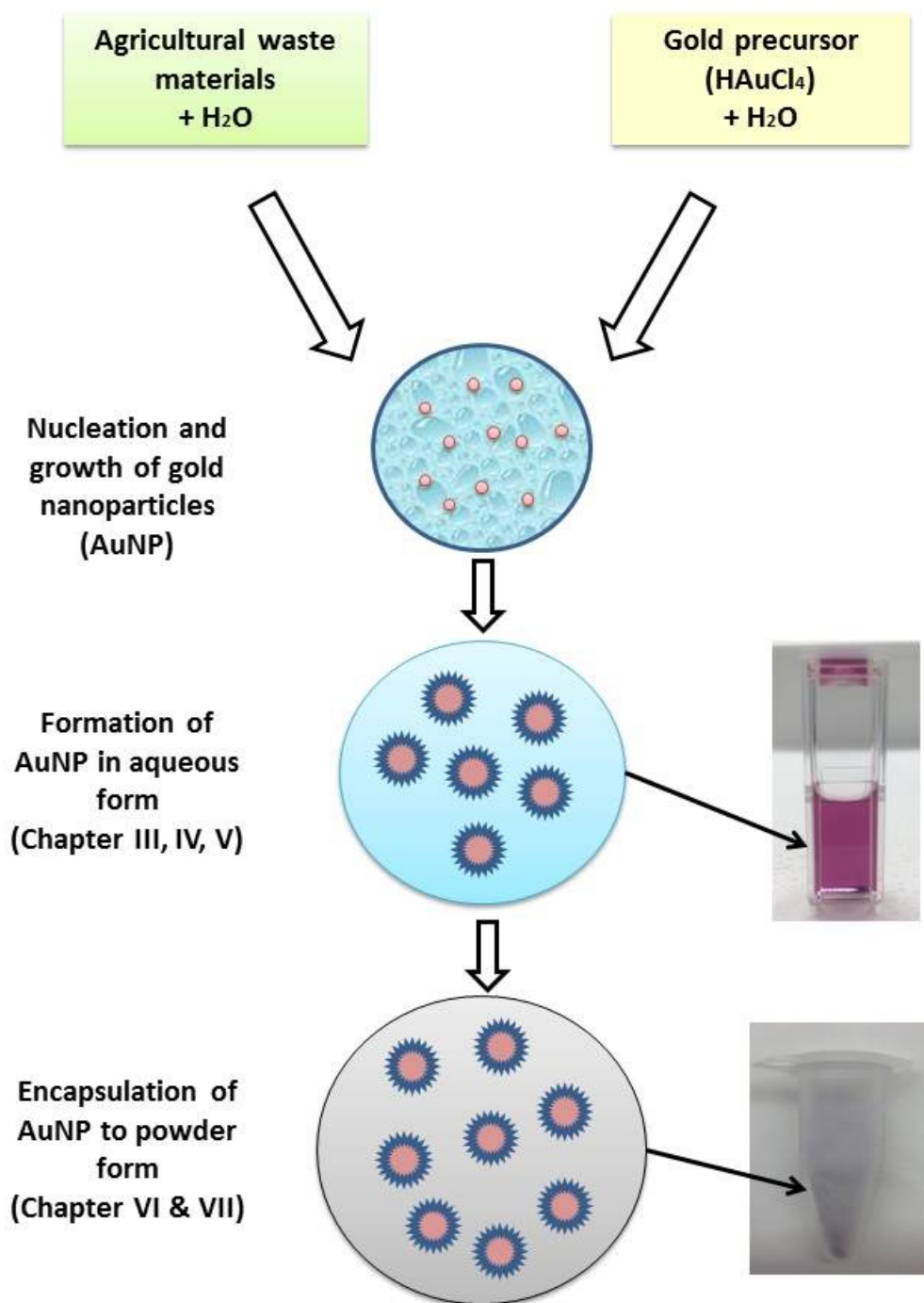


Figure 9.3 Overall summary of this PhD thesis

9.3 Recommendations for future research

During the study, it was observed that gold nanoparticles synthesized using grape seed, stalk, pine needles and maple leaf extracts remained in solution without aggregation or sedimentation for a period of three years. This is an interesting phenomenon to be studied using a zeta potential analyser and other characterization instruments to understand this behaviour.

As the formation of gold nanoparticles with phenolic compounds takes place at a rapid rate, new instrumentation techniques and methodologies have to be developed to understand the mechanisms involved in the formation of nanoparticles.

It was found that parts of grapes, maple and pine can be used to synthesize gold nanoparticles. Further studies are required to understand the role played by the compounds present in these plant materials and their interactions to aid the formation of gold nanoparticles.

More investigation is required to understand the FTIR data and the information provided from the fingerprint region of the spectra.

Further research and development of microwave assisted processing of nanomaterials is required which will lead to more effective and efficient nanomaterial possessing particular properties.

Currently, batch type systems are used to produce nanoparticles. A continuous production unit could be designed for the synthesis of gold nanoparticles.

The good news is that there is a progressive future for nanotechnology.

REFERENCE

- Abbasi, S., Rahimi, S. 2008. Microwave-assisted encapsulation of citric acid using hydrocolloids. *International Journal of Food Science & Technology*, 43(7), 1226-1232.
- Abraham, M.A., Nguyen, N. 2003. "Green Engineering: Defining the Principles"—Results from the Sandestin Conference. *Environmental Progress*, 22(4), 233-236.
- Ahmad, N., Sharma, S., Rai, R. 2012. Rapid green synthesis of silver and gold nanoparticles using peels of *Punica granatum*. *Adv Mater Let*, 3, 376-380.
- Amarnath, K., Mathew, N., Nellore, J., Siddarth, C., Kumar, J. 2011. Facile synthesis of biocompatible gold nanoparticles from *Vitis vinifera* and its cellular internalization against HBL-100 cells. *Cancer Nanotechnology*, 2(1), 121-132.
- Amato, I., Carroll, L. 1999. Nanotechnology: shaping the world atom by atom. National Science and Technology Council, Committee on Technology, Interagency Working Group on Nanoscience, Engineering, and Technology.
- American Institute of Physics- Quantum Mechanics: The Uncertainty Principle. Retrieved from: <http://www.aip.org/history/heisenberg/p08.htm>. Accessed 4 April, 2015.
- Anastas, P.T., Warner, J.C. 2000. Green chemistry: theory and practice. Oxford university press.

- Anastas, P.T., Zimmerman, J.B. 2003. Design Through the 12 Principles of Green Engineering. *Environmental Science & Technology*, 37(5), 94A-101A.
- Ankrum, J.A., Miranda, O.R., Ng, K.S., Sarkar, D., Xu, C., Karp, J.M. 2014. Engineering cells with intracellular agent-loaded microparticles to control cell phenotype. *Nature protocols*, 9(2), 233-245.
- ASTM E2456-06. 2006. Standard Terminology Relating to Nanotechnology, ASTM International, West Conshohocken, PA, Retrieved from: www.astm.org. Accessed 5 April, 2015.
- Astray, G., Gonzalez-Barreiro, C., Mejuto, J., Rial-Otero, R., Simal-Gandara, J. 2009. A review on the use of cyclodextrins in foods. *Food Hydrocolloids*, 23(7), 1631-1640.
- Astray, G., Mejuto, J.C., Morales, J., Rial-Otero, R., Simal-Gándara, J. 2010. Factors controlling flavors binding constants to cyclodextrins and their applications in foods. *Food Research International*, 43(4), 1212-1218.
- Augustin, M.A., Hemar, Y. 2009. Nano- and micro-structured assemblies for encapsulation of food ingredients. *Chemical Society Reviews*, 38(4), 902-912.
- Aykaç, A., Martos-Maldonado, M.C., Casas-Solvas, J.M., Quesada-Soriano, I., García-Maroto, F., García-Fuentes, L., Vargas-Berenguel, A. 2013. β -Cyclodextrin-Bearing Gold Glyconanoparticles for the Development of Site Specific Drug Delivery Systems. *Langmuir*, 30(1), 234-242.

- Baigent, C., Müller, G. 1980. A colloidal gold prepared with ultrasonics. *Experientia*, 36(4), 472-473.
- Baldwin, I., Schultz, J., Ward, D. 1987. Patterns and sources of leaf tannin variation in yellow birch (*Betula allegheniensis*) and sugar maple (*Acer saccharum*). *Journal of Chemical Ecology*, 13(5), 1069-1078.
- Bankar, A., Joshi, B., Ravi Kumar, A., Zinjarde, S. 2010. Banana peel extract mediated synthesis of gold nanoparticles. *Colloids and Surfaces B: Biointerfaces*, 80(1), 45-50.
- Baruwati, B., Varma, R.S. 2009. High Value Products from Waste: Grape Pomace Extract—A Three-in-One Package for the Synthesis of Metal Nanoparticles. *ChemSusChem*, 2(11), 1041-1044.
- Baş, D., Boyacı, İ.H. 2007. Modeling and optimization I: Usability of response surface methodology. *Journal of Food Engineering*, 78(3), 836-845.
- Begum, N.A., Mondal, S., Basu, S., Laskar, R.A., Mandal, D. 2009. Biogenic synthesis of Au and Ag nanoparticles using aqueous solutions of Black Tea leaf extracts. *Colloids and Surfaces B: Biointerfaces*, 71(1), 113-118.
- Bermejo, E., Becue, T., Lacour, C., Quarton, M. 1997. Synthesis of nanoscaled iron particles from freeze-dried precursors. *Powder Technology*, 94(1), 29-34.
- Betts, K. 2005. A greener route to gold nanoparticles. *Environmental Science & Technology*, 39(5), 104-105.

- Bezerra, M.A., Santelli, R.E., Oliveira, E.P., Villar, L.S., Escaleira, L.A. 2008. Response surface methodology (RSM) as a tool for optimization in analytical chemistry. *Talanta*, 76(5), 965-977.
- Bhushan, B. 2010. Introduction to nanotechnology. Springer handbook of nanotechnology, 1-13.
- Bilati, U., Allémann, E., Doelker, E. 2005. Poly (D, L-lactide-co-glycolide) protein-loaded nanoparticles prepared by the double emulsion method-processing and formulation issues for enhanced entrapment efficiency. *Journal of microencapsulation*, 22(2), 205-214.
- Binnig, G., Quate, C.F., Gerber, C. 1986. Atomic Force Microscope. *Physical Review Letters*, 56(9), 930-933.
- Binnig, G., Rohrer, H. 1987. Scanning tunneling microscopy—from birth to adolescence. *reviews of modern physics*, 59(3), 615-625.
- Birrell, G., Hedberg, K., Griffith, O. 1987. Pitfalls of immunogold labeling: analysis by light microscopy, transmission electron microscopy, and photoelectron microscopy. *Journal of Histochemistry & Cytochemistry*, 35(8), 843-853.
- Bonenfant, D., Niquette, P., Mimeault, M., Furtos-Matei, A., Hausler, R. 2009. UV-VIS and FTIR spectroscopic analyses of inclusion complexes of nonylphenol and nonylphenol ethoxylate with β -cyclodextrin. *Water Research*, 43(14), 3575-3581.

- Bouwmeester, H., Brandhoff, P., Marvin, H.J.P., Weigel, S., Peters, R.J.B. 2014. State of the safety assessment and current use of nanomaterials in food and food production. *Trends in Food Science & Technology*, 40(2), 200-210.
- Brust, M., Kiely, C.J. 2002. Some recent advances in nanostructure preparation from gold and silver particles: a short topical review. *Colloids and Surfaces A: Physicochemical and Engineering Aspects*, 202(2–3), 175-186.
- Brust, M., Walker, M., Bethell, D., Schiffrin, D.J., Whyman, R. 1994. Synthesis of thiol-derivatised gold nanoparticles in a two-phase liquid–liquid system. *J. Chem. Soc., Chem. Commun.*(7), 801-802.
- Bueno, J.M., Sáez-Plaza, P., Ramos-Escudero, F., Jiménez, A.M., Fett, R., Asuero, A.G. 2012. Analysis and Antioxidant Capacity of Anthocyanin Pigments. Part II: Chemical Structure, Color, and Intake of Anthocyanins. *Critical Reviews in Analytical Chemistry*, 42(2), 126-151.
- Buschmann, H.-J., Schollmeyer, E. 2002. Applications of cyclodextrins in cosmetic products: a review. *Journal of cosmetic science*, 53(3), 185-192.
- Cao, Y., Irwin, P.C., Younsi, K. 2004. The future of nanodielectrics in the electrical power industry. *Dielectrics and Electrical Insulation, IEEE Transactions on*, 11(5), 797-807.
- Castillo, J., Benavente-Garcia, O., Lorente, J., Alcaraz, M., Redondo, A., Ortuno, A., Del Rio, J. 2000. Antioxidant activity and radioprotective effects against chromosomal damage induced in vivo by X-rays of flavan-3-ols (Procyanidins)

- from grape seeds (*Vitis vinifera*): comparative study versus other phenolic and organic compounds. *Journal of agricultural and food chemistry*, 48(5), 1738-1745.
- Castro, L., Blazquez, M.L., Munoz, J.A., Gonzalez, F., Garcia-Balboa, C., Ballester, A. 2011. Biosynthesis of gold nanowires using sugar beet pulp. *Process Biochemistry*.
- Cegnar, M., Kos, J., Kristl, J. 2004. Cystatin incorporated in poly (lactide-co-glycolide) nanoparticles: development and fundamental studies on preservation of its activity. *European Journal of Pharmaceutical Sciences*, 22(5), 357-364.
- Chen, L., Remondetto, G.E., Subirade, M. 2006. Food protein-based materials as nutraceutical delivery systems. *Trends in Food Science & Technology*, 17(5), 272-283.
- Choi, S.U. 2009. Nanofluids: from vision to reality through research. *Journal of Heat Transfer*, 131(3), 033106.
- Choi, S.U.S., Eastman, J.A. 1995. Enhancing thermal conductivity of fluids with nanoparticles. American Society of Mechanical Engineers, Fluids Engineering Division (Publication) FED. pp. 99-105.
- Clark, D.E., Folz, D.C., West, J.K. 2000. Processing materials with microwave energy. *Materials Science and Engineering: A*, 287(2), 153-158.

- Coles, D., Frewer, L. 2013. Nanotechnology applied to European food production—A review of ethical and regulatory issues. *Trends in Food Science & Technology*, 34(1), 32-43.
- Crozier, A., Clifford, M.N., Ashihara, H. 2008. Plant secondary metabolites: occurrence, structure and role in the human diet. John Wiley & Sons.
- Csaba, N., Caamaño, P., Sánchez, A., Domínguez, F., Alonso, M.J. 2005. PLGA: poloxamer and PLGA: poloxamine blend nanoparticles: new carriers for gene delivery. *Biomacromolecules*, 6(1), 271-278.
- Cushen, M., Kerry, J., Morris, M., Cruz-Romero, M., Cummins, E. 2012. Nanotechnologies in the food industry – Recent developments, risks and regulation. *Trends in Food Science & Technology*, 24(1), 30-46.
- Daniel, M.C., Astruc, D. 2004. Gold Nanoparticles: Assembly, Supramolecular Chemistry, Quantum-Size-Related Properties, and Applications Toward Biology, Catalysis, and Nanotechnology. *Chemical Reviews*, 104(1), 293-346.
- Das, S.K., Choi, S.U.S., Yu, W., Pradeep, T. 2008. *Nanofluids Science and Technology*. John Wiley & Sons, Inc., , Hoboken, New Jersey.
- De Mey, J., Moeremans, M. 1986. The preparation of colloidal gold probes and their use as marker in electron microscopy. in: *Advanced techniques in biological electron microscopy III*, Springer, pp. 229-271.
- Del Valle, E.M.M. 2004. Cyclodextrins and their uses: a review. *Process Biochemistry*, 39(9), 1033-1046.

- Drexler, K.E. 1981. Molecular engineering: An approach to the development of general capabilities for molecular manipulation. *Proceedings of the National Academy of Sciences*, 78(9), 5275-5278.
- Du, L., Xian, L., Feng, J.-X. 2011. Rapid extra-/intracellular biosynthesis of gold nanoparticles by the fungus *Penicillium* sp. *Journal of Nanoparticle Research*, 13(3), 921-930.
- Dubey, S.P., Lahtinen, M., Sillanpää, M. 2010. Tansy fruit mediated greener synthesis of silver and gold nanoparticles. *Process Biochemistry*, 45(7), 1065-1071.
- Dudda, B., Shin, D. 2013. Effect of nanoparticle dispersion on specific heat capacity of a binary nitrate salt eutectic for concentrated solar power applications. *International Journal of Thermal Sciences*, 69(0), 37-42.
- Durán, N., Marcato, P., Durán, M., Yadav, A., Gade, A., Rai, M. 2011. Mechanistic aspects in the biogenic synthesis of extracellular metal nanoparticles by peptides, bacteria, fungi, and plants. *Applied Microbiology and Biotechnology*, 90(5), 1609-1624.
- Edwards, P.P., Thomas, J.M. 2007. Gold in a Metallic Divided State—From Faraday to Present-Day Nanoscience. *Angewandte Chemie International Edition*, 46(29), 5480-5486.
- Eijkel, J.C., Van Den Berg, A. 2005. Nanofluidics: what is it and what can we expect from it? *Microfluidics and Nanofluidics*, 1(3), 249-267.

- Ezhilarasi, P.N., Karthik, P., Chhanwal, N., Anandharamakrishnan, C. 2013. Nanoencapsulation Techniques for Food Bioactive Components: A Review. Food and Bioprocess Technology, 6(3), 628-647.
- Faraday, M. 1857. Experimental Relations of Gold (and other Metals) to Light. Philosophical Transactions of the Royal Society of London, 147(1857), 145-181.
- Fathi, M., Martín, Á., McClements, D.J. 2014. Nanoencapsulation of food ingredients using carbohydrate based delivery systems. Trends in Food Science & Technology, 39(1), 18-39.
- Feynman, R.P. 1960. There's plenty of room at the bottom. Engineering and science, 23(5), 22-36.
- Fitzgibbons, K., McNiven, C. 2006. Towards a nanotechnology statistical framework. Blue sky indicators conference II on, 25-27 September 2006, Ottawa, Canada. pp. 1-2.
- Fothergill, J.C. 2007. Ageing, Space Charge and Nanodielectrics: Ten Things We Don't Know About Dielectrics. Solid Dielectrics, 2007. ICSD '07. IEEE International Conference on, 8-13 July 2007. pp. 1-10.
- Fratini, A., Pellegrini, N., Nicastro, D., Sanctis, O.d. 2005. Effect of amine groups in the synthesis of Ag nanoparticles using aminosilanes. Materials Chemistry and Physics, 94(1), 148-152.
- Frens, G. 1973. Controlled nucleation for the regulation of the particle size in monodisperse gold suspensions. Nature, 241(105), 20-22.

- Gade, A., Gaikwad, S., Tiwari, V., Yadav, A., Ingle, A., Rai, M. 2010. Biofabrication of silver nanoparticles by *Opuntia ficus-indica*: In Vitro antibacterial activity and study of the mechanism involved in the synthesis. *Current Nanoscience*, 6(4), 370-375.
- Galindo-Rodríguez, S.A., Puel, F., Briançon, S., Allémann, E., Doelker, E., Fessi, H. 2005. Comparative scale-up of three methods for producing ibuprofen-loaded nanoparticles. *European Journal of Pharmaceutical Sciences*, 25(4–5), 357-367.
- Gan, P.P., Ng, S.H., Huang, Y., Li, S.F.Y. 2012. Green synthesis of gold nanoparticles using palm oil mill effluent (POME): A low-cost and eco-friendly viable approach. *Bioresource Technology*, 113(0), 132-135.
- Genç, R.k., Clergeaud, G., Ortiz, M., O’Sullivan, C.K. 2011. Green Synthesis of Gold Nanoparticles Using Glycerol-Incorporated Nanosized Liposomes. *Langmuir*, 27(17), 10894-10900.
- Ghoreishi, S.M., Behpour, M., Khayatkashani, M. 2011. Green synthesis of silver and gold nanoparticles using *Rosa damascena* and its primary application in electrochemistry. *Physica E: Low-dimensional Systems and Nanostructures*, 44(1), 97-104.
- Gimeno, M., Laguna, A. 2003. Some recent highlights in gold chemistry. *Gold Bulletin*, 36(3), 83-92.
- Gray, E.P., Bruton, T.A., Higgins, C.P., Halden, R.U., Westerhoff, P., Ranville, J.F. 2012. Analysis of gold nanoparticle mixtures: a comparison of hydrodynamic

- chromatography (HDC) and asymmetrical flow field-flow fractionation (AF4) coupled to ICP-MS. *Journal of Analytical Atomic Spectrometry*, 27(9), 1532-1539.
- Green, C., Vaughan, A. 2008. Nanodielectrics - How Much Do We Really Understand? [Feature Article]. *Electrical Insulation Magazine*, IEEE, 24(4), 6-16.
- Guo, L., Huang, Q., Li, X.-y., Yang, S. 2001. Iron nanoparticles: synthesis and applications in surface enhanced Raman scattering and electrocatalysis. *Physical Chemistry Chemical Physics*, 3(9), 1661-1665.
- Guo, L., Wang, L.H., Sun, B., Yang, J.Y., Zhao, Y.Q., Dong, Y.X., Spranger, M.I., Wu, C.F. 2007. Direct in vivo evidence of protective effects of grape seed procyanidin fractions and other antioxidants against ethanol-induced oxidative DNA damage in mouse brain cells. *Journal of agricultural and food chemistry*, 55(14), 5881-5891.
- Guo, S., Wang, E. 2007. Synthesis and electrochemical applications of gold nanoparticles. *Analytica chimica acta*, 598(2), 181-192.
- Hammer, B., Norskov, J.K. 1995. Why gold is the noblest of all the metals. *Nature*, 376(6537), 238-240.
- Handford, C.E., Dean, M., Henchion, M., Spence, M., Elliott, C.T., Campbell, K. 2014. Implications of nanotechnology for the agri-food industry: Opportunities, benefits and risks. *Trends in Food Science & Technology*, 40(2), 226-241.

- Haiss, W., Thanh, N.T.K., Aveyard, J., Fernig, D.G. 2007. Determination of Size and Concentration of Gold Nanoparticles from UV–Vis Spectra. *Analytical Chemistry*, 79(11), 4215-4221.
- Hatto, P. 2009. International standards for risk management in nanotechnology. *Nature Nanotechnology*, 4(4), 205-205.
- HeeáKook, Y., TaxáOh, E., JooáPark, H. 2009. Cyclodextrin-covered gold nanoparticles for targeted delivery of an anti-cancer drug. *Journal of Materials Chemistry*, 19(16), 2310-2315.
- Hirayama, F., Uekama, K. 1999. Cyclodextrin-based controlled drug release system. *Advanced Drug Delivery Reviews*, 36(1), 125-141.
- Hornyak, G.L., Moore, J.J., Tibbals, H.F., Dutta, J. 2008. *Fundamentals of Nanotechnology*. Taylor & Francis. 71- 113.
- Huang, J., Li, Q., Sun, D., Lu, Y., Su, Y., Yang, X., Wang, H., Wang, Y., Shao, W., He, N. 2007. Biosynthesis of silver and gold nanoparticles by novel sundried *Cinnamomum camphora* leaf. *Nanotechnology*, 18(10), 105104.
- Hubert, B., Atkinson, J., Guerret, M., Hoffman, M., Devissaguet, J.P., Maincent, P. 1991. The preparation and acute antihypertensive effects of a nanocapsular form of darodipine, a dihydropyridine calcium entry blocker. *Pharmaceutical Research*, 8(6), 734-738.

- Hyeon, T., Lee, S.S., Park, J., Chung, Y., Na, H.B. 2001. Synthesis of highly crystalline and monodisperse maghemite nanocrystallites without a size-selection process. *Journal of the American Chemical Society*, 123(51), 12798-12801.
- IBM Celebrates 20th Anniversary of Moving Atoms. 2009. Retrieved from: <https://www03.ibm.com/press/us/en/pressrelease/28488.wss>. Accessed 5 April, 2015.
- IBM Research: Major Nanoscale Breakthroughs. IBM Nanotech Leadership. Retrieved from: www.ibm.com/press/attachments/28488.pdf. Accessed 5 April, 2015.
- Iijima, S. 1991. Helical microtubules of graphitic carbon. *Nature*, 354(6348), 56-58.
- International System of Units (Système International d'Unités, SI). 2006. SI Brochure: The International System of Units (SI). International Bureau of Weights and Measures (Bureau International des Poids et Mesures, BIPM). 8th edition, 2006; updated in 2014. Retrieved from: <http://www.bipm.org/en/publications/si-brochure/chapter3.html>. Accessed 9 April, 2015.
- ISO. Nanotechnologies – Vocabulary part 1: Core terms. 2010. International Organization for Standardization (2010). ISO/TS 80004-1:2010. Retrieved from: <https://www.iso.org/> Accessed 9 April, 2015.
- Jain, P.K., Lee, K.S., El-Sayed, I.H., El-Sayed, M.A. 2006. Calculated absorption and scattering properties of gold nanoparticles of different size, shape, and composition: Applications in biological imaging and biomedicine. *Journal of Physical Chemistry B*, 110(14), 7238-7248.

- Jana, N.R., Gearheart, L., Murphy, C.J. 2001. Wet chemical synthesis of silver nanorods and nanowires of controllable aspect ratio. . Chemical Communications(7), 617-618.
- Jincheng, W., Xiaoyu, Z., Sihao, C. 2010. Preparation and properties of nanocapsulated capsaicin by complex coacervation method. Chemical Engineering Communications, 197(7), 919-933.
- Kalishwaralal, K., Deepak, V., Ram Kumar Pandian, S., Gurunathan, S. 2009. Biological synthesis of gold nanocubes from *Bacillus licheniformis*. Bioresource Technology, 100(21), 5356-5358.
- Kamat, P.V., Flumiani, M., Hartland, G.V. 1998. Picosecond dynamics of silver nanoclusters. Photoejection of electrons and fragmentation. The Journal of Physical Chemistry B, 102(17), 3123-3128.
- Kapoor, R. 2010. Some observations on the metal-based preparations in Indian systems of medicine.
- Karathanos, V.T., Mourtzinis, I., Yannakopoulou, K., Andrikopoulos, N.K. 2007. Study of the solubility, antioxidant activity and structure of inclusion complex of vanillin with β -cyclodextrin. Food Chemistry, 101(2), 652-658.
- Karn, B. 2008. The road to green nanotechnology. Journal of Industrial Ecology, 12(3), 263-266.
- Kauffman, G. 1985a. The role of gold in alchemy. Part I. Gold Bulletin, 18(1), 31-44.
- Kauffman, G. 1985b. The role of gold in alchemy. Part II. Gold Bulletin, 18(2), 69-78.

- Kennedy, J.A., Hayasaka, Y., Vidal, S., Waters, E.J., Jones, G.P. 2001. Composition of Grape Skin Proanthocyanidins at Different Stages of Berry Development. *Journal of agricultural and food chemistry*, 49(11), 5348-5355.
- Khitrova, G., Gibbs, H.M. 2008. Solid-state physics: Join the dots. *Nature*, 451(7176), 256-256.
- Korgel, B.A., Fullam, S., Connolly, S., Fitzmaurice, D. 1998. Assembly and self-organization of silver nanocrystal superlattices: ordered “soft spheres”. *The Journal of Physical Chemistry B*, 102(43), 8379-8388.
- Krishnaswamy, K., Orsat, V., Gariépy, Y., Thangavel, K. 2013. Optimization of Microwave-Assisted Extraction of Phenolic Antioxidants from Grape Seeds (*Vitis vinifera*). *Food and Bioprocess Technology*, 6(2), 441-455.
- Kroto, H.W., Heath, J.R., O'Brien, S.C., Curl, R.F., Smalley, R.E. 1985. C 60: buckminsterfullerene. *Nature*, 318(6042), 162-163.
- Kuppusamy, P., Yusoff, M.M., Ichwan, S.J., Parine, N.R., Maniam, G.P., Govindan, N. 2014. *Commelina nudiflora* L. edible weed as a novel source for gold nanoparticles synthesis and studies on different physical–chemical and biological properties. *Journal of Industrial and Engineering Chemistry*. 27, 59-67.
- Leicester, H.M. 1971. The historical background of chemistry. Courier Corporation. 53-61.

- Leiva, A., Saldías, C., Quezada, C., Toro-Labbé, A., Espinoza-Beltrán, F.J., Urzúa, M., Gargallo, L., Radic, D. 2009. Gold-copolymer nanoparticles: poly ([epsilon]-caprolactone)/poly (N-vinyl-2-pyrrolydone) biodegradable triblock copolymer as stabilizer and reductant. *European Polymer Journal*, 45(11), 3035-3042.
- Lewis, T.J. 1994. Nanometric dielectrics. *Dielectrics and Electrical Insulation*, IEEE Transactions on, 1(5), 812-825.
- Li, C.-J., Chen, L. 2006. Organic chemistry in water. *Chemical Society Reviews*, 35(1), 68-82.
- Li, N., Xu, L. 2010. Thermal analysis of β -cyclodextrin/Berberine chloride inclusion compounds. *Thermochimica Acta*, 499(1-2), 166-170.
- Li, V.H., Wood, R.W., Kreuter, J., Harmia, T., Robinson, J.R. 1986. Ocular drug delivery of progesterone using nanoparticles. *Journal of microencapsulation*, 3(3), 213-218.
- Li, Y., Zhou, J.e., Tung, S., Schneider, E., Xi, S. 2009. A review on development of nanofluid preparation and characterization. *Powder Technology*, 196(2), 89-101.
- Liao, X., Raghavan, G., Yaylayan, V. 2001. Dielectric properties of alcohols (C1 - C5) at 2450 MHz and 915 MHz. *Journal of Molecular Liquids*, 94(1), 51-60.
- Liu, Z., Jiao, Y., Wang, Y., Zhou, C., Zhang, Z. 2008. Polysaccharides-based nanoparticles as drug delivery systems. *Advanced Drug Delivery Reviews*, 60(15), 1650-1662.

- Loftsson, T., Duchêne, D. 2007. Cyclodextrins and their pharmaceutical applications. *International journal of pharmaceutics*, 329(1–2), 1-11.
- Lowe, P.J., Temple, C.S. 1994. Calcitonin and insulin in isobutylcyanoacrylate nanocapsules: protection against proteases and effect on intestinal absorption in rats. *Journal of pharmacy and pharmacology*, 46(7), 547-552.
- Machín, R., Isasi, J.R., Vélaz, I. 2012. β -Cyclodextrin hydrogels as potential drug delivery systems. *Carbohydrate Polymers*, 87(3), 2024-2030.
- Mafuné, F., Kohno, J.-y., Takeda, Y., Kondow, T. 2002. Full physical preparation of size-selected gold nanoparticles in solution: laser ablation and laser-induced size control. *The Journal of Physical Chemistry B*, 106(31), 7575-7577.
- Mahal, A., Khullar, P., Kumar, H., Kaur, G., Singh, N., Jelokhani-Niaraki, M., Bakshi, M.S. 2013. Green Chemistry of Zein Protein Toward the Synthesis of Bioconjugated Nanoparticles: Understanding Unfolding, Fusogenic Behavior, and Hemolysis. *ACS Sustainable Chemistry & Engineering*, 1(6), 627-639.
- Mallick, K., Wang, Z.L., Pal, T. 2001. Seed-mediated successive growth of gold particles accomplished by UV irradiation: a photochemical approach for size-controlled synthesis. *Journal of Photochemistry and Photobiology A: Chemistry*, 140(1), 75-80.
- Mansoori, G.A. 2005. Principles of nanotechnology: molecular-based study of condensed matter in small systems. World Scientific Singapore. 1- 27.

- Myers, R.H., Montgomery, D.C., Anderson -Cook, C.M. 2009. Response Surface Methodology. John Wiley & Sons, Inc., New Jersey. 155-196.
- McKenzie, L.C., Hutchison, J.E. 2004. Green nanoscience. *Chimica Oggi- Chemistry Today*, 22(9), 30-33.
- Meda, V., Orsat, V., Raghavan, V. 2005. 4 - Microwave heating and the dielectric properties of foods. in: *The microwave processing of foods*, (Eds.) H. Schubert, M. Regier, Woodhead Publishing, pp. 61-75.
- Mishra, B., Patel, B.B., Tiwari, S. 2010. Colloidal nanocarriers: a review on formulation technology, types and applications toward targeted drug delivery. *Nanomedicine: Nanotechnology, Biology and Medicine*, 6(1), 9-24.
- Mühlpfordt, H. 1982. The preparation of colloidal gold particles using tannic acid as an additional reducing agent. *Cellular and Molecular Life Sciences*, 38(9), 1127-1128.
- Müller, E.W. 1957. Study of Atomic Structure of Metal Surfaces in the Field Ion Microscope. *Journal of Applied Physics*, 28(1), 1-6.
- Müller, E.W. 1955. Work function of tungsten single crystal planes measured by the field emission microscope. *Journal of Applied Physics*, 26(6), 732-737.
- Mulvaney, P. 1996. Surface plasmon spectroscopy of nanosized metal particles. *Langmuir*, 12(3), 788-800.
- Murashov, V., Howard, J. 2009. Essential features for proactive risk management. *Nature Nanotechnology*, 4(8), 467-470.

- Murashov, V., Howard, J. 2008. The US must help set international standards for nanotechnology. *Nat Nano*, 3(11), 635-636.
- Muralidharan, V.S., Subramania, A. 2008. *Nanoscience and Technology*. Taylor & Francis. 1- 30.
- Nadagouda, M.N., Hoag, G., Collins, J., Varma, R.S. 2009. Green Synthesis of Au Nanostructures at Room Temperature Using Biodegradable Plant Surfactants. *Crystal Growth & Design*, 9(11), 4979-4983.
- Namazi, H., Heydari, A. 2014. Synthesis of β -cyclodextrin-based dendrimer as a novel encapsulation agent. *Polymer International*, 63(8), 1447-1455.
- National Institute for Nanotechnology (NINT). NINT Innovation Center, Edmonton, Alberta. Retrieved from: <http://www.nint-innt.ca/>. Accessed 11 April, 2015.
- National Nanotechnology Initiative (NNI) Fiscal Year 2015 Budget. National Science and Technology Council, Committee on Technology: Subcommittee on Nanoscale Science, Engineering, and Technology, USA. Retrieved from: <http://nano.gov/node/1128> and <http://www.nano.gov/nni-pca>. Accessed 11 April, 2015.
- Nelson, J.K., Fothergill, J.C., Dissado, L.A., Peasgood, W. 2002. Towards an understanding of nanometric dielectrics. *Electrical Insulation and Dielectric Phenomena*, 2002 Annual Report Conference on, 2002. pp. 295-298.
- Newton, D.E. 2002. *Recent advances and issues in molecular nanotechnology*. Greenwood Press. 107-120.

- NIOSH. 2006. Approaches to Safe Nanotechnology: An Information Exchange with NIOSH. National Institute for Occupational Safety and Health (NIOSH), USA.
- Nouailhat, A. 2008. An Introduction to Nanosciences and Nanotechnology. John Wiley & Sons.
- Nune, S.K., Chanda, N., Shukla, R., Katti, K., Kulkarni, R.R., Thilakavathy, S., Mekapothula, S., Kannan, R., Katti, K.V. 2009. Green nanotechnology from tea: phytochemicals in tea as building blocks for production of biocompatible gold nanoparticles. *J. Mater. Chem.*, 19(19), 2912-2920.
- Obare, S.O., Hollowell, R.E., Murphy, C.J. 2002. Sensing strategy for lithium ion based on gold nanoparticles. *Langmuir*, 18(26), 10407-10410.
- Orsat, V. 2010. Effect of Radio-Frequency Heating on Food. In *Novel Food Processing: Effects on Rheological and Functional Properties*. Ahmed, J., Ramaswamy, H., Kasapis, S. and Boye, J. I. Eds. CRC Press, Florida, USA. 7-20.
- Paciotti, G.F., Myer, L., Weinreich, D., Goia, D., Pavel, N., McLaughlin, R.E., Tamarkin, L. 2004. Colloidal gold: A novel nanoparticle vector for tumor directed drug delivery. *Drug Delivery: Journal of Delivery and Targeting of Therapeutic Agents*, 11(3), 169-183.
- FAOSTAT, 2012. Retrieved from: <http://faostat.fao.org/>
- Faulk, P.W., Taylor, M.G. 1971. Communication to the editors: an immunocolloid method for the electron microscope. *Immunochemistry*, 8(11), 1081-1083.

- Pande, S., Ghosh, S.K., Praharaj, S., Panigrahi, S., Basu, S., Jana, S., Pal, A., Tsukuda, T., Pal, T. 2007. Synthesis of Normal and Inverted Gold–Silver Core–Shell Architectures in β -Cyclodextrin and Their Applications in SERS. *The Journal of Physical Chemistry C*, 111(29), 10806-10813.
- Paul, S., Chugh, A. 2011. Assessing the Role of Ayurvedic ‘Bhasms’ as Ethno-nanomedicine in the Metal Based Nanomedicine Patent Regime. *Journal of Intellectual Property Rights*, 16, 509-515.
- Peng, G., Tisch, U., Adams, O., Hakim, M., Shehada, N., Broza, Y.Y., Billan, S., Abdah-Bortnyak, R., Kuten, A., Haick, H. 2009. Diagnosing lung cancer in exhaled breath using gold nanoparticles. *Nature Nanotechnology*, 4(10), 669-673.
- Pfaltzgraff, L.A., Cooper, E.C., Budarin, V., Clark, J.H. 2013. Food waste biomass: a resource for high-value chemicals. *Green Chemistry*, 15(2), 307-314.
- Philip, D. 2009. Honey mediated green synthesis of gold nanoparticles. *Spectrochimica Acta Part A: Molecular and Biomolecular Spectroscopy*, 73(4), 650-653.
- Pinent, M., Blay, M., Blade, M., Salvado, M., Arola, L., Ardevol, A. 2004. Grape seed-derived procyanidins have an antihyperglycemic effect in streptozotocin-induced diabetic rats and insulinomimetic activity in insulin-sensitive cell lines. *Endocrinology*, 145(11), 4985.

- Pinho, E., Grootveld, M., Soares, G., Henriques, M. 2014. Cyclodextrins as encapsulation agents for plant bioactive compounds. *Carbohydrate Polymers*, 101(0), 121-135.
- Poole Jr, C.P., Owens, F.J. 2003. *Introduction to nanotechnology*. John Wiley & Sons.
- Pradeep, T. 2007. *Nano: the essentials*. Tata McGraw-Hill Education.
- Prasain, J.K., Peng, N., Dai, Y., Moore, R., Arabshahi, A., Wilson, L., Barnes, S., Michael Wyss, J., Kim, H., Watts, R.L. 2009. Liquid chromatography tandem mass spectrometry identification of proanthocyanidins in rat plasma after oral administration of grape seed extract. *Phytomedicine*, 16(2–3), 233-243.
- Puglisi, A., Spencer, J., Clarke, J., Milton, J. 2012. Microwave-assisted synthesis of 6-amino- β -cyclodextrins. *Journal of Inclusion Phenomena and Macrocyclic Chemistry*, 73(1-4), 475-478.
- Puliti, G., Paolucci, S., Sen, M. 2011. Nanofluids and their properties. *Applied Mechanics Reviews*, 64(3), 030803.
- Radwan, M.A., Aboul-Enein, H.Y. 2002. The effect of oral absorption enhancers on the in vivo performance of insulin-loaded poly (ethylcyanoacrylate) nanospheres in diabetic rats. *Journal of microencapsulation*, 19(2), 225-235.
- Rao, J.P., Geckeler, K.E. 2011. Polymer nanoparticles: Preparation techniques and size-control parameters. *Progress in Polymer Science*, 36(7), 887-913.

- Reed, M., Randall, J., Aggarwal, R., Matyi, R., Moore, T., Wetsel, A. 1988. Observation of discrete electronic states in a zero-dimensional semiconductor nanostructure. *Physical Review Letters*, 60(6), 535.
- Reis, C.P., Neufeld, R.J., Ribeiro, A.J., Veiga, F. 2006. Nanoencapsulation I. Methods for preparation of drug-loaded polymeric nanoparticles. *Nanomedicine: Nanotechnology, Biology and Medicine*, 2(1), 8-21.
- Roco, M. 2011. The Long View of Nanotechnology Development: The National Nanotechnology Initiative at 10 Years. in: *Nanotechnology Research Directions for Societal Needs in 2020*, Vol. 1, Springer Netherlands, pp. 1-28.
- Roco, M.C., Bainbridge, W.S. 2005. Societal implications of nanoscience and nanotechnology: Maximizing human benefit. *Journal of Nanoparticle Research*, 7(1), 1-13.
- Daw, Rosamund. 2012. Nanotechnology is ancient history. In: *Nanotechnology world*, Vol. 2012, Guardian News and Media Limited. London. The Guardian, April 24, 2012.
- Rossi, M., Cubadda, F., Dini, L., Terranova, M.L., Aureli, F., Sorbo, A., Passeri, D. 2014. Scientific basis of nanotechnology, implications for the food sector and future trends. *Trends in Food Science & Technology*, 40(2), 127-148.
- Roth, J. 1982. The preparation of protein A-gold complexes with 3 nm and 15 nm gold particles and their use in labelling multiple antigens on ultra-thin sections. *The Histochemical Journal*, 14(5), 791-801.

- Routray, W., Orsat, V. 2013. Dielectric Properties of Concentration-Dependent Ethanol + Acids Solutions at Different Temperatures. *Journal of Chemical & Engineering Data*. 58 (6), 1650-1661.
- Sabliov, C.M., Astete, C.E. 2008. Encapsulation and controlled release of antioxidants and vitamins. in: *Delivery and Controlled Release of Bioactives in Foods and Nutraceuticals*, (Ed.) N. Garti, Woodhead Publishing, pp. 297-330.
- Salvati, R., Longo, A., Carotenuto, G., De Nicola, S., Pepe, G., Nicolais, L., Barone, A. 2005. UV-vis spectroscopy for on-line monitoring of Au nanoparticles size during growth. *Applied surface science*, 248(1-4), 28-31.
- Sau, T.K., Rogach, A.L. 2012. Colloidal Synthesis of Noble Metal Nanoparticles of Complex Morphologies. in: *Complex-Shaped Metal Nanoparticles*, Wiley-VCH Verlag GmbH & Co. KGaA, pp. 7-90.
- Schmid, G., Corain, B. 2003. Nanoparticulated gold: Syntheses, structures, electronics, and reactivities. *European Journal of Inorganic Chemistry*(17), 3081-3098.
- Schmidt, K. 2007. Green nanotechnology: it's easier than you think. Technical Report, Project on Emerging Nanotechnologies, 1-36.
- Schwarz, A.E. 2009. Green Dreams of Reason. *Green Nanotechnology Between Visions of Excess and Control. NanoEthics*, 3(2), 109-118.
- Seijo, B., Fattal, E., Roblot-Treupel, L., Couvreur, P. 1990. Design of nanoparticles of less than 50 nm diameter: preparation, characterization and drug loading. *International journal of pharmaceutics*, 62(1), 1-7.

- Shankar, S.S., Rai, A., Ankamwar, B., Singh, A., Ahmad, A., Sastry, M. 2004. Biological synthesis of triangular gold nanoprisms. *Nature Materials*, 3(7), 482-488.
- Shankar, S.S., Ahmad, A., Pasricha, R., Sastry, M. 2003. Bioreduction of chloroaurate ions by geranium leaves and its endophytic fungus yields gold nanoparticles of different shapes. *J. Mater. Chem.*, 13(7), 1822-1826.
- Shankar, S.S., Rai, A., Ahmad, A., Sastry, M. 2005. Controlling the optical properties of lemongrass extract synthesized gold nanotriangles and potential application in infrared-absorbing optical coatings. *Chemistry of Materials*, 17(3), 566-572.
- Shimoni, E. 2008. Starch as an encapsulation material to control digestion rate in the delivery of active food components. in: *Delivery and Controlled Release of Bioactives in Foods and Nutraceuticals*, (Ed.) N. Garti, Woodhead Publishing, pp. 279-293.
- Shin, D., Banerjee, D. 2011. Enhancement of specific heat capacity of high-temperature silica-nanofluids synthesized in alkali chloride salt eutectics for solar thermal-energy storage applications. *International Journal of Heat and Mass Transfer*, 54(5), 1064-1070.
- Singh, V., Khullar, P., Dave, P.N., Kaur, G., Bakshi, M.S. 2013. Ecofriendly Route To Synthesize Nanomaterials for Biomedical Applications: Bioactive Polymers on Shape-Controlled Effects of Nanomaterials under Different Reaction Conditions. *ACS Sustainable Chemistry & Engineering*, 1(11), 1417-1431.

- Smitha, S.L., Gopchandran, K.G. 2013. Surface enhanced Raman scattering, antibacterial and antifungal active triangular gold nanoparticles. *Spectrochimica Acta - Part A: Molecular and Biomolecular Spectroscopy*, 102, 114-119.
- Souquet, J.-M., Labarbe, B., Le Guernevé, C., Cheynier, V., Moutounet, M. 2000. Phenolic composition of grape stems. *Journal of agricultural and food chemistry*, 48(4), 1076-1080.
- Song, J., Kim, B. 2009. Rapid biological synthesis of silver nanoparticles using plant leaf extracts. *Bioprocess and Biosystems Engineering*, 32(1), 79-84.
- Song, J.Y., Jang, H.-K., Kim, B.S. 2009. Biological synthesis of gold nanoparticles using *Magnolia kobus* and *Diopyros kaki* leaf extracts. *Process Biochemistry*, 44(10), 1133-1138.
- Sperling, R.A., Gil, P.R., Zhang, F., Zanella, M., Parak, W.J. 2008. Biological applications of gold nanoparticles. *Chemical Society Reviews*, 37(9), 1896-1908.
- Stancanelli, R., Ficarra, R., Cannavà, C., Guardo, M., Calabrò, M.L., Ficarra, P., Ottanà, R., Maccari, R., Crupi, V., Majolino, D., Venuti, V. 2008. UV-vis and FTIR-ATR characterization of 9-fluorenon-2-carboxyester/(2-hydroxypropyl)- β -cyclodextrin inclusion complex. *Journal of Pharmaceutical and Biomedical Analysis*, 47(4-5), 704-709.
- Stražičar, M., Andrenšek, S., Šmidovnik, A. 2008. Effect of β -cyclodextrin on antioxidant activity of coumaric acids. *Food Chemistry*, 110(3), 636-642.

- Strong, L.E., West, J.L. 2011. Thermally responsive polymer–nanoparticle composites for biomedical applications. *Wiley Interdisciplinary Reviews: Nanomedicine and Nanobiotechnology*. 3(3), 307-317.
- Szejtli, J. 1998. Introduction and general overview of cyclodextrin chemistry. *Chemical Reviews*, 98(5), 1743-1754.
- Szente, L., Szejtli, J. 2004. Cyclodextrins as food ingredients. *Trends in Food Science & Technology*, 15(3-4), 137-142.
- Tahmooresnejad, L., Beaudry, C., Schiffauerova, A. 2015. The role of public funding in nanotechnology scientific production: Where Canada stands in comparison to the United States. *Scientometrics*, 102(1), 753-787.
- Taleb, A., Petit, C., Pileni, M.P. 1997. Synthesis of Highly Monodisperse Silver Nanoparticles from AOT Reverse Micelles: A Way to 2D and 3D Self-Organization. *Chemistry of Materials*, 9(4), 950-959.
- Taniguchi, N. 1974. On the basic concept of nanotechnology. *Proc. Intl. Conf. Prod. Eng. Tokyo, Part II, Japan Society of Precision Engineering*. pp. 18-23.
- "The Nobel Prize in Physics 1986". *Nobelprize.org*. Nobel Media AB 2014. Retrieved from http://www.nobelprize.org/nobel_prizes/physics/laureates/1986/. Accessed 5 April, 2015.
- "The Nobel Prize in Chemistry 1996". *Nobelprize.org*. Nobel Media AB 2014 from http://www.nobelprize.org/nobel_prizes/chemistry/laureates/1996/ Accessed 5 April, 2015.

- The Royal Institution of Great Britain. London. Retrieved from: <http://www.rigb.org/ourhistory/michael-faraday/about>. Accessed 5 April, 2015
- Tiede, K., Boxall, A.B.A., Tear, S.P., Lewis, J., David, H., Hassellöv, M. 2008. Detection and characterization of engineered nanoparticles in food and the environment. *Food Additives & Contaminants: Part A*, 25(7), 795-821.
- Torreggiani, A., Jurasekova, Z., Sanchez-Cortes, S., Tamba, M. 2008. Spectroscopic and pulse radiolysis studies of the antioxidant properties of (+)catechin: metal chelation and oxidizing radical scavenging. *Journal of Raman Spectroscopy*, 39(2), 265-275.
- Turkevich, J., Stevenson, P.C., Hillier, J. 1951. A study of the nucleation and growth processes in the synthesis of colloidal gold. *Discussions of the Faraday Society*, 11, 55-75.
- Vajjha, R.S., Das, D.K. 2009. Experimental determination of thermal conductivity of three nanofluids and development of new correlations. *International Journal of Heat and Mass Transfer*, 52(21), 4675-4682.
- Vauthier, C., Dubernet, C., Fattal, E., Pinto-Alphandary, H., Couvreur, P. 2003. Poly (alkylcyanoacrylates) as biodegradable materials for biomedical applications. *Advanced Drug Delivery Reviews*, 55(4), 519-548.
- Venkatesh, M., Raghavan, G. 2004. An overview of microwave processing and dielectric properties of agri-food materials. *Biosystems Engineering*, 88(1), 1-18.

- Vivekanandhan, S., Schreiber, M., Mason, C., Mohanty, A.K., Misra, M. 2014. Maple Leaf (*Acer* sp.) Extract Mediated Green Process for the Functionalization of ZnO Powders with Silver Nanoparticles. *Colloids and Surfaces B: Biointerfaces*, 113, 169-175.
- Vrignaud, S., Benoit, J.-P., Saulnier, P. 2011. Strategies for the nanoencapsulation of hydrophilic molecules in polymer-based nanoparticles. *Biomaterials*, 32(33), 8593-8604.
- Wang, J.C., Chen, S.H., Xu, Z.C. 2008. Synthesis and Properties Research on the Nanocapsulated Capsaicin by Simple Coacervation Method. *Journal of Dispersion Science and Technology*, 29(5), 687-695.
- Warriner, K., Reddy, S.M., Namvar, A., Neethirajan, S. 2014. Developments in nanoparticles for use in biosensors to assess food safety and quality. *Trends in Food Science & Technology*, 40(2), 183-199.
- Watnasirichaikul, S., Davies, N.M., Rades, T., Tucker, I.G. 2000. Preparation of biodegradable insulin nanocapsules from biocompatible microemulsions. *Pharmaceutical Research*, 17(6), 684-689.
- Weber, H.A., Hodges, A.E., Guthrie, J.R., O'Brien, B.M., Robaugh, D., Clark, A.P., Harris, R.K., Algaier, J.W., Smith, C.S. 2006. Comparison of Proanthocyanidins in Commercial Antioxidants: Grape Seed and Pine Bark Extracts. *Journal of agricultural and food chemistry*, 55(1), 148-156.

- White, R.J., Luque, R., Budarin, V.L., Clark, J.H., Macquarrie, D.J. 2009. Supported metal nanoparticles on porous materials. Methods and applications. Chemical Society Reviews, 38(2), 481-494.
- Wong, S., Karn, B. 2012. Ensuring sustainability with green nanotechnology. Nanotechnology, 23(29), 290201.
- Xu, H., Zeiger, B.W., Suslick, K.S. 2013. Sonochemical synthesis of nanomaterials. Chemical Society Reviews, 42(7), 2555-2567.
- Xue, Q., Liu, Z., Guo, Y., Guo, S. 2015. Cyclodextrin functionalized graphene–gold nanoparticle hybrids with strong supramolecular capability for electrochemical thrombin aptasensor. Biosensors and Bioelectronics, 68(0), 429-436.
- Yamakoshi, J., Saito, M., Kataoka, S., Tokutake, S. 2002. Procyanidin-rich extract from grape seeds prevents cataract formation in hereditary cataractous (ICR/f) rats. Journal of agricultural and food chemistry, 50(17), 4983-4988.
- Yang, N., WeiHong, L., Hao, L. 2014. Biosynthesis of Au nanoparticles using agricultural waste mango peel extract and its in vitro cytotoxic effect on two normal cells. Materials Letters, 134, 67-70.
- Yates, B.J., Dionysiou, D.D. 2006. Chapter 17 Green engineering and nanotechnology. in: Sustainability Science and Engineering, (Ed.) M.A. Abraham, Vol. Volume 1, Elsevier, pp. 349-365.
- Yokel, R.A., MacPhail, R.C. 2011. Engineered nanomaterials: exposures, hazards, and risk prevention. J Occup Med Toxicol, 6(7).

- Yu, W., Xie, H. 2012. A review on nanofluids: preparation, stability mechanisms, and applications. *Journal of Nanomaterials*, 2012, 1.
- Zeng, H., Du, X.W., Singh, S.C., Kulinich, S.A., Yang, S., He, J., Cai, W. 2012. Nanomaterials via laser ablation/irradiation in liquid: a review. *Advanced Functional Materials*, 22(7), 1333-1353.
- Zeng, S., Yong, K.T., Roy, I., Dinh, X.Q., Yu, X., Luan, F. 2011. A review on functionalized gold nanoparticles for biosensing applications. *Plasmonics*, 6(3), 491-506.
- Zhu, J., Liu, S., Palchik, O., Koltypin, Y., Gedanken, A. 2000. Shape-controlled synthesis of silver nanoparticles by pulse sonoelectrochemical methods. *Langmuir*, 16(16), 6396-6399.

Last page of my thesis

Writing is the painting of the voice - Voltaire

I have tried to color my PhD painting with curiosity and passion.

Thank you very much, for your valuable time.

Sincerely,

Kiruba Krishnaswamy

